Ozone Formation Sensitivity to NOx and VOC Emissions in the LADCO Region

APPENDICES

Prepared by:
Angela F. Dickens
Lake Michigan Air Directors Consortium

Please direct questions/comments to dickens@ladco.org

September 9, 2022

Table of Contents

APPENDIX 1

Supplemental Figures: Ground-Based $HCHO/NO_2$ Analysis

This appendix contains supplemental figures for the ground-based $HCHO/NO_2$ ratio study of ozone formation in the LADCO region. These figures include:

- A figure showing how $HCHO/NO_2$ ratios change with different ozone MDA8 concentrations.
- A figure showing the $HCHO/NO_2$ ratios on days with MDA8 values greater than 70 ppb.
- Figures showing the $HCHO/NO_2$ ratios on high-ozone days for each year at each monitor.

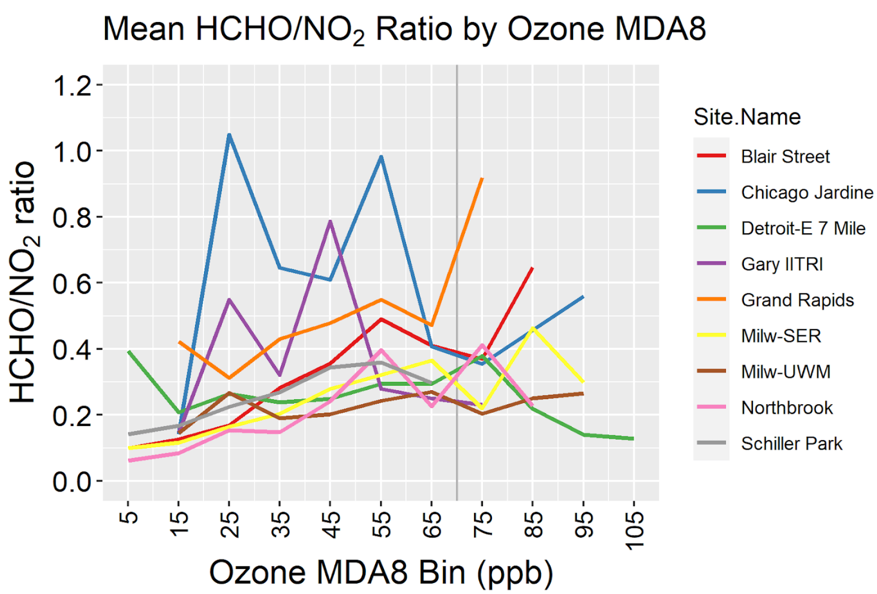

Figure A1.1. Mean $HCHO/NO_2$ ratio for each nonattainment area, plotted by ozone MDA8 values. MDA8 values were binned into 10-ppb-wide concentration bins. $HCHO/NO_2$ ratios are the means for all years of data available for each monitor.

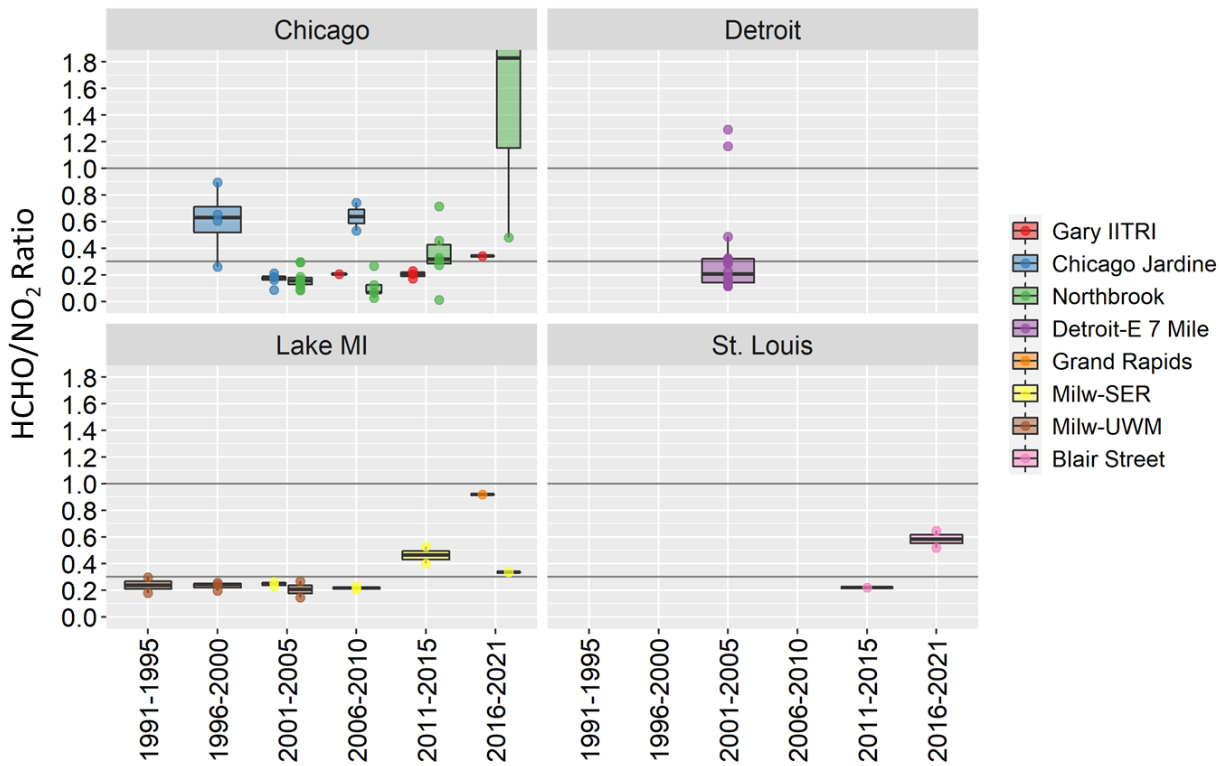

Figure A1.2. Ground-based $HCHO/NO_2$ ratios for monitors in or near LADCO nonattainment areas on days with MDA8 ozone greater than 70 ppb. Data are shown for six groupings of years.[1] Note that the Northbrook monitor in Chicago had one day off the scale shown ($HCHO/NO_2$ of 3.2) in 2016-2021. The gray lines mark the ratio thresholds between VOC-sensitive (< 0.3), transitional (0.3-1), and NOx-sensitive (> 1) chemistry based on ratio thresholds from Blanchard (2020).

[1] In the boxplots, the line goes through the median value, the box encloses the middle 50% of values, and the "whiskers" include most values. Data points representing individual days are shown as circles.

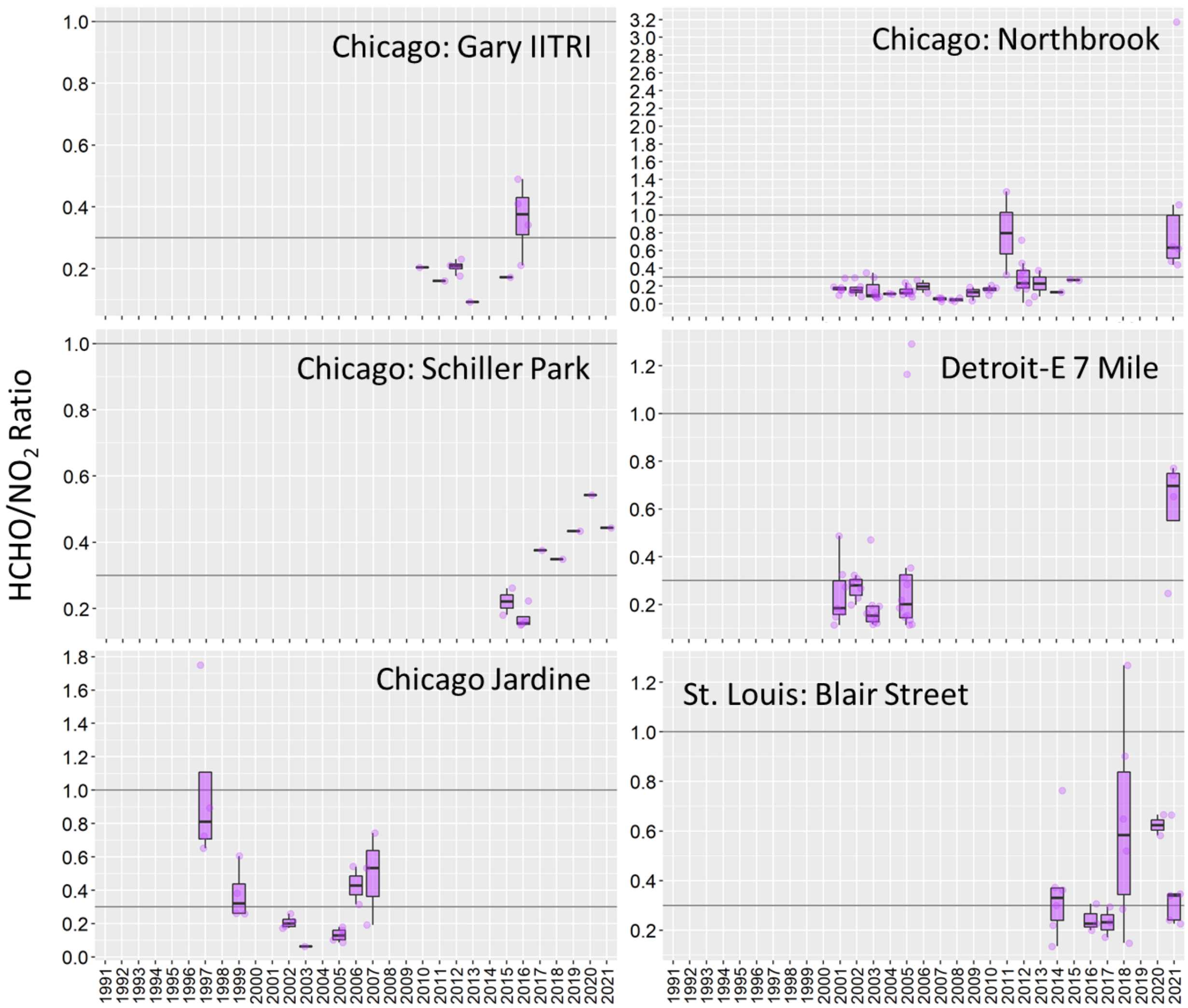

Figure A1.3. Ground-based $HCHO/NO_2$ ratios for each year at monitors in the Chicago, Detroit, and St. Louis nonattainment areas on days with MDA8 ozone greater than 60 ppb.

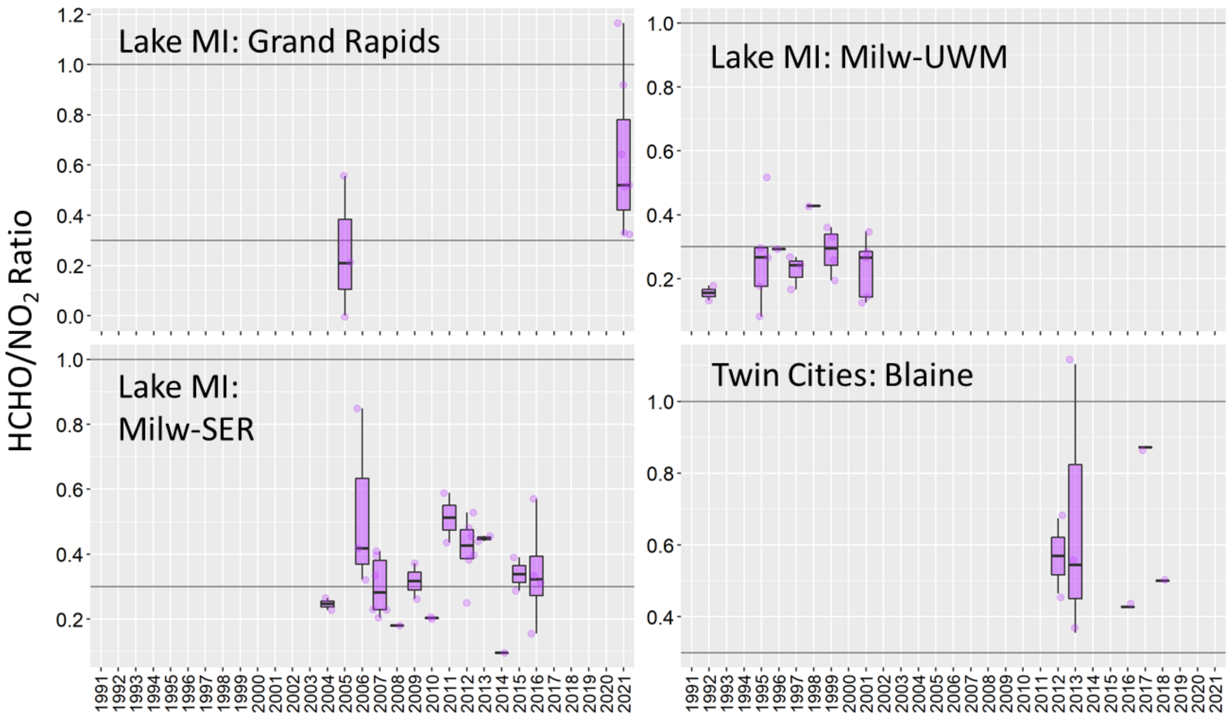

Figure A1.4. Ground-based $HCHO/NO_2$ ratios for each year at monitors in the Lake Michigan region and in the Twin Cities on days with MDA8 ozone greater than 60 ppb.

APPENDIX 2

Supplemental Figures: TROPOMI Satellite HCHO/NO_2 Observations

This appendix contains supplemental figures and tables for the TROPOMI satellite-based HCHO/NO_2 ratio study of ozone formation in the LADCO region. These figures and tables include:

- A table of the exceedance days in each nonattainment area
- Maps showing the grid cells included in each nonattainment area
- Maps of ozone season average NO_2 and HCHO columns, HCHO/NO_2 ratios, and ozone formation sensitivity regimes in the nonattainment areas
- A table showing the amounts of ozone and ozone precursors and indicator ratio values from the CAMx model and TROPOMI satellite analyses on exceedance days

Table A2.1. Exceedance days in each nonattainment area used for the TROPOMI analysis and the number of sites within the nonattainment area with exceedances on that day. Exceedance days had at least one monitor within the nonattainment area with an ozone MDA8 value above 70 ppb. Only exceedances with concurrent TROPOMI HCHO and NO_2 data are included.

Chicago		Cincinnati		Cleveland		Detroit		Louisville		Sheboygan		St. Louis		Western MI	
33 days	#	*19 days*	#	*18 days*	#	*21 days*	#	*14 days*	#	*12 days*	#	*24 days*	#	*14 days*	#
20180524	12	20180525	6	20180517	2	20180524	1	20180607	2	20180524	2	20180523	1	20180525	3
20180525	13	20180527	1	20180525	5	20180525	6	20180608	3	20180525	1	20180524	10	20180527	3
20180526	12	20180607	2	20180528	4	20180527	1	20180615	3	20180526	1	20180528	13	20180528	1
20180527	15	20180608	2	20180529	2	20180528	6	20180616	1	20180527	1	20180601	4	20180529	3
20180528	12	20180615	7	20180616	2	20180529	4	20180617	1	20180629	2	20180605	5	20180531	2
20180529	1	20180616	4	20180617	2	20180607	2	20180628	1	20180630	1	20180606	12	20180615	1
20180607	1	20180617	1	20180629	4	20180608	2	20180713	5	20180708	1	20180608	6	20180617	2
20180615	9	20180628	1	20180630	1	20180617	2	20180714	4	20180712	1	20180615	2	20180709	3
20180616	3	20180629	1	20180709	2	20180629	5	20180810	1	20180713	1	20180711	2	20180713	3
20180628	1	20180713	4	20180710	2	20180703	1	20180914	1	20180804	2	20180712	7	20180802	1
20180629	2	20180714	8	20180713	1	20180708	1	20190628	1	20190709	1	20180713	8	20190702	2
20180703	5	20190626	1	20180714	4	20180709	2	20190710	1	20190725	1	20180801	2	20190705	1
20180708	3	20190710	3	20180715	7	20180713	6	20190713	2			20180803	6	20190710	3
20180709	9	20190713	3	20190628	2	20180715	2	20190805	2			20180911	1	20190728	1
20180711	3	20190714	3	20190629	1	20180804	5					20190629	4		
20180713	6	20190805	3	20190710	2	20190627	4					20190713	11		
20180715	7	20190819	2	20190713	2	20190701	2					20190717	1		
20180803	1	20190910	1	20190804	1	20190710	4					20190719	1		
20180804	2	20190920	1			20190715	2					20190720	1		
20180813	1					20190727	1					20190721	1		
20180814	1					20190812	1					20190805	8		
20190605	2											20190819	2		
20190626	1											20190918	2		
20190628	1											20190919	6		
20190629	4														
20190703	1														
20190705	1														
20190708	1														
20190709	11														
20190713	1														
20190725	2														
20190802	1														
20190803	2														

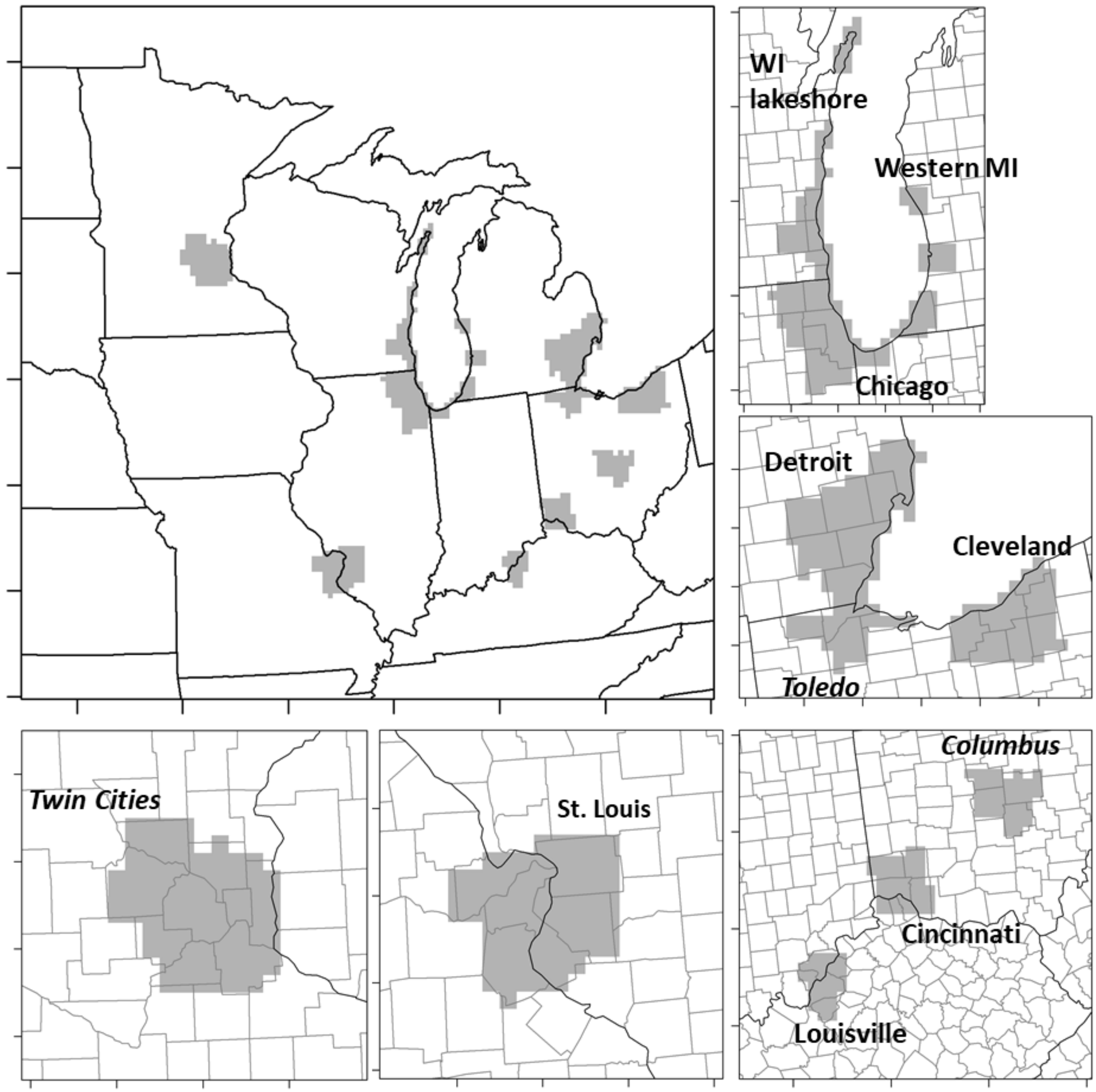

Figure A2.1. Maps showing the grid cells included in each nonattainment area (in gray). Areas not discussed in the main body of the report are labeled in italics. These areas are discussed below. Figure A3 includes the breakdown of the nonattainment areas in the Lakes Michigan and Erie regions.

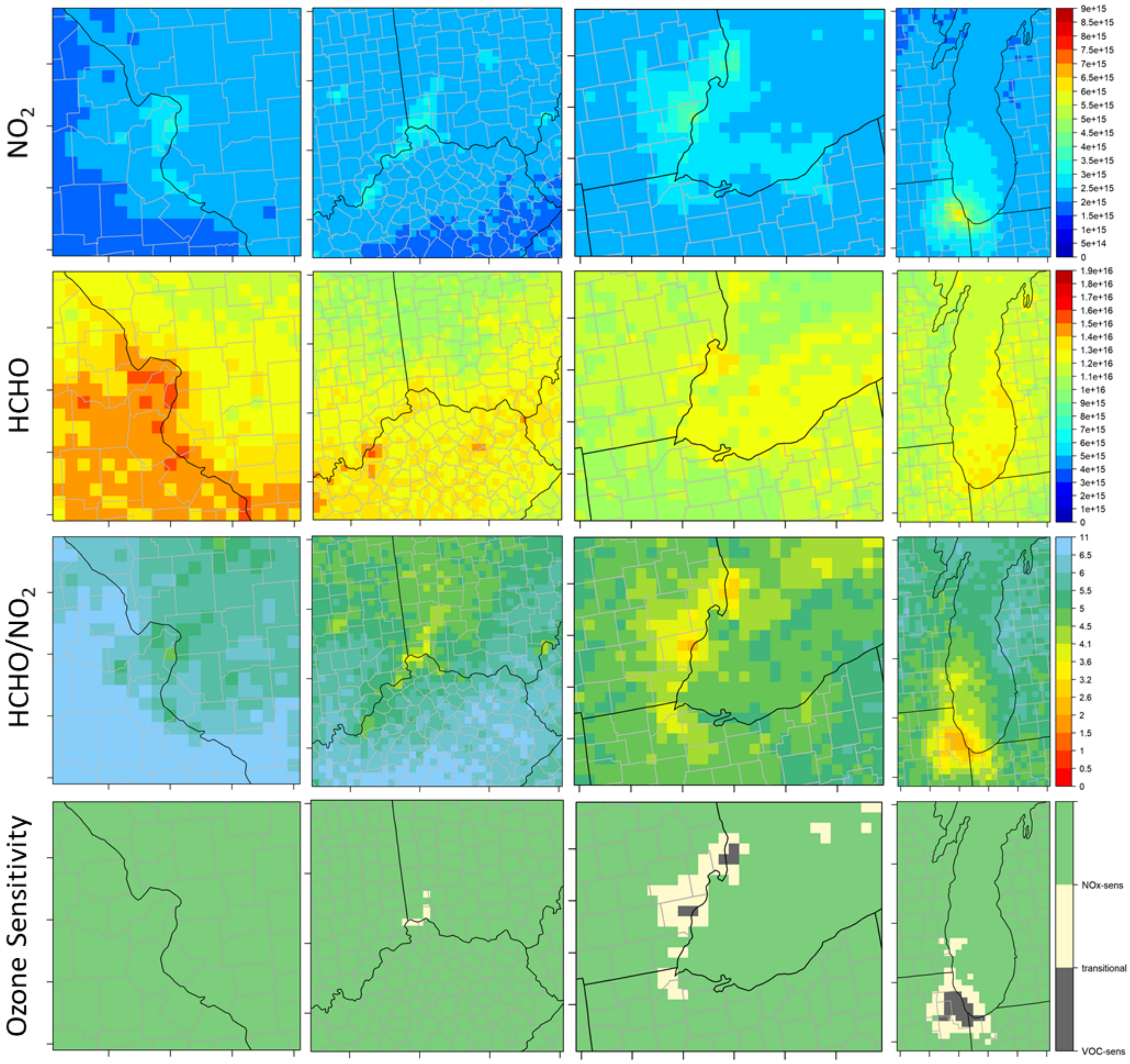

Figure A2.2. Maps of ozone season average (top) NO_2 columns (mol/cm^2), (2nd row) HCHO columns (mol/cm^2), (3rd row) $HCHO/NO_2$ ratios, and (bottom) ozone formation sensitivity regimes in (left) St. Louis, (second) Louisville and Cincinnati, (third) Detroit and Cleveland, and (right) Chicago, the Wisconsin lakeshore and Western Michigan.

Table A2.2. Concentrations (ppb) or columns (mol/cm^2) of ozone and ozone precursors and sensitivity indicator ratios for grid cells containing ground monitors on exceedance days in nonattainment or maintenance areas in the LADCO region.

	Model Concentrations (ppb) and Ratios																					TROPOMI Columns and Ratios		
	Ozone			HCHO			NO_2			$HCHO/NO_2$			H_2O_2			HNO_3			H_2O_2/HNO_3			HCHO (mol/cm^2)	NO_2 (mol/cm^2)	$HCHO/NO_2$
Site	2016	2020	2028	2016	2020	2028	2016	2020	2028	2016	2020	2028	2016	2020	2028	2016	2020	2028	2016	2020	2028			
Allegan County, MI (Western MI)																								
260050003	63.88	59.62	56.11	2.34	2.27	2.24	1.30	1.07	0.77	1.92	2.26	3.06	1.72	1.74	1.75	2.06	1.73	1.37	0.93	1.14	1.44	1.34E+16	2.73E+15	4.92
Berrien County, MI (Western MI)																								
260210014	67.76	63.33	59.09	2.69	2.62	2.55	1.15	0.91	0.66	2.54	3.07	4.18	1.83	1.87	1.88	2.52	2.08	1.66	0.85	1.05	1.35	1.35E+16	2.58E+15	5.25
Chicago, IL-IN-WI																								
170310001	68.51	65.35	61.77	3.09	3.00	2.87	4.13	3.24	2.27	0.88	1.08	1.46	1.25	1.29	1.33	2.34	1.93	1.50	0.78	0.95	1.29	1.38E+16	4.43E+15	3.12
170310032	67.08	63.85	61.90	2.88	2.81	2.74	5.88	5.17	3.47	0.56	0.64	0.90	1.29	1.33	1.37	2.94	2.51	1.99	0.62	0.74	0.99	1.34E+16	5.98E+15	2.24
170310076	68.20	65.74	62.30	3.15	3.04	3.07	6.50	5.00	4.84	0.56	0.70	0.71	1.20	1.25	1.27	2.83	2.35	1.93	0.64	0.80	1.00	1.47E+16	7.37E+15	2.00
170311003	68.21	65.42	62.85	3.07	2.97	2.95	6.08	4.92	3.98	0.62	0.75	0.91	1.22	1.27	1.30	2.91	2.44	1.99	0.56	0.69	0.86	1.45E+16	5.87E+15	2.48
170311601	66.78	63.47	60.13	2.98	2.93	2.82	3.50	3.09	1.97	0.94	1.04	1.54	1.29	1.31	1.36	2.06	1.75	1.32	0.87	1.01	1.38	1.33E+16	4.74E+15	2.81
170313103	66.99	64.41	56.74	3.70	3.61	3.88	9.36	8.27	12.31	0.45	0.49	0.34	1.14	1.18	1.19	2.95	2.50	2.24	0.60	0.72	0.81	1.53E+16	6.46E+15	2.36
170314002	66.61	64.24	62.26	3.07	2.97	2.92	7.62	6.09	4.50	0.49	0.60	0.78	1.21	1.26	1.30	2.96	2.48	1.99	0.59	0.72	0.95	1.40E+16	8.13E+15	1.73
170314007	69.22	66.26	62.63	3.57	3.46	3.42	5.33	4.23	3.80	0.81	0.99	1.16	1.19	1.24	1.25	2.58	2.14	1.82	0.70	0.86	1.10	1.46E+16	4.60E+15	3.16
170314201	69.22	66.26	62.63	3.57	3.46	3.42	5.33	4.23	3.80	0.81	0.99	1.16	1.19	1.24	1.25	2.58	2.14	1.82	0.70	0.86	1.10	1.46E+16	4.60E+15	3.16
170317002	69.06	65.63	62.43	2.96	2.87	2.80	3.45	2.78	2.07	1.11	1.34	1.76	1.44	1.49	1.54	2.98	2.48	1.97	0.66	0.81	1.06	1.35E+16	4.27E+15	3.16
170436001	68.79	65.54	61.91	3.35	3.25	3.11	4.29	3.41	2.27	0.89	1.08	1.51	1.24	1.28	1.33	2.19	1.81	1.36	0.80	0.97	1.30	1.24E+16	4.59E+15	2.70
170890005	63.57	60.09	56.47	2.85	2.79	2.71	2.69	2.23	1.66	1.18	1.39	1.78	1.40	1.43	1.45	1.72	1.43	1.10	1.06	1.26	1.65	1.35E+16	3.11E+15	4.33
170971007	65.25	61.71	58.62	2.74	2.73	2.64	2.26	2.28	1.57	1.43	1.39	1.91	1.47	1.49	1.54	2.62	2.23	1.74	0.86	0.97	1.29	1.24E+16	3.39E+15	3.67
171110001	61.77	58.14	54.18	2.82	2.73	2.61	1.93	1.56	1.14	1.62	1.95	2.50	1.41	1.44	1.45	1.50	1.24	0.93	1.23	1.48	1.94	1.30E+16	2.77E+15	4.69
171971011	56.07	53.06	49.36	2.12	2.07	2.01	1.14	0.94	0.70	2.05	2.44	3.18	1.66	1.65	1.63	1.43	1.22	0.93	1.48	1.72	2.21	1.38E+16	2.56E+15	5.38
180890022	66.67	63.09	60.13	2.82	2.77	2.72	3.79	3.53	2.68	0.85	0.90	1.15	1.53	1.56	1.58	2.78	2.38	1.90	0.77	0.91	1.18	1.48E+16	4.82E+15	3.06
180892008	65.77	61.97	59.90	2.84	2.76	2.74	5.32	5.26	3.75	0.58	0.58	0.80	1.35	1.38	1.40	2.71	2.34	1.88	0.69	0.81	1.05	1.45E+16	6.01E+15	2.42
181270024	65.81	62.13	59.38	3.11	3.06	2.99	4.20	4.40	2.94	0.81	0.76	1.10	1.47	1.49	1.51	2.59	2.27	1.75	0.79	0.89	1.22	1.46E+16	5.05E+15	2.90
181270026	62.45	58.92	54.12	2.62	2.54	2.41	1.53	1.23	0.88	1.91	2.28	3.04	1.59	1.59	1.60	1.71	1.41	1.06	1.26	1.48	1.99	1.37E+16	2.92E+15	4.71
550590019	61.62	58.72	56.25	3.14	3.26	2.95	3.96	3.87	2.29	0.89	0.96	1.41	1.30	1.23	1.42	2.75	2.40	1.73	0.71	0.76	1.22	1.31E+16	2.79E+15	4.69
550590025	59.45	55.92	52.70	2.51	2.45	2.37	1.83	1.45	1.05	1.74	2.09	2.79	1.40	1.43	1.45	1.97	1.61	1.28	1.08	1.31	1.69	1.29E+16	2.79E+15	4.62
Cincinnati, OH-KY																								
210373002	70.71	66.18	61.54	3.62	3.50	3.36	3.15	2.36	1.48	1.26	1.61	2.43	1.63	1.68	1.71	2.22	1.77	1.32	0.92	1.19	1.56	1.57E+16	2.81E+15	5.59
390170004	68.61	64.31	59.37	2.90	2.82	2.72	1.82	1.43	0.98	1.75	2.13	2.92	1.74	1.76	1.77	2.11	1.71	1.26	0.96	1.17	1.57	1.43E+16	2.93E+15	4.87
390170018	67.71	63.65	59.69	2.89	2.86	2.80	3.21	2.88	1.88	1.01	1.10	1.61	1.61	1.63	1.65	2.31	1.94	1.44	0.81	0.97	1.31	1.27E+16	3.40E+15	3.75
390179991	61.72	57.67	53.53	2.50	2.43	2.36	0.69	0.57	0.46	3.91	4.49	5.41	1.85	1.86	1.83	1.79	1.47	1.14	1.19	1.43	1.80	1.28E+16	2.30E+15	5.57
390250022	66.26	61.53	56.94	3.18	3.06	2.96	1.19	0.92	0.65	3.04	3.73	4.94	1.69	1.71	1.71	1.84	1.46	1.11	1.14	1.45	1.83	1.31E+16	2.65E+15	4.96
390610006	70.23	65.92	60.97	3.21	3.11	2.99	3.48	2.62	1.66	1.02	1.30	1.92	1.58	1.62	1.67	2.23	1.79	1.27	0.81	1.04	1.46	1.56E+16	3.41E+15	4.57
390610010	72.38	67.90	63.27	3.46	3.36	3.32	2.08	1.61	1.25	1.80	2.19	2.76	1.68	1.74	1.74	2.37	1.90	1.47	0.86	1.08	1.35	1.47E+16	3.56E+15	4.13
390610040	70.83	66.64	62.02	3.48	3.37	3.25	4.35	3.19	2.02	0.89	1.17	1.73	1.55	1.60	1.65	2.33	1.87	1.34	0.78	1.02	1.41	1.60E+16	3.47E+15	4.61
391650007	66.38	62.19	57.64	2.77	2.70	2.65	1.79	1.47	1.16	1.75	2.10	2.52	1.69	1.71	1.72	2.11	1.73	1.29	0.93	1.15	1.53	1.34E+16	2.91E+15	4.60

Site	Model Concentrations (ppb) and Ratios																					TROPOMI Columns and Ratios		
	Ozone			HCHO			NO_2			$HCHO/NO_2$			H_2O_2			HNO_3			H_2O_2/HNO_3			HCHO (mol/cm^2)	NO_2 (mol/cm^2)	$HCHO/NO_2$
	2016	2020	2028	2016	2020	2028	2016	2020	2028	2016	2020	2028	2016	2020	2028	2016	2020	2028	2016	2020	2028			
Cleveland, OH																								
390350034	70.18	68.46	64.40	3.42	3.54	3.26	5.93	5.29	2.99	0.64	0.75	1.18	1.35	1.30	1.45	2.88	2.64	1.79	0.47	0.50	0.81	1.40E+16	2.57E+15	5.46
390350060	65.35	61.97	58.80	2.85	2.78	2.67	4.42	3.61	2.50	0.76	0.90	1.26	1.26	1.30	1.31	1.96	1.64	1.25	0.75	0.92	1.21	1.52E+16	3.46E+15	4.37
390350064	65.33	61.70	57.89	2.95	2.86	2.77	2.89	2.29	1.93	1.18	1.46	1.61	1.31	1.34	1.33	1.74	1.45	1.13	0.94	1.15	1.44	1.39E+16	2.75E+15	5.07
390355002	66.52	62.66	58.90	2.75	2.65	2.53	2.58	1.94	1.40	1.18	1.51	1.98	1.37	1.41	1.41	1.82	1.49	1.15	0.84	1.05	1.35	1.19E+16	2.76E+15	4.31
390550004	64.68	60.21	56.27	2.43	2.34	2.26	0.76	0.62	0.50	3.39	3.98	4.76	1.39	1.43	1.40	1.35	1.07	0.86	1.16	1.47	1.78	1.34E+16	2.40E+15	5.58
390850003	70.67	68.56	64.17	3.65	3.88	3.43	5.01	4.81	2.83	0.77	0.87	1.28	1.42	1.35	1.52	2.81	2.55	1.76	0.51	0.53	0.88	1.35E+16	2.53E+15	5.36
390850007	70.94	68.77	64.58	4.06	4.32	3.83	4.72	4.57	2.93	0.88	0.96	1.33	1.47	1.40	1.56	2.85	2.58	1.84	0.55	0.58	0.90	1.29E+16	2.49E+15	5.17
390930018	63.44	59.65	56.04	2.71	2.63	2.50	2.04	1.79	1.20	1.49	1.74	2.33	1.31	1.33	1.33	1.63	1.40	1.07	0.99	1.19	1.52	1.30E+16	2.57E+15	5.05
391030004	60.90	57.04	52.92	2.27	2.22	2.14	0.78	0.66	0.51	3.02	3.49	4.37	1.49	1.50	1.47	1.37	1.12	0.86	1.30	1.54	1.93	1.35E+16	2.33E+15	5.80
391331001	65.54	61.05	56.41	2.85	2.74	2.60	1.39	1.11	0.80	2.12	2.55	3.31	1.39	1.42	1.41	1.40	1.12	0.86	1.11	1.40	1.83	1.38E+16	2.28E+15	6.08
391530020	65.90	61.68	56.92	2.89	2.79	2.61	2.38	1.80	1.18	1.32	1.67	2.36	1.36	1.40	1.40	1.53	1.22	0.91	1.04	1.31	1.74	1.24E+16	2.52E+15	4.91
Detroit, MI																								
260990009	61.56	59.15	53.61	2.46	2.40	2.26	1.31	1.08	0.77	2.12	2.51	3.21	1.34	1.41	1.39	1.59	1.32	0.95	1.09	1.33	1.72	1.28E+16	3.80E+15	3.38
260991003	64.64	62.17	56.98	2.63	2.57	2.40	3.92	2.90	1.86	0.73	0.95	1.37	1.20	1.30	1.31	1.96	1.55	1.10	0.71	0.96	1.36	1.38E+16	4.73E+15	2.93
261250001	65.38	62.75	57.82	3.00	2.91	2.71	4.57	3.19	1.93	0.74	1.01	1.52	1.19	1.30	1.31	2.01	1.55	1.10	0.72	1.00	1.39	1.47E+16	4.41E+15	3.34
261470005	59.80	58.61	53.95	2.72	2.77	2.57	1.74	1.64	1.15	1.68	1.90	2.48	1.26	1.30	1.28	1.64	1.53	1.15	1.22	1.32	1.71	1.25E+16	3.60E+15	3.49
261610008	62.34	58.82	54.84	2.74	2.64	2.57	1.89	1.49	1.21	1.63	1.99	2.43	1.40	1.48	1.42	1.68	1.37	1.11	1.10	1.42	1.70	1.18E+16	3.10E+15	3.80
261619991	58.71	54.31	50.67	2.61	2.44	2.34	0.57	0.44	0.36	5.34	6.25	7.11	1.47	1.53	1.48	1.46	1.12	0.89	1.35	1.74	2.00	1.24E+16	2.71E+15	4.57
261630001	64.05	61.21	56.55	2.95	2.88	2.77	2.55	1.96	1.51	1.22	1.53	1.96	1.34	1.42	1.38	1.64	1.36	1.07	0.92	1.16	1.44	1.26E+16	3.93E+15	3.21
261630019	65.03	62.68	57.80	2.72	2.69	2.52	4.55	3.53	2.07	0.65	0.81	1.28	1.21	1.31	1.32	2.08	1.67	1.17	0.66	0.87	1.26	1.43E+16	5.74E+15	2.50
261630093	65.38	62.75	57.82	3.00	2.91	2.71	4.57	3.19	1.93	0.74	1.01	1.52	1.19	1.30	1.31	2.01	1.55	1.10	0.72	1.00	1.39	1.47E+16	4.41E+15	3.34
261630094	65.38	62.75	57.82	3.00	2.91	2.71	4.57	3.19	1.93	0.74	1.01	1.52	1.19	1.30	1.31	2.01	1.55	1.10	0.72	1.00	1.39	1.47E+16	4.41E+15	3.34
Door County, WI (WI Lakeshore)																								
550290004	47.33	45.46	42.25	1.90	1.88	1.81	0.76	0.71	0.52	3.14	3.35	4.27	1.39	1.37	1.36	1.15	1.00	0.80	1.81	1.96	2.44	1.36E+16	2.27E+15	6.01
Louisville, KY-IN																								
180190008	67.47	63.43	58.36	3.37	3.31	3.17	1.24	1.08	0.79	2.96	3.27	4.34	1.72	1.75	1.75	2.09	1.71	1.33	0.98	1.18	1.54	1.51E+16	2.88E+15	5.26
180431004	68.85	64.80	59.26	3.68	3.55	3.37	2.17	1.68	1.17	1.84	2.27	3.08	1.60	1.64	1.66	2.02	1.63	1.24	0.96	1.18	1.58	1.68E+16	3.28E+15	5.12
210290006	69.40	65.38	60.28	4.49	4.42	4.15	1.74	1.63	1.12	2.91	3.13	4.29	1.80	1.78	1.78	1.91	1.57	1.27	1.22	1.44	1.76	1.56E+16	2.63E+15	5.93
211110027	69.09	64.55	59.39	3.74	3.61	3.43	2.77	2.06	1.47	1.45	1.87	2.53	1.63	1.70	1.69	2.04	1.58	1.25	1.00	1.29	1.62	1.71E+16	2.85E+15	6.01
211110051	73.47	69.85	64.32	4.20	4.17	4.00	1.95	1.84	1.25	2.36	2.47	3.44	1.67	1.67	1.72	2.28	1.93	1.48	0.94	1.08	1.40	1.60E+16	4.67E+15	3.44
211110067	72.02	68.51	63.20	3.86	3.77	3.86	5.51	4.42	4.87	0.75	0.90	0.84	1.48	1.54	1.53	2.61	2.11	1.79	0.71	0.88	1.03	2.00E+16	3.81E+15	5.25
211850004	65.48	61.06	56.33	3.34	3.26	3.10	1.32	1.05	0.79	2.75	3.30	4.32	1.70	1.74	1.72	1.93	1.51	1.24	1.07	1.34	1.67	1.63E+16	2.78E+15	5.88
Manitowoc County, WI (WI Lakeshore)																								
550710007	54.90	51.95	48.98	2.21	2.18	2.09	1.92	1.56	1.12	1.21	1.49	1.94	1.43	1.42	1.47	1.24	1.06	0.84	8.74	10.67	14.00	1.47E+16	2.72E+15	5.40

	Model Concentrations (ppb) and Ratios																					TROPOMI Columns and Ratios		
	Ozone			HCHO			NO_2			$HCHO/NO_2$			H_2O_2			HNO_3			H_2O_2/HNO_3			HCHO	NO_2	HCHO/
Site	2016	2020	2028	2016	2020	2028	2016	2020	2028	2016	2020	2028	2016	2020	2028	2016	2020	2028	2016	2020	2028	(mol/cm^2)	(mol/cm^2)	NO_2
Milwaukee, WI																								
550790010	68.90	65.06	61.44	2.75	2.71	2.70	3.23	2.85	2.44	0.92	1.02	1.18	1.56	1.60	1.64	2.79	2.32	1.84	0.72	0.87	1.14	1.33E+16	3.07E+15	4.33
550790026	61.39	57.35	57.92	2.96	3.06	2.87	8.51	8.48	4.47	0.37	0.39	0.68	1.43	1.31	1.55	2.91	2.41	1.84	0.55	0.63	1.05	1.58E+16	3.13E+15	5.05
550790085	62.88	60.01	58.19	2.93	2.98	2.80	5.09	4.65	2.51	0.72	0.82	1.38	1.39	1.35	1.53	2.79	2.38	1.71	0.69	0.85	1.59	1.38E+16	2.95E+15	4.68
550890008	61.23	57.52	53.53	2.60	2.53	2.43	1.50	1.24	0.88	1.94	2.29	3.05	1.44	1.46	1.47	1.63	1.36	1.02	1.03	1.23	1.62	1.42E+16	2.45E+15	5.80
550890009	64.28	60.84	57.46	2.27	2.22	2.23	1.12	0.97	0.79	2.66	3.05	3.56	1.53	1.55	1.58	2.41	2.06	1.61	0.95	1.13	1.47	1.23E+16	2.63E+15	4.67
551010020	68.34	64.80	63.49	3.14	3.23	3.00	5.55	5.24	3.20	0.59	0.66	0.97	1.24	1.14	1.43	3.63	3.07	2.21	0.39	0.43	0.89	1.40E+16	3.11E+15	4.52
551330027	59.42	56.08	52.26	2.59	2.52	2.44	2.26	1.79	1.31	1.31	1.60	2.08	1.52	1.53	1.52	1.49	1.25	0.97	1.34	1.58	2.01	1.25E+16	2.46E+15	5.10
Muskegon County, MI (Western MI)																								
261210039	63.49	59.70	56.07	2.13	2.08	2.06	0.68	0.56	0.45	4.12	4.66	5.68	1.87	1.88	1.88	2.17	1.83	1.43	1.05	1.23	1.55	1.32E+16	2.73E+15	4.83
Sheboygan County, WI (WI Lakeshore)																								
551170006	62.22	58.68	54.96	2.29	2.22	2.16	2.02	1.59	1.09	1.24	1.52	2.13	1.24	1.26	1.29	1.88	1.57	1.23	0.86	1.07	1.47	1.17E+16	2.70E+15	4.33
551170009	61.23	57.53	53.72	2.18	2.12	2.06	1.38	1.07	0.75	1.83	2.25	3.05	1.33	1.36	1.37	1.78	1.48	1.16	1.00	1.23	1.62	1.45E+16	2.59E+15	5.60
St. Louis, MO-IL																								
171190008	65.30	60.44	56.35	3.61	3.69	3.45	2.19	2.00	1.39	1.76	1.93	2.58	1.70	1.69	1.73	1.69	1.37	1.02	1.23	1.44	1.92	1.30E+16	2.87E+15	4.53
171191009	62.04	57.02	52.85	3.32	3.35	3.10	1.82	1.41	0.93	2.02	2.61	3.58	1.70	1.70	1.72	1.42	1.12	0.84	1.36	1.67	2.22	1.41E+16	2.34E+15	6.00
171191010	65.30	60.44	56.35	3.61	3.69	3.45	2.19	2.00	1.39	1.76	1.93	2.58	1.70	1.69	1.73	1.69	1.37	1.02	1.23	1.44	1.92	1.30E+16	2.87E+15	4.53
171193007	65.30	60.44	56.35	3.61	3.69	3.45	2.19	2.00	1.39	1.76	1.93	2.58	1.70	1.69	1.73	1.69	1.37	1.02	1.23	1.44	1.92	1.30E+16	2.87E+15	4.53
171199991	55.88	51.31	47.99	2.66	2.70	2.56	0.67	0.57	0.47	4.29	5.00	5.70	1.94	1.91	1.90	1.36	1.09	0.85	1.66	1.99	2.49	1.34E+16	2.35E+15	5.70
171630010	65.65	61.02	56.11	3.66	3.73	3.45	2.82	2.20	1.57	1.43	1.84	2.34	1.71	1.72	1.76	1.68	1.34	0.98	1.15	1.41	1.96	1.54E+16	3.03E+15	5.07
290990019	66.87	62.79	55.83	5.13	5.10	4.39	2.23	1.87	1.11	2.38	2.82	4.04	2.06	2.04	2.03	1.40	1.19	0.84	1.75	1.98	2.69	1.67E+16	2.90E+15	5.76
291831002	69.70	65.25	61.13	4.11	4.29	3.98	2.56	3.05	1.88	1.72	1.49	2.22	1.75	1.72	1.77	2.12	1.83	1.39	1.07	1.15	1.55	1.40E+16	3.20E+15	4.35
291831004	66.10	61.74	56.73	3.80	3.84	3.56	1.23	1.07	0.81	3.65	4.16	5.10	2.17	2.18	2.15	1.70	1.38	1.08	1.68	1.97	2.41	1.48E+16	2.59E+15	5.70
291890005	62.79	58.45	53.29	4.83	4.76	4.24	1.04	0.87	0.59	4.90	5.79	7.50	2.22	2.21	2.12	1.23	1.03	0.82	2.15	2.49	2.88	1.68E+16	2.37E+15	7.11
291890014	69.46	64.72	58.22	4.73	4.67	4.18	2.56	2.03	1.30	1.99	2.46	3.40	2.03	2.06	2.05	1.60	1.29	0.95	1.53	1.85	2.44	1.64E+16	2.61E+15	6.30
295100085	67.72	64.24	58.78	4.19	4.27	3.90	6.44	5.05	3.13	0.77	1.01	1.45	1.55	1.57	1.65	2.01	1.63	1.09	0.91	1.10	1.69	1.68E+16	3.51E+15	4.78

APPENDIX 3

Supplemental Figures: Model-Based Indicator Ratios

This appendix contains supplemental figures and tables for the CAMx model-based indicator ratio analysis of ozone formation in the LADCO region. These figures and tables include:

- A table of ozone exceedance days for each nonattainment area
- Figures showing the seasonal trends in ozone-related parameters
- A figure showing the relationships between sensitivity ratios and ozone concentrations
- Figures and maps showing the concentrations of ozone sensitivity indicator compounds
- Maps of ozone sensitivity indicator ratios and ozone formation sensitivity classifications

For a table showing the amounts of ozone precursors and indicator ratio values from the CAMx model and TROPOMI satellite analyses see Table A2.2 in the previous appendix.

Ozone exceedance days in each nonattainment area

Table A3.1. Ozone exceedance days in 2016 as determined by the CAMx model. The "model" column indicates whether the day was an exceedance in the aa2a (2020), abc (2028), or both models. LADCO applied a threshold of 65 (rather than 70) ppb to determine exceedances for the Twin Cities area.

Chicago		Cincinnati		Cleveland		Detroit		Louisville	
23 days	model	23 days	model	12 days	model	13-14 days	model	24 days	model
4/18/2016	both	4/18/2016	both	4/17/2016	both	5/27/2016	both	4/18/2016	both
6/10/2016	both	6/11/2016	both	6/19/2016	both	6/19/2016	both	6/9/2016	both
6/11/2016	both	6/13/2016	both	6/25/2016	both	6/25/2016	both	6/10/2016	both
6/15/2016	both	6/24/2016	both	6/26/2016	both	7/8/2016	both	6/11/2016	both
6/18/2016	both	6/25/2016	both	7/7/2016	both	7/12/2016	both	6/13/2016	both
6/19/2016	both	6/26/2016	both	7/8/2016	both	7/23/2016	both	6/16/2016	both
6/24/2016	both	7/19/2016	both	7/12/2016	both	7/27/2016	both	6/24/2016	both
6/25/2016	both	7/20/2016	both	7/21/2016	both	7/28/2016	both	6/25/2016	both
7/6/2016	both	7/21/2016	both	7/23/2016	both	8/2/2016	both	6/30/2016	both
7/7/2016	both	7/23/2016	both	8/27/2016	both	8/3/2016	both	7/11/2016	both
7/18/2016	both	7/24/2016	both	8/30/2016	both	8/4/2016	both	7/19/2016	both
7/19/2016	both	7/29/2016	both	9/22/2016	both	8/10/2016	both	7/21/2016	both
7/20/2016	both	8/2/2016	both			8/26/2016	both	7/23/2016	both
7/22/2016	both	8/3/2016	both			8/29/2016	2028	7/27/2016	both
7/23/2016	both	8/4/2016	both					8/2/2016	both
7/25/2016	both	8/5/2016	both					8/3/2016	both
7/26/2016	both	8/26/2016	both					8/5/2016	both
7/27/2016	both	8/28/2016	both					8/26/2016	both
7/31/2016	both	8/30/2016	both					8/30/2016	both
8/2/2016	both	9/13/2016	both					9/14/2016	both
8/3/2016	both	9/14/2016	both					9/22/2016	both
8/4/2016	both	9/22/2016	both					9/23/2016	both
8/10/2016	both	9/23/2016	both					9/24/2016	both
								9/25/2016	2028

St. Louis		Western MI		WI lakeshore		Toledo		Twin Cities (65 ppb)	
23 days	model	17 days	model	13 days	model	2 days	model	3 days	model
6/9/2016	both	4/18/2016	both	5/25/2016	both	7/23/2016	both	6/11/2016	both
6/10/2016	both	5/24/2016	both	6/15/2016	both	8/4/2016	both	7/21/2016	both
6/16/2016	both	6/10/2016	both	6/19/2016	both			7/22/2016	both
6/18/2016	both	6/11/2016	both	6/25/2016	both				
6/24/2016	both	6/15/2016	both	7/7/2016	both				
6/27/2016	both	7/5/2016	both	7/20/2016	both				
6/29/2016	both	7/6/2016	both	7/22/2016	both				
7/5/2016	both	7/7/2016	both	7/23/2016	both				
7/9/2016	both	7/20/2016	both	7/27/2016	both				
7/19/2016	both	7/22/2016	both	8/4/2016	both				
7/22/2016	both	7/23/2016	both	8/10/2016	both				
7/23/2016	both	7/27/2016	both	8/11/2016	both				
7/26/2016	both	8/4/2016	both	9/5/2016	both				
7/31/2016	both	8/10/2016	both						
8/2/2016	2020	8/11/2016	both						
8/4/2016	both	8/19/2016	both						
8/10/2016	both	9/22/2016	both						
8/17/2016	both								
8/29/2016	both								
9/20/2016	both								
9/21/2016	both								
9/22/2016	both								
9/23/2016	both								

Seasonal trends in ozone-related parameters

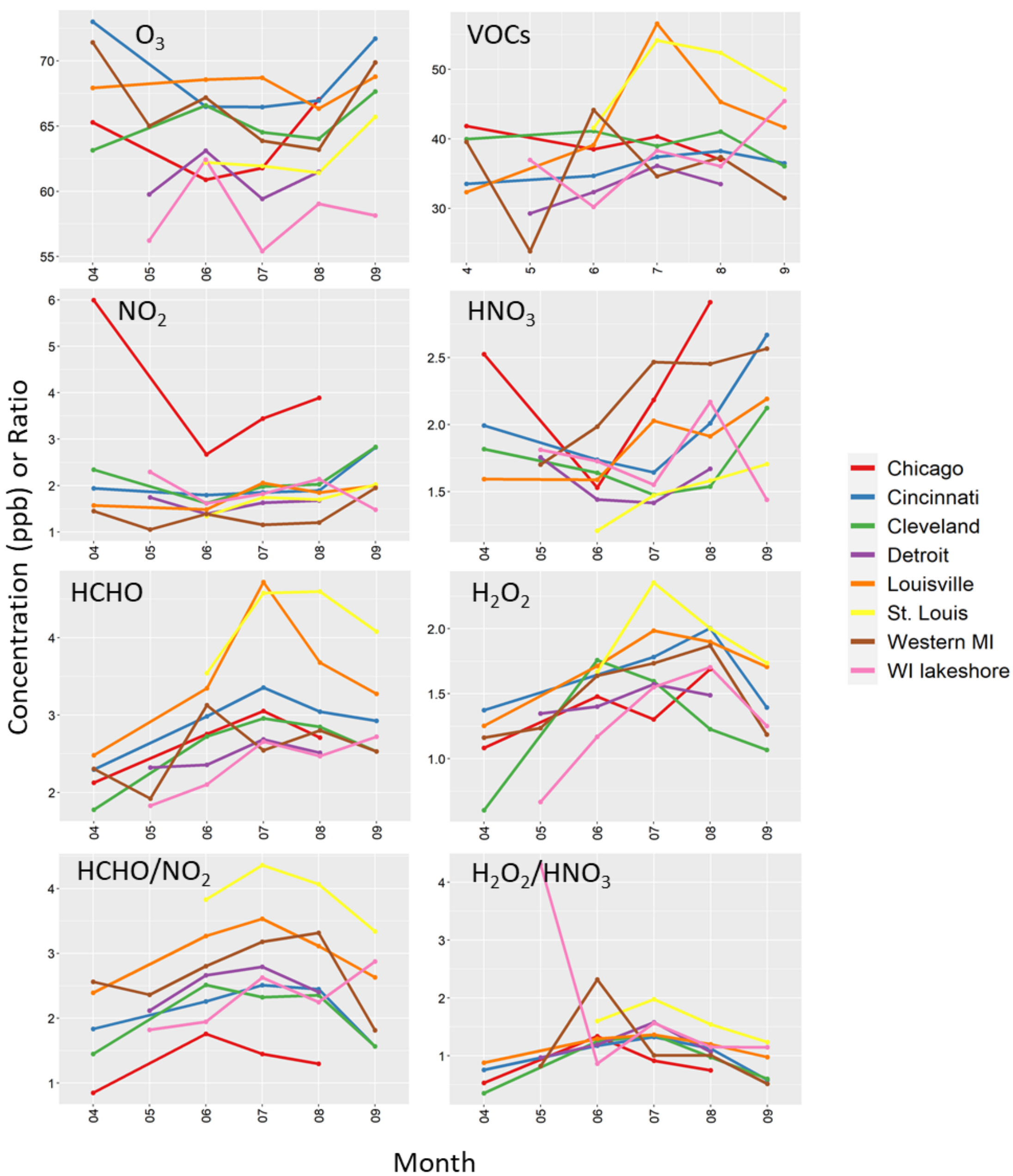

Figure A3.1. Monthly patterns in mean pollutant concentrations and ratios on exceedance days in the nonattainment areas for the 2016 base year using the LADCO_2016aa2a modeling run. Values are shown for the early afternoon (13-16:59 LDT).

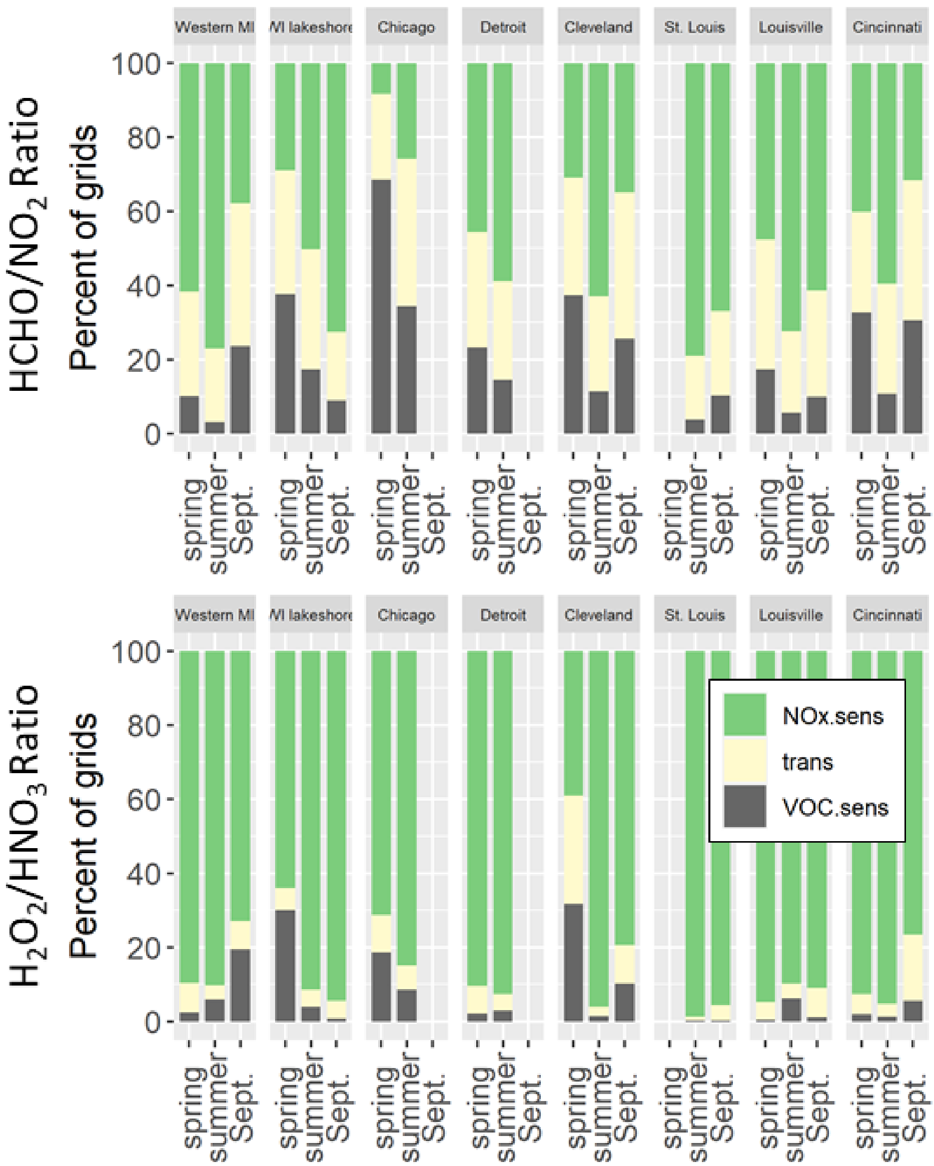

Figure A3.2. Seasonal trends in ozone sensitivity classification based on (top) $HCHO/NO_2$ ratios and (bottom) H_2O_2/HNO_3 ratios in the spring (April-May), summer (June-August), and September.

Relationships between sensitivity ratios and ozone concentrations

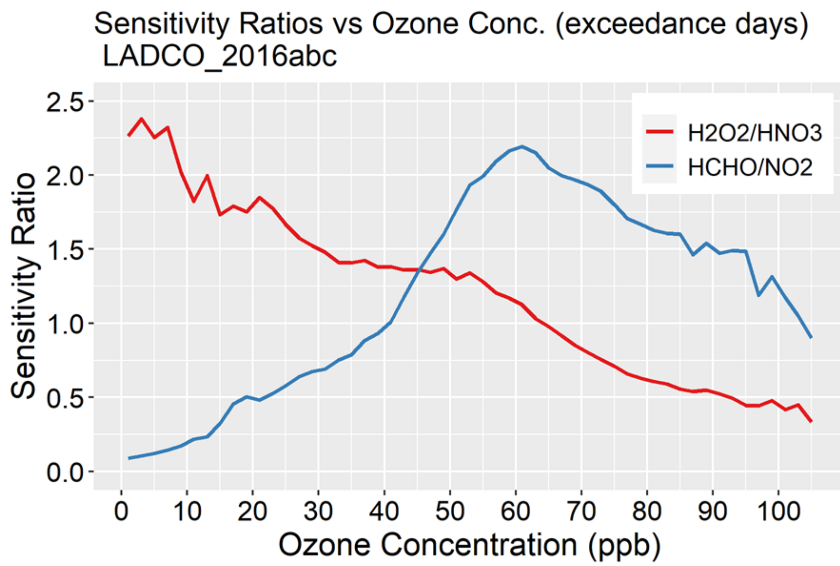

Figure A3.3. Plots of mean early afternoon $HCHO/NO_2$ and H_2O_2/HNO_3 ratios on ozone exceedance days in the LADCO region versus ozone concentration.

Ozone sensitivity indicator compounds

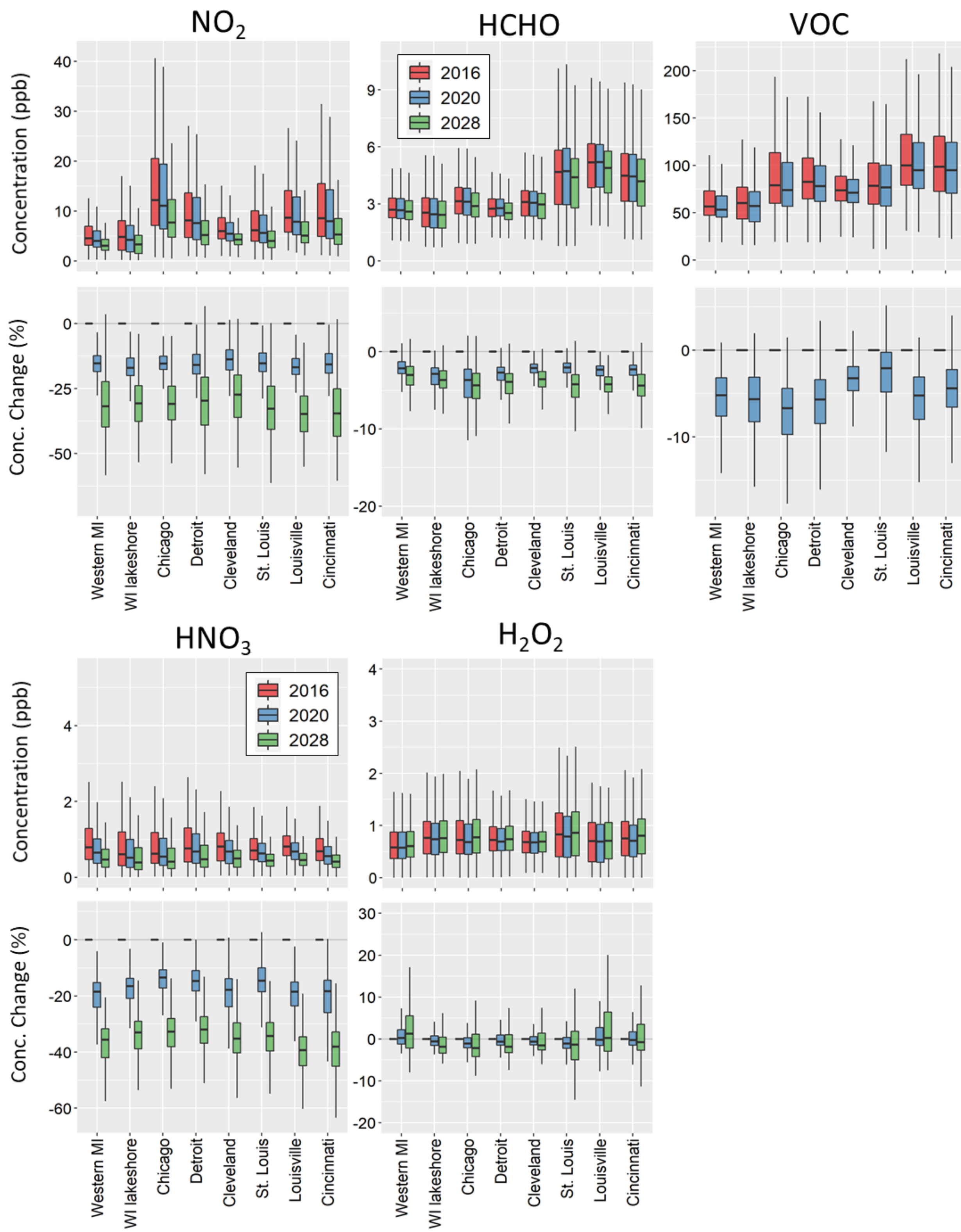

Figure 3.4. Modeled concentrations of pollutants and concentration changes as percentage of 2016 values in the early afternoon (13:00-16:59 LDT) on exceedance days in the nonattainment areas. The 2016 values are from the LADCO_2016abc model run. Boxplots for Western Michigan and the Wisconsin lakeshore combine values for multiple nonattainment areas in these regions. Appendix 6 shows the results for each individual nonattainment area.

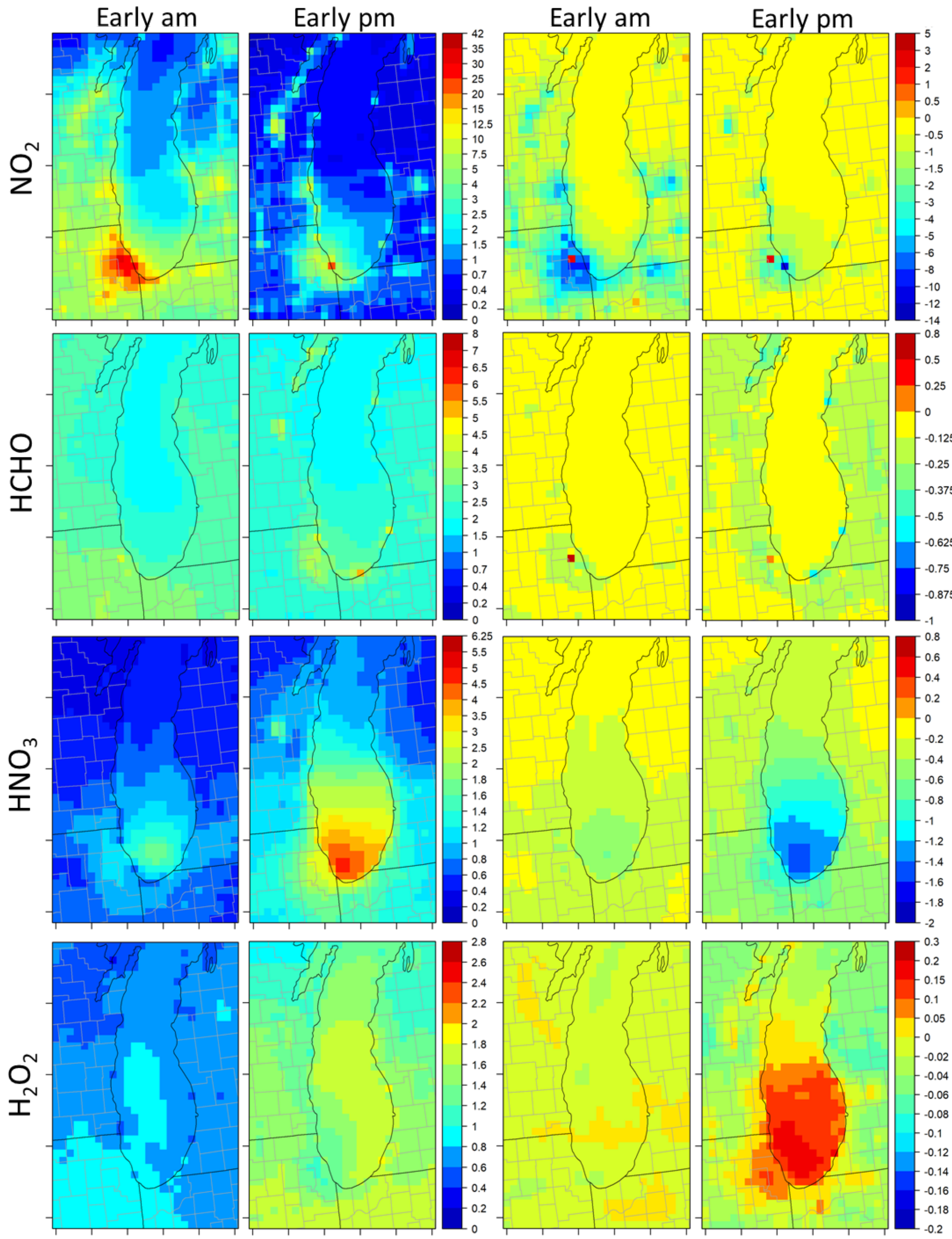

Figure A3.5. Mean concentrations of ozone sensitivity indicator compounds on ozone exceedance days in Chicago in 2016 (left) and the change in compound concentrations between 2016 and 2028 (right). Concentrations are shown for the early morning (5-8:59 LDT) and early afternoon (13:00-16:59 LDT) from the abc model.

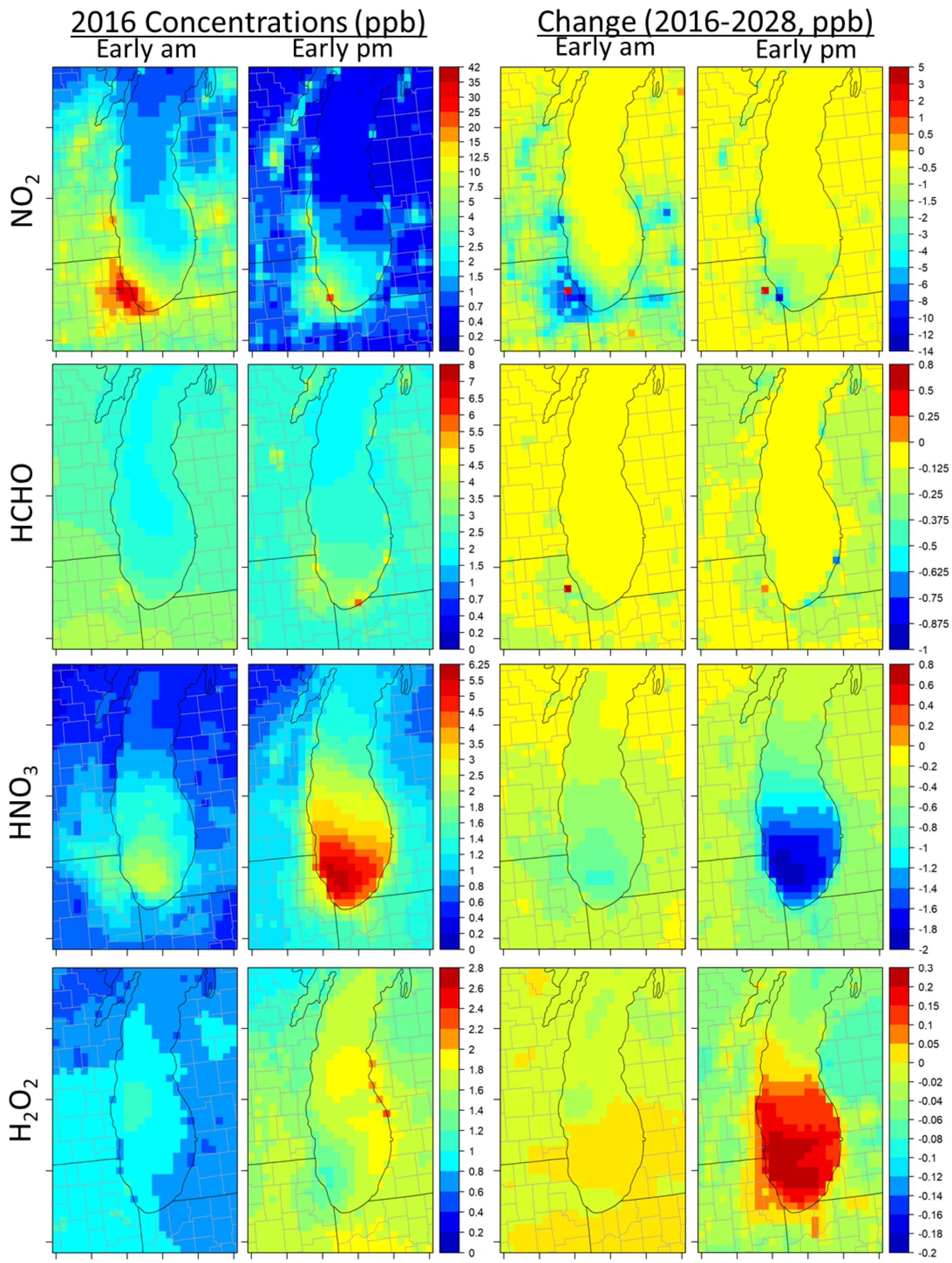

Figure A3.6. Mean concentrations of ozone sensitivity indicator compounds on ozone exceedance days on the Wisconsin lakeshore in 2016 (left) and the change in compound concentrations between 2016 and 2028 (right). Concentrations are shown for the early morning (5-8:59 LDT) and early afternoon (13:00-16:59 LDT) from the abc model.

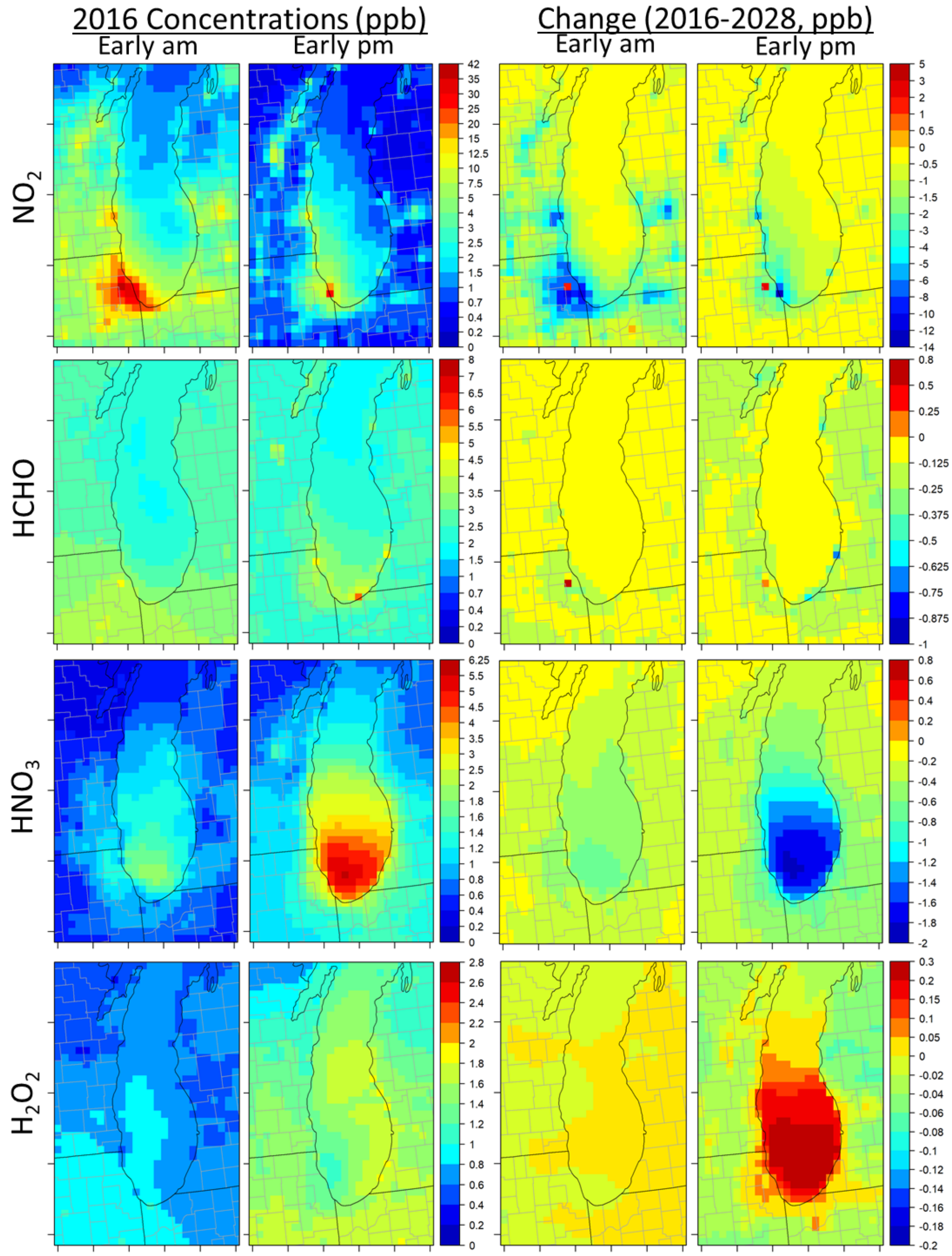

Figure A3.7. Mean concentrations of ozone sensitivity indicator compounds on ozone exceedance days in Western Michigan in 2016 (left) and the change in compound concentrations between 2016 and 2028 (right). Concentrations are shown for the early morning (5-8:59 LDT) and early afternoon (13:00-16:59 LDT) from the abc model.

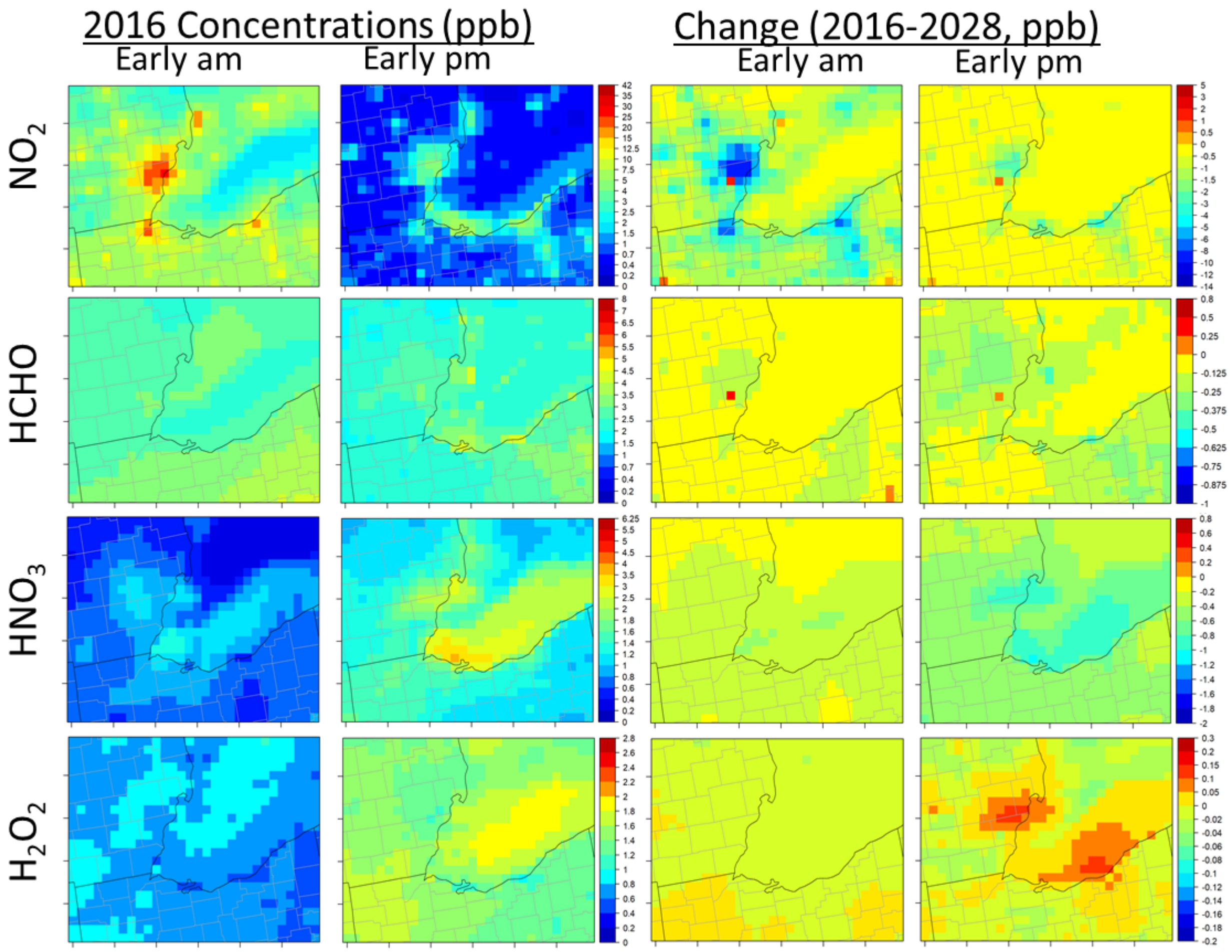

Figure A3.8. Mean concentrations of ozone sensitivity indicator compounds on ozone exceedance days in Detroit in 2016 (left) and the change in compound concentrations between 2016 and 2028 (right). Concentrations are shown for the early morning (5-8:59 LDT) and early afternoon (13:00-16:59 LDT) from the abc model.

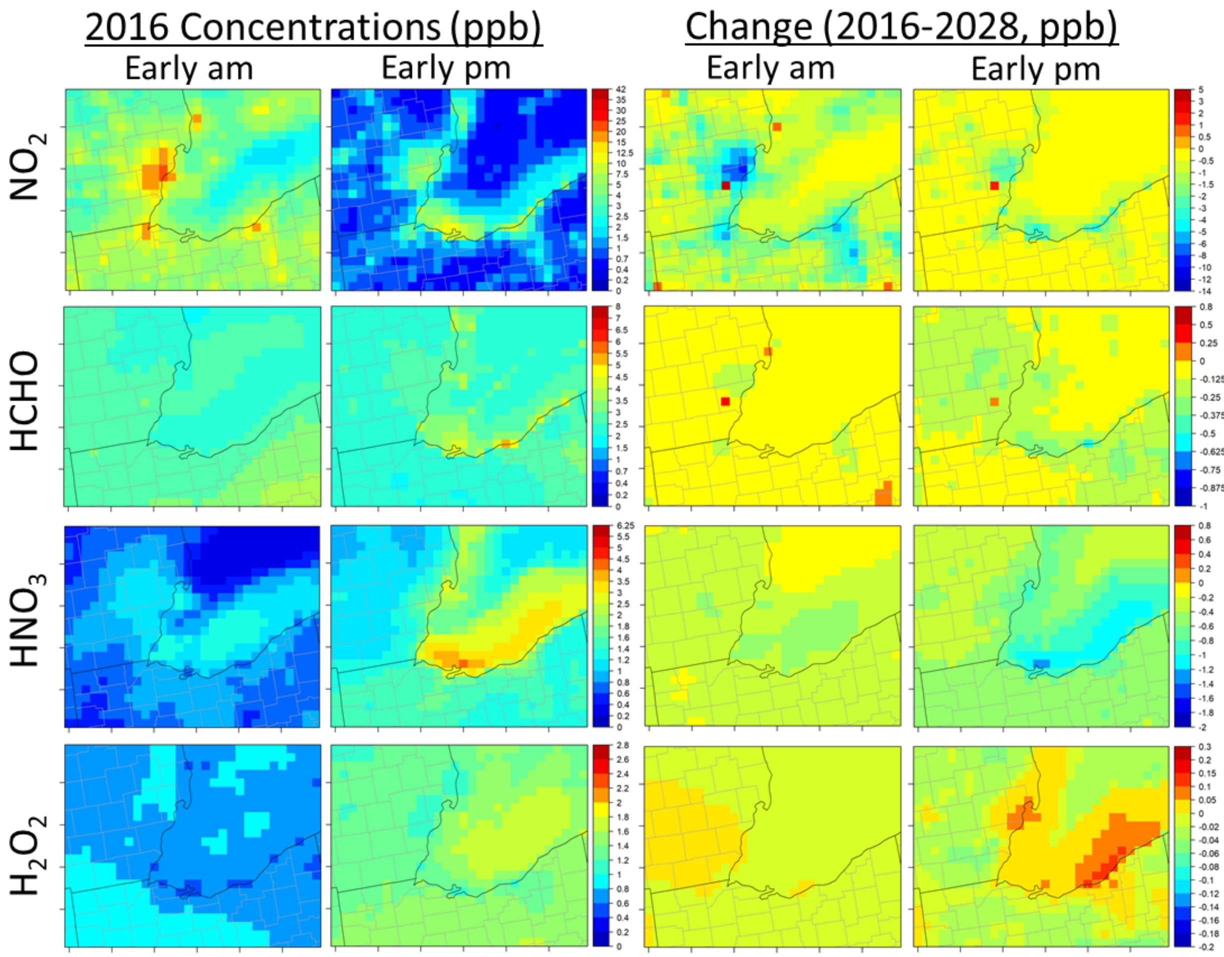

Figure A3.9. Mean concentrations of ozone sensitivity indicator compounds on ozone exceedance days in Cleveland in 2016 (left) and the change in compound concentrations between 2016 and 2028 (right). Concentrations are shown for the early morning (5-8:59 LDT) and early afternoon (13:00-16:59 LDT) from the abc model.

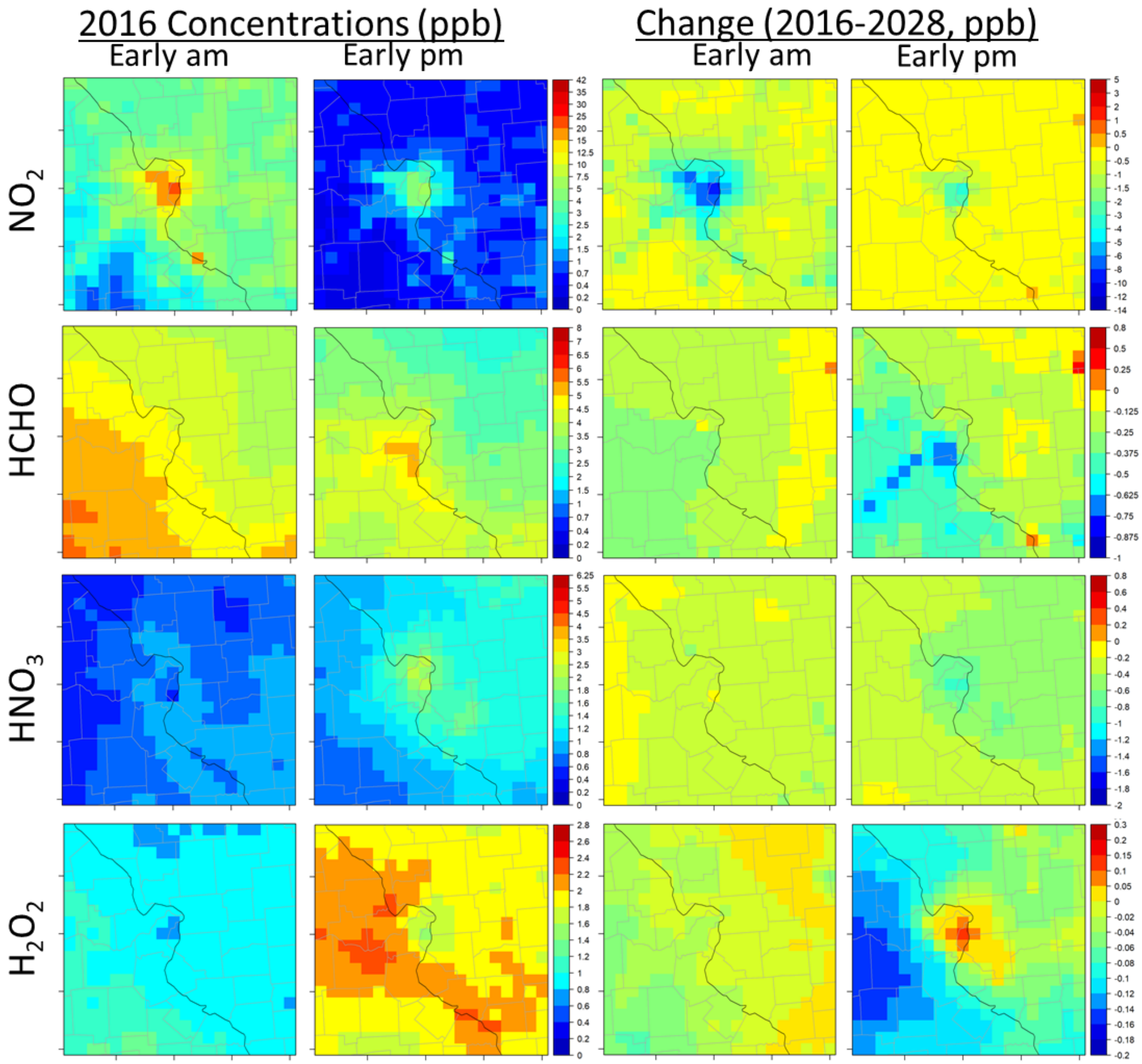

Figure A3.10. Mean concentrations of ozone sensitivity indicator compounds on ozone exceedance days in St. Louis in 2016 (left) and the change in compound concentrations between 2016 and 2028 (right). Concentrations are shown for the early morning (5-8:59 LDT) and early afternoon (13:00-16:59 LDT) from the abc model.

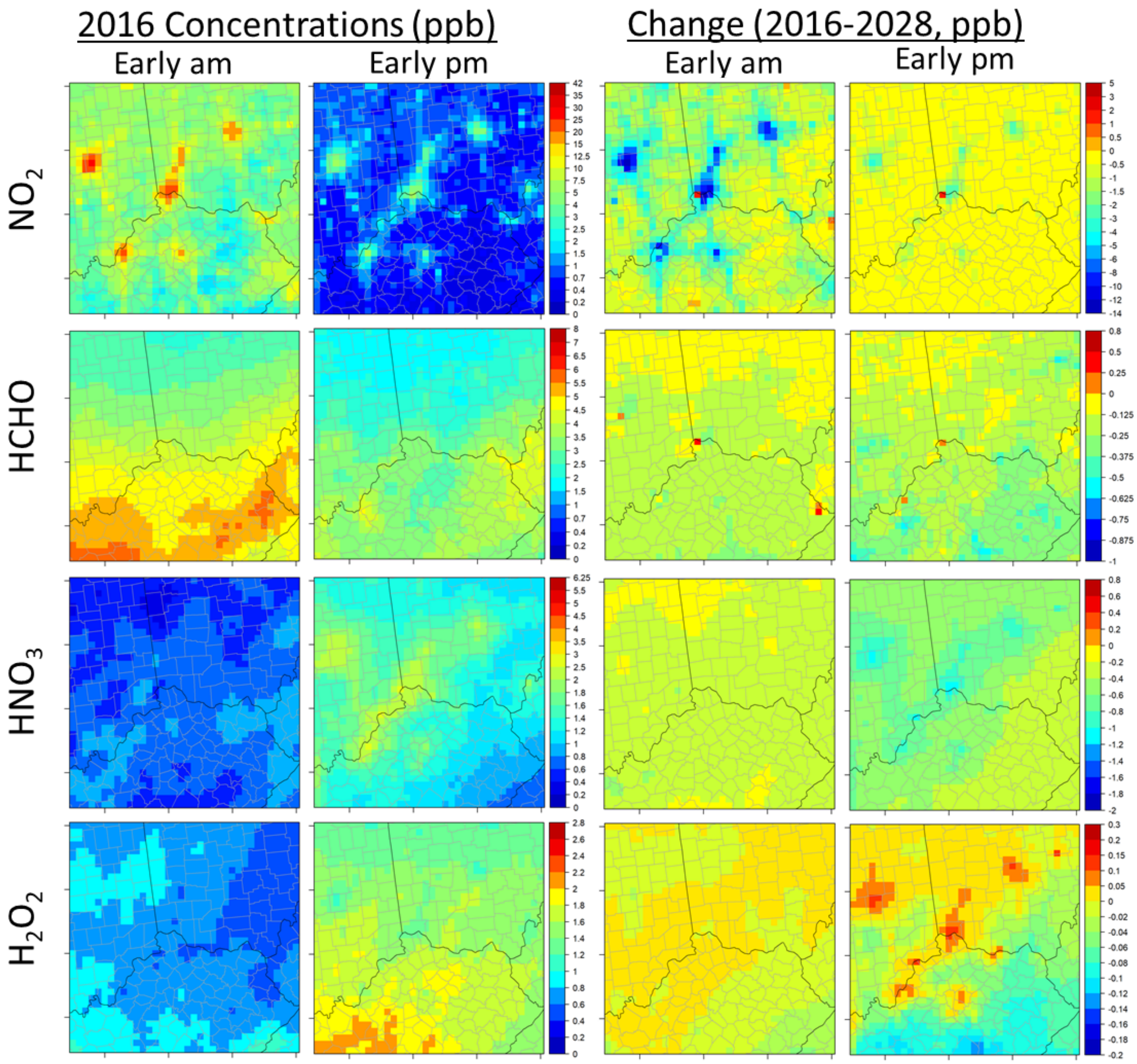

Figure A3.11. Mean concentrations of ozone sensitivity indicator compounds on ozone exceedance days in Louisville in 2016 (left) and the change in compound concentrations between 2016 and 2028 (right). Concentrations are shown for the early morning (5-8:59 LDT) and early afternoon (13:00-16:59 LDT) from the abc model.

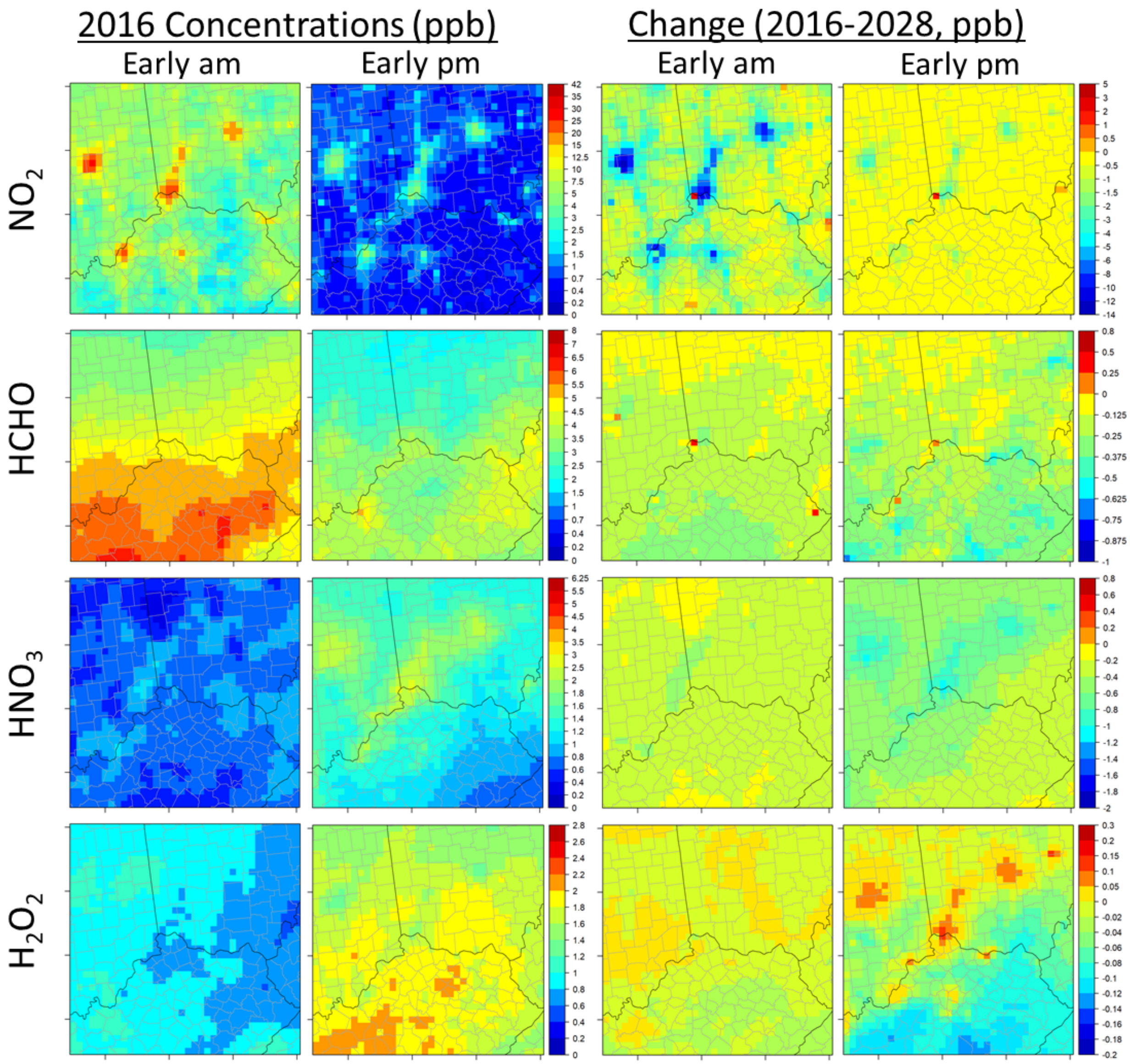

Figure A3.12. Mean concentrations of ozone sensitivity indicator compounds on ozone exceedance days in Cincinnati in 2016 (left) and the change in compound concentrations between 2016 and 2028 (right). Concentrations are shown for the early morning (5-8:59 LDT) and early afternoon (13:00-16:59 LDT) from the abc model.

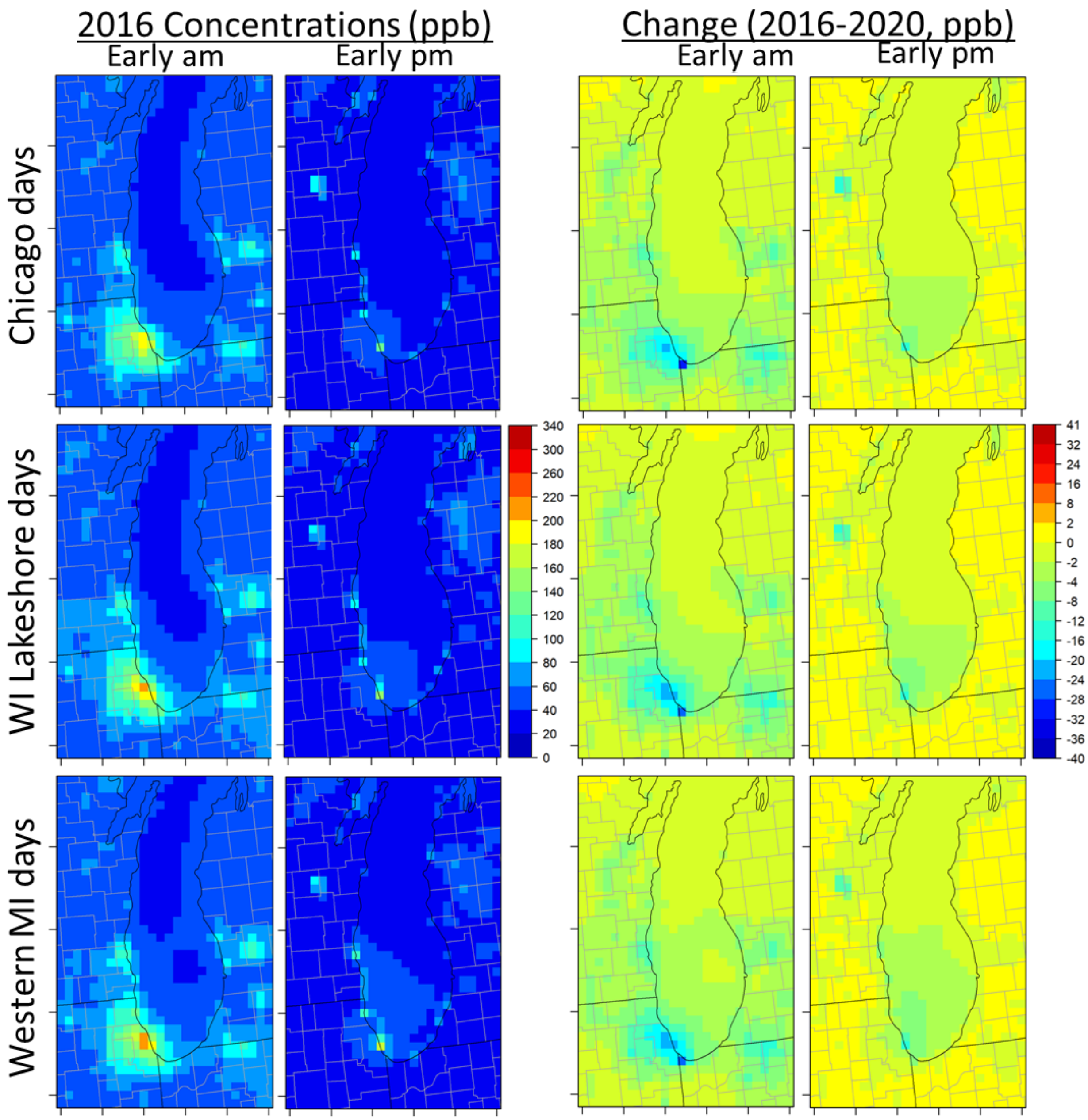

Figure A3.13. Mean concentrations of VOCs on ozone exceedance days in (top) Chicago, (middle) Wisconsin lakeshore, and (bottom) Western Michigan in 2016 (left) and the change in compound concentrations between 2016 and 2020 (right). Concentrations are shown for the early morning (5-8:59 LDT) and early afternoon (13:00-16:59 LDT) from the aa2a model.

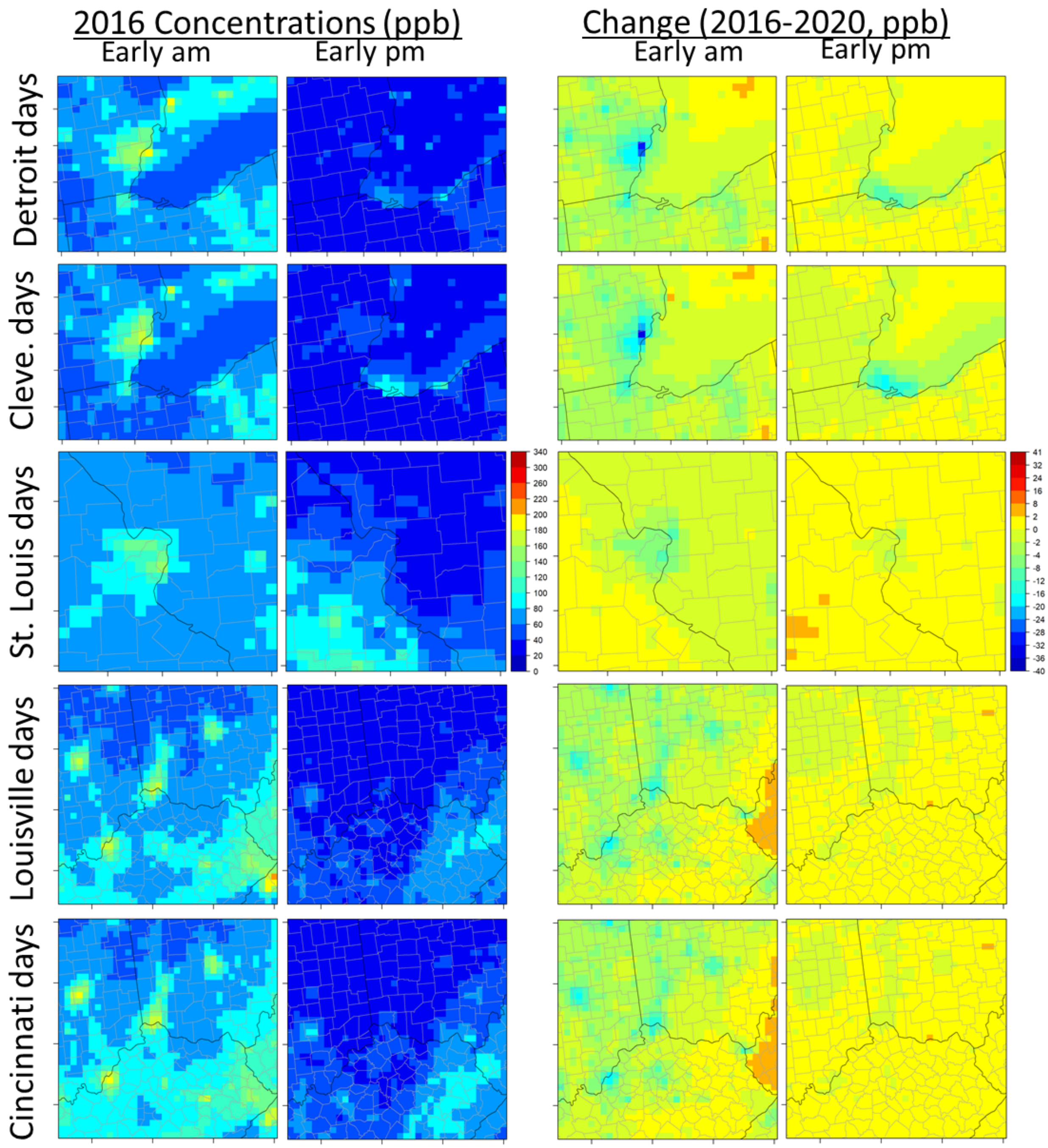

Figure A3.14. Mean concentrations of VOCs on ozone exceedance days in Detroit, Cleveland, St. Louis, Louisville, and Cincinnati in 2016 (left) and the change in compound concentrations between 2016 and 2020 (right). Concentrations are shown for the early morning (5-8:59 LDT) and early afternoon (13:00-16:59 LDT) from the aa2a model.

Ozone sensitivity indicator ratios and classifications

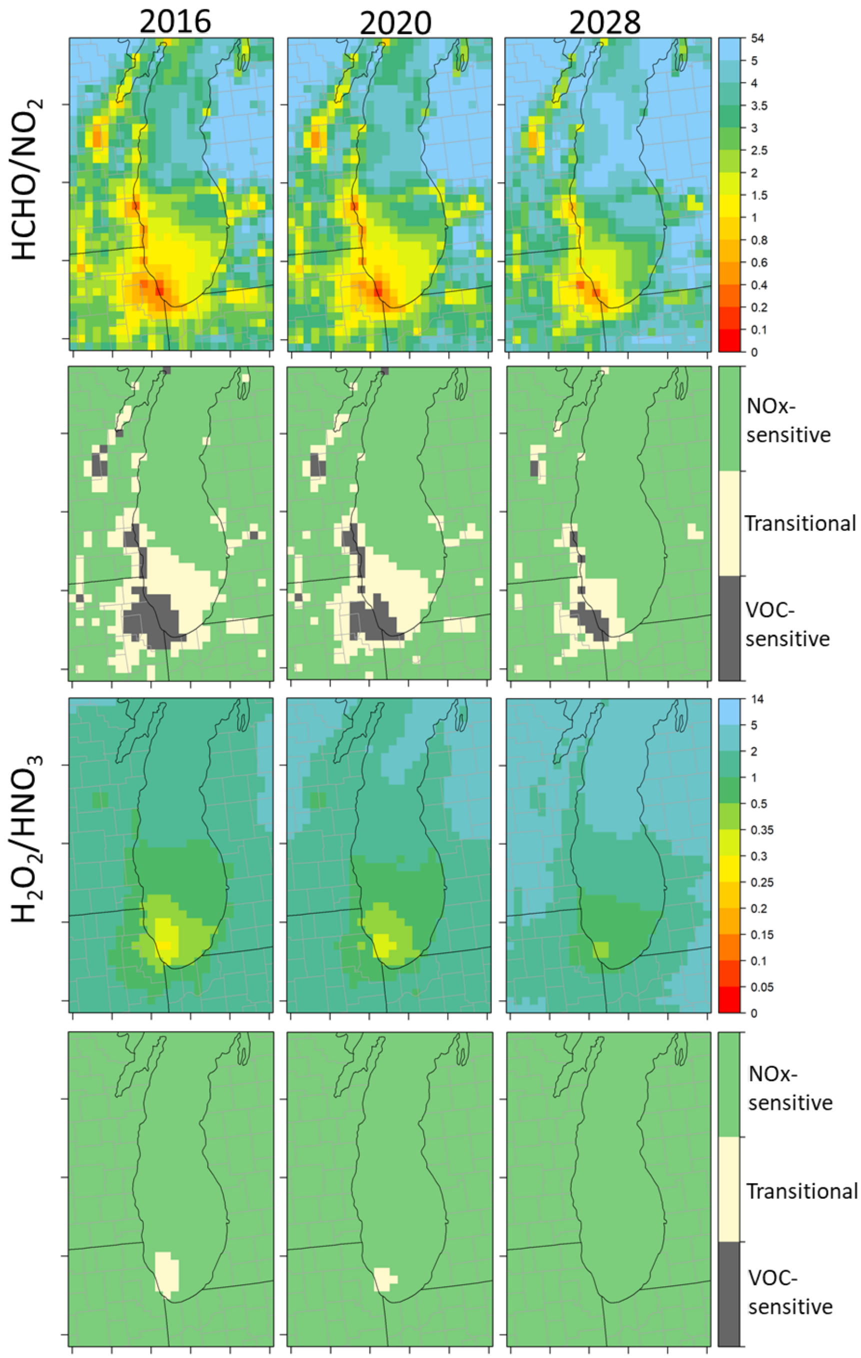

Figure A3.15. Mean ozone sensitivity indicator ratios and the derived ozone formation sensitivity regimes on ozone exceedance days in Chicago in (left) 2016, (middle) 2020, and (right) 2028 in the early afternoon (13:00-16:59 LDT). 2016 and 2028 values are from the abc model, and 2020 values are from the aa2a model.

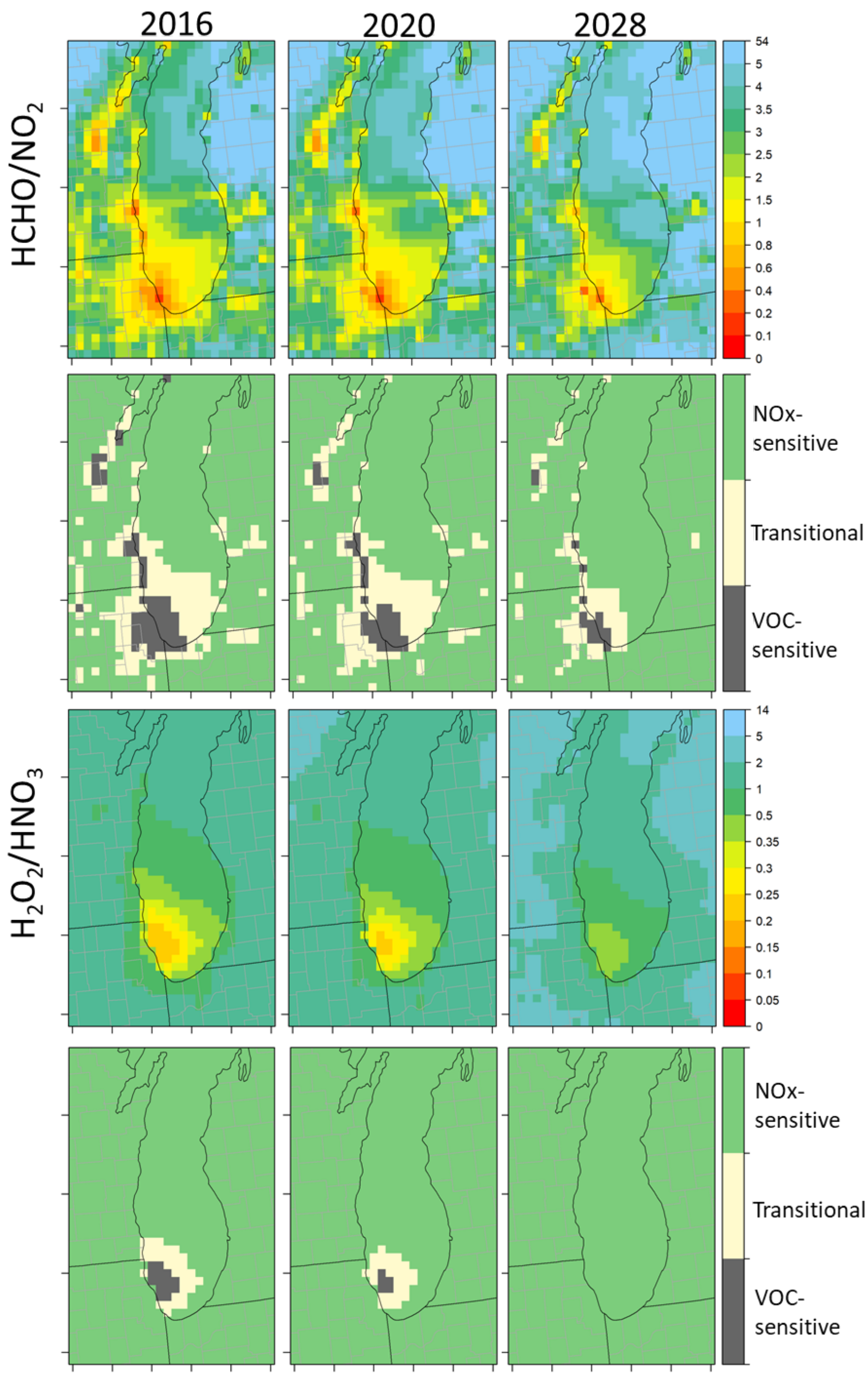

Figure A3.16. Mean ozone sensitivity indicator ratios and the derived ozone formation sensitivity regimes on ozone exceedance days on the Wisconsin lakeshore in (left) 2016, (middle) 2020, and (right) 2028 in the early afternoon (13:00-16:59 LDT). 2016 and 2028 values are from the abc model, and 2020 values are from the aa2a model.

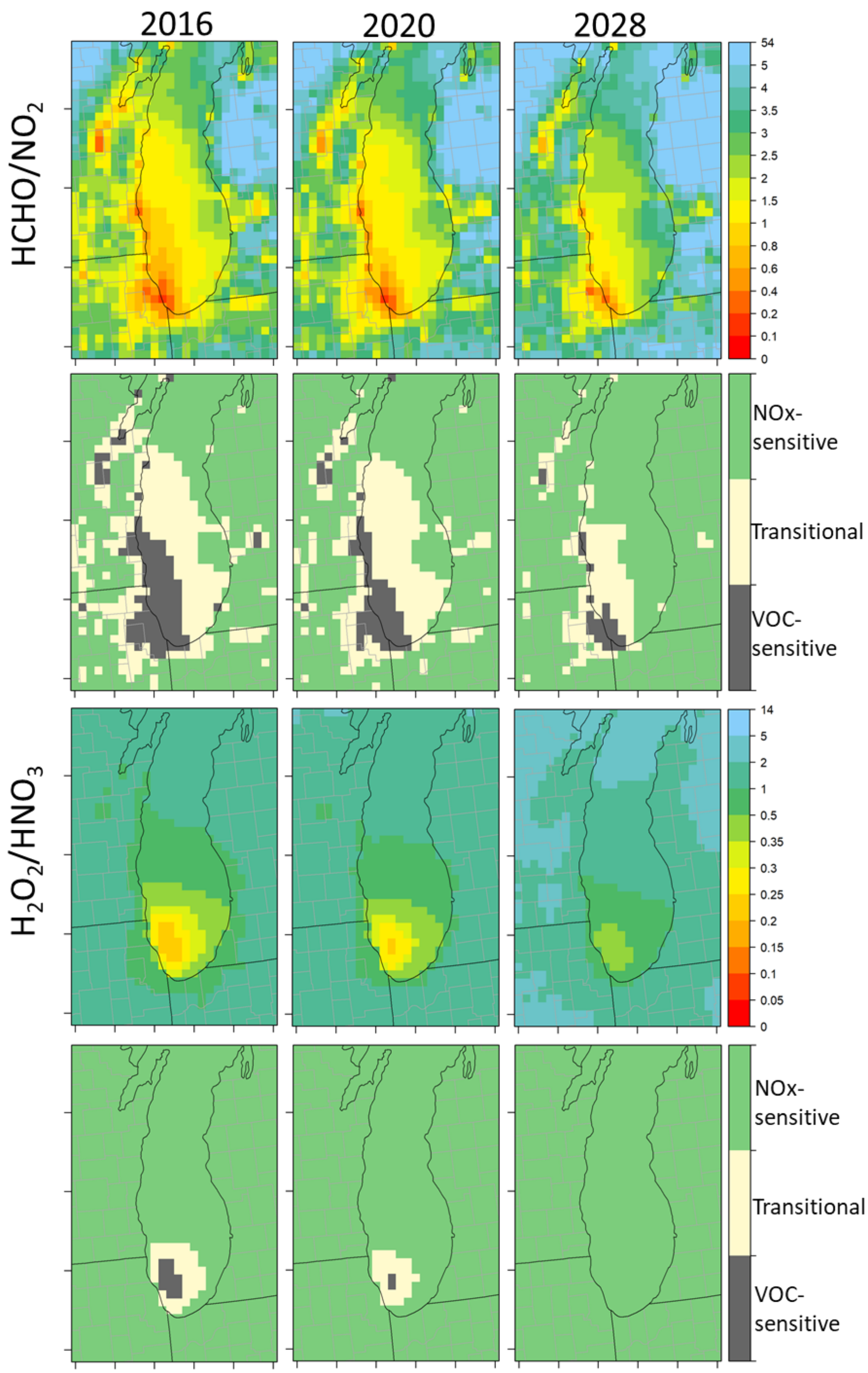

Figure A3.17. Mean ozone sensitivity indicator ratios and the derived ozone formation sensitivity regimes on ozone exceedance days in Western Michigan in (left) 2016, (middle) 2020, and (right) 2028 in the early afternoon (13:00-16:59 LDT). 2016 and 2028 values are from the abc model, and 2020 values are from the aa2a model.

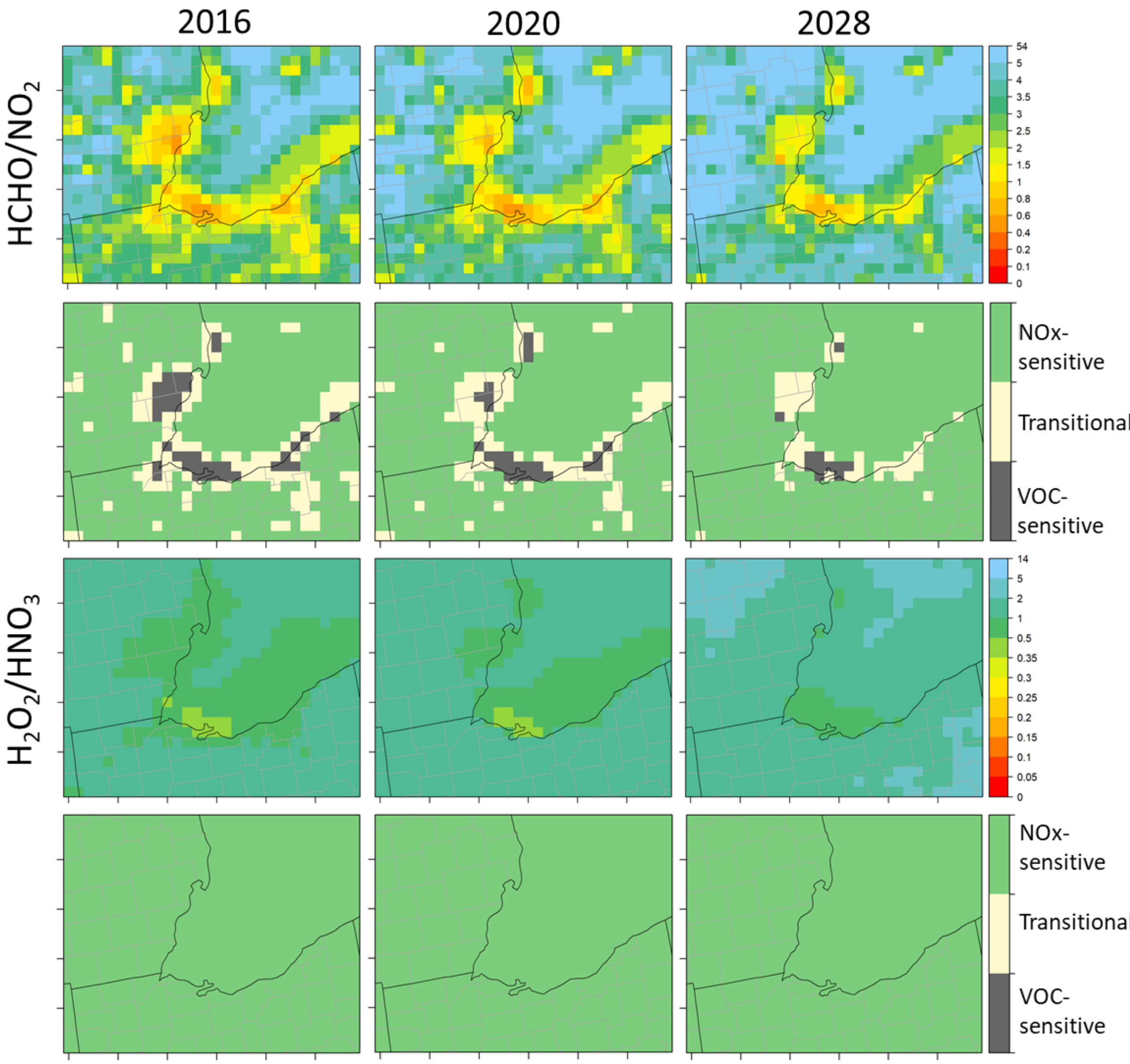

Figure A3.18. Mean ozone sensitivity indicator ratios and the derived ozone formation sensitivity regimes on ozone exceedance days in Detroit in (left) 2016, (middle) 2020, and (right) 2028 in the early afternoon (13:00-16:59 LDT). 2016 and 2028 values are from the abc model, and 2020 values are from the aa2a model.

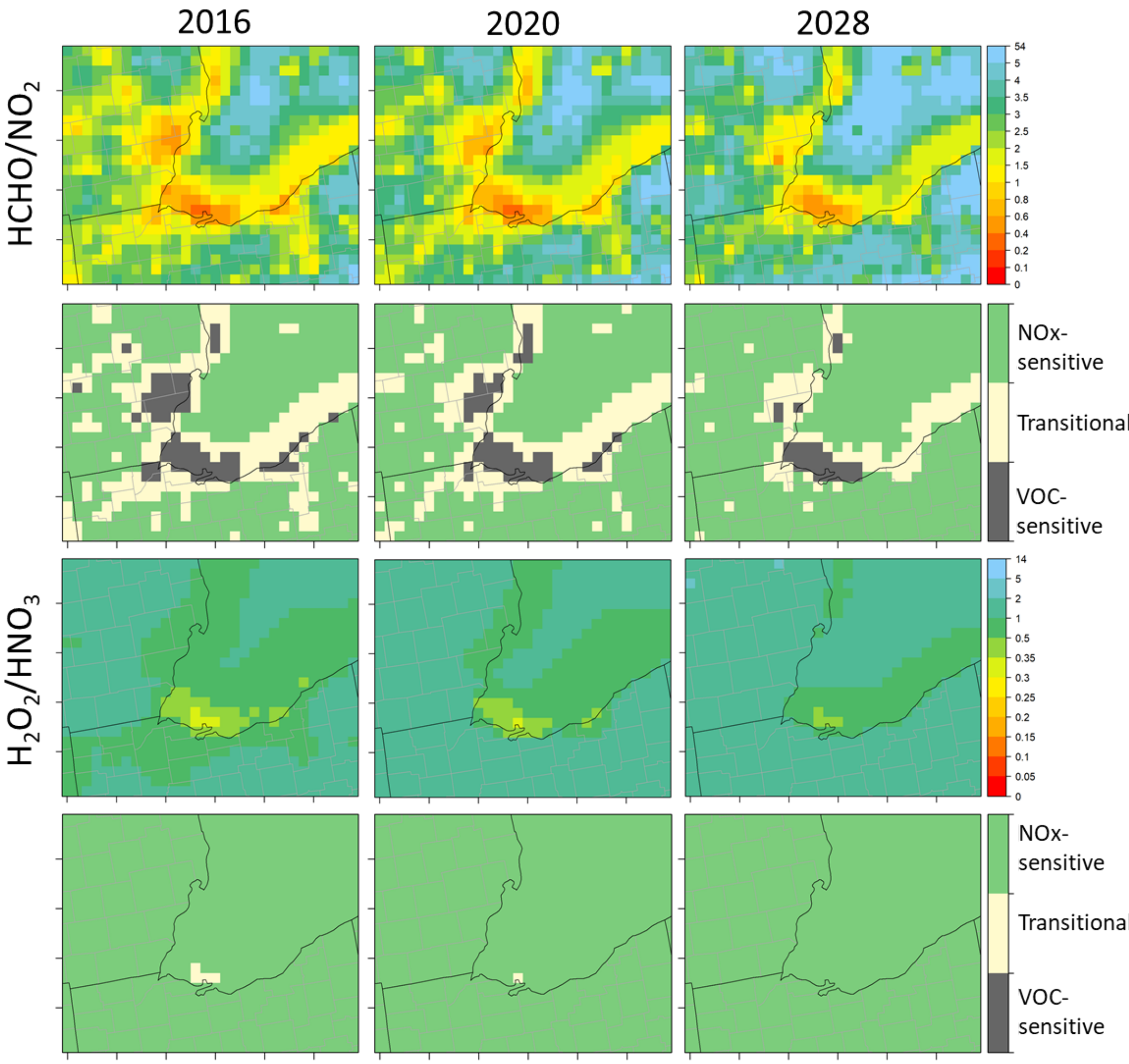

Figure A3.19. Mean ozone sensitivity indicator ratios and the derived ozone formation sensitivity regimes on ozone exceedance days in Cleveland in (left) 2016, (middle) 2020, and (right) 2028 in the early afternoon (13:00-16:59 LDT). 2016 and 2028 values are from the abc model, and 2020 values are from the aa2a model.

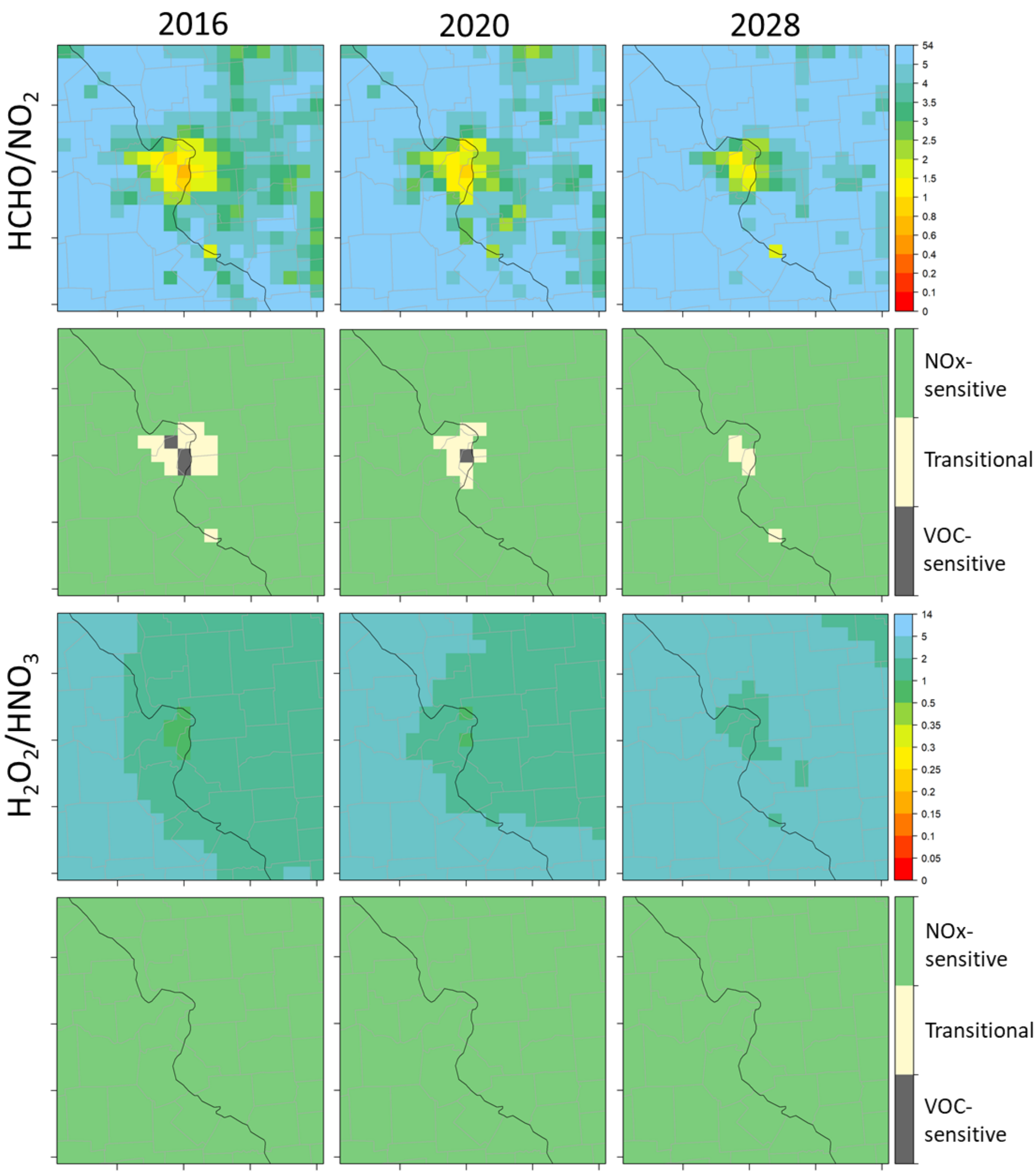

Figure A3.20. Mean ozone sensitivity indicator ratios and the derived ozone formation sensitivity regimes on ozone exceedance days in St. Louis in (left) 2016, (middle) 2020, and (right) 2028 in the early afternoon (13:00-16:59 LDT). 2016 and 2028 values are from the abc model, and 2020 values are from the aa2a model.

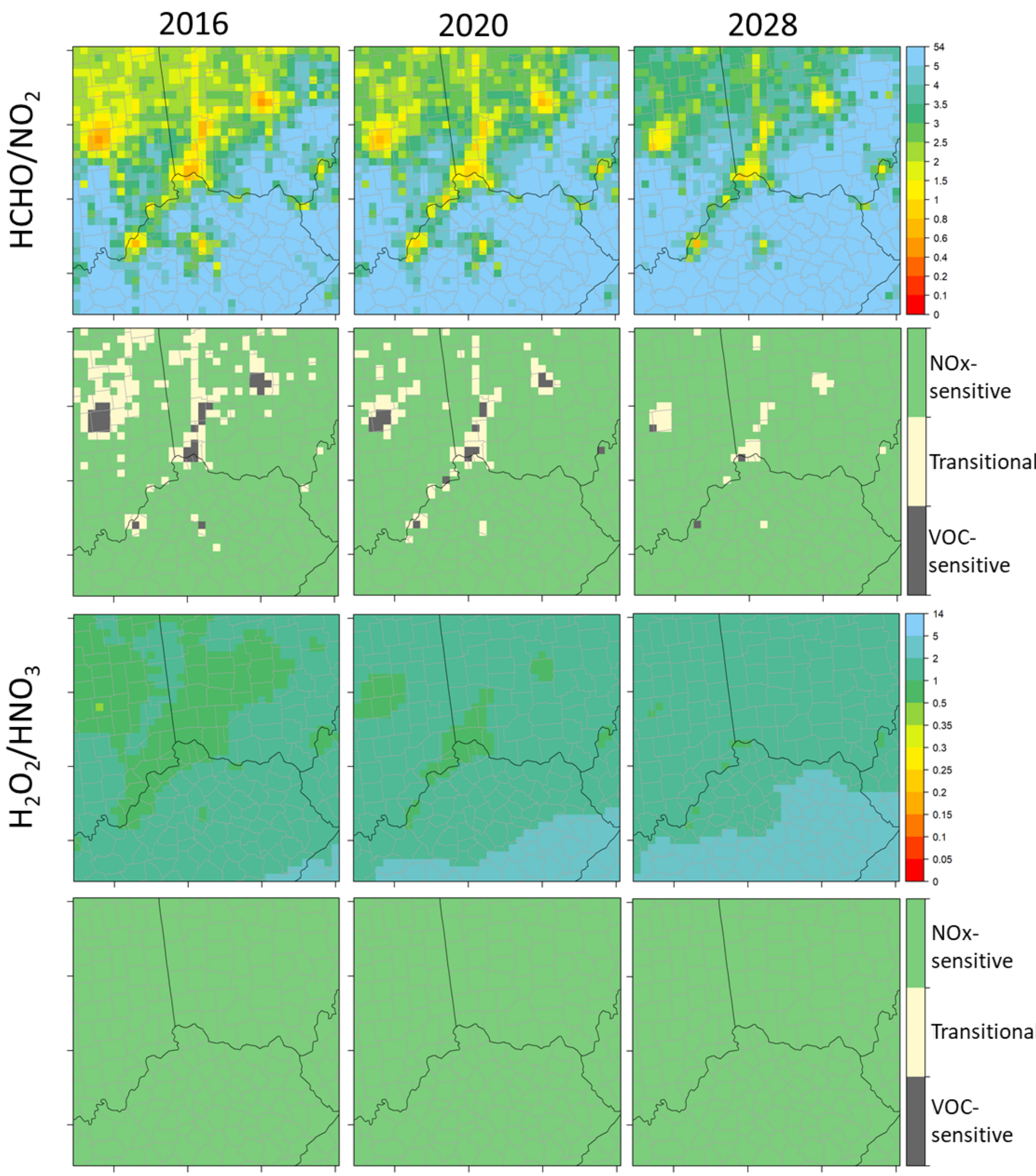

Figure A3.21. Mean ozone sensitivity indicator ratios and the derived ozone formation sensitivity regimes on ozone exceedance days in Louisville in (left) 2016, (middle) 2020, and (right) 2028 in the early afternoon (13:00-16:59 LDT). 2016 and 2028 values are from the abc model, and 2020 values are from the aa2a model.

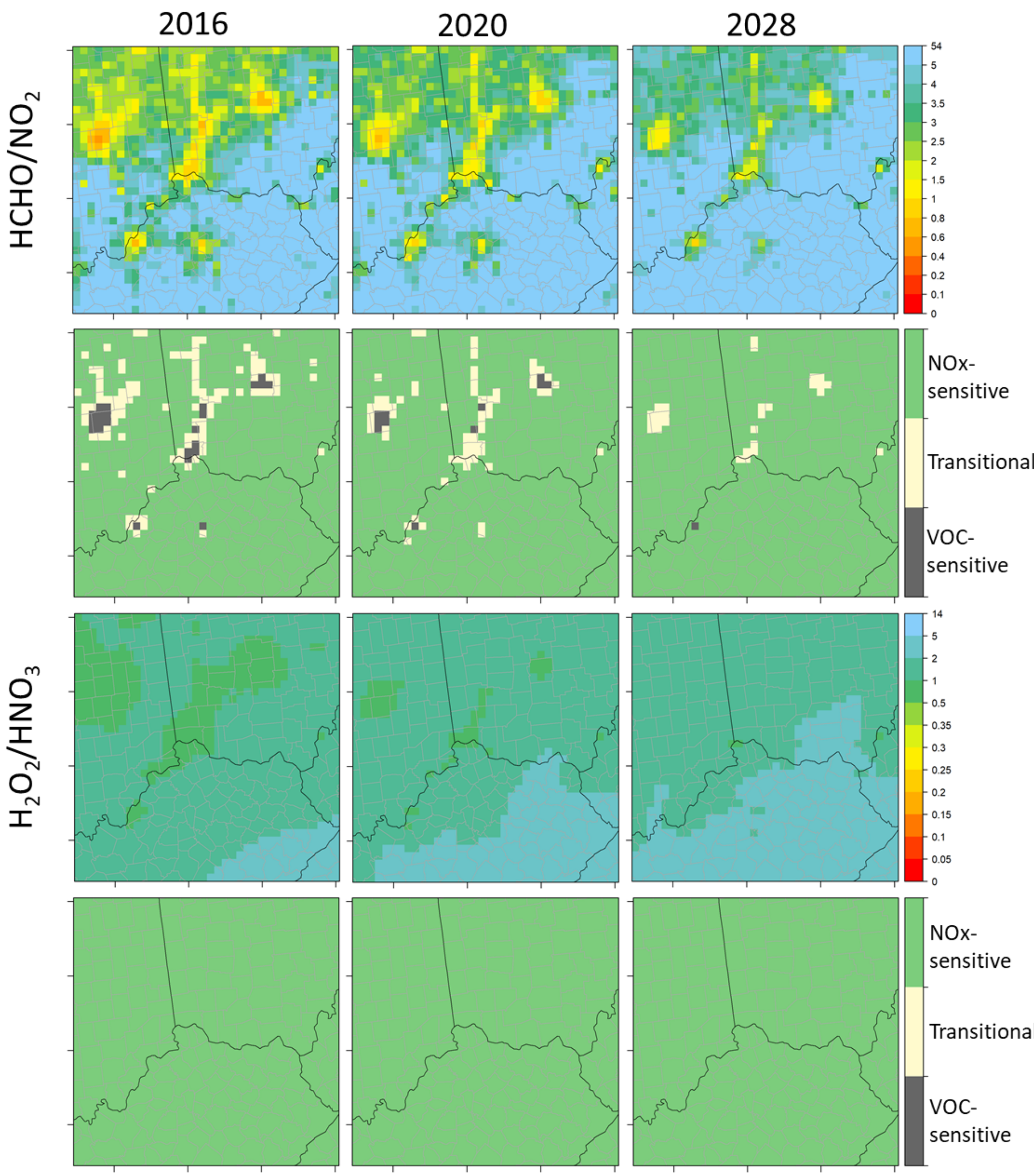

Figure A3.22. Mean ozone sensitivity indicator ratios and the derived ozone formation sensitivity regimes on ozone exceedance days in Cincinnati in (left) 2016, (middle) 2020, and (right) 2028 in the early afternoon (13:00-16:59 LDT). 2016 and 2028 values are from the abc model, and 2020 values are from the aa2a model.

APPENDIX 4

Supplemental Figures: Weekday-Weekend Analysis

This appendix contains supplemental figures and tables for the weekday-weekend analysis of ozone formation chemistry. These figures and tables include:

- Supplemental information about the CART analyses, including:
  - CART inputs and ctree_control settings used for each CART analysis
  - Notes on the Wisconsin North Lake (Sheboygan) CART analysis
  - Meteorological parameters used in the CART analyses
  - Motivation for excluding 2015 meteorology
  - CART trees
- Weekday-weekend differences in maximum daily temperature on all ozone season days
- Weekday-weekend differences in select meteorological parameters on ozone-conducive days
- Relationship of p values to Weekday-Weekend mean MDA8 differences
- Trends in VOCs in the Chicago area
- Weekday-weekend analysis of additional urban core monitors

Supplemental Information about the CART Analyses

CART inputs and ctree_control settings used for each CART analysis

To conduct the CART analyses, we provided an array of daily meteorological parameters as the input variables and ozone MDA8 values as the response variables. Table A1 lists the ozone monitors and airport meteorological stations whose data was used for each CART analysis, and Table A2 lists the meteorological parameters used from each meteorological station.

As discussed in the main document, we adjusted the values of three different parameters under *ctree_control* in the partykit package in *R*: *maxdepth, minsplit* and *minbucket*. We set *maxsurrogate* to 3 for all of the CART runs. *Maxdepth* limits the maximum depth of the tree, *minsplit* sets the minimum number of days in a node to allow it to be further split, and *minbucket* sets the minimum number of days allowed in a terminal node. We set *maxdepth* to either 4 or 5 and *minsplit* to twice *minbucket*. Table A1 lists the values of these parameters for each CART analysis. Values were adjusted in part based on the number of monitors used in the analysis: analyses with more monitors generally had higher values of *minsplit* and *minbucket*.

Table A4.1. Ozone monitors and meteorological stations used in the CART analysis and values of *ctree_control* parameters used in each CART analysis.

CART analysis	Ozone monitors	Airport met station	*maxdepth*	*minsplit*	*minbucket*	Terminal nodes
Lake MI: WI North Lake (Sheboygan)	Sheboygan Kohler Andrae	Manitowoc (MTW)	5	200	100	11
Lake MI: Milwaukee North	Bayside, Grafton, Harrington Beach	Milwaukee (MKE)	4	400	200	13
Lake MI: Western MI	Holland, Coloma, Muskegon	Muskegon (MKG)	4	400	200	14

Chicago: Far North	Chiwaukee, Zion	Chicago O'Hare (ORD)	4	200	100	16
Chicago: Central	Alsip, Chicago SWFP, Chicago Taft HS, Lemont, Cicero, Northbrook, Evanston, Des Plaines	Chicago O'Hare (ORD)	5	1000	500	17
Chicago: Indiana Lake	Gary-IITRI, Hammond, Ogden Dunes, Valparaiso	Chicago O'Hare (ORD)	4	400	200	15
Detroit	New Haven, Warren, Port Huron, Allen Park, Detroit-E 7 Mile, Oak Park	Detroit (DTW)	4	600	300	13
Cleveland	District 6, Berea BOE, Mayfield, Eastlake	Cleveland (CLE)	4	400	200	16
St. Louis	Alton-Clara Barton Sch, Maryville, Wood River, West Alton, Orchard Farm, Alton-HM Sch	St. Louis (STL)	5	800	400	15
Louisville	Bates, Watson Ln, Carrithers MS	Louisville (SDF)	5	400	200	11
Cincinnati	Sycamore, Colerain, Taft	Cincinnati (LUK)	4	400	200	14

Notes on the Wisconsin North Lake (Sheboygan) CART analysis

The CART analysis for the WI North Lake monitor group deliberately only relied upon ozone data from the Sheboygan monitor rather than also including data from the Manitowoc and Newport monitors. Previous CART analyses[2] showed that all three of these WI North Lake monitors had ozone on days with strong southerly transport and/or southerly winds and maximum temperatures above 75 °F. However, the Sheboygan monitor also had high ozone on days with more moderate southerly winds; the Manitowoc and Newport monitors did not have high ozone on these days. We chose to use a CART analysis based on only the Sheboygan monitor to be more inclusive of high-ozone days at the Sheboygan Kohler Andrae monitor. However, this choice will include more lower ozone days for the Manitowoc and Newport monitors.

Meteorological parameters used in the CART analyses

Table A4.2. Daily meteorological parameters used in the CART analyses

Parameter	Description	Units
avg_S_am	Average Morning Wind South (v) Vector	meters/second (m/s)
avg_S_pm	Average Morning Wind South (v) Vector	meters/second (m/s)
avg_S_win	Average Wind South (v) Vector	meters/second (m/s)
avg_W_am	Average Morning Wind West (u) Vector	meters/second (m/s)
avg_W_pm	Average Afternoon Wind West (u) Vector	meters/second (m/s)
avg_W_win	Average Wind West (u) Vector	meters/second (m/s)
dp_{avg}	Average Daily Dew Point Temperature	Degrees Fahrenheit (°F)
dp_{max}	Maximum Daily Dew Point Temperature	Degrees Fahrenheit (°F)
foghrs	Hours of Fog	Hours
hazehrs	Hours of Haze	Hours
lag_S_wn	Previous Day Wind South (V) Vector	meters/second (m/s)

2 https://www.ladco.org/wp-content/uploads/Projects/Ozone/LADCO_O3_CART-Analysis_27Oct2021-FINAL-with-Appendices.pdf

Parameter	Description	Units
lag_W_wn	Previous Day Wind West (U) Vector	meters/second (m/s)
$lagStP_{avg}$	Previous Day Station Pressure	millibars (mb)
$lagT_{max}$	Previous Day Max Temp	Degrees Fahrenheit (°F)
$lagws_{avg}$	Previous Day Avg Wind Speed	meters/second (m/s)
mr_{max}	Maximum Water Vapor Mixing Ratio	grams/kilogram (g/kg)
precip	24 hr Precipitation	inches
presschange	24-hr Pressure Change	millibars (mb)
rainhrs	Hours of Rain	hours
RH_{avg}	Average Daily Relative Humidity	Percent (%)
RH_{avgmid}	Average Midday Relative Humidity	Percent (%)
$RH_{avgnight}$	Average Nighttime Relative Humidity	Percent (%)
SLP_{avg}	Average Sea Level Pressure	millibars (mb)
StP_{avg}	Average Station Pressure	millibars (mb)
Ta_{avg}	Average Apparent Temperature	Degrees Fahrenheit (°F)
Ta_{max}	Maximum Apparent Temperature	Degrees Fahrenheit (°F)
Ta_{min}	Minimum Apparent Temperature	Degrees Fahrenheit (°F)
T_{avgam}	Average Morning Temperature	Degrees Fahrenheit (°F)
T_{avgpm}	Average Afternoon Temperature	Degrees Fahrenheit (°F)
Tem_{2day}	Average 2-day Temperature	Degrees Fahrenheit (°F)
Tem_{3day}	Average 3-day Temperature	Degrees Fahrenheit (°F)
tempchange	24-hr Temperature Change"	Degrees Fahrenheit (°F)
T_{max}	Maximum Daily Temperature	Degrees Fahrenheit (°F)
trandir	24-hr Transport Direction	Degrees (°)
trandis	24-hr Transport Distance	kilometers (km)
$tran_{south}$	Southerly (v) Component of 24-hr Transport Vector	kilometers (km)

Parameter	Description	Units
$tran_w$	Vertical (z) Component of 24-hr Transport Vector	kilometers (km)
$tran_{west}$	Westerly (u) Component of 24-hr Transport Vector	kilometers (km)
wd_{avg}	Average Daily Wind Direction	Degrees (°)
wd_{avgam}	Average Morning Wind Direction	Degrees (°)
wd_{avgpm}	Average Afternoon Wind Direction	Degrees (°)
weekday	Day of Week	
wndrun	24-hr Scalar Wind Run	kilometers (km)
ws_{2day}	Average 2-day Wind Speed	meters/second (m/s)
ws_{3day}	Average 3-day Wind Speed	meters/second (m/s)
ws_{avg}	Average Daily Wind Speed	meters/second (m/s)
ws_{avgam}	Average Morning Wind Speed	meters/second (m/s)
ws_{avgpm}	Average Afternoon Wind Speed	meters/second (m/s)

Temperature analysis supporting exclusion of 2015 meteorology

Temperatures at airports in the LADCO region provided by U.S. EPA for the year 2015 seem to be skewed either high or low. For example, Figure A4.1 shows that temperatures skewed high at Chicago O'Hare, with peak temperatures in the 90s (°F). No other year shown has peak temperatures in the 90s. 2015 summer temperatures were below average in the Chicago area (Figure A4.3), so this distribution seems highly unlikely. Figure A4.2 shows that temperatures skewed low at Cincinnati Municipal Airport, with peak temperatures in the mid- to low-70s. While summer temperatures in Cincinnati were 1-2 °F below average, the temperatures in 2009 and 2014 were even lower, and these years had peak temperatures in the upper 70s to low 80s. It appears likely that these temperatures were incorrect as well.

LADCO has excluded this data from the CART analyses because of the apparent issues with this data.

Figure A4.1. Annual afternoon temperature distributions at Chicago O'Hare International Airport, with 2015 data highlighted.

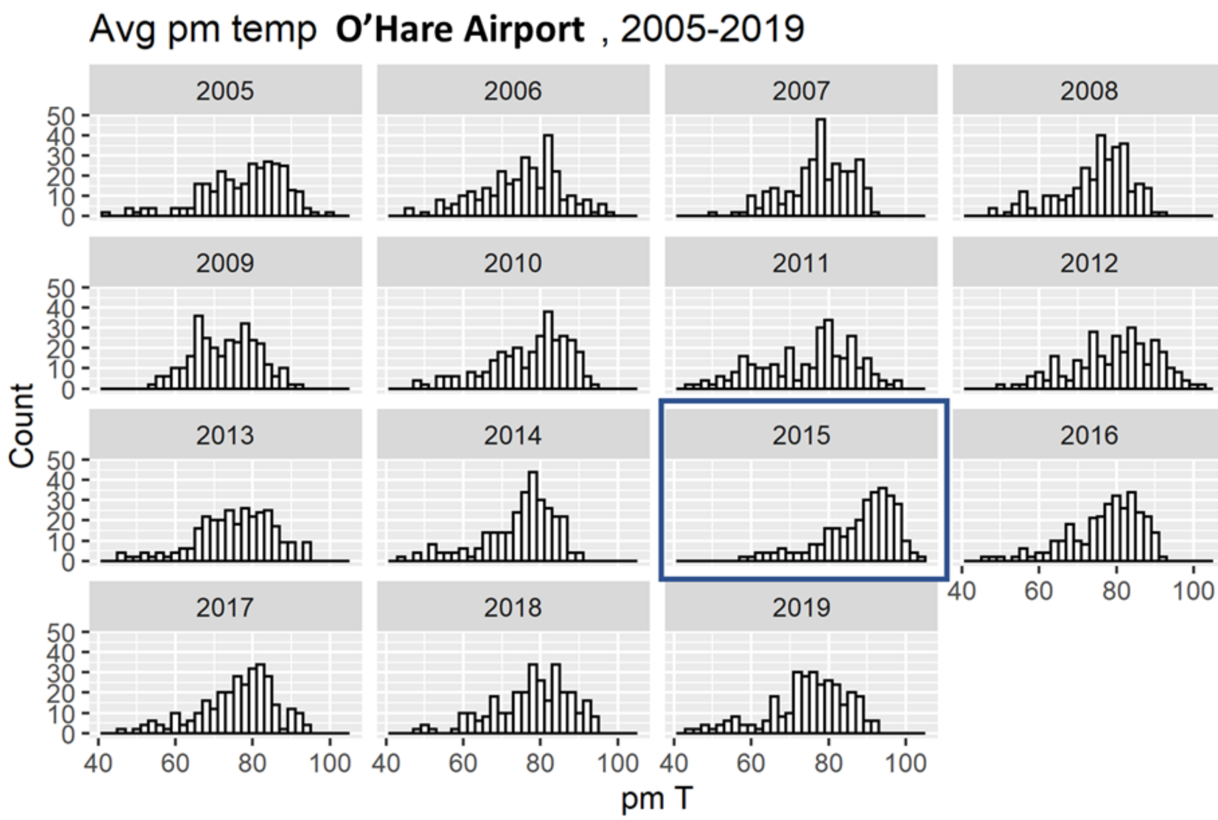

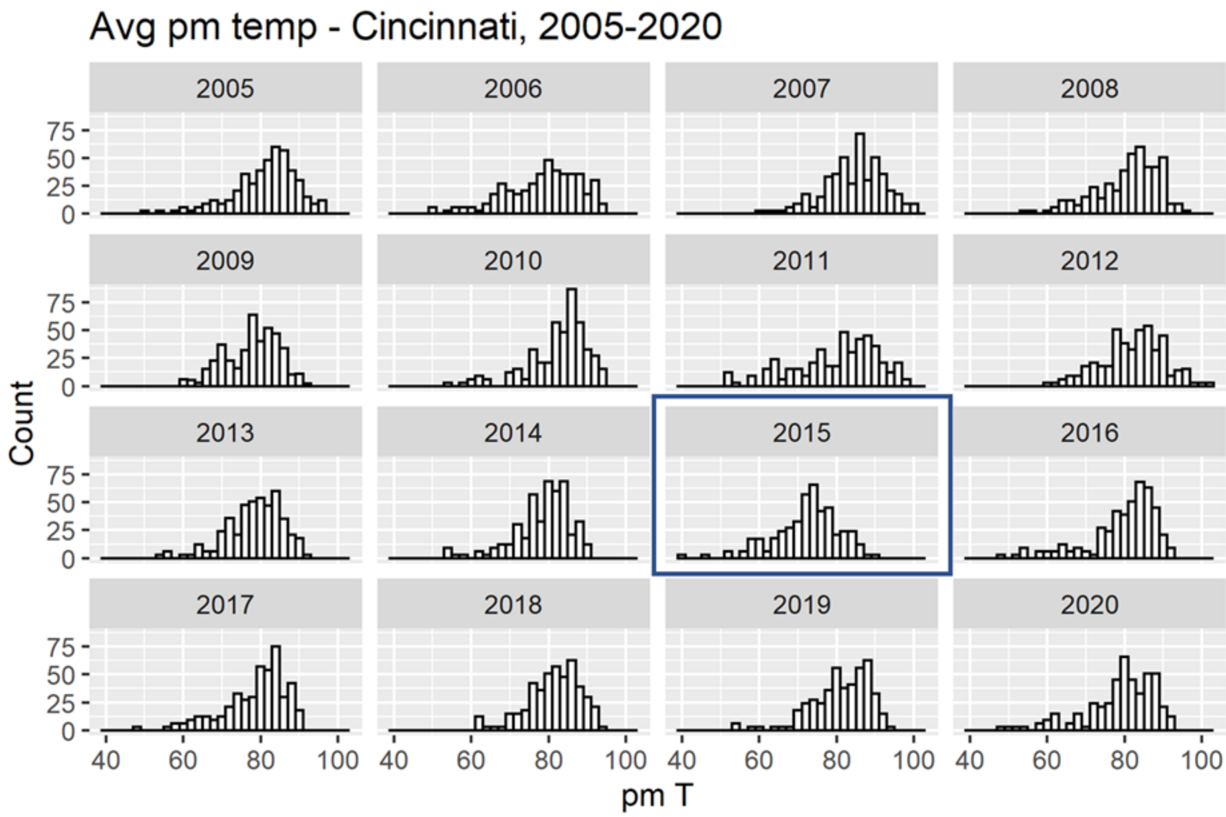

Figure A4.2. Annual afternoon temperature distributions at Cincinnati Municipal Airport-Lunken Field, with 2015 data highlighted.

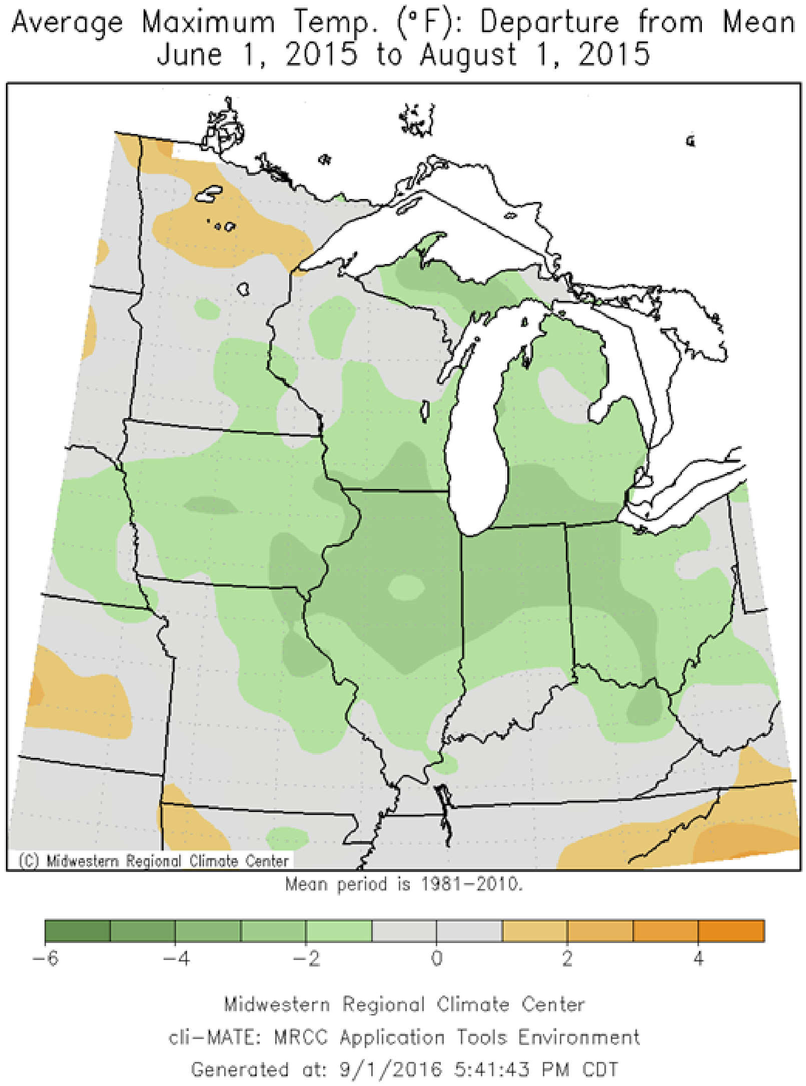

Figure A4.3. Average maximum temperature for June through August 2015, shown as the departure from the mean (in °F).

CART trees

Figure A4.4. CART Tree for the Lake MI: Wisconsin North Lake (Sheboygan) monitor group. The boxplots show the range of ozone MDA8 values (ppb) observed within each set of meteorological conditions ("node").

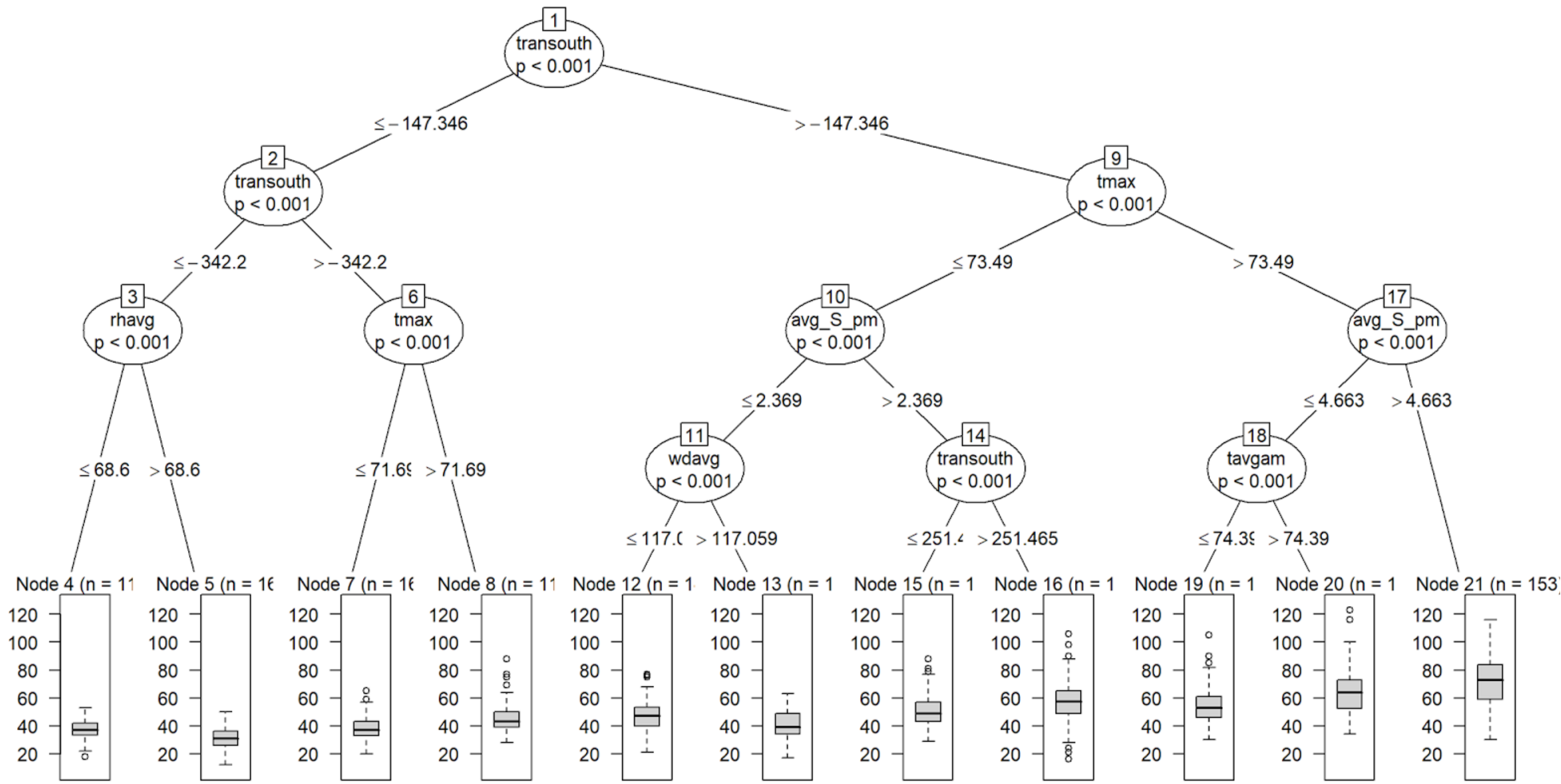

Figure A4.5. CART Tree for the Lake MI: Milwaukee North monitor group. The boxplots show the range of ozone MDA8 values (ppb) observed within each set of meteorological conditions ("node").

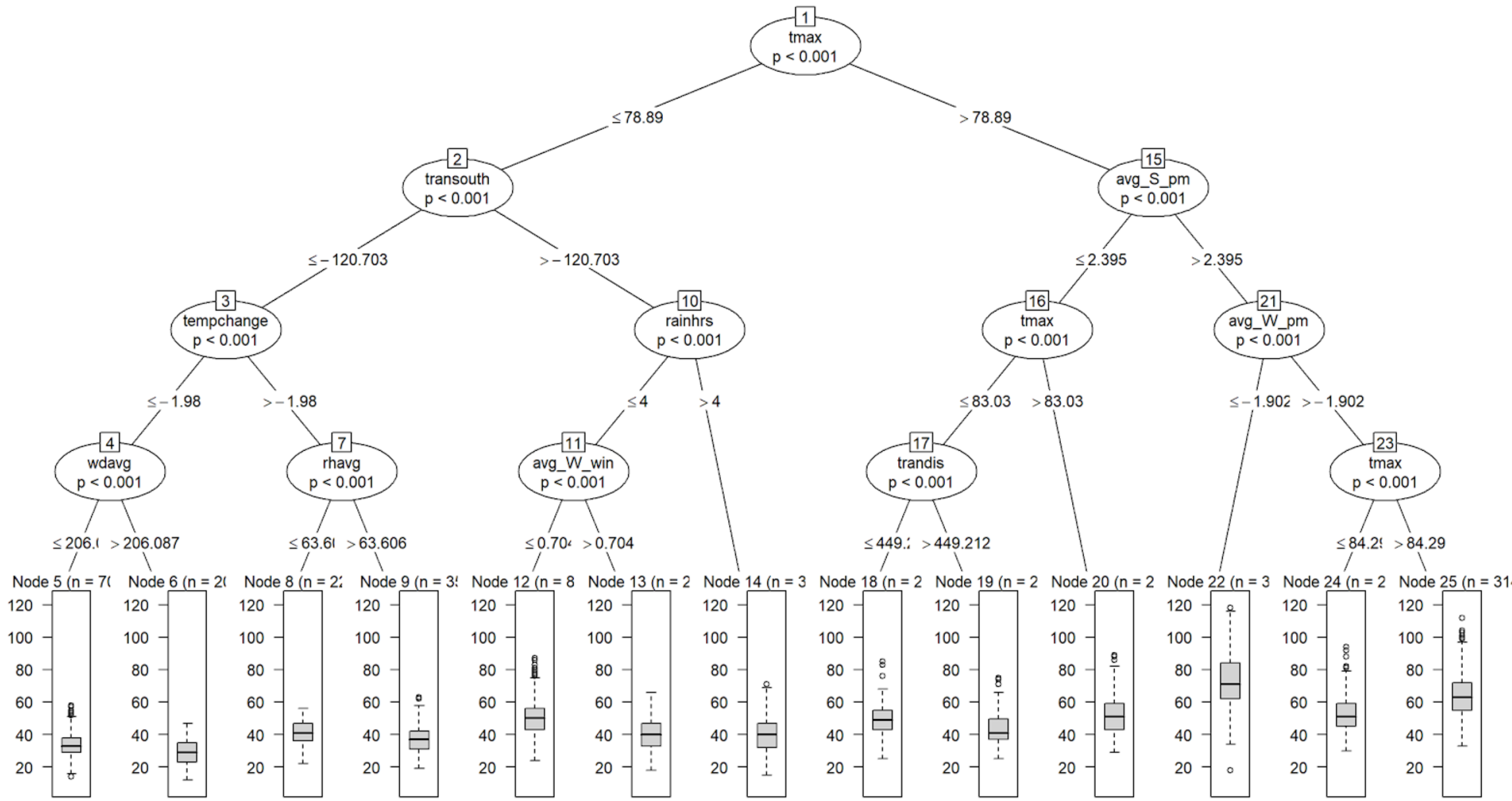

Figure A4.6. CART Tree for the Lake MI: Western Michigan monitor group. The boxplots show the range of ozone MDA8 values (ppb) observed within each set of meteorological conditions ("node").

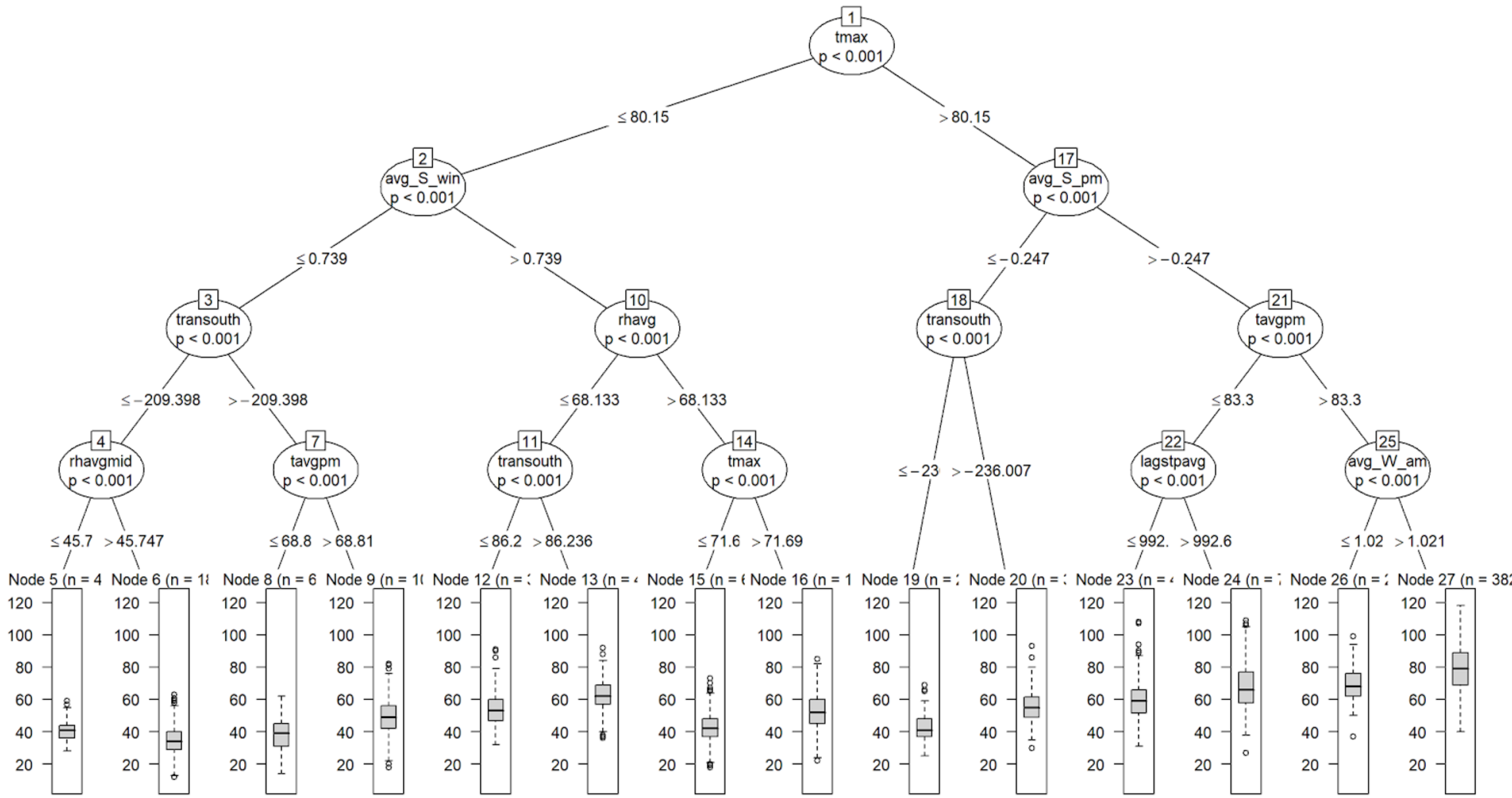

Figure A4.7. CART Tree for the Chicago: Far North monitor group. The boxplots show the range of ozone MDA8 values (ppb) observed within each set of meteorological conditions ("node").

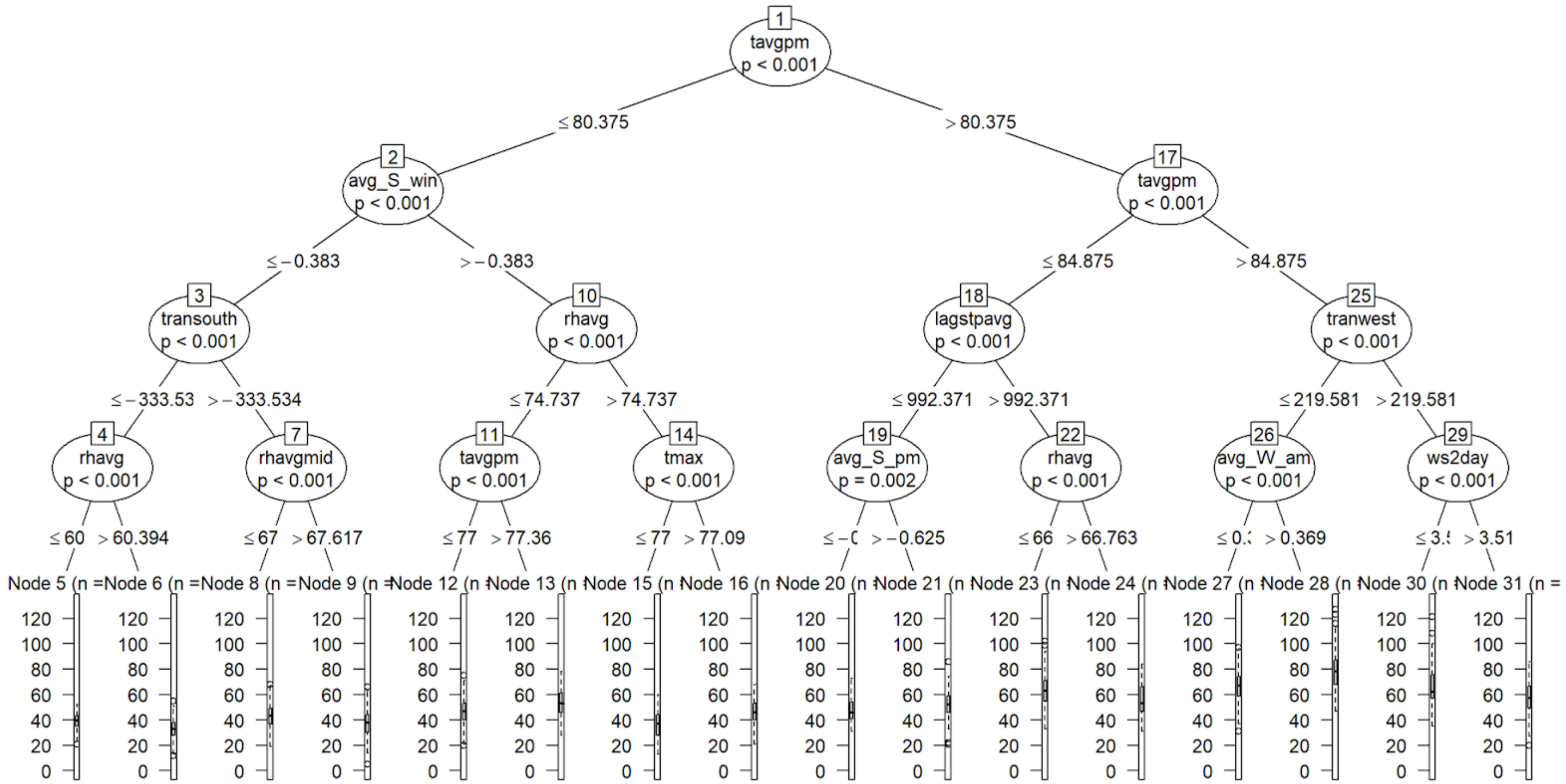

Figure A4.8. CART Tree for the Chicago: Central monitor group. The boxplots show the range of ozone MDA8 values (ppb) observed within each set of meteorological conditions ("node").

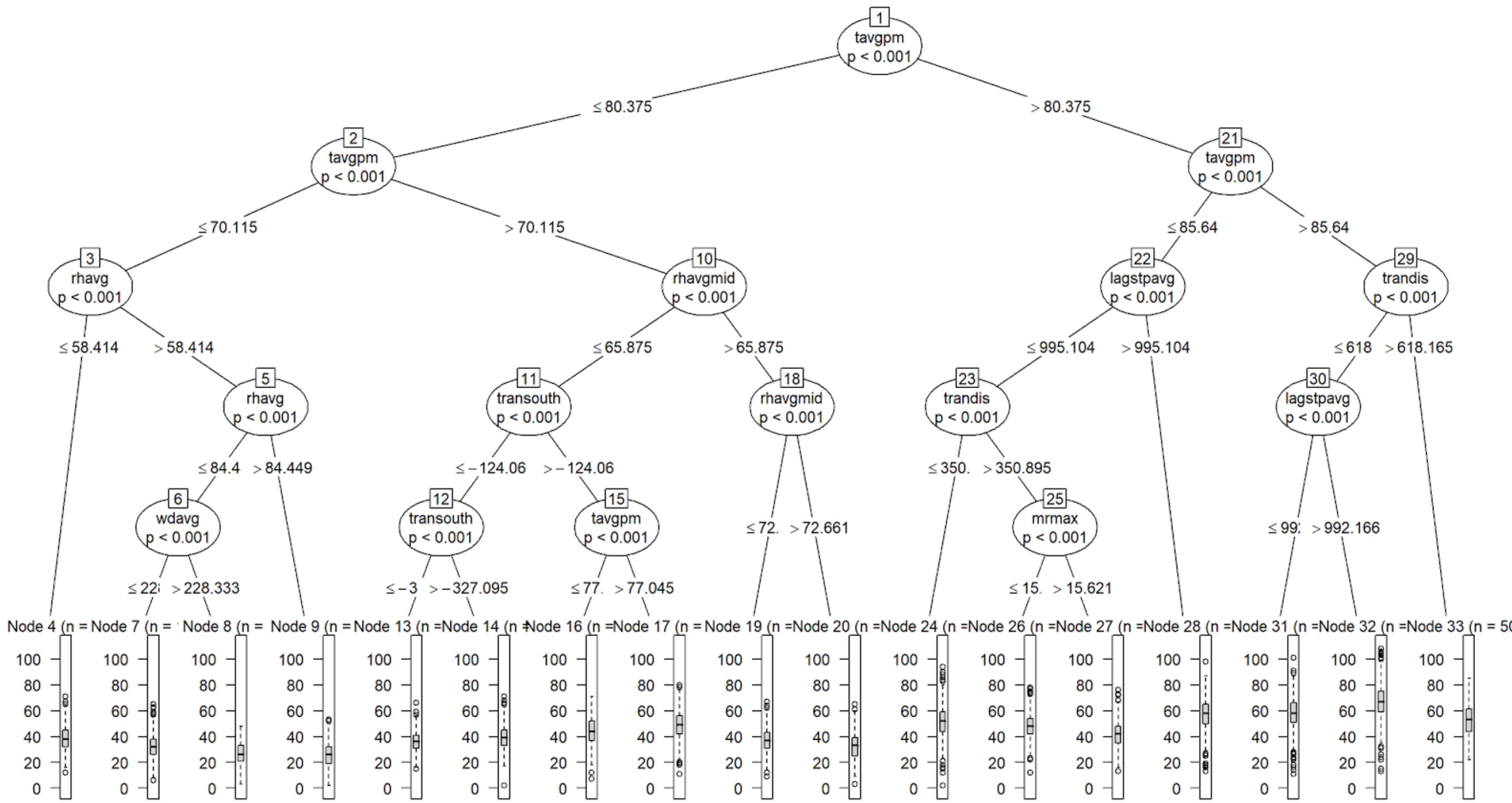

Figure A4.9. CART Tree for the Chicago: Indiana Lake monitor group. The boxplots show the range of ozone MDA8 values (ppb) observed within each set of meteorological conditions ("node").

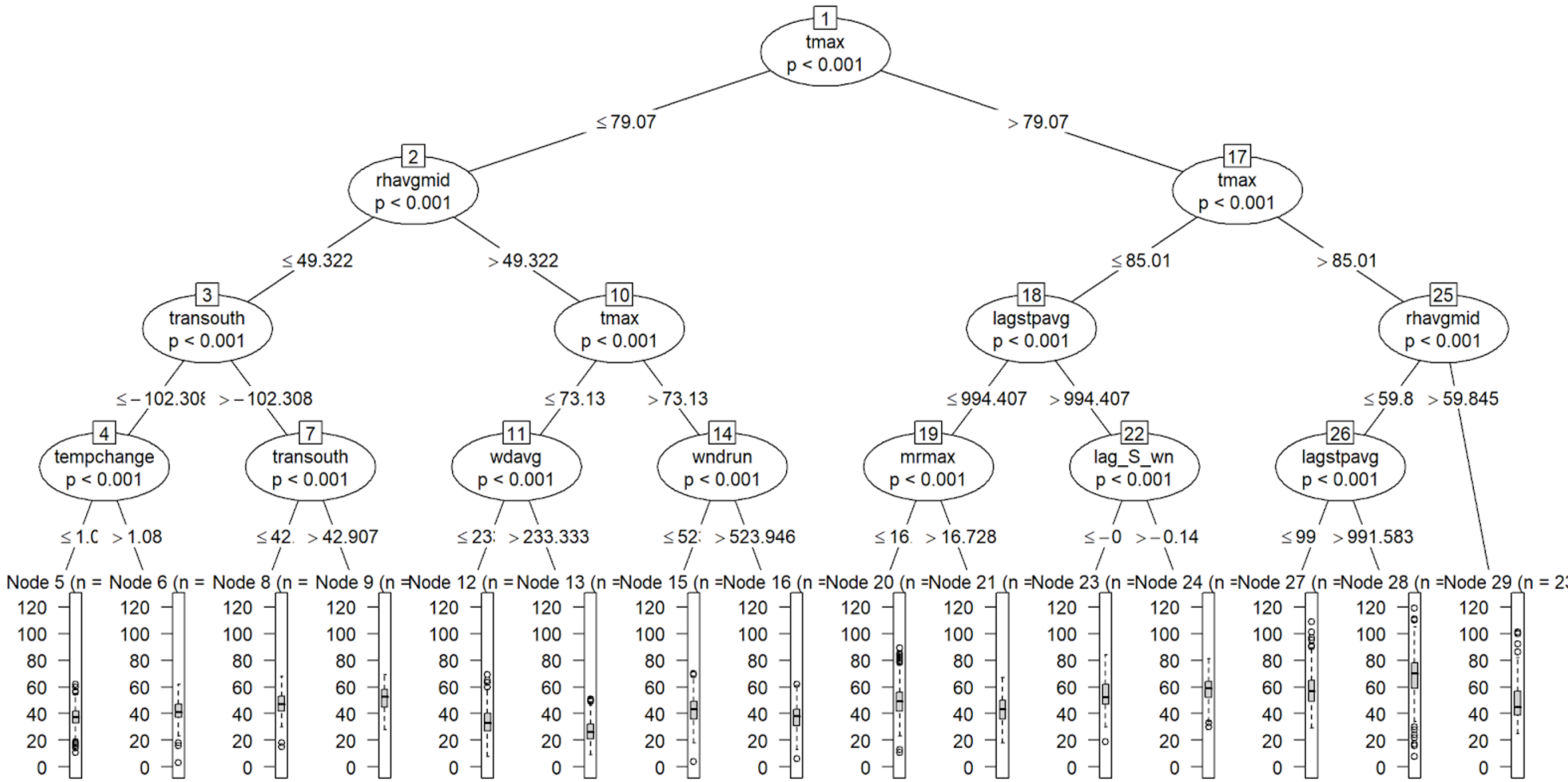

Figure A4.10. CART Tree for the Detroit nonattainment area. The boxplots show the range of ozone MDA8 values (ppb) observed within each set of meteorological conditions ("node").

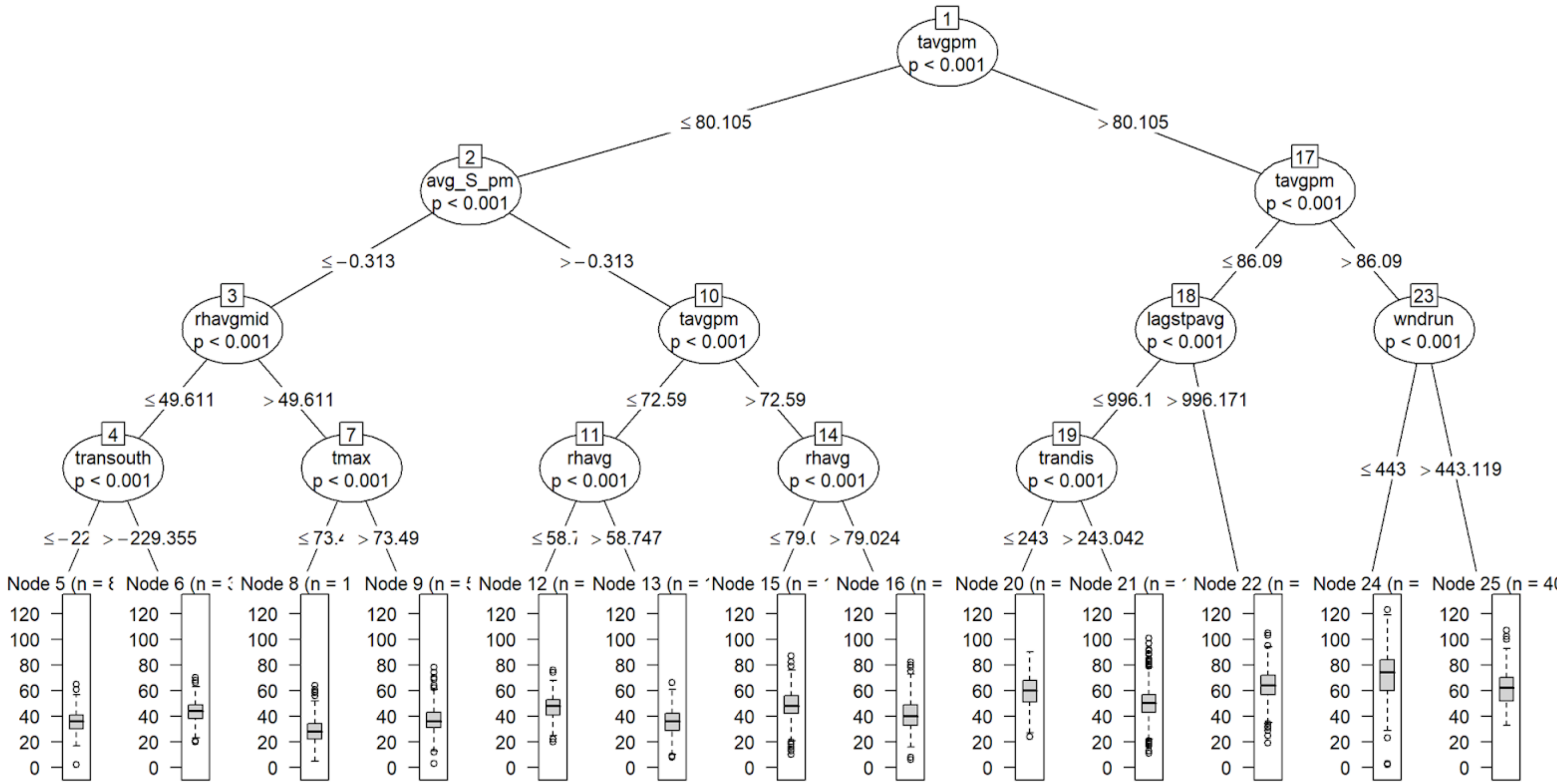

Figure A4.11. CART Tree for the Cleveland nonattainment area. The boxplots show the range of ozone MDA8 values (ppb) observed within each set of meteorological conditions ("node").

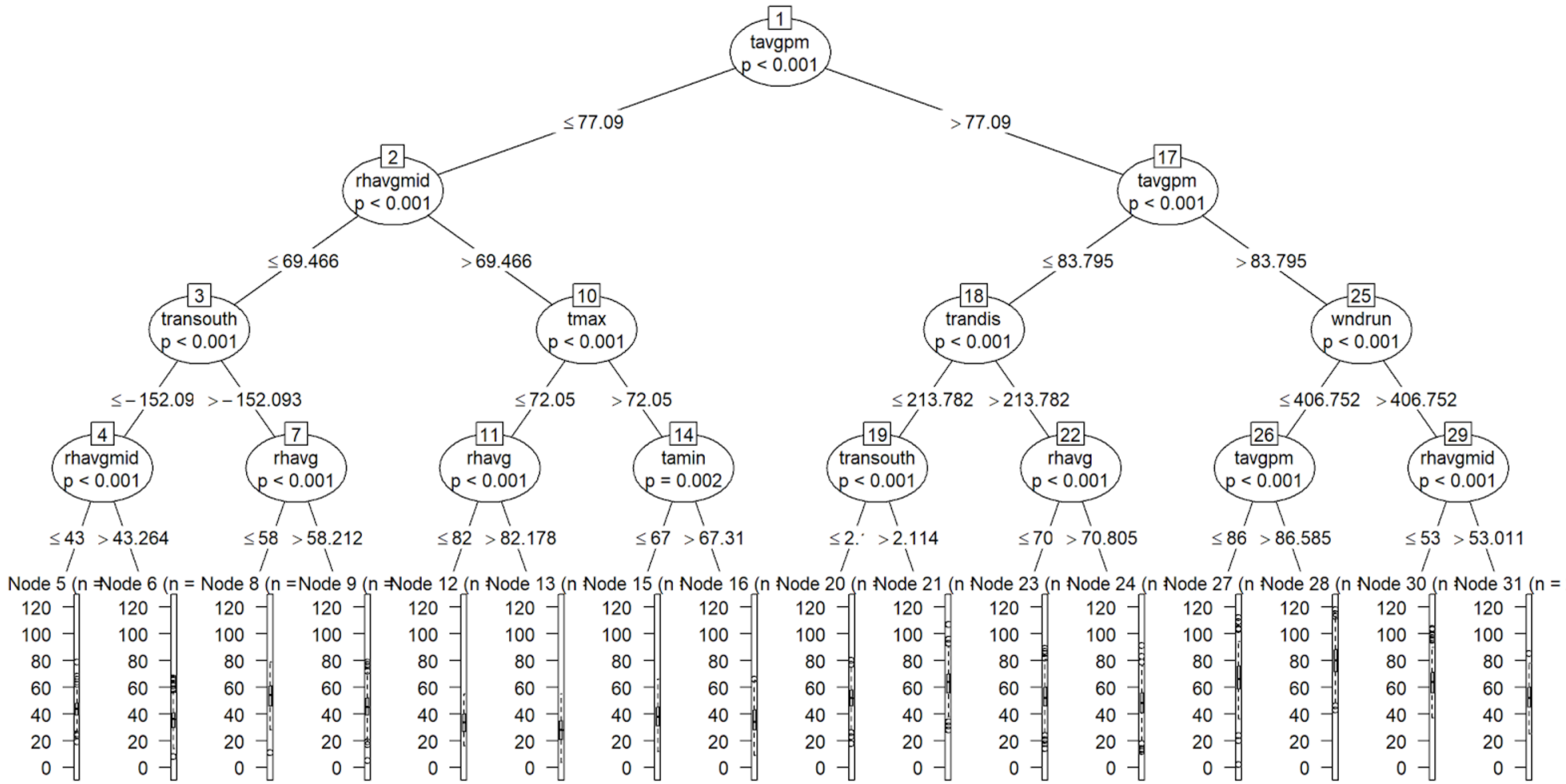

Figure A4.12. CART Tree for the St. Louis nonattainment area. The boxplots show the range of ozone MDA8 values (ppb) observed within each set of meteorological conditions ("node").

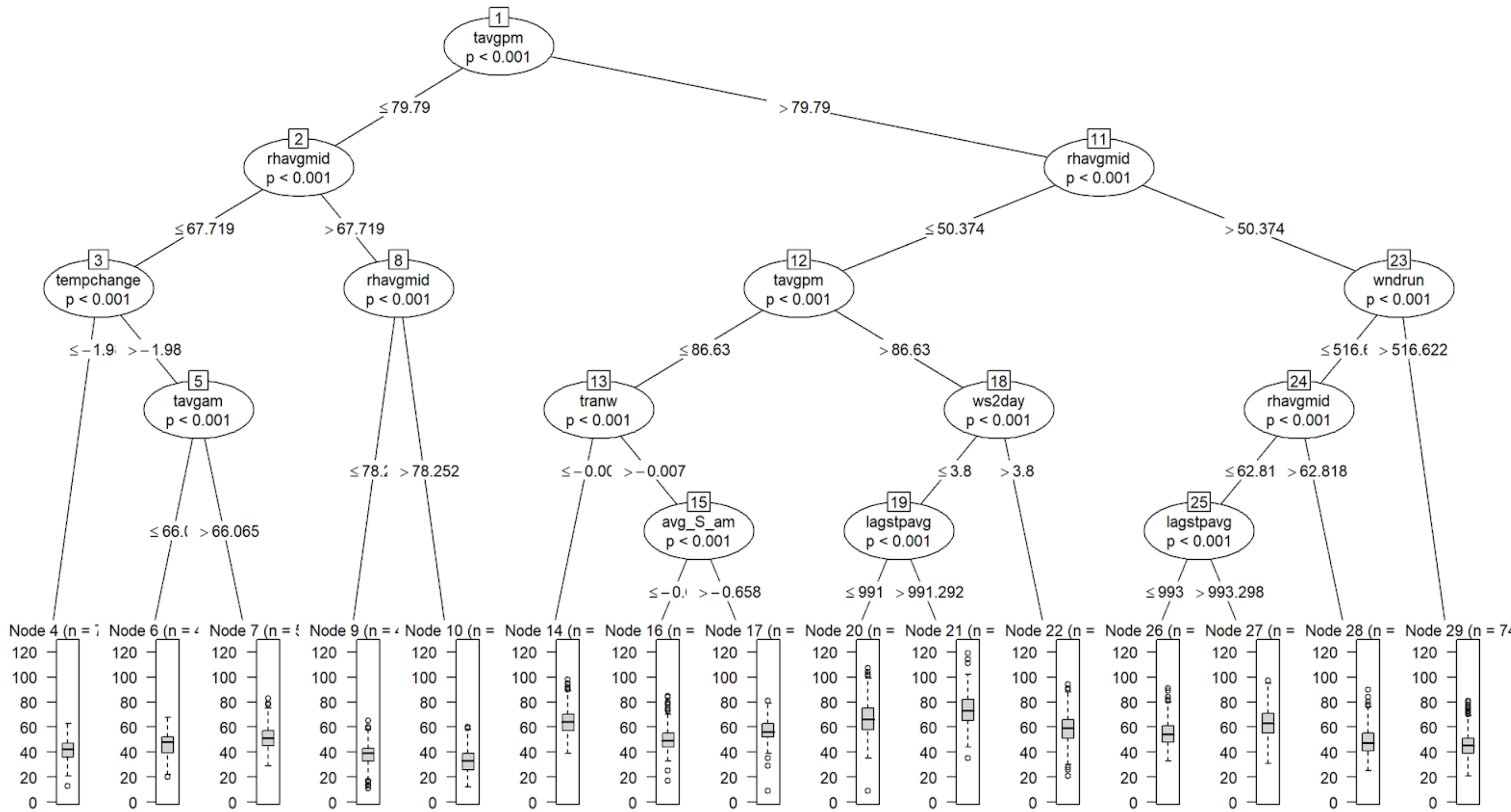

Figure A4.13. CART Tree for the Louisville nonattainment area. The boxplots show the range of ozone MDA8 values (ppb) observed within each set of meteorological conditions ("node").

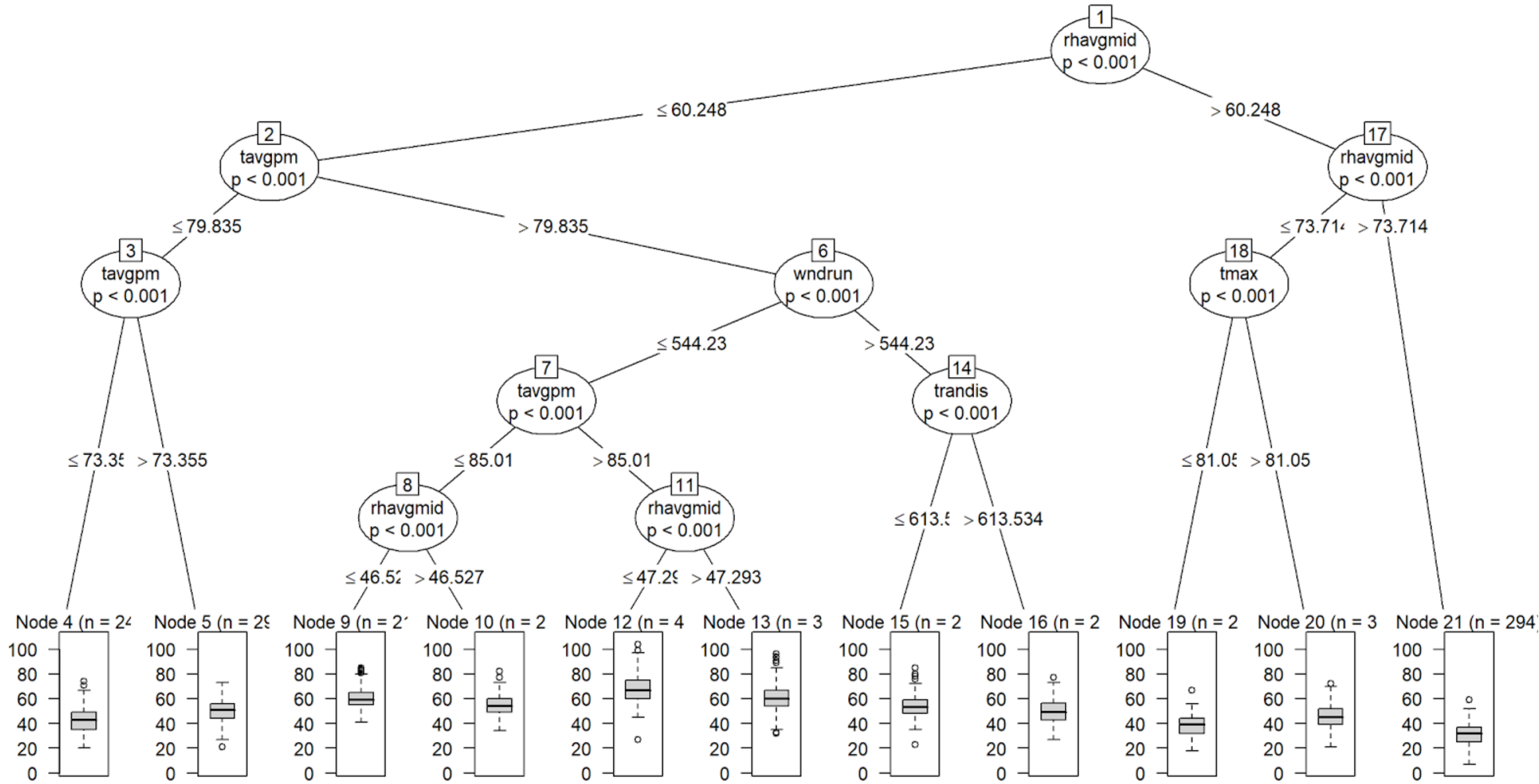

Figure A4.14. CART Tree for the Cincinnati nonattainment area. The boxplots show the range of ozone MDA8 values (ppb) observed within each set of meteorological conditions ("node").

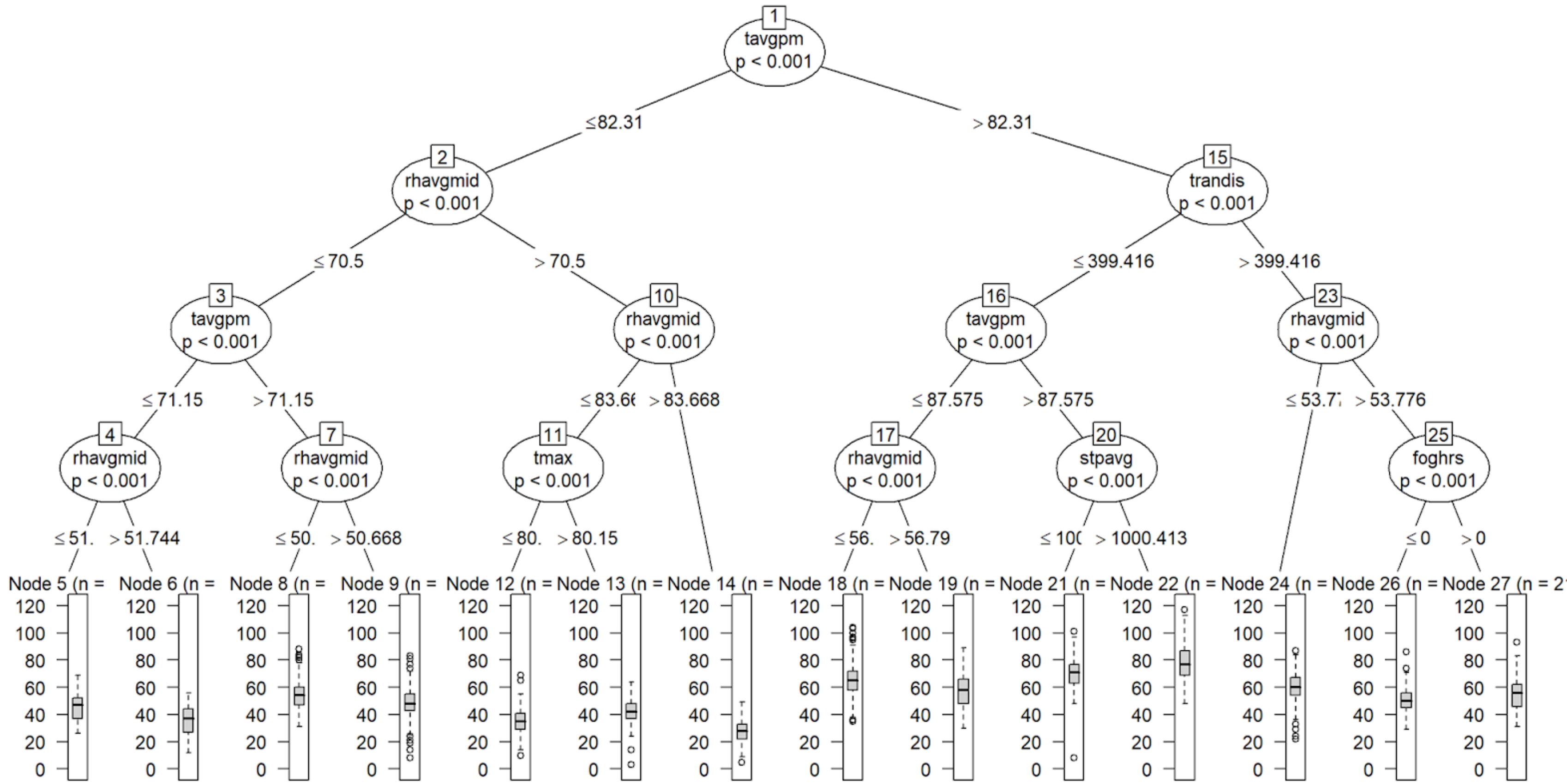

Weekday-weekend differences in maximum daily temperature on all ozone season days

This figure shows the W-W differences in maximum daily temperature on all ozone season days in the different nonattainment areas. W-W differences were determined by subtracting the weekend average maximum daily temperature from the weekday average maximum daily temperature.

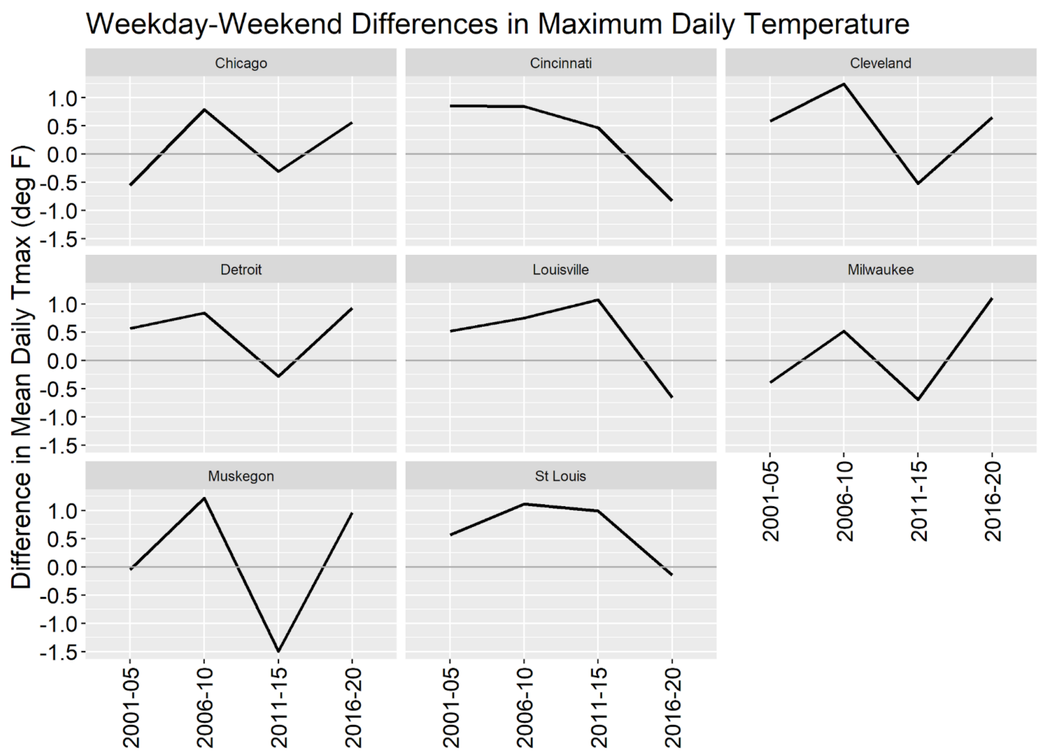

Figure A4.15. Weekday-weekend differences in maximum daily temperature on all ozone season days in the Great Lakes nonattainment areas.

Weekday-weekend differences in select meteorological parameters on ozone-conducive days

These figures show the weekday-weekend differences in the meteorological parameters that were used to split the high-ozone nodes in all of the areas. W-W differences were determined by subtracting the weekend averages on ozone-conducive days from the weekday averages for each parameter.

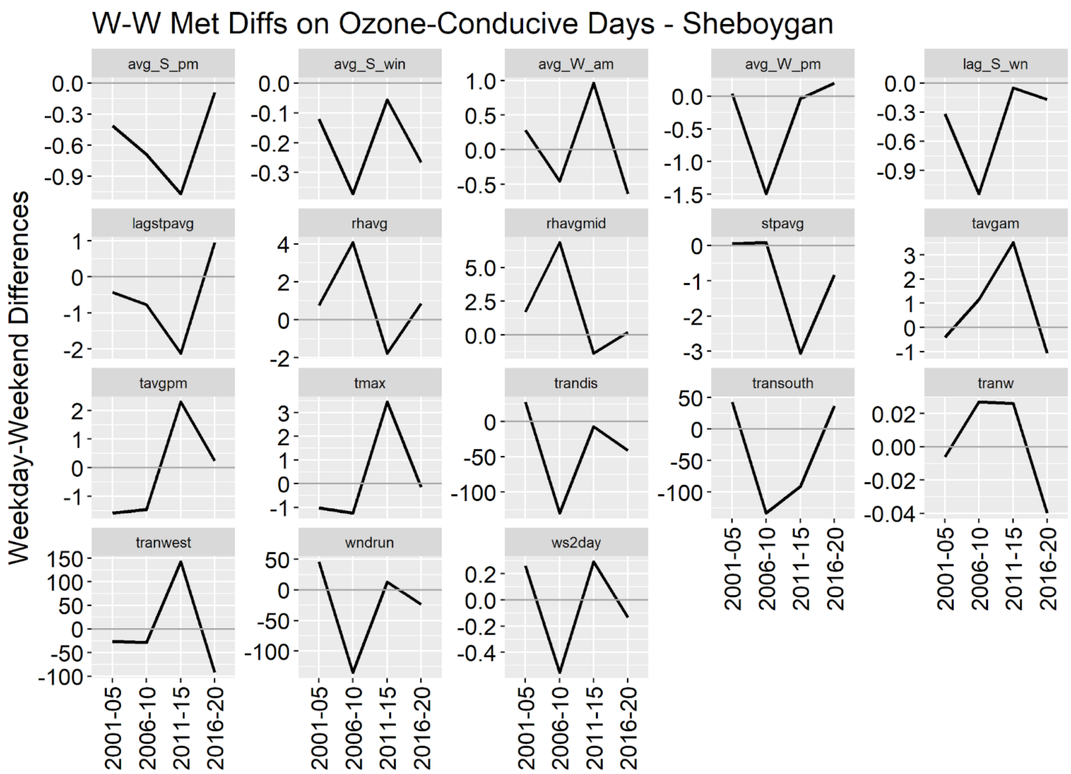

Figure A4.16. Weekday-weekend differences in meteorological parameters on ozone-conducive days in the Sheboygan CART analyses.

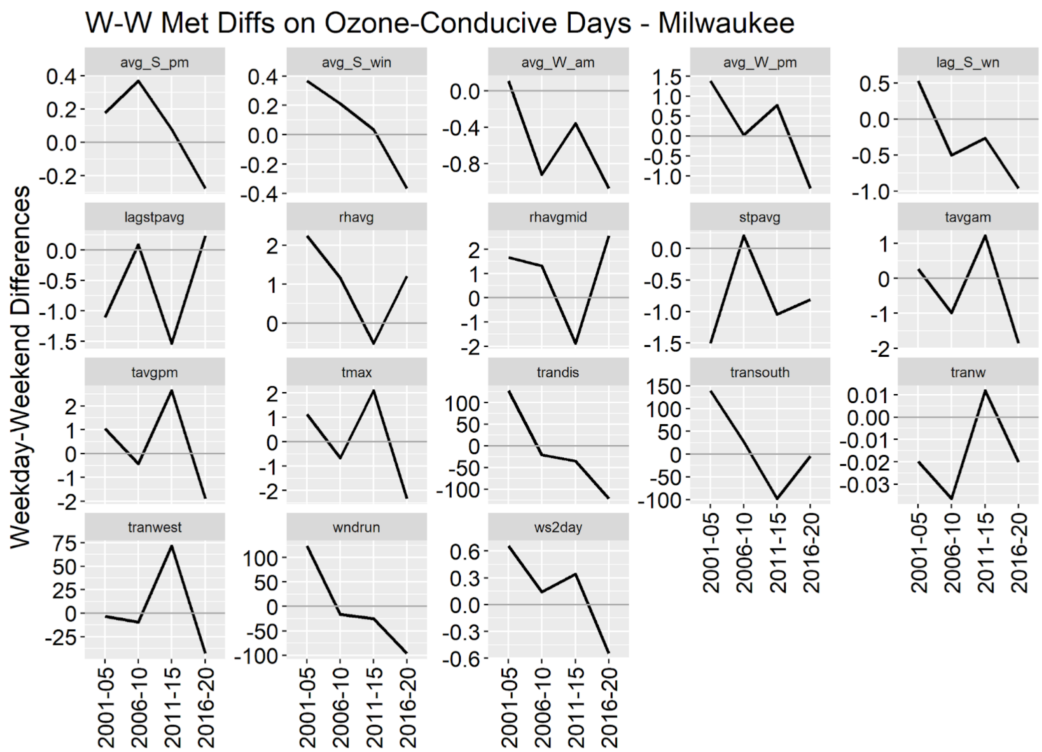

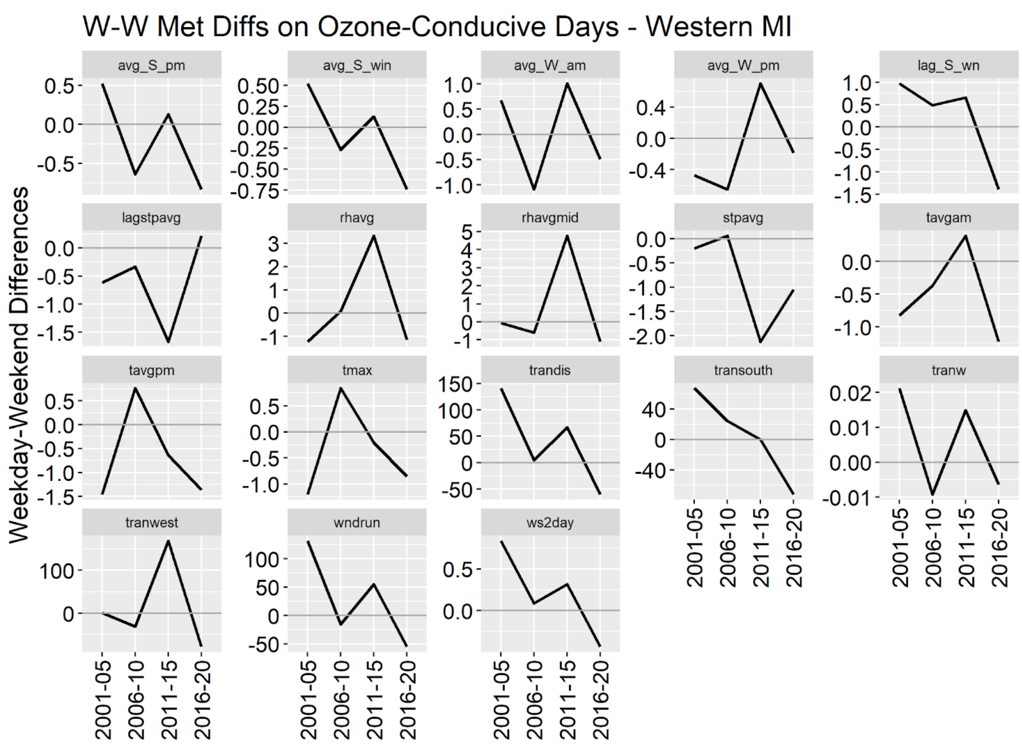

Figure A4.17. Weekday-weekend differences in meteorological parameters on ozone-conducive days in (top) the Milwaukee North and (bottom) Western Michigan CART analyses.

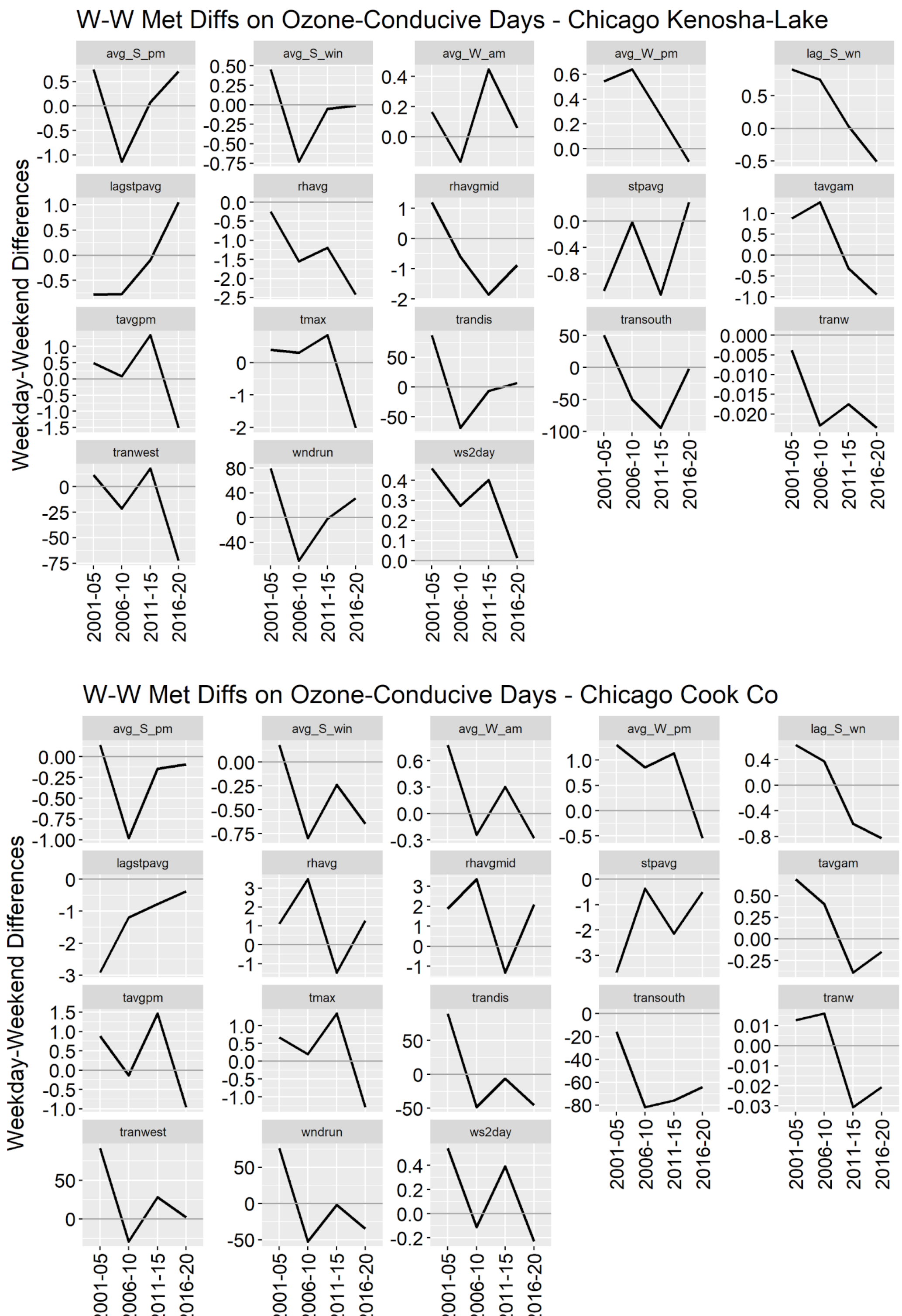

Figure A4.18. Weekday-weekend differences in meteorological parameters on ozone-conducive days in (top) the Chicago: Far North (Kenosha-Lake) and (bottom) the Chicago: Central CART analyses.

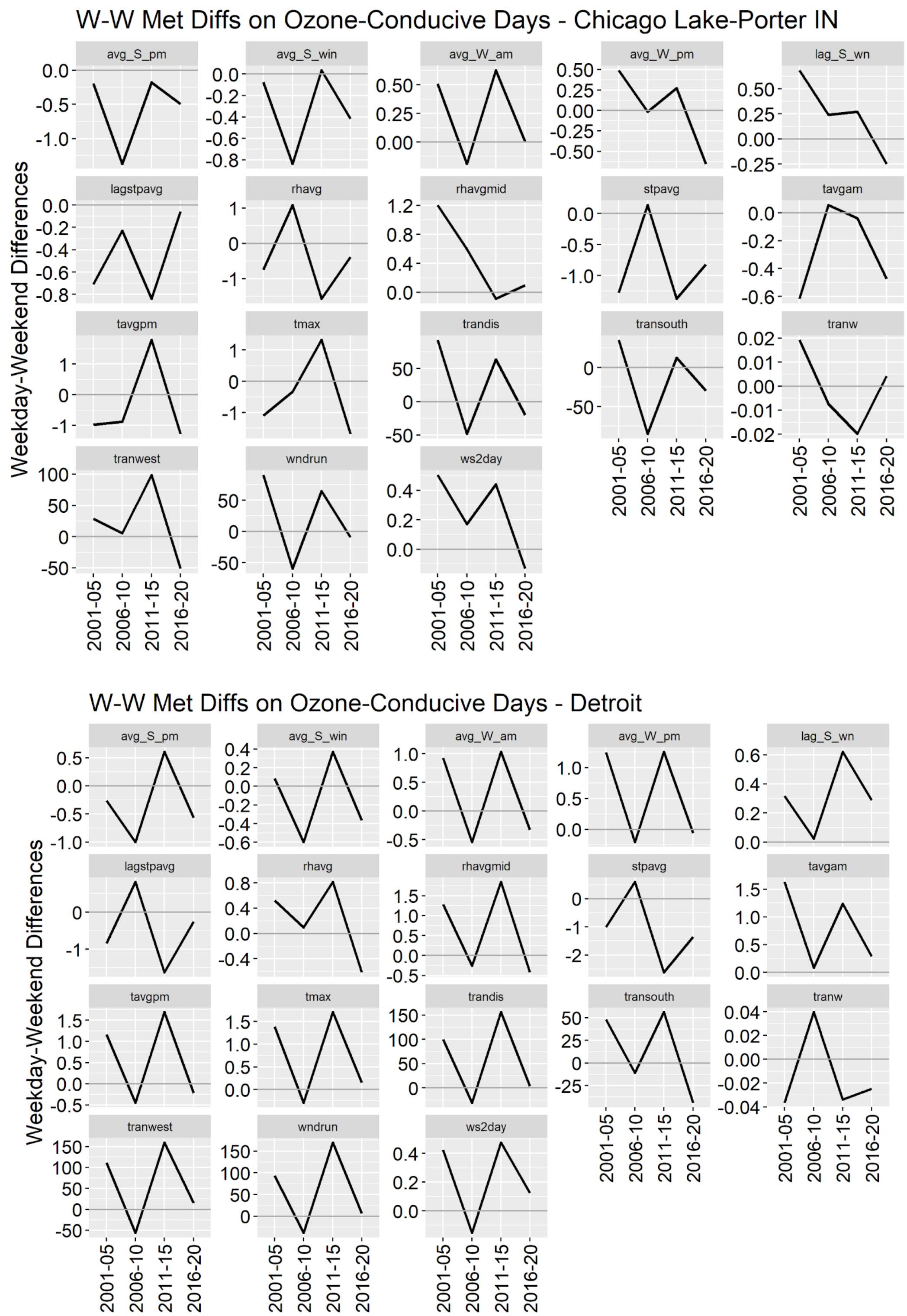

Figure A4.19. Weekday-weekend differences in meteorological parameters on ozone-conducive days in (top) the Chicago: Indiana Lake (Lake-Porter) and (bottom) Detroit CART analyses.

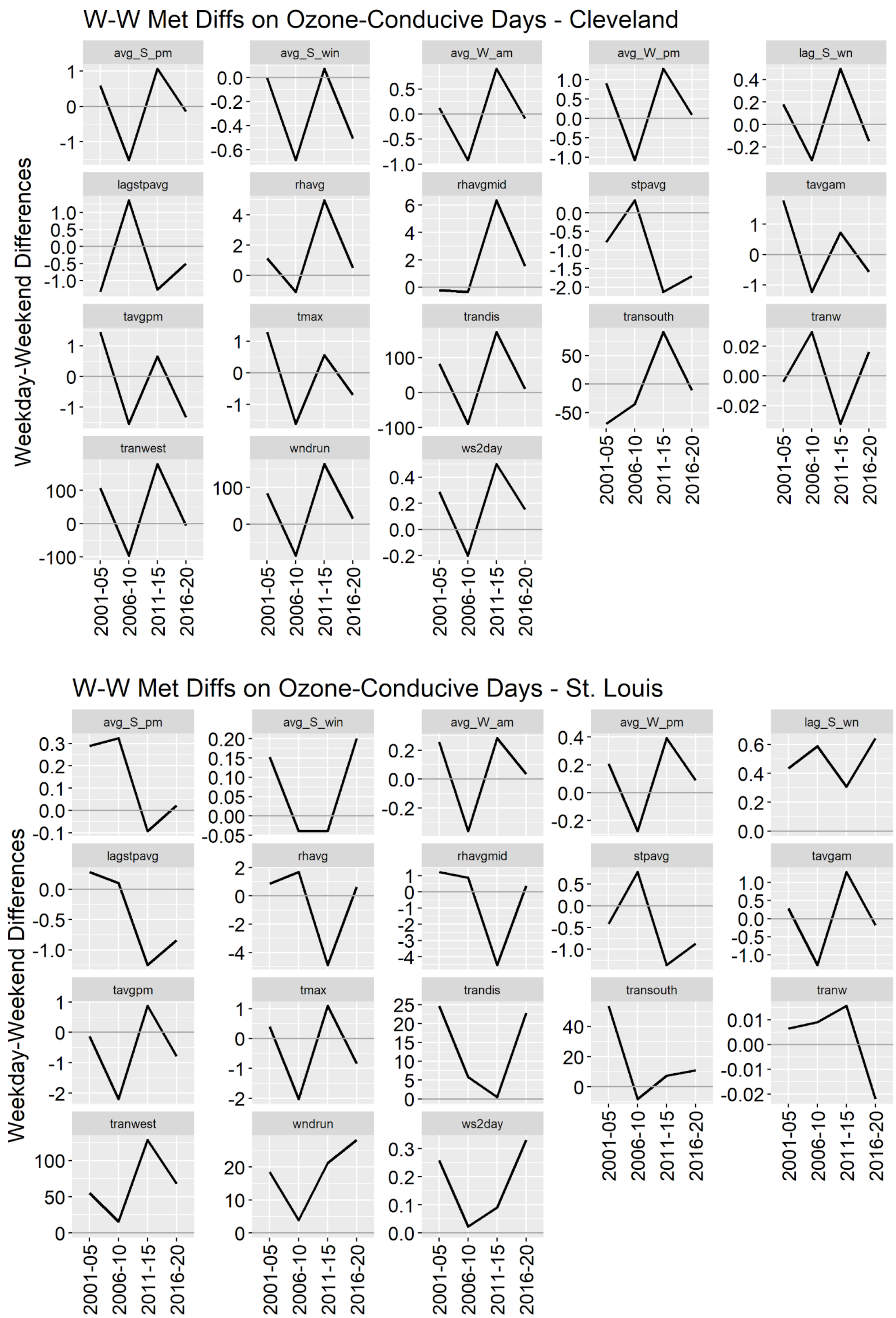

Figure A4.20. Weekday-weekend differences in meteorological parameters on ozone-conducive days in (top) the Cleveland and (bottom) St. Louis CART analyses.

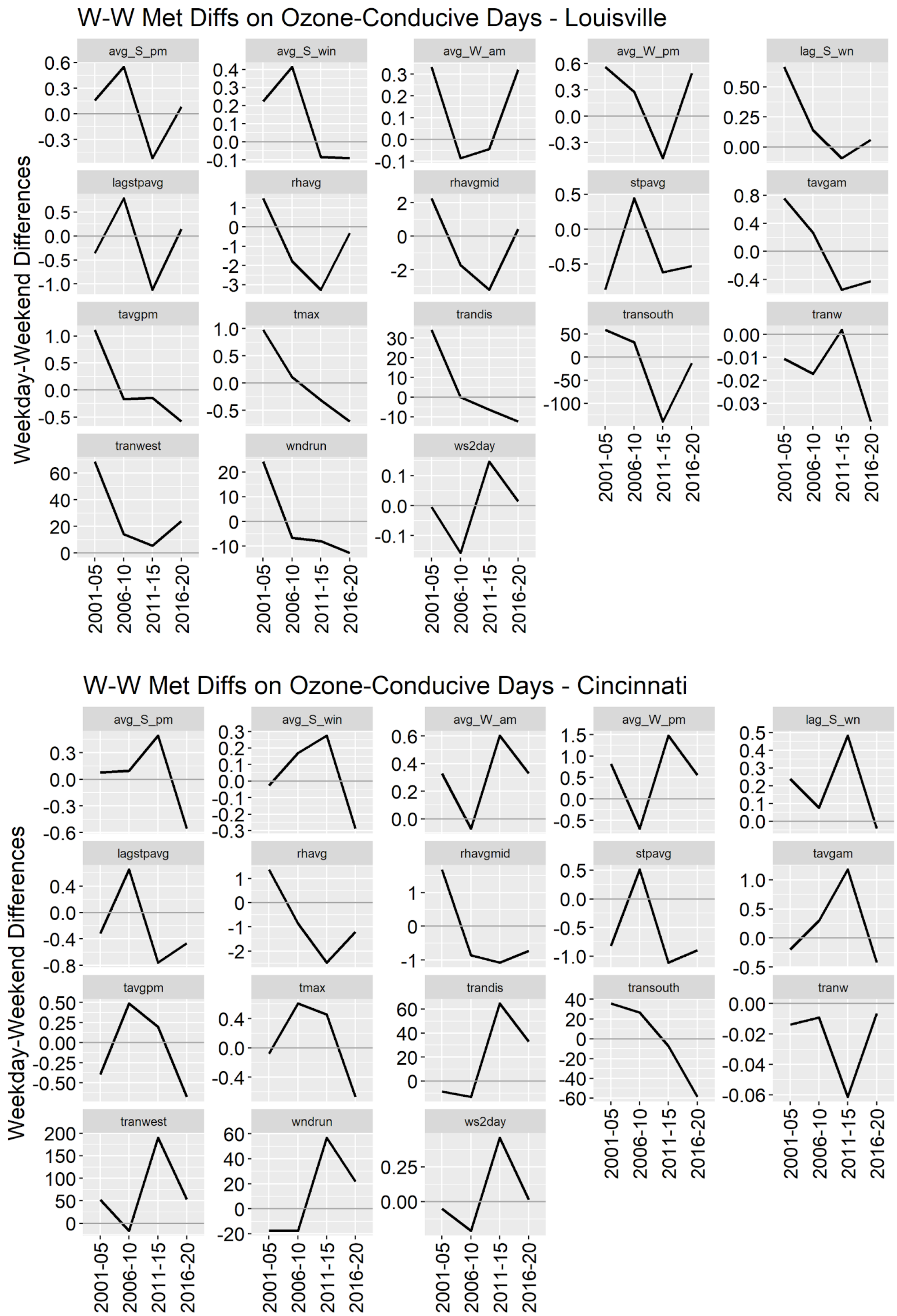

Figure A4.21. Weekday-weekend differences in meteorological parameters on ozone-conducive days in (top) the Louisville and (bottom) Cincinnati CART analyses.

Relationship of p values to Weekday-Weekend mean MDA8 differences

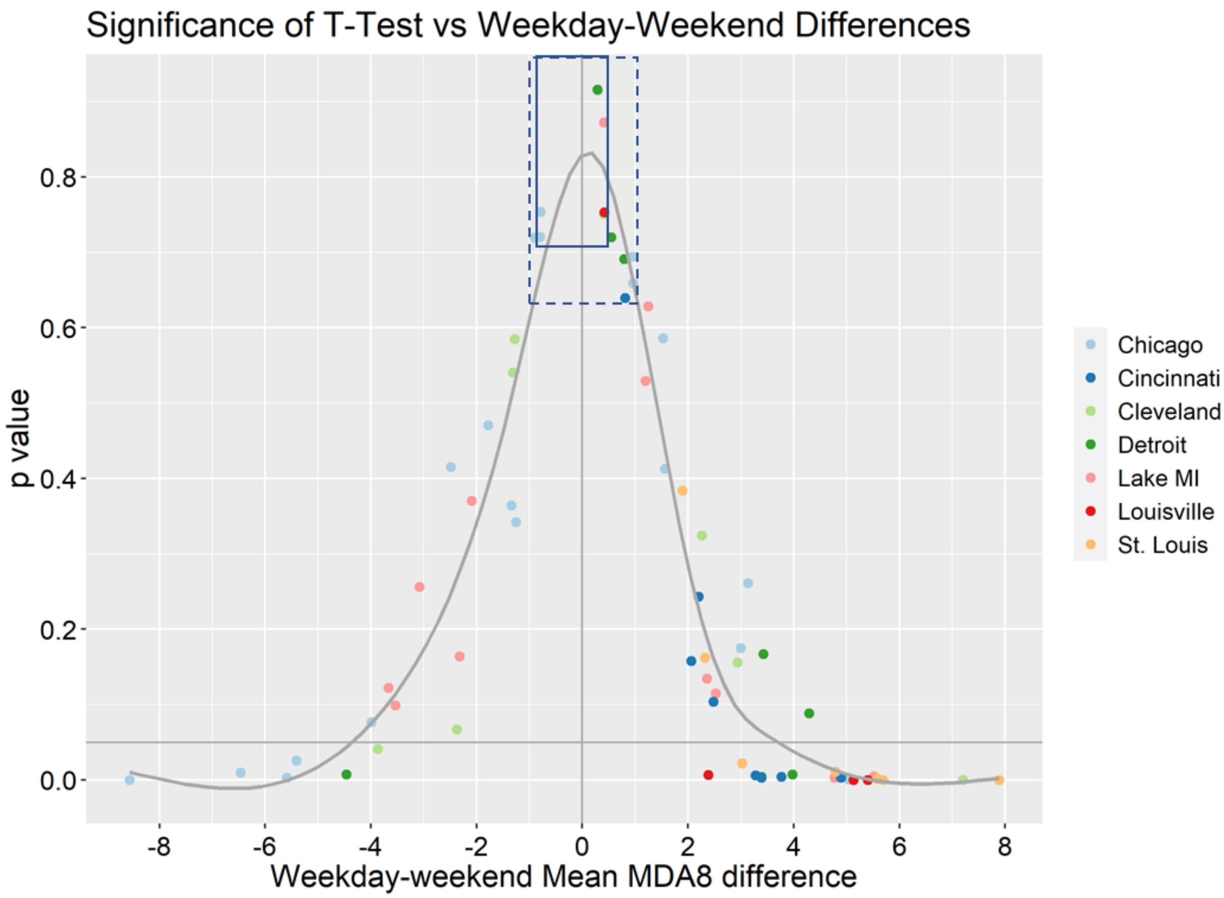

Figure A4.22. Plot of p values from the Welch's t-test versus the W-W mean MDA8 difference for the different monitor groups and sets of years. The solid box encloses the top 10% of points with the highest p values, and the dashed box encloses the top 20% of points with the highest p values.

Trends in VOCs in the Chicago and Detroit areas

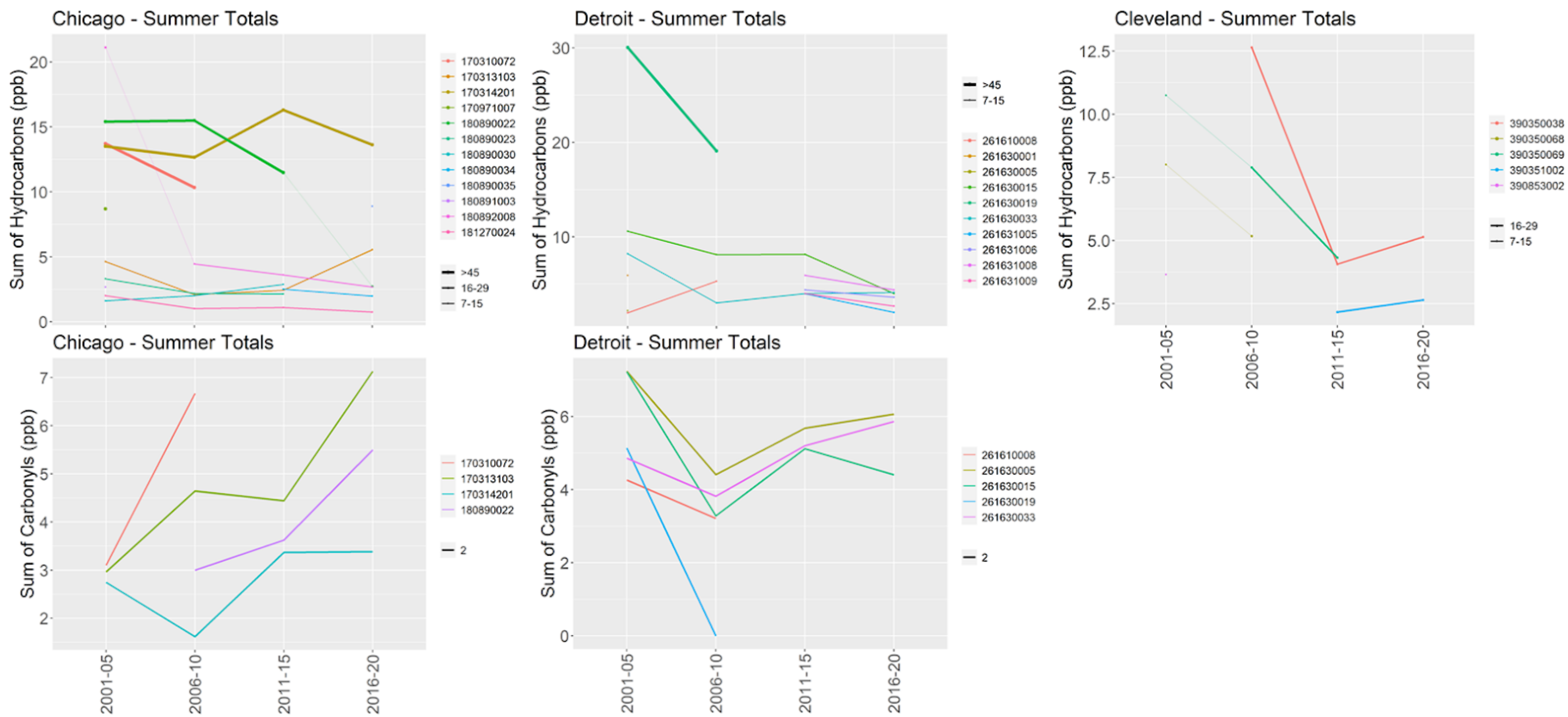

Figure A4.23. Trends in total hydrocarbon (top) and carbonyl (bottom, only including formaldehyde and acetaldehyde) VOCs at monitors in the Chicago (left), Detroit (middle), and Cleveland (right) areas. Carbonyls were not measured in Cleveland. The thickness of the lines and points indicates how many of the hydrocarbon or carbonyl compounds were measured at that site in those years. The thinnest lines connect points indicating different numbers of monitors.

Weekday-weekend analysis of additional monitors of interest

LADCO performed additional weekday-weekend analyses on monitors in several areas. Most of these sites are single monitors located in an urban core. They were not included in the primary analysis because they could not be paired with other, nearby monitors that had similar trends. Examination of the W-W trends for these individual monitors is informative, although the analyses are likely more uncertain since they are based on a single monitor. In addition to monitors in urban cores, we examined a lakeshore monitor in Toledo that has been measuring high values of ozone.

The W-W analyses were run using the data inputs described in Table A4.3. Monitors are mapped out in Figure A4.24. Note that the Toledo analysis relied on ozone-conducive days (determined via CART analysis) and NO_2 in nearby Detroit because of the lack of data for Toledo. The NO_2 trends for the Milwaukee monitor are shown in Figure A4.25; NO_2 trends for the other areas were already presented in Figure 3.4 of the main document.

Table A4.3. Data inputs used for the W-W analyses of additional areas.

Area of interest	Ozone Monitor(s)	Years of Operation	CART Analysis Used	NO_2 monitors used
Milwaukee Central	Milw SER DNR (550790026) Milw 16th St (550790010)	2001-2020 2003-2020	Milwaukee North	Milwaukee (Milw SER DNR)
Toledo	Lo Service (390950034) Cooley Canal (390950035)	2001-2015* 2016-2020	Detroit	Detroit
St. Louis Central	Blair Street (295100085)	2005-2020	St. Louis	St. Louis
Louisville Central	Cannons Lane (211110067)	2010-2020	Louisville	Louisville

*The Lo Service monitor operated through 2016, but we used 2016 data from Cooley Canal instead.

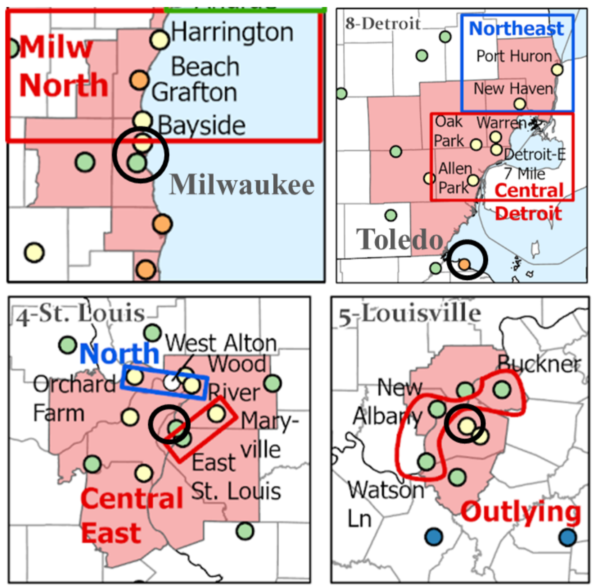

Figure A4.24. Map showing the location of the additional monitors, which are circled in black.

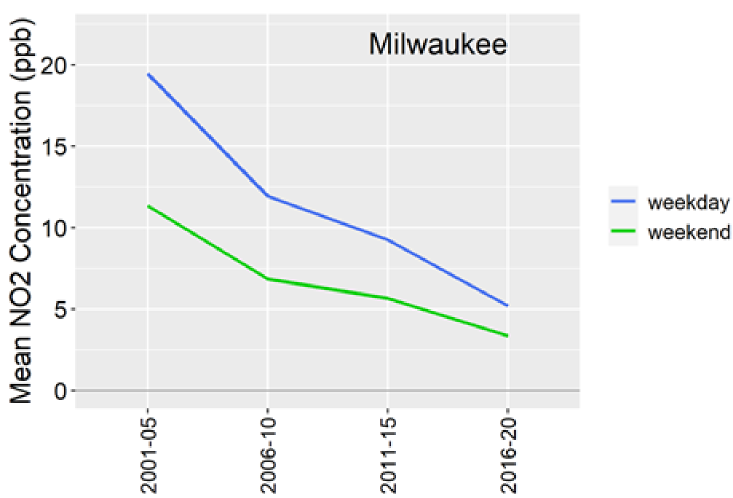

Figure A4.25. Mean nonattainment area concentrations of NO_2 on ozone-conducive weekdays and weekend days in Milwaukee. NO_2 concentrations were measured during midday hours (9:00-14:59 LST) from May through September.

These additional areas showed similar reductions in mean MDA8 values on weekdays and weekends as found in the areas described in the main document (Figure A4.26). W-W mean MDA8 differences are shown in Figure AA.27, along with trends for nearby areas. In general, the trends at the urban core ("Central") monitors closely tracked those at nearby monitors. The

Milwaukee Central trends were very similar to those at the Milwaukee North monitors, although the Central monitors were more VOC-sensitive at all time points. This is consistent with an understanding that VOC-sensitivity peaks in urban cores due to NOx-suppression in these areas. St. Louis Central tracks St. Louis Central East values more closely than those in St. Louis North. This makes sense given the proximity of the Central monitor to the Central East monitors (Figure AA.24). The Louisville Central monitor tracks the Louisville outlying monitors closely as well. The trends at the Toledo monitors followed a similar trend to those at the Detroit Central monitors, although the Toledo values were shifted to more positive (NOx-sensitive) values (compare Figure A4.27 with Figure 3.6 in the main document). Overall, this demonstrates that while urban cores tended to be more VOC-sensitive in some areas, particularly in Chicago and Milwaukee, these differences were not evident in areas such as St. Louis and Louisville.

Examination of plots of mean MDA8 values versus NO_2 (Figure A4.28) show similar findings as those in the other areas (Figure 3.8 in the main document). In addition to NO_2 reductions, VOC reductions appeared to contribute to ozone reductions in all of the areas, including in St. Louis and Louisville, where ozone formation was strongly NOx-sensitive.

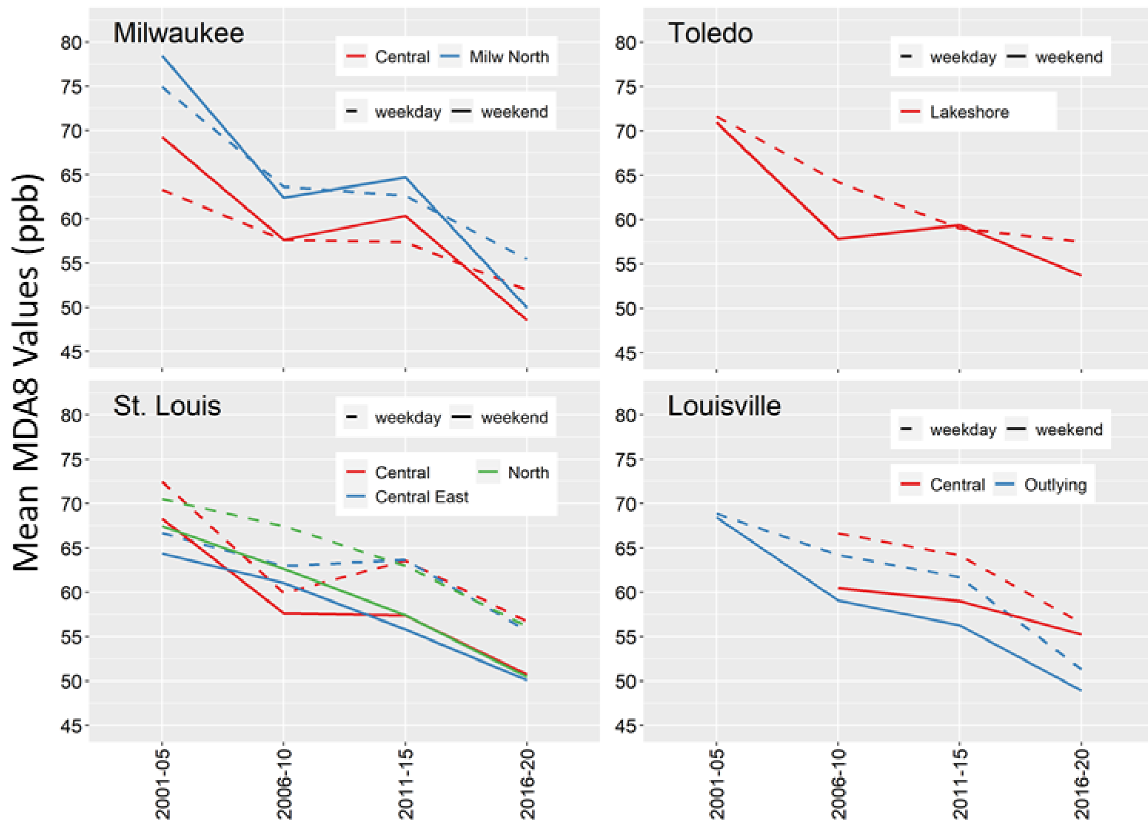

Figure A4.26. Trends in mean maximum daily 8-hour ozone (MDA8) concentrations on weekdays (Tue-Thu) and weekends (Sun) in the different monitor groups within the nonattainment areas.

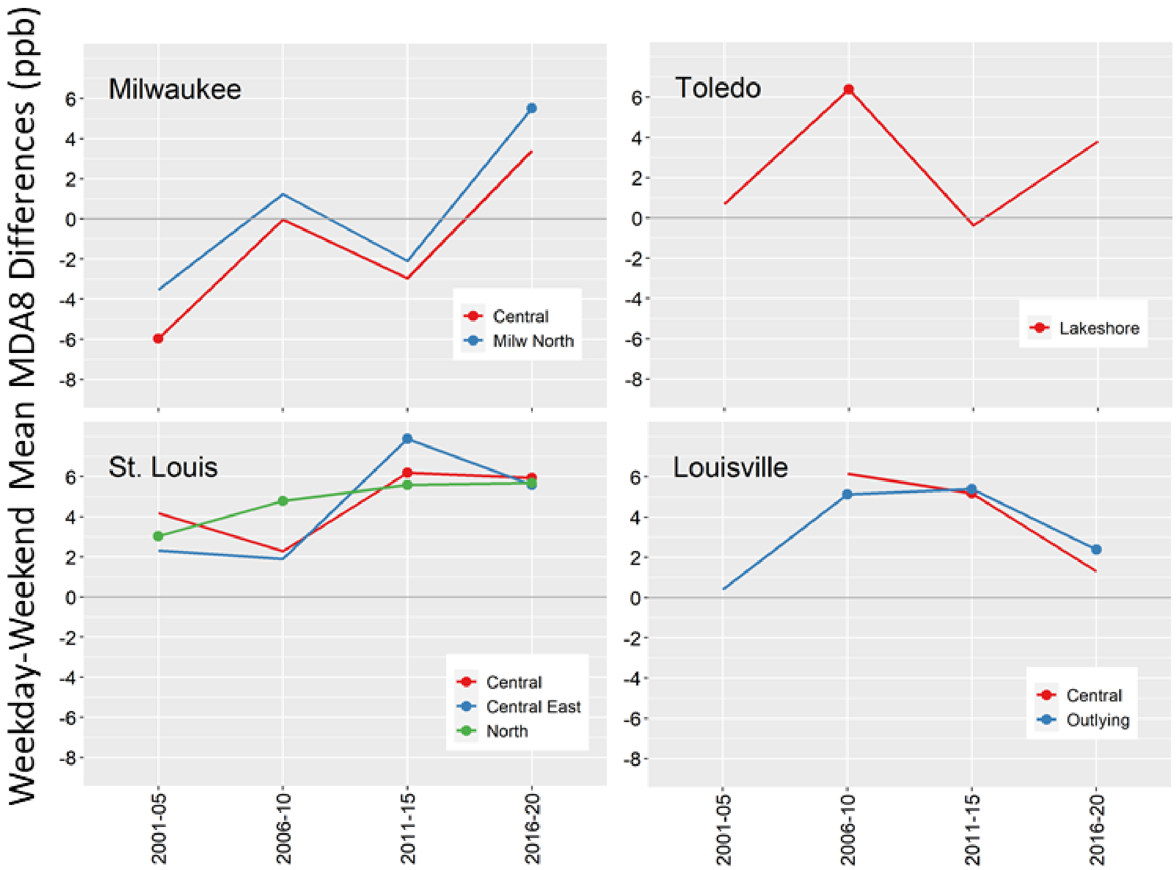

Figure A4.27. The weekday-weekend (W-W) difference in the mean MDA8 value for the LADCO nonattainment areas. The filled circles indicate statistically significant W-W differences. Positive values indicate NOx sensitivity and negative values indicate VOC sensitivity.

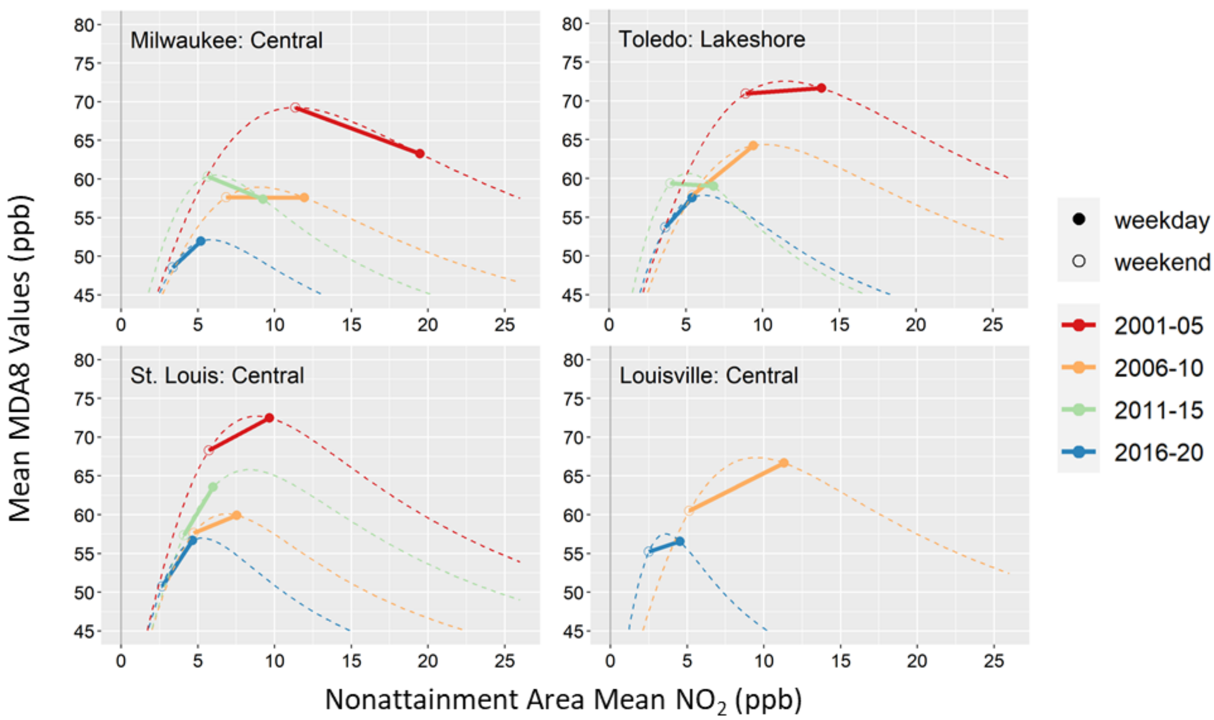

Figure A4.28. Plots of mean maximum daily 8-hour average (MDA8) ozone concentrations versus midday nonattainment area mean NO_2 concentrations on ozone-conducive weekdays (solid symbols) and weekend days (open symbols) during four sets of years. Curves (dashed lines) are included as visual aids and are not meant to be quantitative; these curves were developed as described in the text using an analytical model in which VOCR was tuned and the curve was scaled to fit the ozone MDA8 values. Louisville had no MDA8 monitoring data in the Central area during the 2001-05 period and no NO_2 data for ozone-conducive days during the 2011-15 period.

APPENDIX 5

Supplemental Figures: Ozone Trends over Space and Time

This appendix contains supplemental figures and tables for the analysis of ozone formation in the LADCO region using ozone trends over space and time. These figures and tables include:

- Maps of NO_2 concentrations in the LADCO region
- A list of monitoring sites and distances from the city centers
- Maps of ozone concentrations in all time periods
- Combined plots of ozone over distance and over time
- Ozone trends on a rolling 5-year average basis
- Ozone trends in Milwaukee and Toledo

Maps of NO_2 Concentrations in the LADCO Region

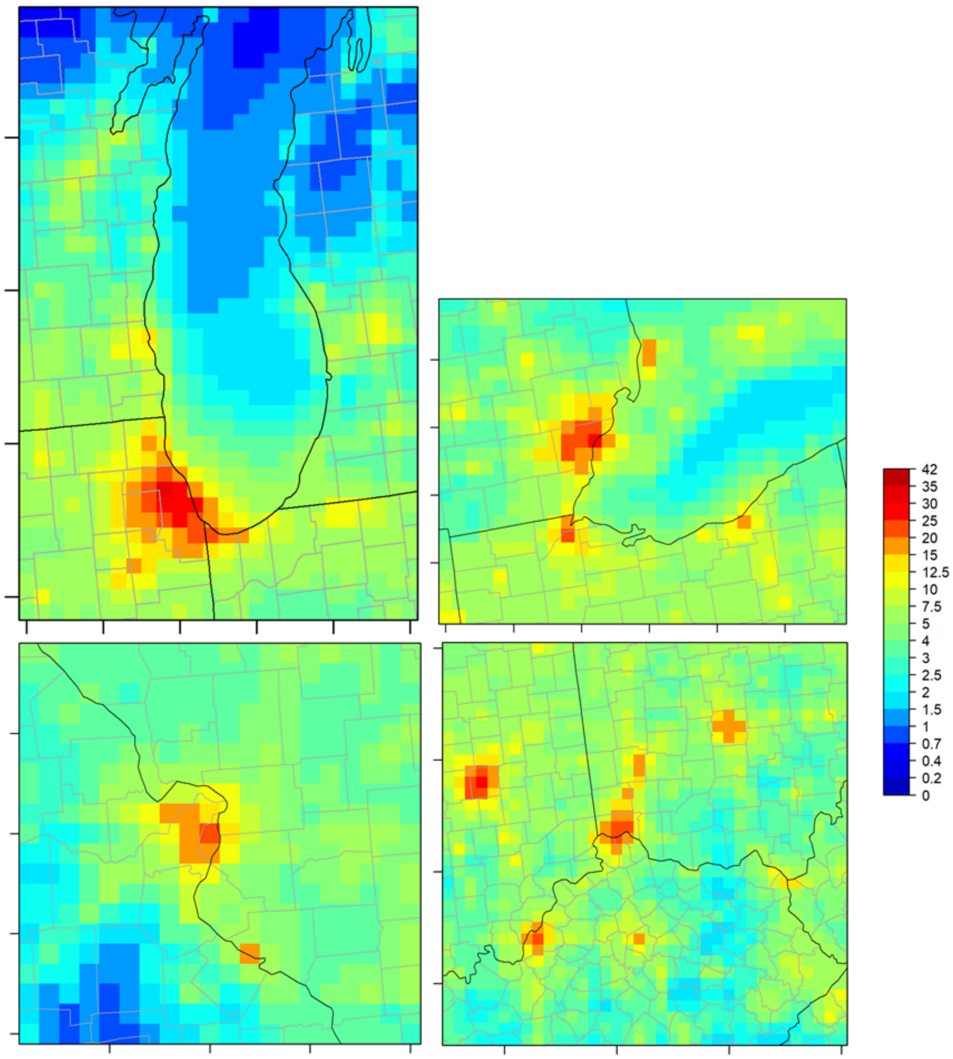

Figure A5.1. Average early morning (5:00-8:59 am CDT) NO_2 concentrations (ppb) on ozone season days from LADCO 12 km modeling (abc model run). Maps are shown for (top left) the Lake Michigan region, (top right) Detroit and Cleveland, (bottom left) St. Louis, and (bottom right) Louisville and Cincinnati.

VOC monitoring trends

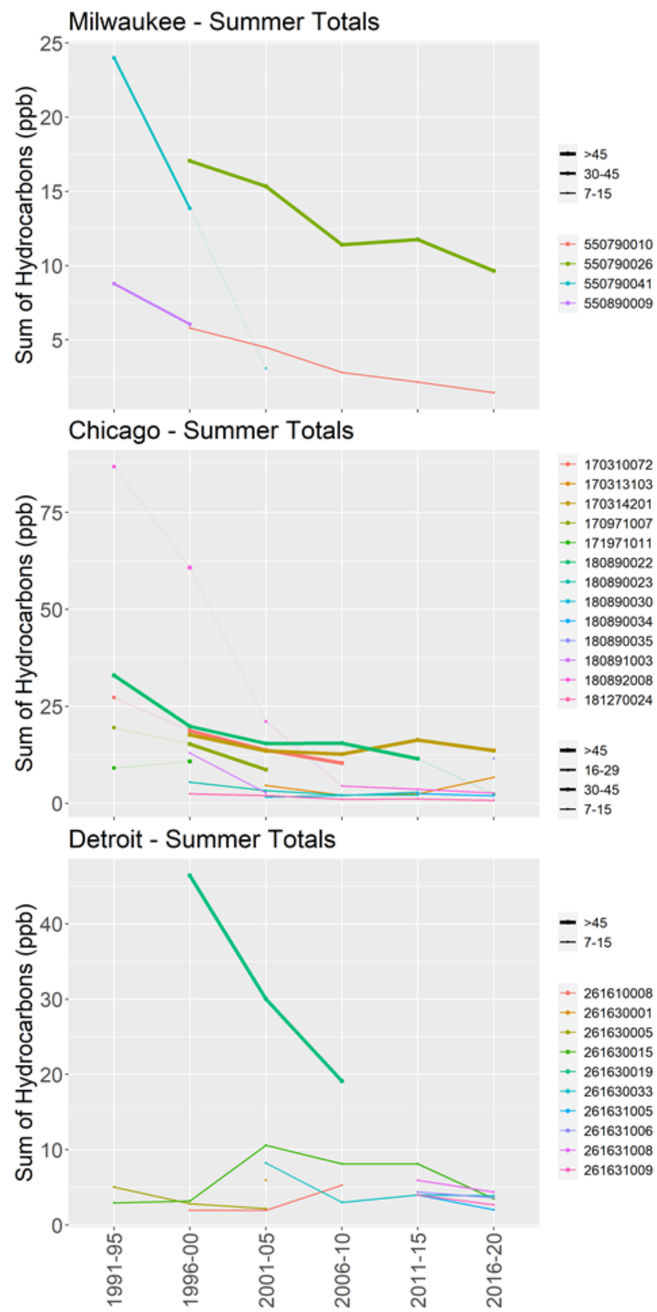

Figure A5.2. Sums of monitored hydrocarbons in the three nonattainment areas that had monitors measuring a complete or nearly complete set of PAMS compounds. The thickness of the lines and points indicates how many of the 54 PAMS hydrocarbon compounds were measured at that site in those years. The thinnest lines connect points indicating different numbers of monitors.

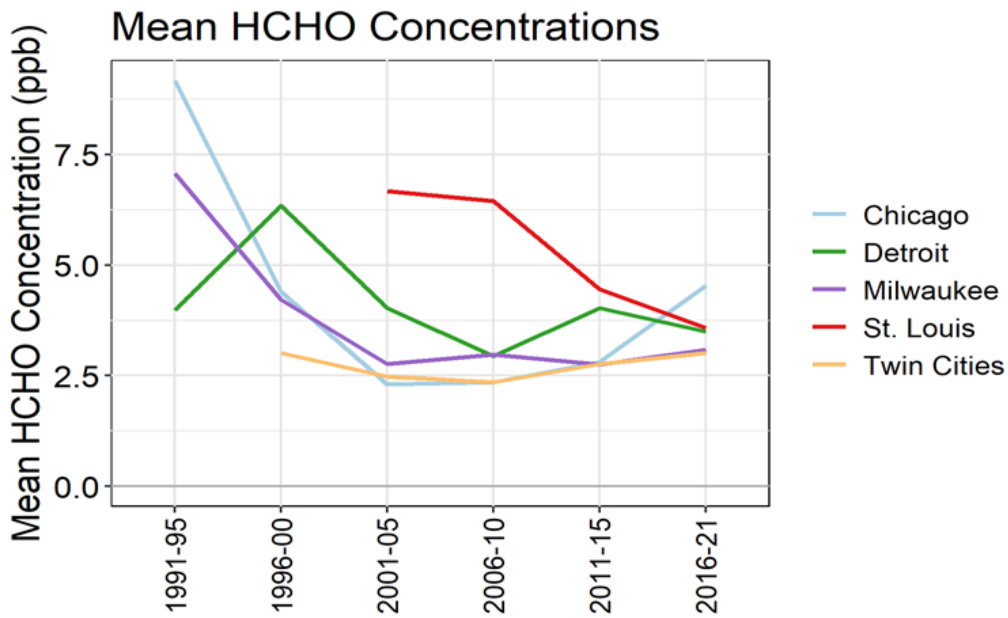

Figure A5.3. Trends in mean monitored formaldehyde (HCHO) concentrations. The lines show the mean concentrations in June through August at all monitors in the region, averaged by nonattainment area and by year grouping.

List of monitoring sites and distances from the city centers

Table A5.1. List of monitor sites in each urban area and the distance from the city center (km) for each monitoring site.

Chicago	
Site	**km**
170310042	0.6
170310063	0.7
170310072	2.4
170314002	10.5
170310064	10.6
170310037	11.1
170310032	15.9
170310076	16.2
170311003	17.4
170317002	20.1
170310050	20.3
170313103	22.2
170310001	25.1
180890030	25.2
170314007	27.4
170314006	28.1
170318003	28.5
180892008	29.5
170314201	31.6
170436001	37.5
170970001	37.9
170311601	38.3
180891016	40.0
180890022	41.1
181270024	46.6
171971008	49.1
181270020	53.3
170973001	53.7
170890005	56.2
170971002	58.5
171110001	62.9
180910005	62.9
181270026	64.5
170971007	66.5
550590019	70.5
180890024	71.1
550590002	76.7
550590025	81.8
180910010	83.7
171971011	87.1
550590022	87.3
551010017	93.2

Cincinnati	
Site	**km**
390610040	3.0
211170007	3.6
210370003	7.3
210373002	9.9
390610010	19.2
390610006	23.5
390170023	31.2
390250022	32.6
210150003	35.5
391651002	45.0
391650007	45.2
390170018	48.4
390179991	50.9
390271002	72.6
390570006	79.7
212090001	79.8
391130037	82.6
391351001	83.0
391130019	83.6
390230003	94.7

Cleveland	
Site	**km**
390350060	1.9
390350034	11.3
390355002	19.9
390350064	21.4
390850003	29.3
390930018	34.9
390550004	37.1
390850007	45.0
391331001	47.0
391530020	47.1
391030003	48.5
391030004	53.0
391511009	76.8
391514005	79.7
391510016	79.7
391510022	88.4
391550011	91.1
391550009	92.3
391550013	92.4

Detroit	
Site	**km**
261630016	5.3
261630019	11.8
261630001	17.6
261250001	18.7
260991003	20.6
261610008	46.9
260990009	49.1
261470030	49.9
261610005	55.2
261619991	71.4
390950034	76.1
390950035	76.1
390950081	76.6
260910007	83.4
261470005	84.4
390950024	86.8
260490021	94.8
260492001	99.2

Louisville	
Site	**km**
211111021	4.5
180431004	8.6
211110067	9.7
180190008	17.6
211110027	20.7
211110051	24.6
210290006	30.1
211850004	32.1
210930006	61.5
181230009	75.4
180710001	79.0
212299991	87.4

Minneapolis	
Site	**km**
270530962	1.6
270031002	18.4
271390505	28.4
271630027	33.2
271636015	35.9
270376018	39.1
271713201	40.9
271636016	44.7
270031001	47.4
551091002	50.2
270495302	59.4
271453052	93.2
550950001	99.5

St. Louis	
Site	**km**
295100072	0.3
295100085	3.3
171630010	3.8
295100086	6.2
295100007	10.9
291893001	13.4
291895001	17.2
291890004	19.1
171192007	23.1
171191009	23.6
290990012	25.3
291890014	25.8
291890006	25.9
290990019	26.2
171193007	27.2
291831002	27.4
291831004	37.2
291890005	46.6
171199991	56.9
171570001	61.6
291130004	73.1
291860005	82.9
171170002	91.8

Table A5.2. List of monitor sites in the Lake Michigan area and the distance from the Chicago city center (km) for each monitoring site.

Cook County		*East Lake*		*West Lake*	
Site	**km**	**Site**	**km**	**Site**	**km**
170310042	0.6	180890030	25.2	170970001	37.9
170310063	0.7	180892008	29.5	170973001	53.7
170310072	2.4	180891016	40.0	170971002	58.5
170314002	10.5	180890022	41.1	170971007	66.5
170310064	10.6	181270024	46.6	550590019	70.5
170310037	11.1	181270020	53.3	550590002	76.7
170310032	15.9	180910005	62.9	550590025	81.8
170310076	16.2	260210014	114.9	550590022	87.3
170311003	17.4	260050003	156.8	551010017	93.2
170317002	20.1	261210039	189.0	551010020	100.1
170310050	20.3	261050007	254.5	550790085	145.9
170313103	22.2	261010922	292.0	550890008	163.8
170310001	25.1	260190003	327.8	550890009	179.9
170314007	27.4			551170004	198.2
170314006	28.1			551170006	198.2
170318003	28.5			550710007	250.5
170314201	31.6			550610002	284.5
170311601	38.3			550290004	376.2

Maps of ozone concentrations in all time periods

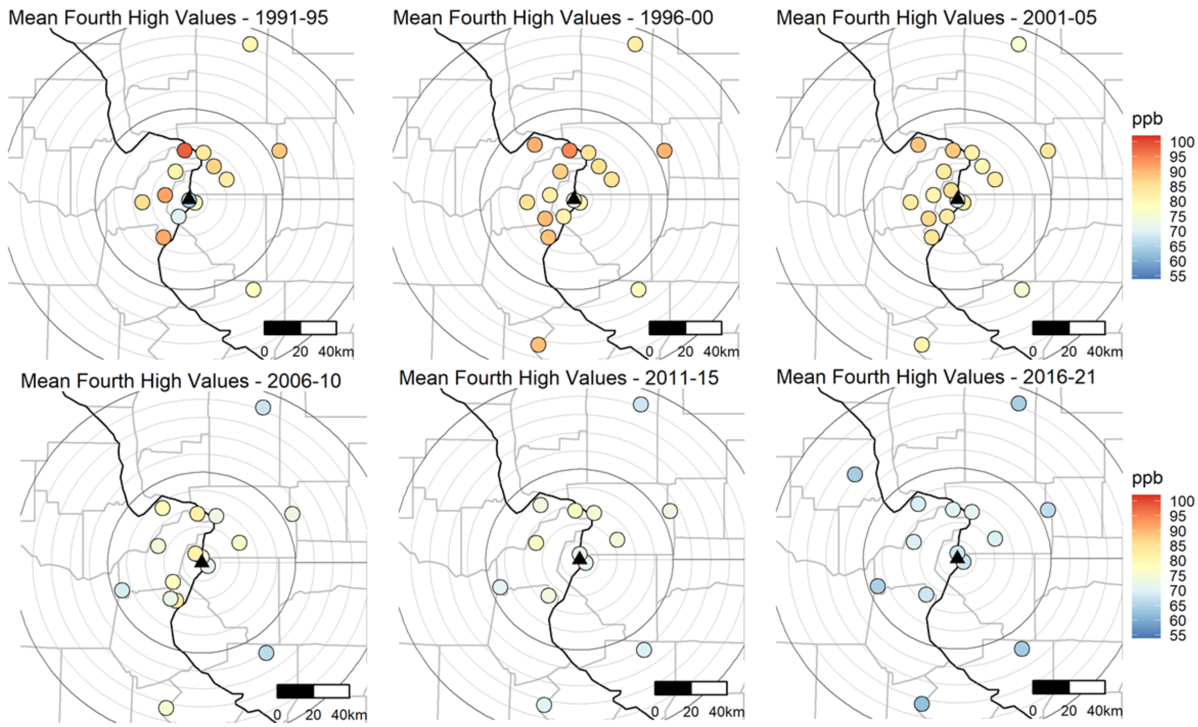

Figure A5.4. Maps of mean annual fourth high maximum daily 8-hour average (MDA8) ozone concentrations in ppb in the St. Louis area in each time period, as labeled. The black triangles show the location of the city center. The concentric circles show the distance from the city center, with the light lines being 10 km apart and the darker lines being 50 km apart.

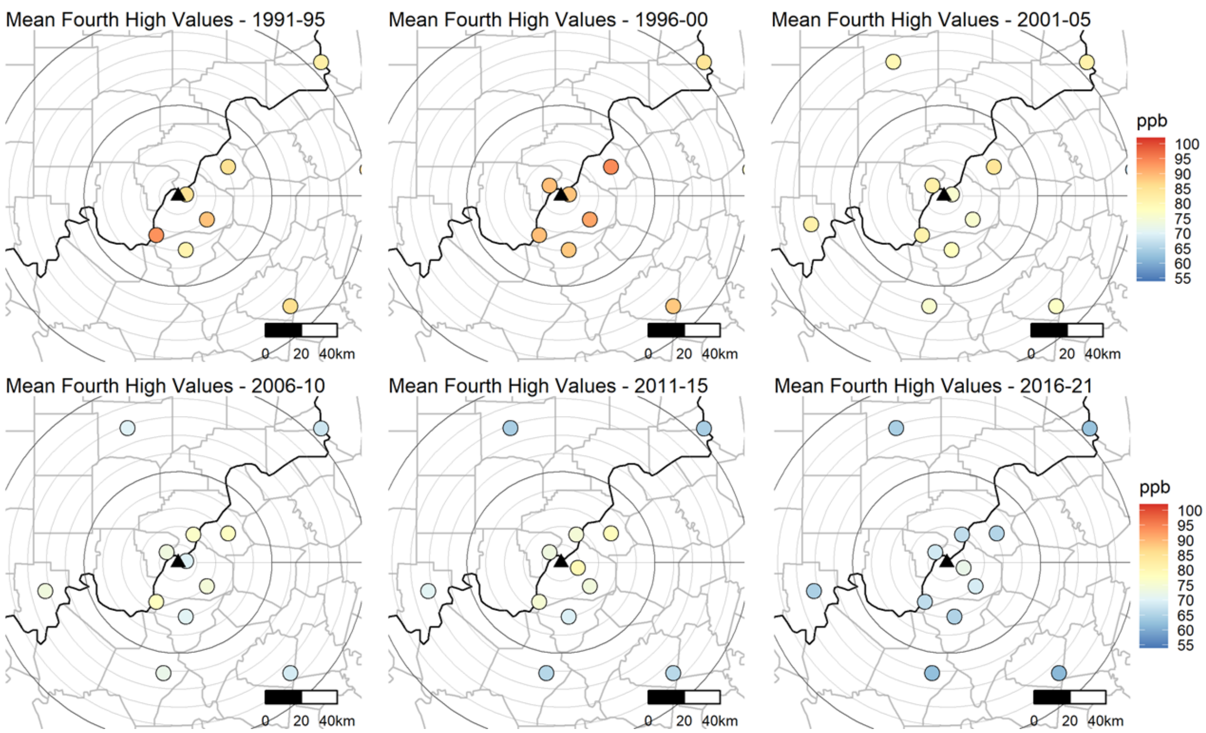

Figure A5.5. Maps of mean annual fourth high maximum daily 8-hour average (MDA8) ozone concentrations in ppb in the Louisville area in each time period, as labeled. The black triangles show the location of the city center. The concentric circles show the distance from the city center, with the light lines being 10 km apart and the darker lines being 50 km apart.

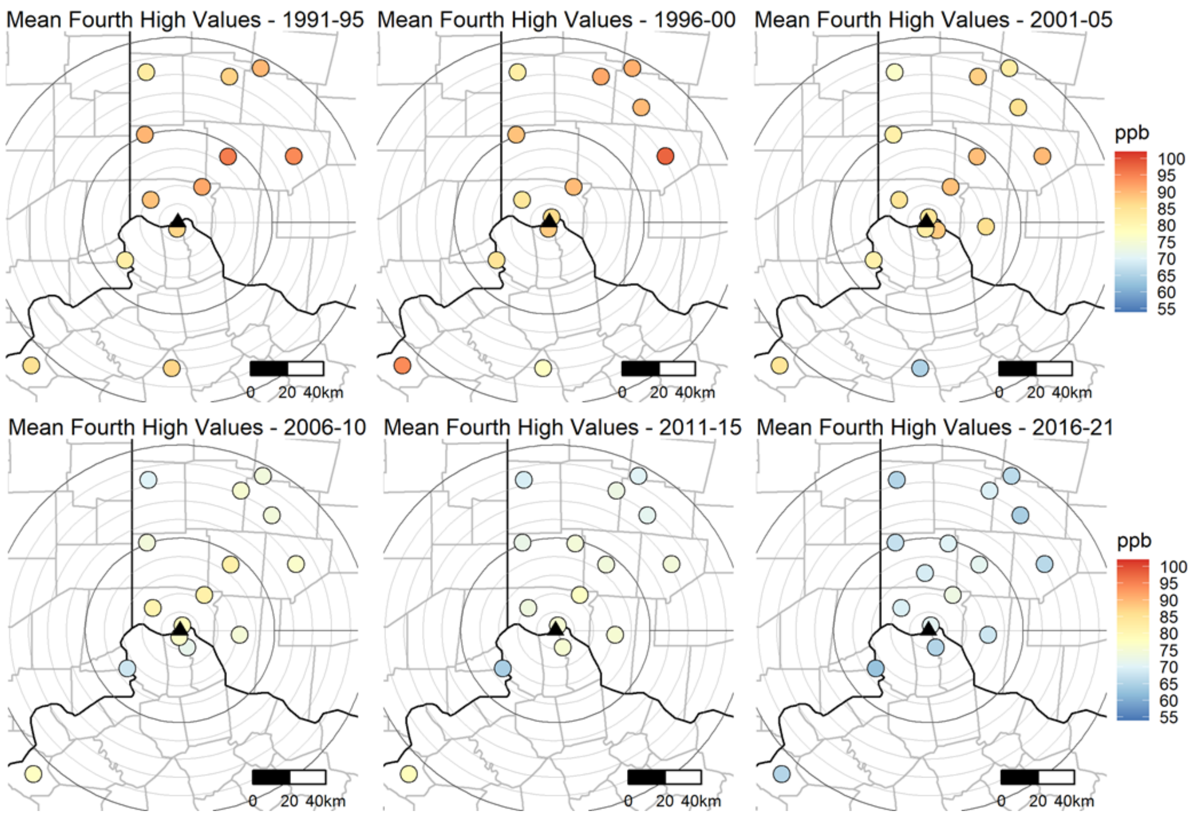

Figure A5.6. Maps of mean annual fourth high maximum daily 8-hour average (MDA8) ozone concentrations in ppb in the Cincinnati area in each time period, as labeled. The black triangles show the location of the city center. The concentric circles show the distance from the city center, with the light lines being 10 km apart and the darker lines being 50 km apart.

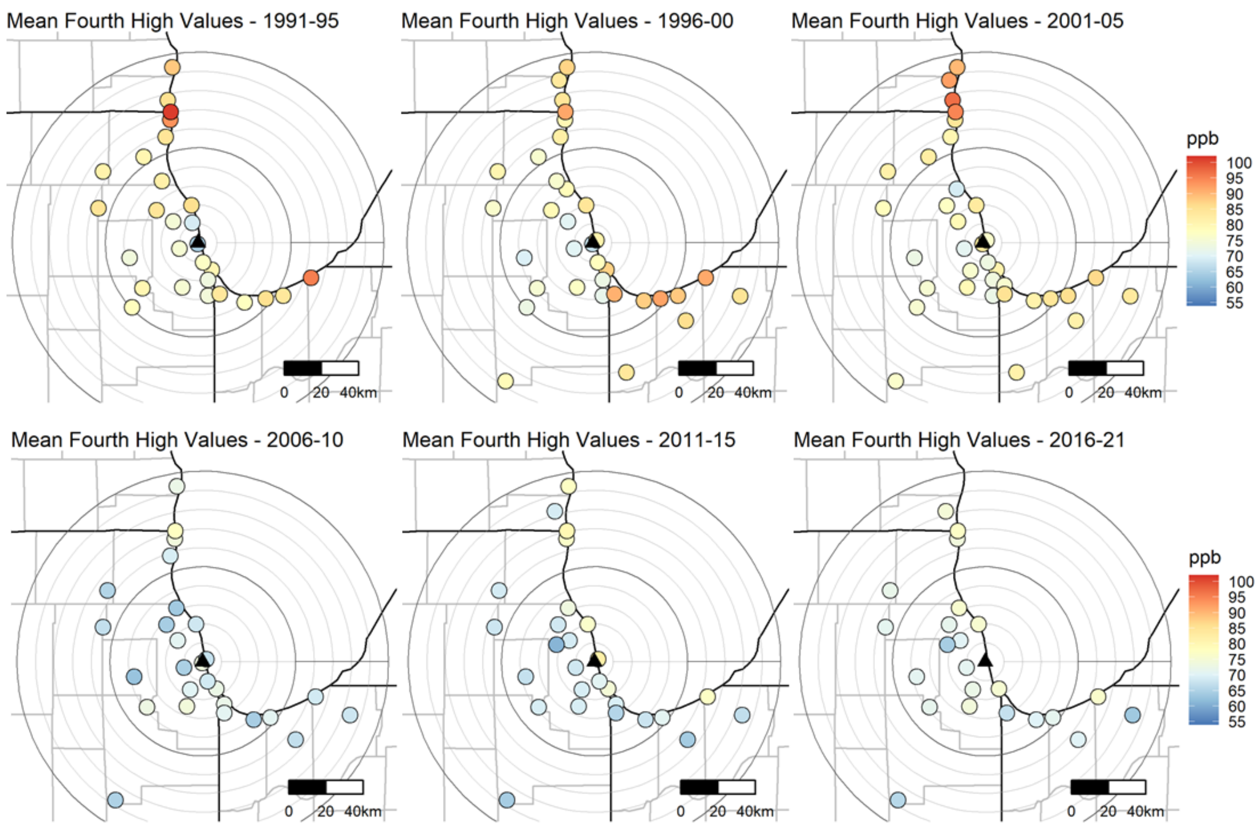

Figure A5.7. Maps of mean annual fourth high maximum daily 8-hour average (MDA8) ozone concentrations in ppb in the Chicago area in each time period, as labeled. The black triangles show the location of the city center. The concentric circles show the distance from the city center, with the light lines being 10 km apart and the darker lines being 50 km apart.

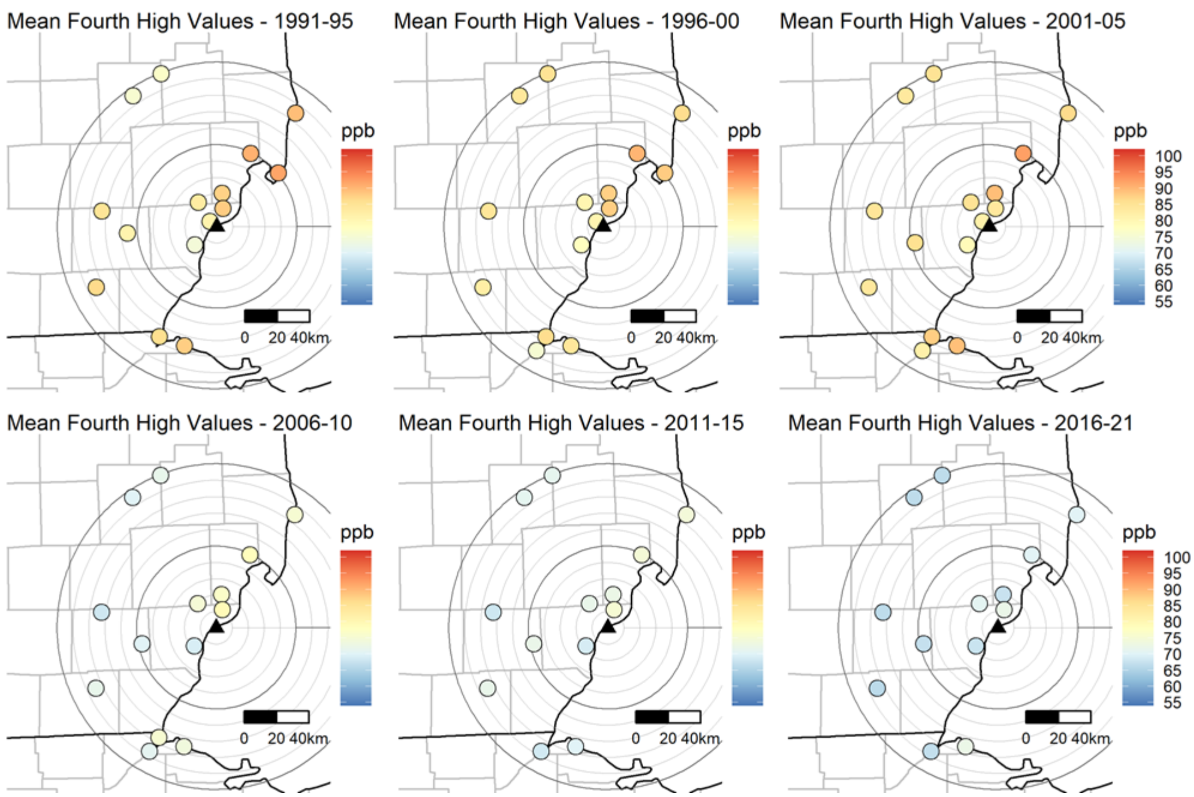

Figure A5.8. Maps of mean annual fourth high maximum daily 8-hour average (MDA8) ozone concentrations in ppb in the Detroit area in each time period, as labeled. The black triangles show the location of the city center. The concentric circles show the distance from the city center, with the light lines being 10 km apart and the darker lines being 50 km apart.

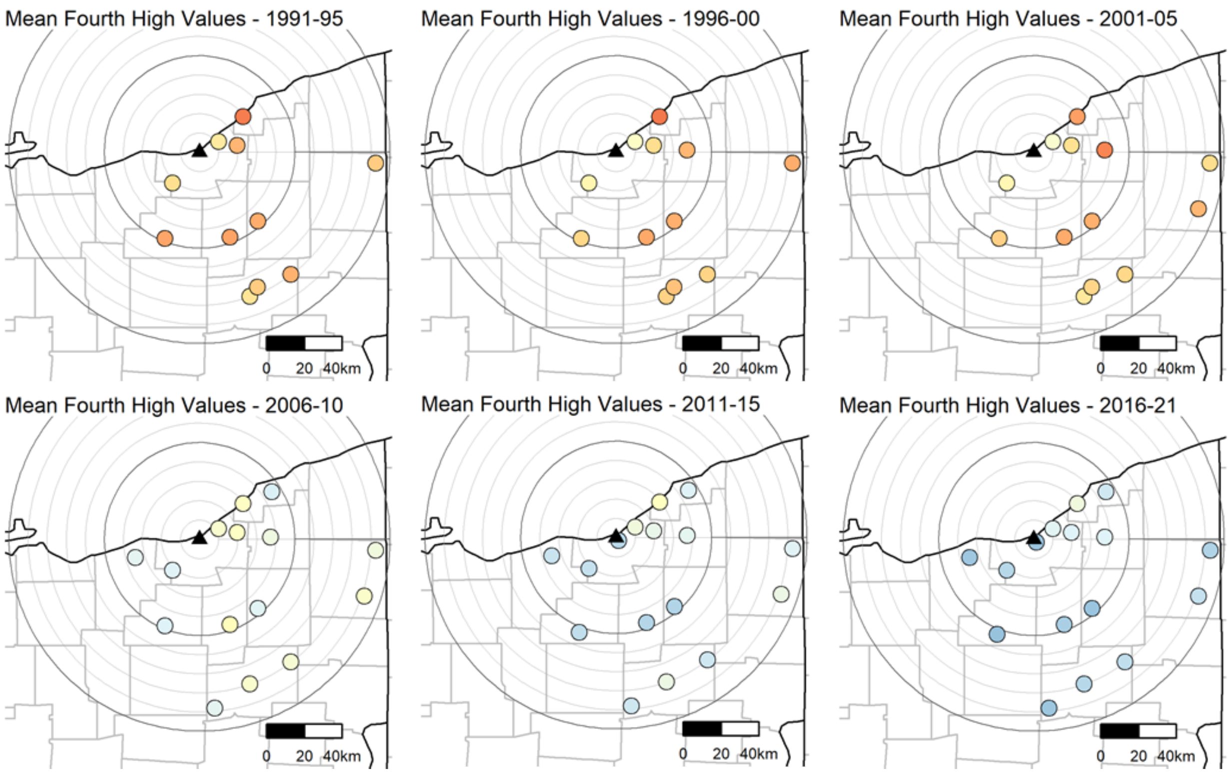

Figure A5.9. Maps of mean annual fourth high maximum daily 8-hour average (MDA8) ozone concentrations in ppb in the Cleveland area in each time period, as labeled. The black triangles show the location of the city center. The concentric circles show the distance from the city center, with the light lines being 10 km apart and the darker lines being 50 km apart.

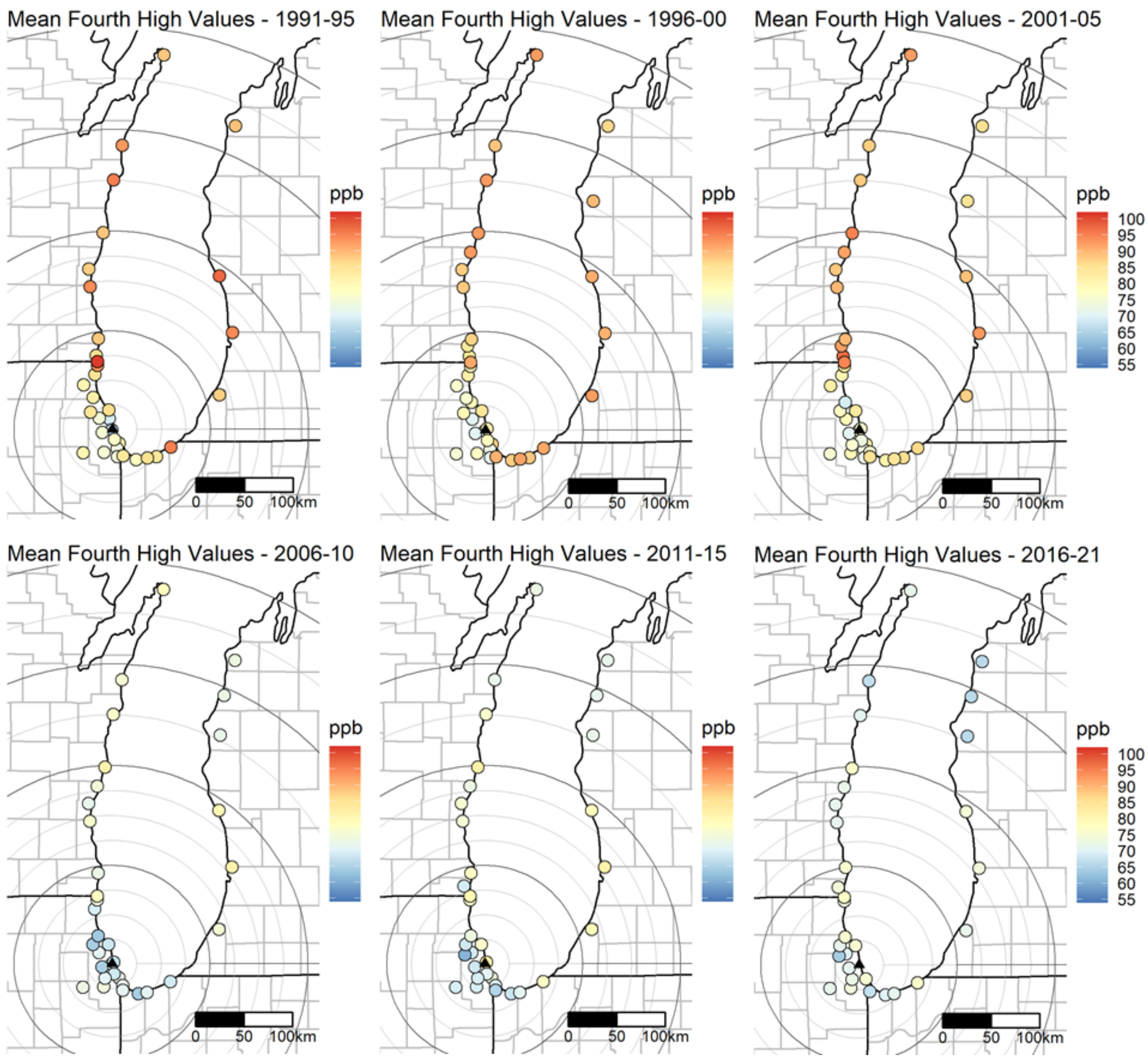

Figure A5.10. Maps of mean annual fourth high maximum daily 8-hour average (MDA8) ozone concentrations in ppb in the Lake Michigan region in each time period, as labeled. The black triangles show the location of the Chicago city center. The concentric circles show the distance from the Chicago city center, with the light lines being 25 or 50 km apart and the darker lines being 100 km apart.

Combined plots of ozone over distance and over time

In generating plots of O_3 fourth high values versus distance from the city center (x) and year (y), we used spatial interpolation between the points to generate surface plots. We used the *gam* (Generalized Additive Model) function in the *mgcv* package in *R* for this, and we used data that was not binned by year or distance for these plots.

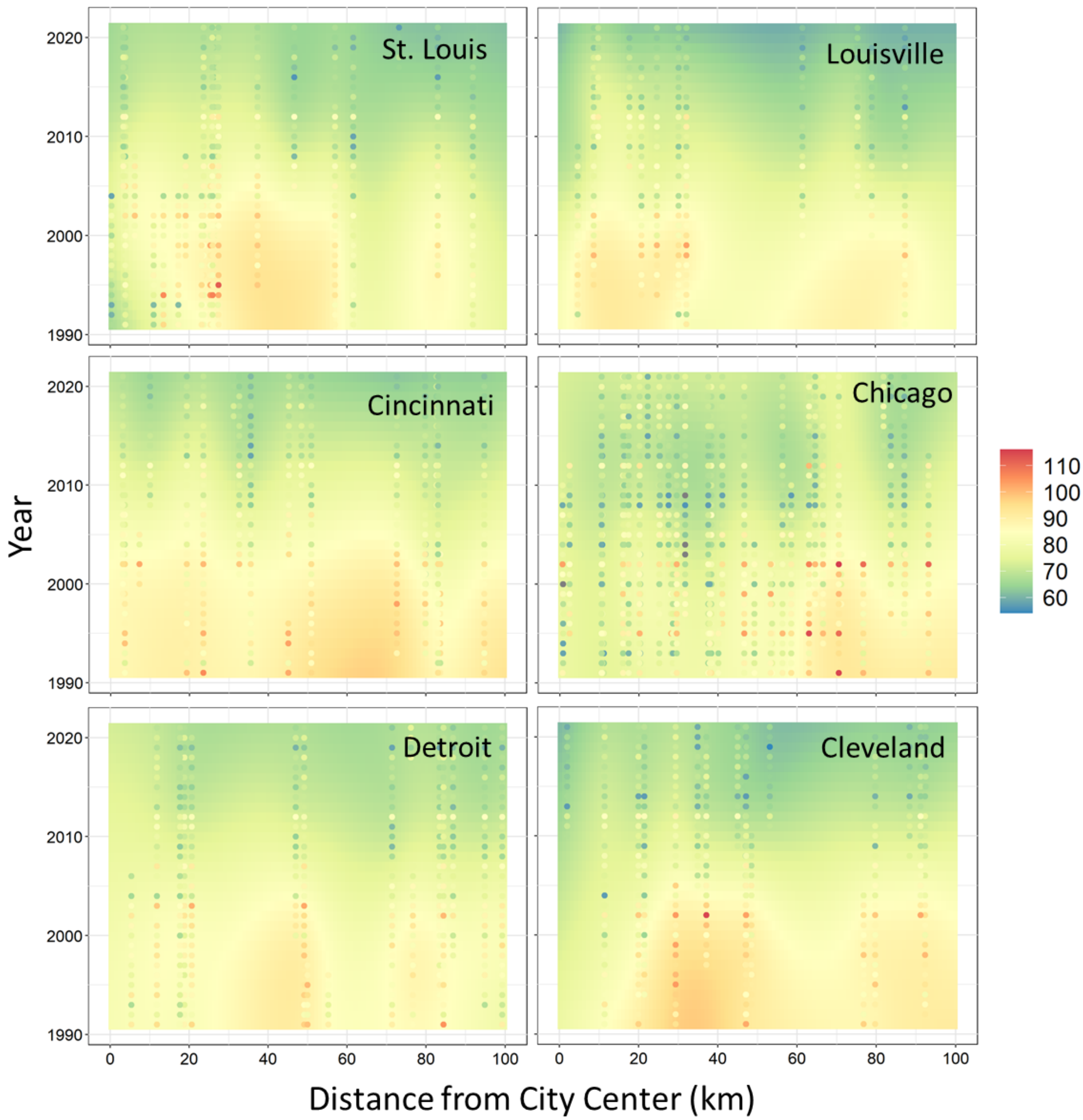

Figure A5.11. Combined plots of ozone fourth high MDA8 concentrations at monitors (in ppb) shown versus distance from the city center (x) and year (y) for the urban nonattainment areas, with data not averaged by distance or year. The shaded surfaces were determined using spatial interpolation with a GAM model.

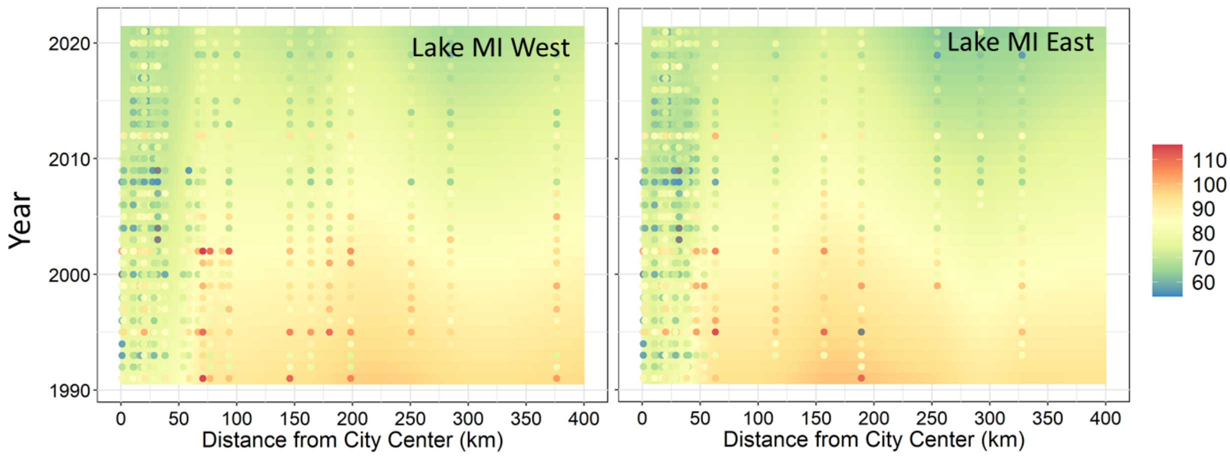

Figure A5.12. Combined plots of ozone fourth high MDA8 concentrations (in ppb) shown versus distance from the city center (x) and year (y) for the (left) western and (right) eastern sides of Lake Michigan, with data not averaged by distance or year. The shaded surfaces were determined using spatial interpolation with a GAM model.

Ozone Trends on a Rolling 5-Year Average Basis

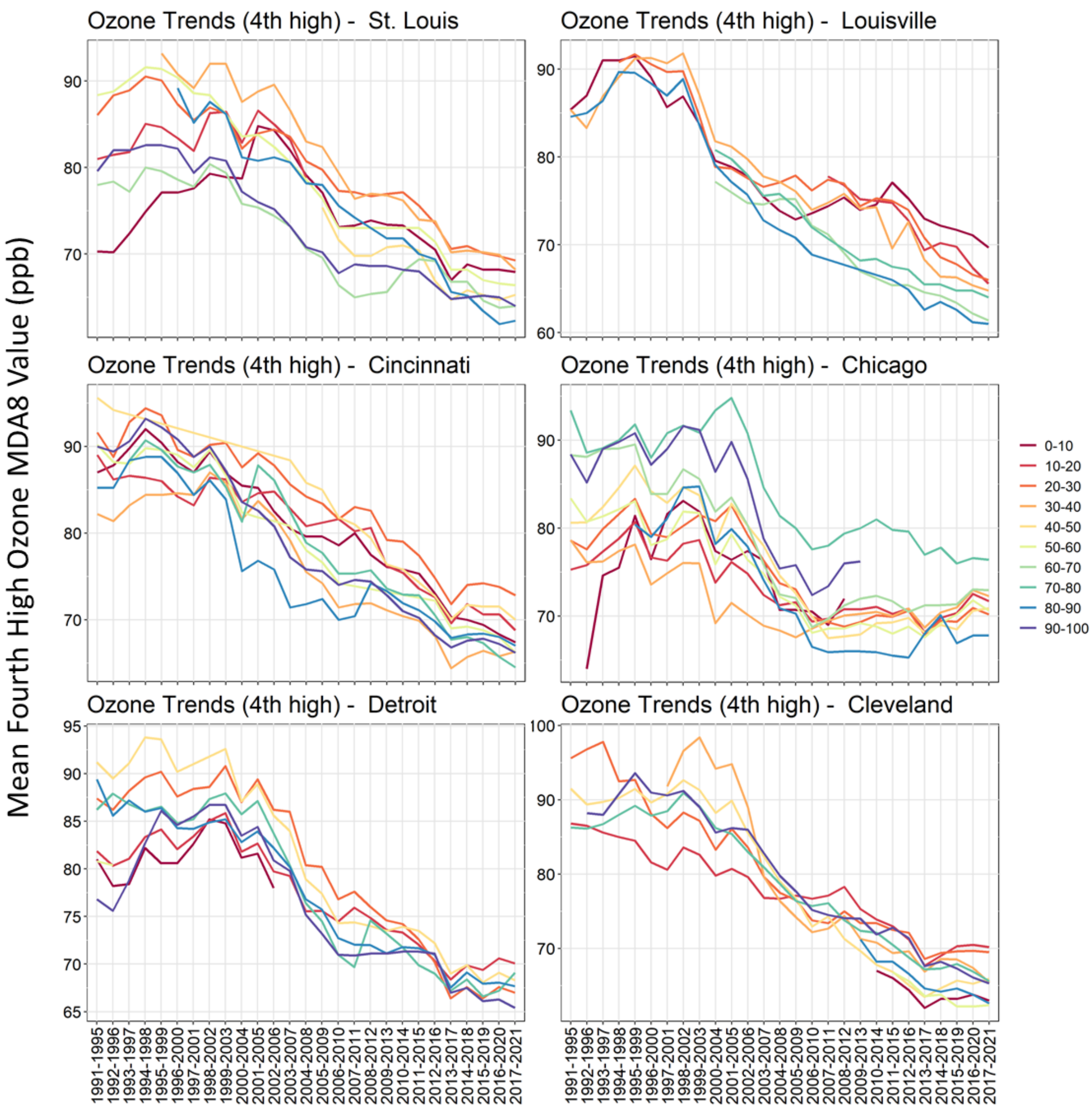

Figure A5.13. Mean fourth high MDA8 ozone concentrations for the urban nonattainment areas plotted versus different year groups, with different lines for the different distance bins. Year groups are shown on a 5-year rolling average basis.

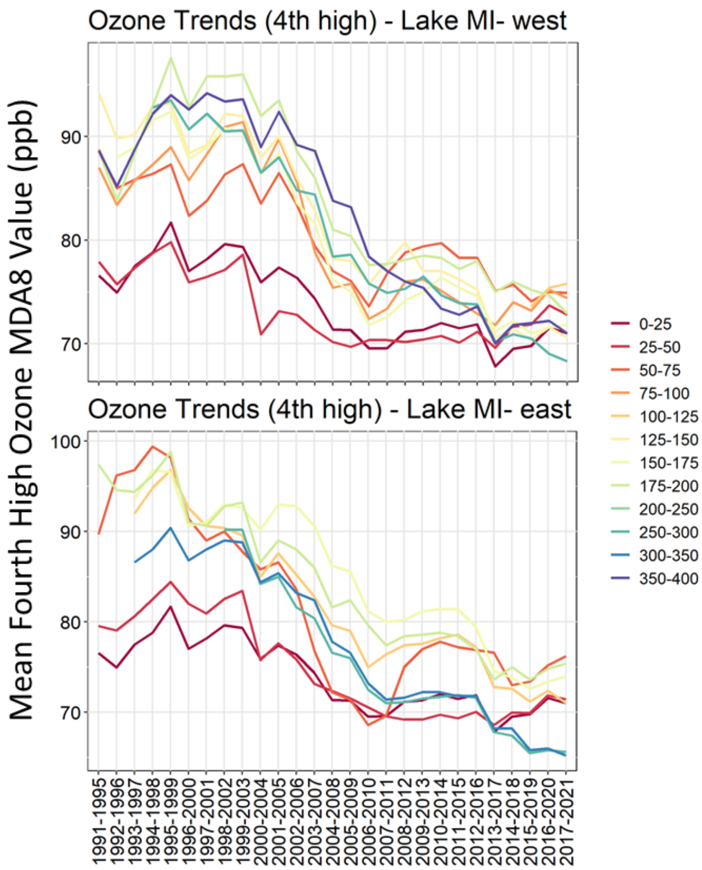

Figure A5.14. Mean fourth high MDA8 ozone concentrations for the Lake Michigan lakeshore region plotted versus different year groups, with different lines for the different distance bins. Year groups are shown on a 5-year rolling average basis.

APPENDIX 6

Sensitivity Observations for Individual Nonattainment Areas around Lake Michigan and Areas of Interest in Ohio

This section applies the sensitivity indicator ratio approaches based on the TROPOMI satellite and CAMx model discussed in the main body of the report to (1) individual nonattainment areas around Lake Michigan in Wisconsin and Michigan and (2) to other areas of interest for ozone formation in Ohio. To simplify comparison of the different parts of the LADCO region, the main report combined four nearby nonattainment areas in Wisconsin (Milwaukee, Sheboygan, Manitowoc, and Door) into one area ("Wisconsin Lakeshore"). The report also combined three nonattainment areas in Michigan (Muskegon, Allegan, and Berrien) into one area ("Western Michigan"). This part of the appendix evaluates the TROPOMI-, CAMx-, and trends-derived results for each individual nonattainment area. Sections 5.2.7 and 5.2.8 of the main document provide a synthesis discussion of ozone formation along these two lakeshores, including references to the figures in this document. This appendix provides and discusses data for each nonattainment area but does not include an additional synthesis discussion.

The report only examined current nonattainment areas in the LADCO region. However, the state of Ohio includes two other areas whose ozone concentrations are of interest. The Columbus, OH area, was originally designated "nonattainment" for the 2015 ozone NAAQS and has since been redesignated to "attainment/maintenance" of this standard. The Toledo, OH area, was designated "attainment" of the 2015 ozone NAAQS but which has had several design values exceeding the level of the 2015 ozone NAAQS. This part of the appendix evaluates the TROPOMI and CAMx-derived sensitivity indicator results for these two areas and compares them with those for nearby nonattainment areas in Detroit, Cleveland, and Cincinnati. TROPOMI results were composited for days that exceeded the standard in Columbus but were not composited for Toledo exceedance days. Accordingly, we evaluated the results in Toledo on days that exceeded the 2015 ozone NAAQS in the nearby areas of Detroit and Cleveland. This appendix includes a synthesis discussion of the data available for both Toledo and Columbus.

Wisconsin Lakeshore and Western Michigan Nonattainment Areas

Figure A6.1 shows the location of each nonattainment area or area of interest and the grid cells included in each area.

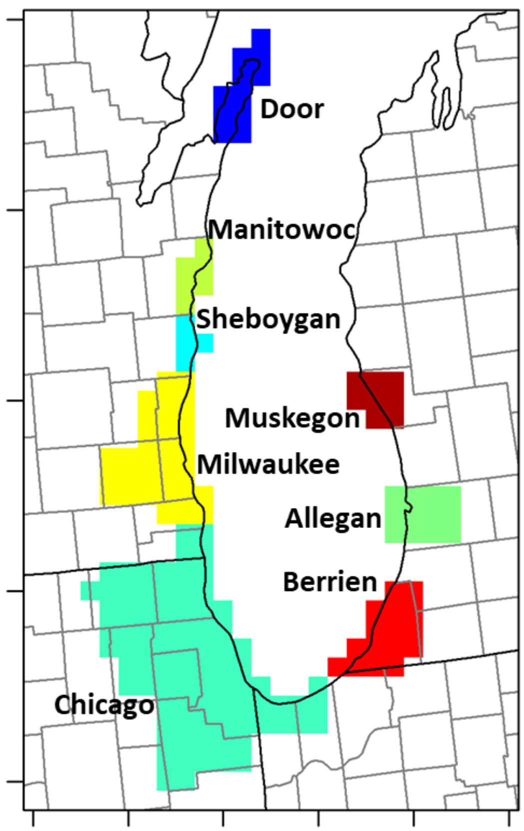

Figure A6.1. Maps showing the grid cells included in each individual nonattainment area in the Lake Michigan region. Nonattainment area grid cells are color-coded by area. The Wisconsin lakeshore area discussed in the report includes the Door, Manitowoc, Sheboygan, and Milwaukee areas. The Western Michigan area includes the Muskegon, Allegan, and Berrien areas.

TROPOMI-Derived Formaldehyde-to-NO_2 ($HCHO/NO_2$) Ratio

Figure A6.2 shows the ozone exceedance day results for the individual nonattainment areas along the Wisconsin lakeshore and in Western Michigan. (Figure # in the main report shows maps of this data.) NO_2 columns are consistently low in these nonattainment areas, around 2.75e15 mol/cm^2, with lower values for the most remote area, Door County, WI and the most variable values in the most urbanized area, Milwaukee. HCHO columns were lowest in the Milwaukee area and highest in Sheboygan, Door and Berrien counties. Median $HCHO/NO_2$ ratios were relatively high, in the NOx-sensitive range, varying from 4.8 to 5.9, with the lowest values in the Milwaukee area and in Allegan County, MI, and the highest values in remote Door County, WI. Ozone formation in 10% of the grid cells in Milwaukee was transitional, however the rest of this nonattainment area had NOx-sensitive ozone formation. Ozone formation in all of the remaining nonattainment areas in Wisconsin and Western Michigan was NOx-sensitive on ozone exceedance days.

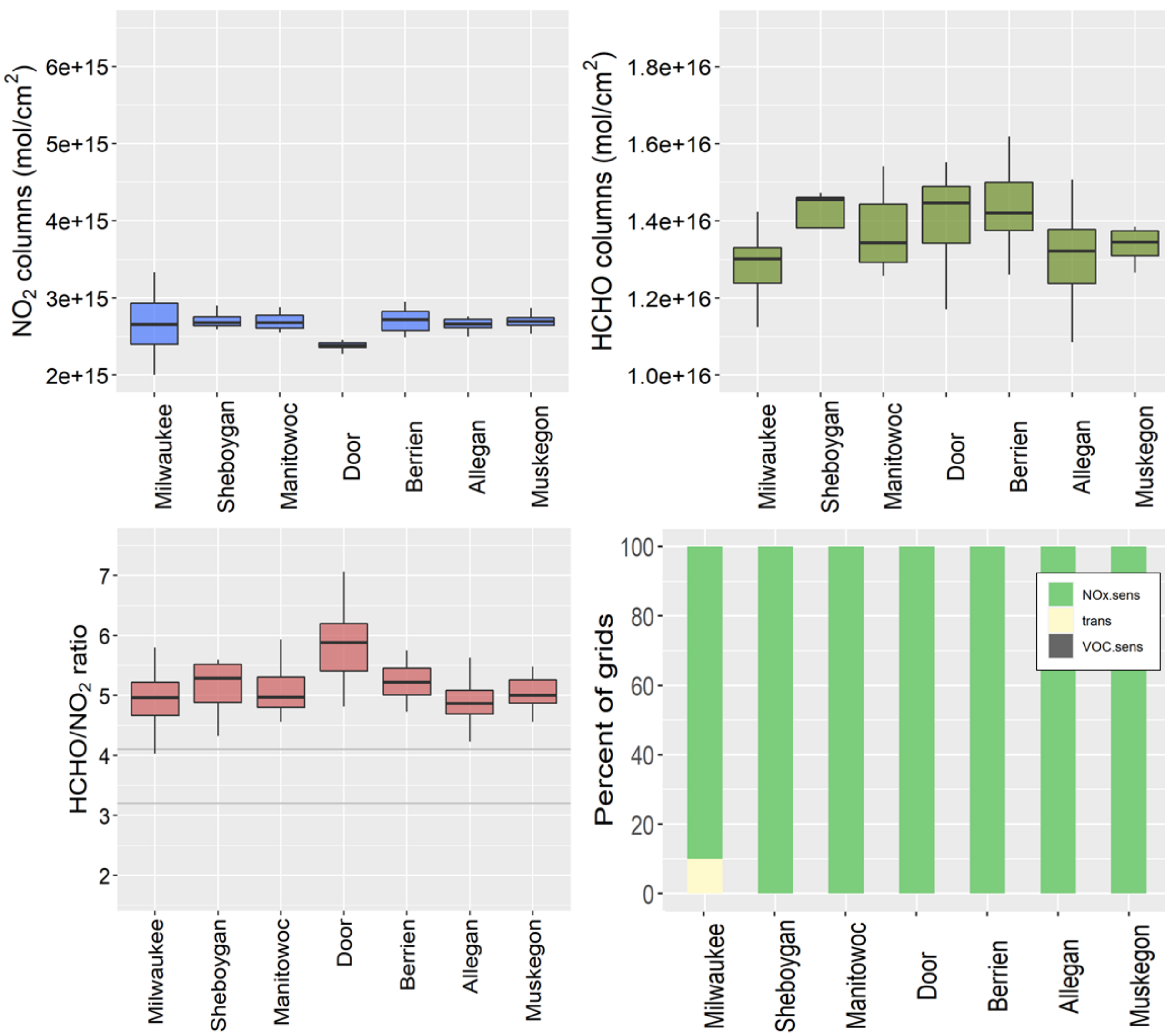

Figure A6.2. TROPOMI data for individual nonattainment areas on exceedance days on the Wisconsin lakeshore and in Western Michigan, as shown in Figure A3. Boxplots of TROPOMI satellite NO_2 columns (top left, mol/cm^2), HCHO columns (top right, mol/cm^2), HCHO/NO_2 ratios (bottom left), and the distribution of ozone formation sensitivity. Sensitivity regimes are determined from HCHO/NO_2 ratios using ratio thresholds from Jin et al. (2020).

Model-Based Indicator Ratios: Formaldehyde-to-NO_2 ($HCHO/NO_2$) and Hydrogen Peroxide-to-Nitric Acid (H_2O_2/HNO_3) Ratios

Figures A6.3 through A6.4 show the model-derived concentrations of ozone, VOCs, and the ozone sensitivity indicator compounds (NO_2, HCHO, HNO_3 and H_2O_2) in the different nonattainment areas along the Wisconsin lakeshore and western Michigan in each of the three model years. The model represents ozone concentrations as decreasing moving farther northward along the lake, with the lowest concentrations in Door County, Wisconsin. The concentrations of NO_2, HCHO, HNO_3, and H_2O_2 follow the opposite trends, with the highest concentrations in the southernmost areas. VOCs follow a more irregular pattern.

The $HCHO/NO_2$ ratios suggest that ozone formation becomes increasingly NOx-sensitive moving northward along the Wisconsin lakeshore (Figure A#). The median value in Milwaukee was transitional in 2016, with about 25% of the grid cell-days being VOC-sensitive, roughly 35% being transitional, and the remaining 40% being NOx-sensitive. Sheboygan, located just north of the Milwaukee area, was more NOx-sensitive than Milwaukee but had a median value in the transitional range in 2016. Both Manitowoc and Door counties were primarily NOx-sensitive in 2016. All of these areas shifted to mostly NOx-sensitive by 2028, including Milwaukee. All of the western Michigan areas were primarily NOx-sensitive in all three years and became more NOx-sensitive over time. Allegan was the most NOx-sensitive of the three areas.

The H_2O_2/HNO_3 ratios suggested that almost all the Wisconsin and Michigan portions of the Lake Michigan region were NOx-sensitive in all years (Figure A#). The Wisconsin lakeshore areas became more NOx-sensitive moving to the north, whereas the ratios in the western Michigan areas were more consistent.

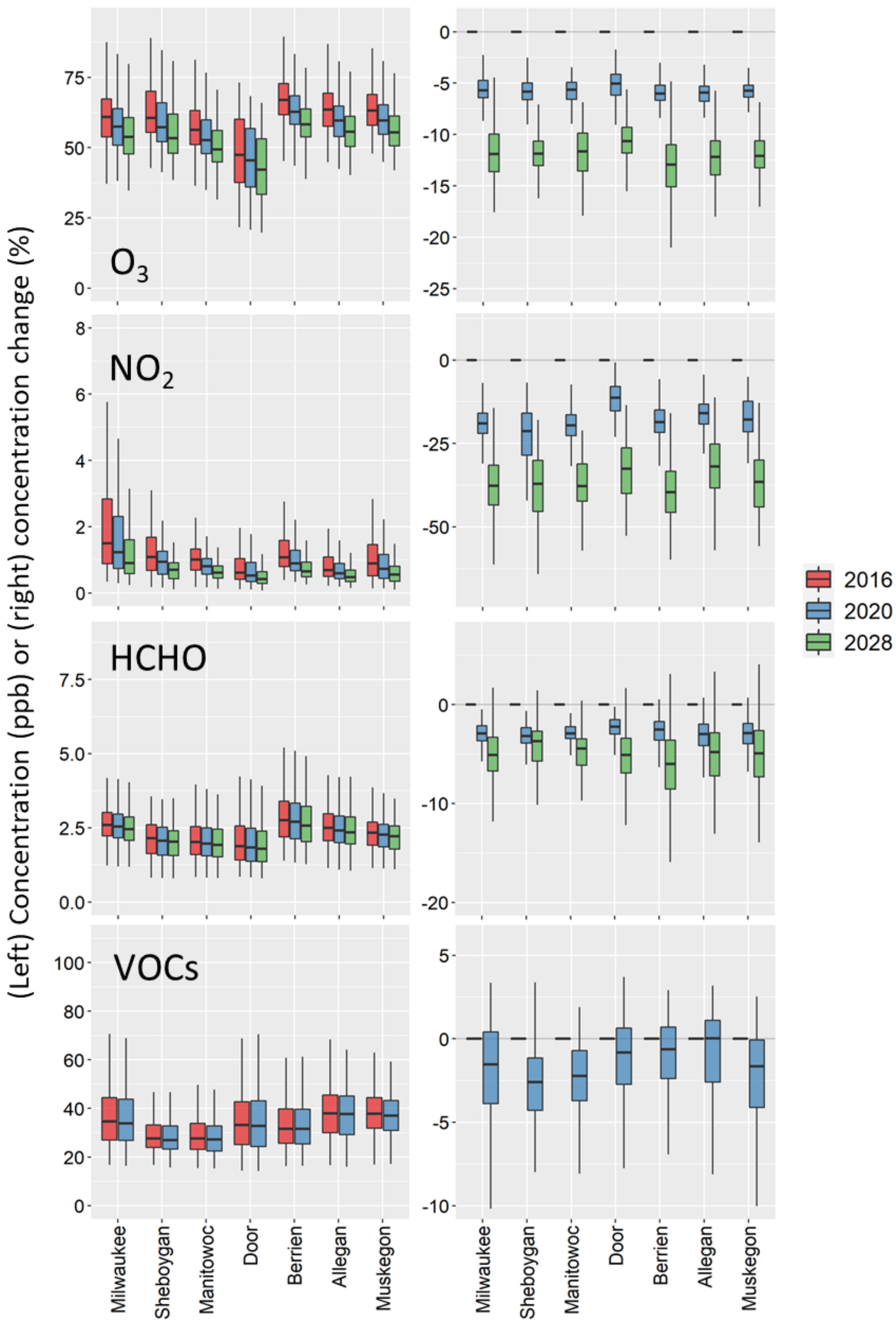

Figure A6.3. Modeled concentrations (left) and percent concentration changes (right) of O_3, NO_2, HCHO, and total VOCs in the early afternoon (13:00-16:59 LDT) on exceedance days in the Wisconsin and western Michigan nonattainment areas. The 2016 values are from the LADCO_2016abc model run except for VOCs, which come from the LADCO_2016aa2a run.

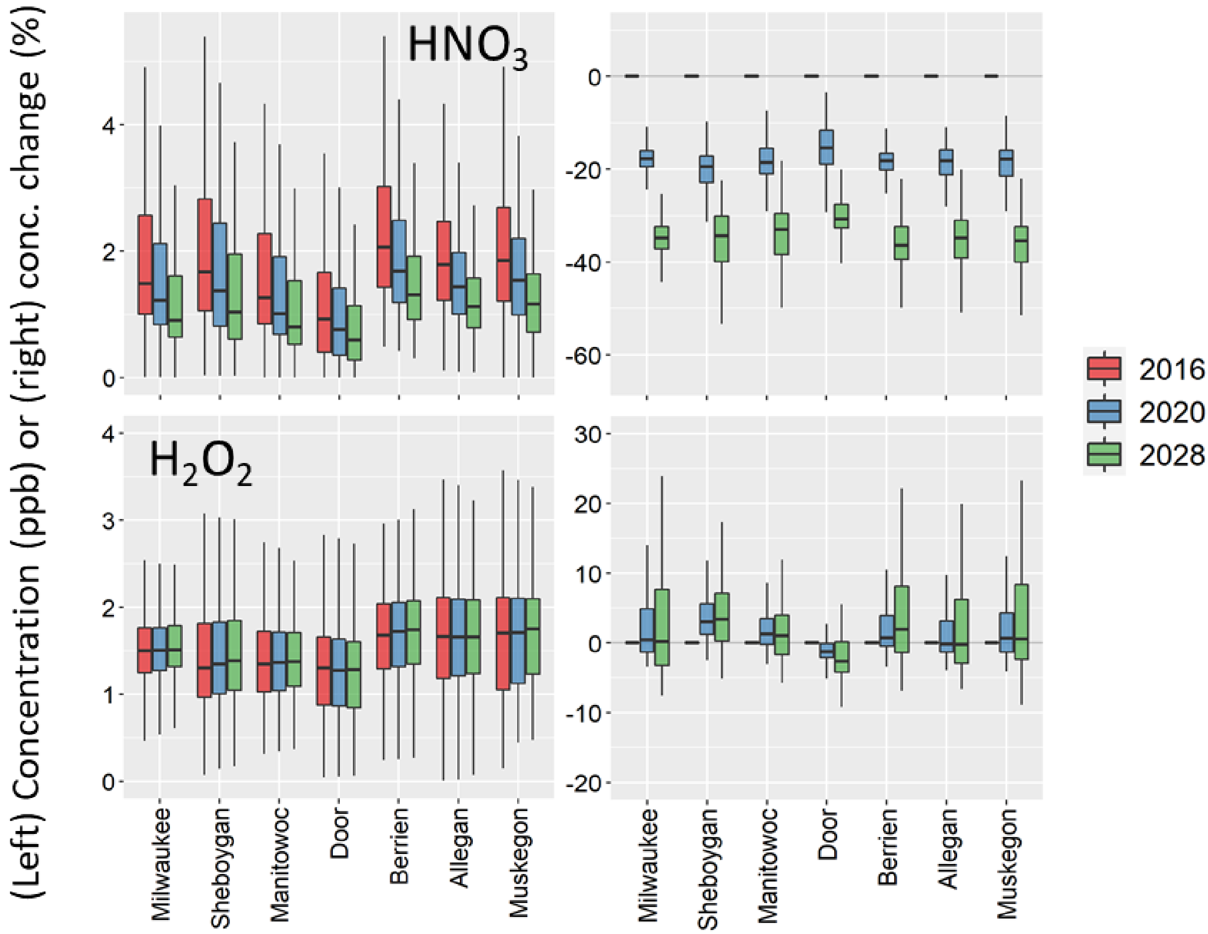

Figure A6.4. Modeled concentrations (left) and percent concentration changes (right) of HNO_3 and H_2O_2 in the early afternoon (13:00-16:59 LDT) on exceedance days in the Wisconsin and western Michigan nonattainment areas. The 2016 values are from the LADCO_2016abc model run except for VOCs, which come from the LADCO_2016aa2a run.

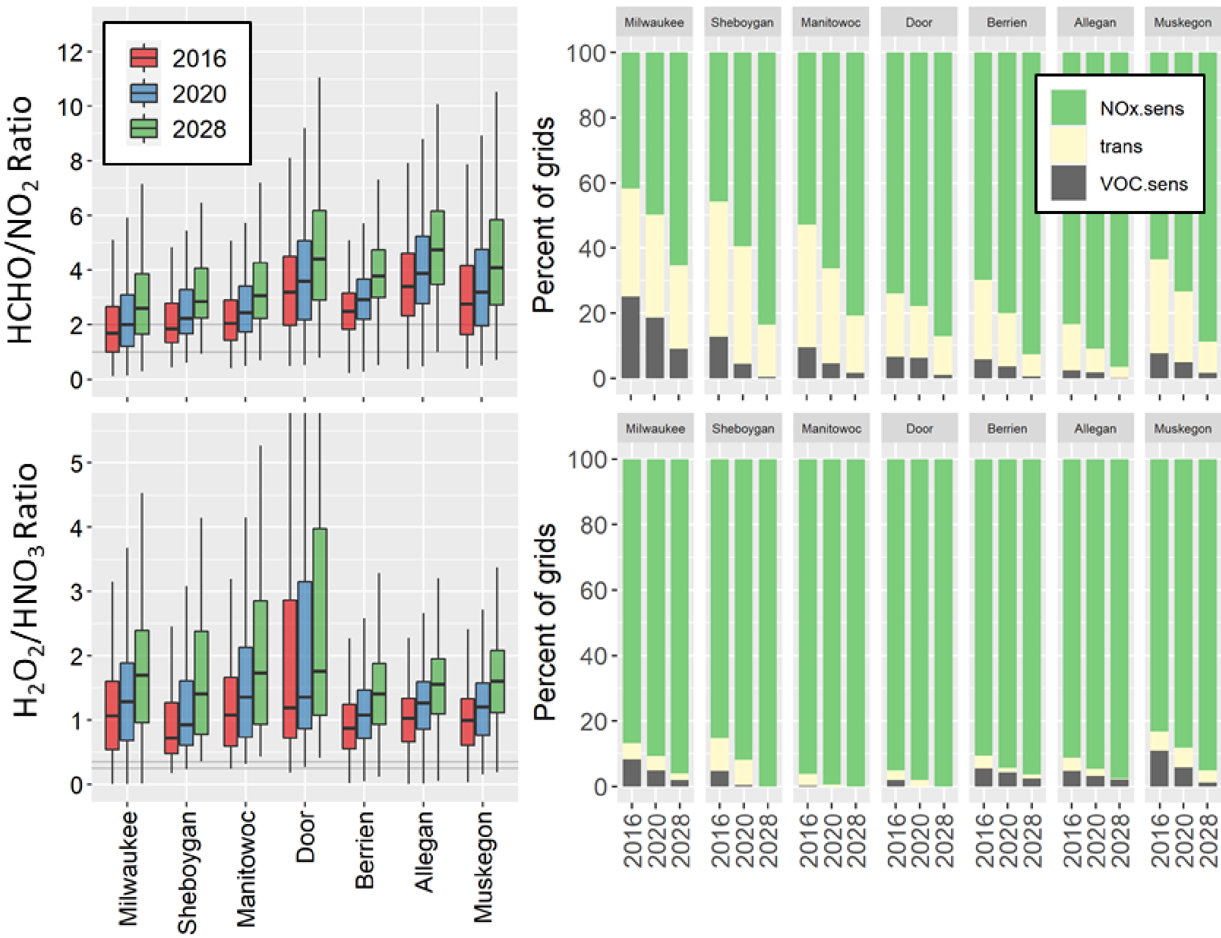

Figure A6.5. Modeled pollutant ratios (left) and ozone formation sensitivity regimes determined from the pollutant ratios (right), for $HCHO/NO_2$ ratios (top) and H_2O_2/HNO_3 ratios (bottom) for the Wisconsin lakeshore and western Michigan nonattainment areas. The gray lines mark the ratio thresholds between VOC-sensitive ($HCHO/NO_2$ < 1; H_2O_2/HNO_3 < 0.25), transitional ($HCHO/NO_2$ of 1-2; H_2O_2/HNO_3 of 0.25-0.35), and NOx-sensitive ($HCHO/NO_2$ > 2; H_2O_2/HNO_3 > 0.35) chemistry. Values are shown for the early afternoon (13:00-16:59 LDT) on exceedance days in the nonattainment areas. The 2016 values are from the LADCO_2016abc model run. Ozone formation sensitivity regimes were determined by applying ratio thresholds from Duncan et al. (2010) to the $HCHO/NO_2$ ratios and from Sillman et al. (2022) to the H_2O_2/HNO_3 ratios.

Ozone Trends over Space and Time in Milwaukee

LADCO analyzed the trends in ozone concentrations over space and over time for the Milwaukee County monitors, as described for the ozone nonattainment areas in Section 4 of the main document. We had excluded most of these monitors from the analysis of the Lake Michigan region because they are impacted by two different types of factors: local, urban emissions and lakeshore processes. Here, we examine trends at these monitors.

Figure A6.6 shows that the highest ozone concentrations in the county have typically been found 10-20 km away from the city center at two monitors. These monitors are located 1.2-2.5 km away from the lakeshore and are likely heavily impacted by lakeshore processes such as transport of ozone plumes via the lake breeze. Concentrations tended to be lowest near the city center. Many of the monitors in the central 10 km are also located near the lakeshore and would presumably be impacted by ozone from the lake breeze. The lower concentrations at these central monitors may indicate the presence of some NOx titration by high NO concentrations in the city center. However, ozone concentrations at these monitors have decreased since the early 2000s, even after the large drop in the mid-2000s, suggesting that ozone formation is not VOC-sensitive (Figure A6.7). The apparent increase in ozone concentrations from the late 2000s to the early 2010s is due in part to the shutdown of a central monitor with relatively low ozone concentrations. Overall, ozone trends in Milwaukee County are difficult to interpret due to the variety of factors affecting them and the changing monitoring network.

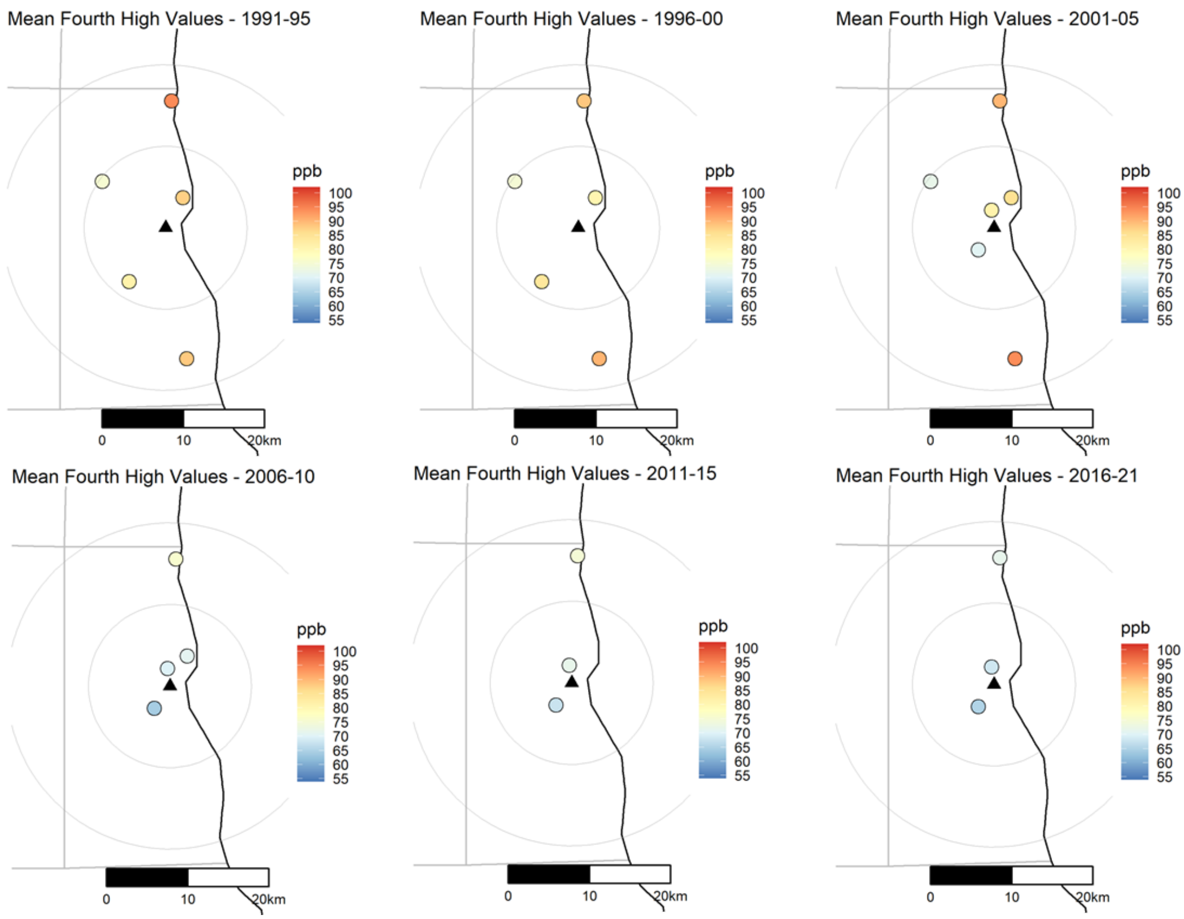

Figure A6.6. Maps of mean annual fourth high maximum daily 8-hour average (MDA8) ozone concentrations in ppb in Milwaukee County in each time period, as labeled. The black triangles show the location of the Milwaukee city center. The concentric circles show the distance from the Milwaukee city center, with the lines being 10 km apart.

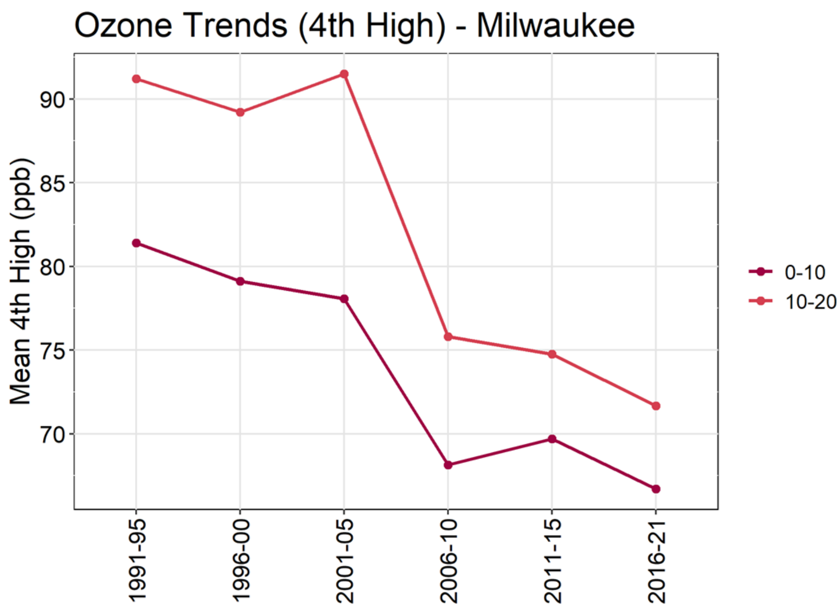

Figure A6.7. Mean fourth high MDA8 ozone concentrations for Milwaukee area monitors plotted versus different year groups, with different lines for the different distance bins.

Areas of Interest in Ohio

Figure A6.8 shows the location of each nonattainment area or area of interest and the grid cells included in each area.

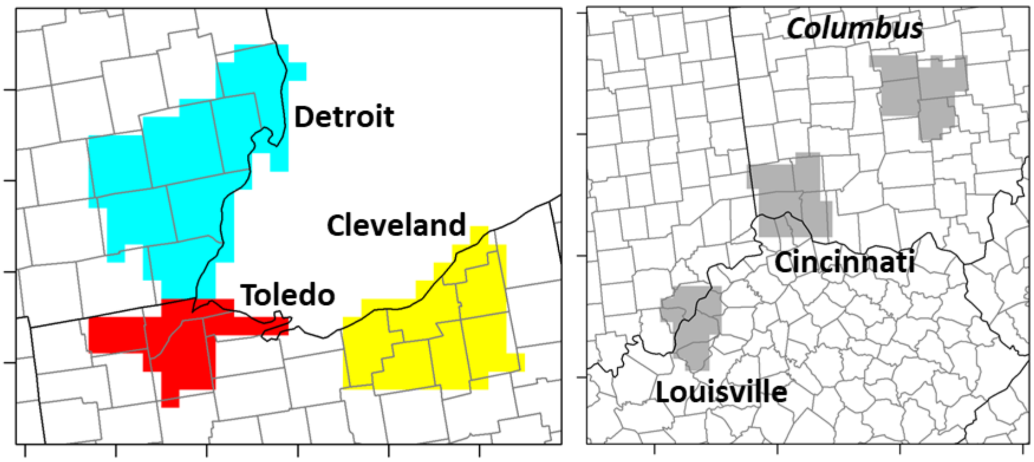

Figure A6.8. Maps showing the grid cells included in the areas of interest in Ohio and southeastern Michigan. Nonattainment area grid cells are color-coded by area in the left panel and shown in gray in the right panel.

TROPOMI-Derived Formaldehyde-to-NO_2 ($HCHO/NO_2$) Ratio

Figure A6.9 compares the ozone exceedance day results for the other areas of interest, Toledo and Columbus, with the nonattainment areas in Ohio and nearby Detroit. (Figure 2.8 in the main report shows maps of this data.) The NO_2 columns in Columbus are the lowest of any of the areas. NO_2 columns in Toledo are very similar on both Detroit and Cleveland exceedance days and are intermediate between the higher values in Detroit to the north and the lower values in Cleveland to the east. HCHO columns are the lowest in Toledo on Cleveland exceedance days, with the next-lowest levels in Columbus. The $HCHO/NO_2$ ratios for Toledo are slightly higher than those observed in Detroit, with the median values falling in the NOx-sensitive range. The $HCHO/NO_2$ ratios in Columbus are much higher, similar to those observed in Cleveland. Roughly a quarter of the grid cells in Toledo had ozone formation in the transitional range, intermediate between observations for neighboring Detroit and Cleveland. Columbus had a small area of VOC-sensitivity and a larger area of transitional chemistry. However, roughly 85% of the grid cells in the Columbus area were NOx-sensitive on ozone exceedance days.

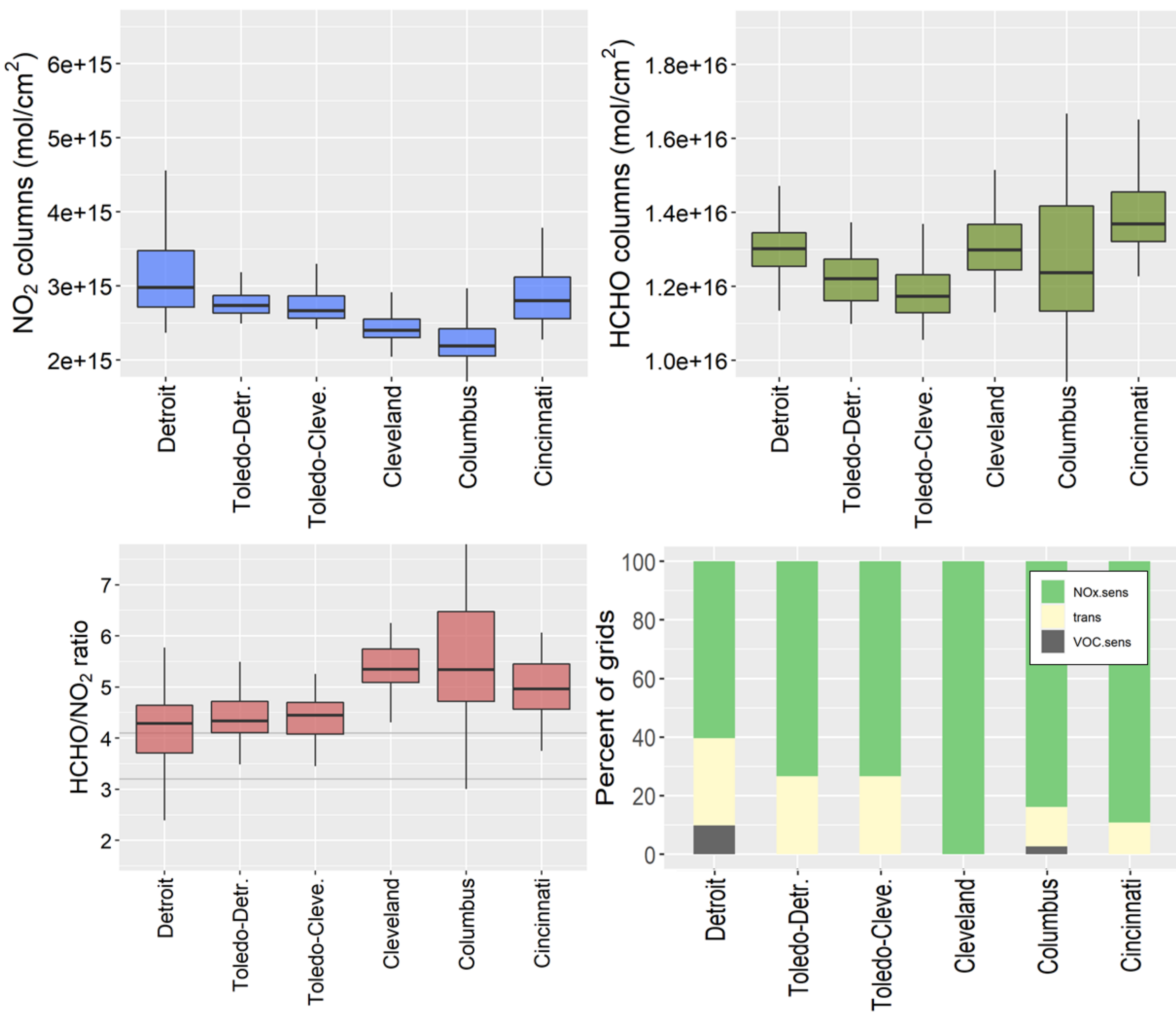

Figure A6.9. TROPOMI data for areas of interest in Ohio and southeastern Michigan on exceedance days, as shown in Figure A3. Boxplots of TROPOMI satellite NO_2 columns (top left, mol/cm^2), HCHO columns (top right, mol/cm^2), HCHO/NO_2 ratios (bottom left), and the distribution of ozone formation sensitivity. Values for Toledo are shown on exceedance days in either Detroit ("Toledo-Detr.") or Cleveland ("Toledo-Cleve."). Sensitivity regimes are determined from HCHO/NO_2 ratios using ratio thresholds from Jin et al. (2020).

Model-Based Indicator Ratios: Formaldehyde-to-NO_2 ($HCHO/NO_2$) and Hydrogen Peroxide-to-Nitric Acid (H_2O_2/HNO_3) Ratios

Figures A6.10 through A6.11 show the model-derived concentrations of ozone, VOCs, and the ozone sensitivity indicator compounds (NO_2, HCHO, HNO_3 and H_2O_2) in the different areas of interest in Ohio and southeast Michigan in each of the three model years. Concentrations of all compounds in Toledo were similar to those in nearby Detroit and Cleveland with the exception of HNO_3 and H_2O_2, which were higher in Toledo, particularly for H_2O_2. These differences are not apparent from mapped concentrations on exceedance days in Detroit or Cleveland (Figure # in the main report). However, the resulting H_2O_2/HNO_3 ratios and ozone sensitivity regimes in Toledo are similar and only slightly higher than those for the other nearby areas. Concentrations of all compounds in Columbus are similar to those in nearby Cincinnati.

The $HCHO/NO_2$ ratios suggest that ozone formation in all of these areas was primarily NOx-sensitive. Ozone formation in Toledo is slightly more NOx-sensitive than in nearby Detroit and Cleveland (Figure A6.12). Ozone formation in Columbus appears similar to that in Cleveland and Cincinnati. As found for the other areas, the H_2O_2/HNO_3 ratios suggested that ozone formation was almost entirely NOx-sensitive. Toledo appeared slightly more NOx-sensitive than Detroit and Cleveland, and Columbus appeared very similar to Cleveland and Cincinnati.

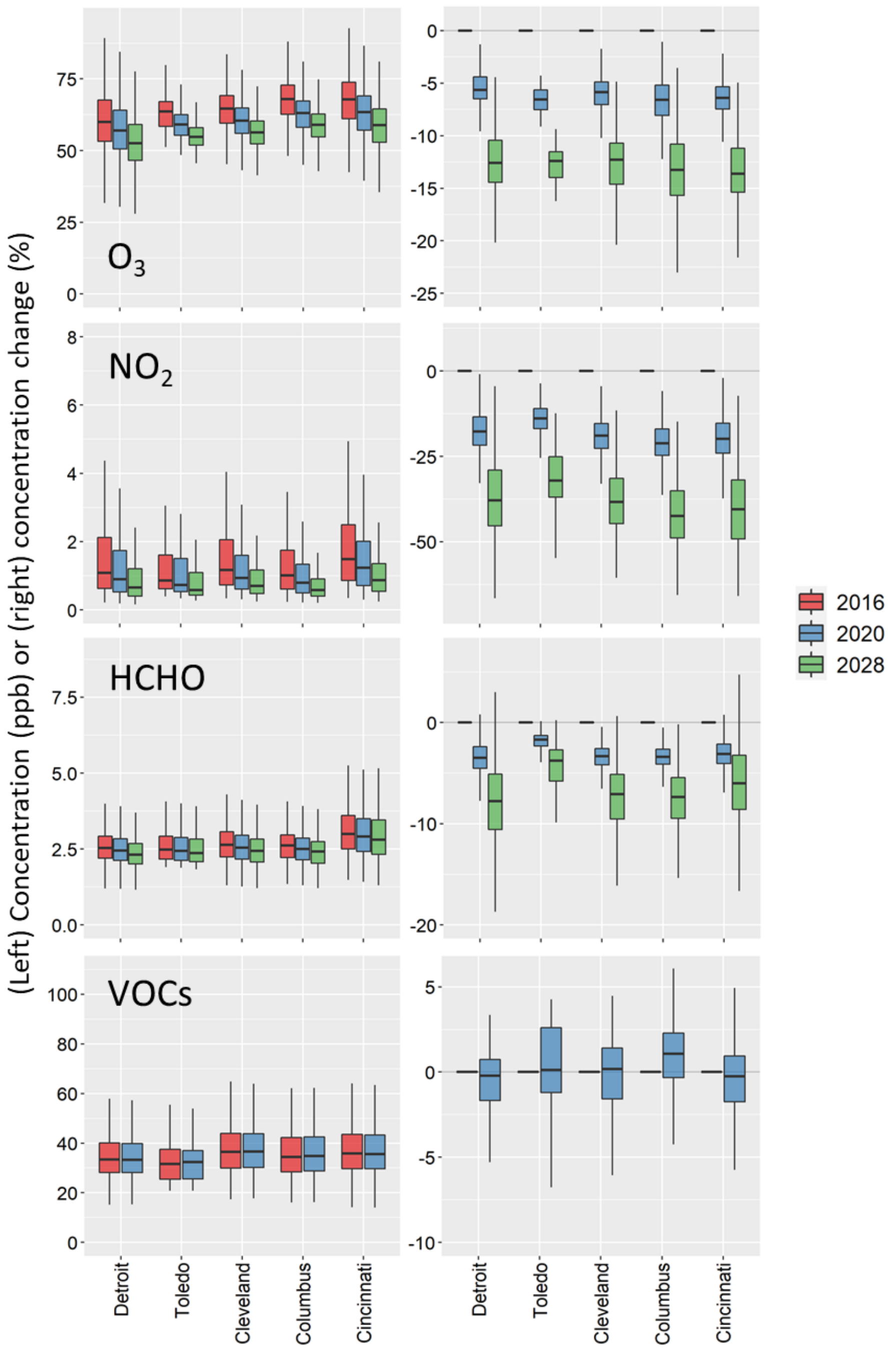

Figure A6.10. Modeled concentrations (left) and percent concentration changes (right) of O_3, NO_2, HCHO, and total VOCs in the early afternoon (13:00-16:59 LDT) on exceedance days in areas of interest in Ohio and southeastern Michigan. The 2016 values are from the LADCO_2016abc model run except for VOCs, which come from the LADCO_2016aa2a run.

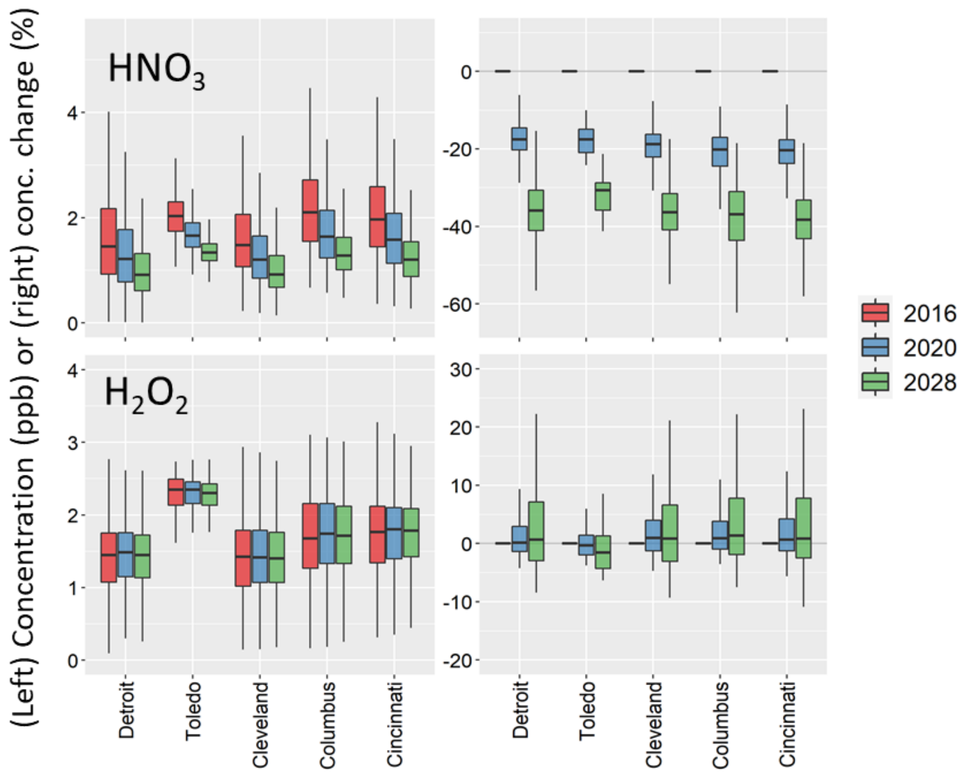

Figure A6.11. Modeled concentrations (left) and percent concentration changes (right) of HNO_3 and H_2O_2 in the early afternoon (13:00-16:59 LDT) on exceedance days in areas of interest in Ohio and southeastern Michigan. The 2016 values are from the LADCO_2016abc model run except for VOCs, which come from the LADCO_2016aa2a run.

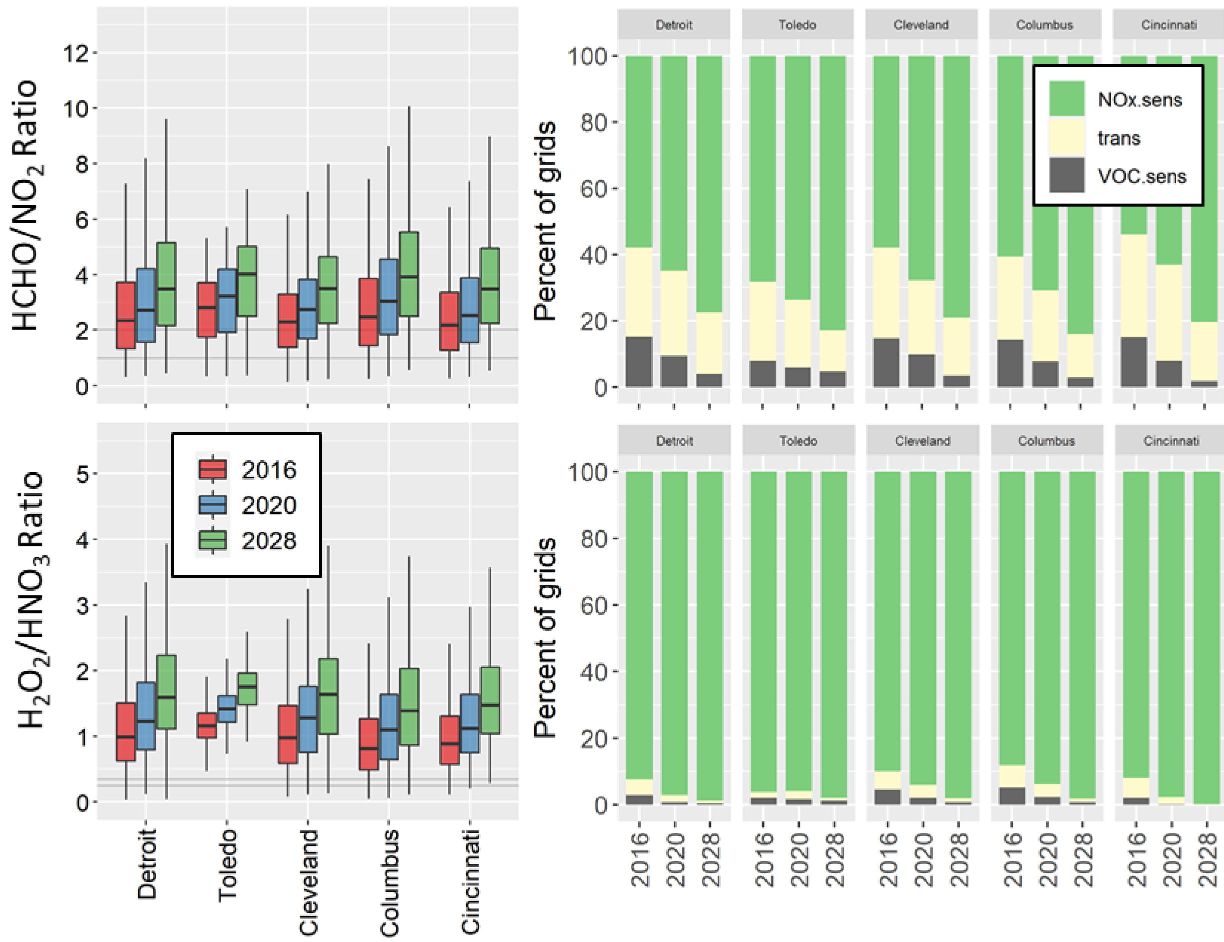

Figure A6.12. Modeled pollutant ratios (left) and ozone formation sensitivity regimes determined from the pollutant ratios (right), for $HCHO/NO_2$ ratios (top) and H_2O_2/HNO_3 ratios (bottom) for areas of interest in Ohio and southeastern Michigan. The gray lines mark the ratio thresholds between VOC-sensitive ($HCHO/NO_2 < 1$; $H_2O_2/HNO_3 < 0.25$), transitional ($HCHO/NO_2$ of 1-2; H_2O_2/HNO_3 of 0.25-0.35), and NOx-sensitive ($HCHO/NO_2 > 2$; $H_2O_2/HNO_3 > 0.35$) chemistry. Values are shown for the early afternoon (13:00-16:59 LDT) on exceedance days in the nonattainment areas. The 2016 values are from the LADCO_2016abc model run. Ozone formation sensitivity regimes were determined by applying ratio thresholds from Duncan et al. (2010) to the $HCHO/NO_2$ ratios and from Sillman et al. (2022) to the H_2O_2/HNO_3 ratios.

Ozone Trends over Space and Time in Toledo

LADCO analyzed the trends in ozone concentrations over space and over time for the Toledo area, as described for the ozone nonattainment areas in Section 4 of the main document. Figure A5.15 shows that ozone concentrations were consistently highest near the Lake Erie lakeshore in the northeast. These high-concentration lakeshore monitors are located in the 0-10 km bin (through 2006-10) and in the 20-30 km bin, although both bins also contain other monitors in most years. This suggests that interpretation of trends versus distance from the lakeshore will not be straightforward in this area. Figure A5.16 shows that ozone concentrations were fairly consistent with distance from the city center within each set of years, with variations of just a few ppb across the 40 km of distance shown. The variations apparent are likely due to the presence or absence of lakeshore monitors in the different bins rather than to chemistry-related factors. Ozone trends over time most clearly demonstrate the dramatic drop in ozone in all distance bins in the mid-2000s, as observed for other areas, particularly in the north. This drop corresponds to implementation of a number of significant emissions control programs nationwide. Many of the other trends may be due to the addition or removal of ozone monitors in different distance bins. However, it is clear that ozone concentrations in each part of the area have decreased over each year period since the early 2000s, which argues against VOC sensitivity in these areas. Figure A5.16 also shows the ozone concentrations at the lakeshore monitors in the 20-30 km bin[3], which currently measure the highest ozone concentrations. Ozone at these lakeshore sites followed similar patterns to the overall patterns in the area, with ozone levels being stable over the last decade. However, given the previous decreases in ozone at these sites previously, it is unlikely that ozone formation is VOC-sensitive. Taken together, this analysis suggests that ozone formation in the Toledo area is primarily NOx-sensitive. The stable ozone concentrations along the lakeshore over the last decade may indicate that ozone formation in this area is transitional, however, this analysis cannot say this definitively.

[3] The Lo Service monitor (390950034) operated from at least 1991 through 2016 and was replaced by the nearby Cooley Canal monitor (390950035) in 2016.

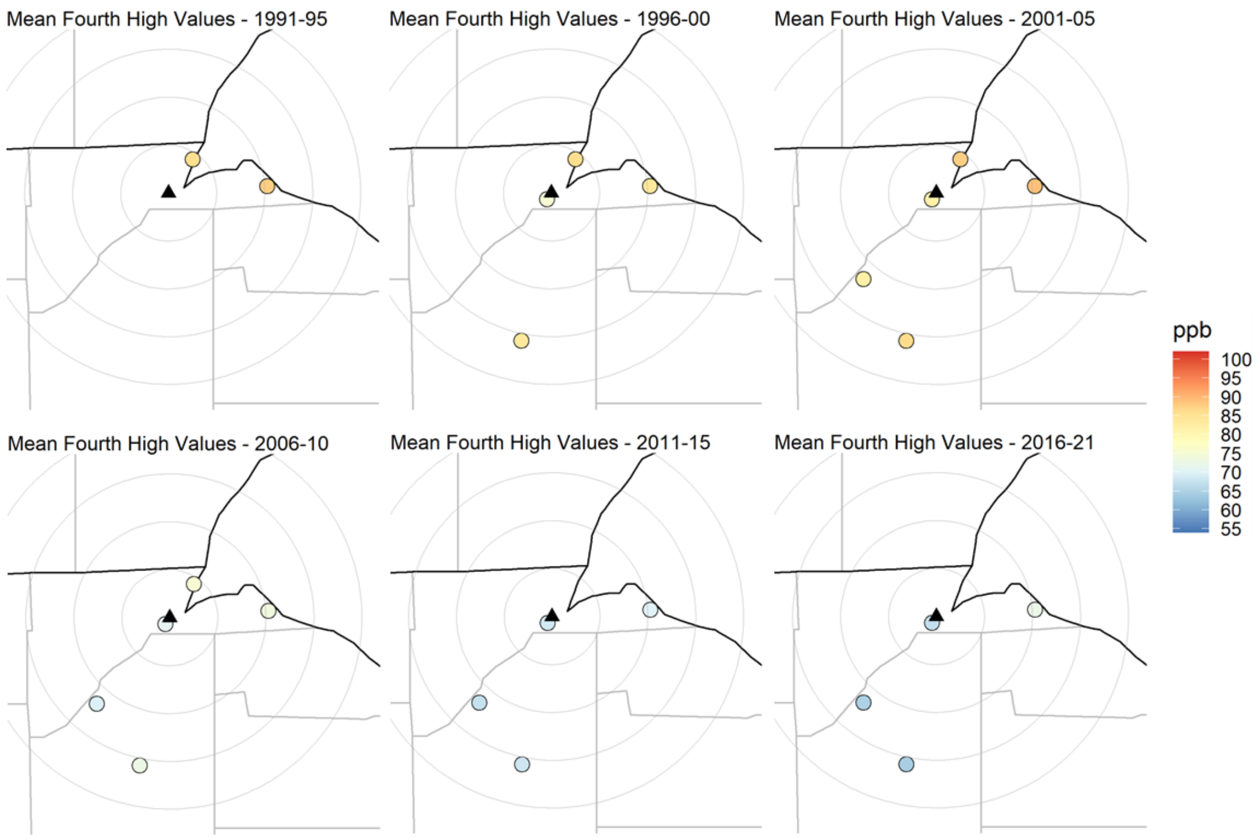

Figure A6.13. Maps of mean annual fourth high maximum daily 8-hour average (MDA8) ozone concentrations in ppb in the Toledo area in each time period, as labeled. The black triangles show the location of the Toledo city center. The concentric circles show the distance from the Toledo city center, with the lines being 10 km apart.

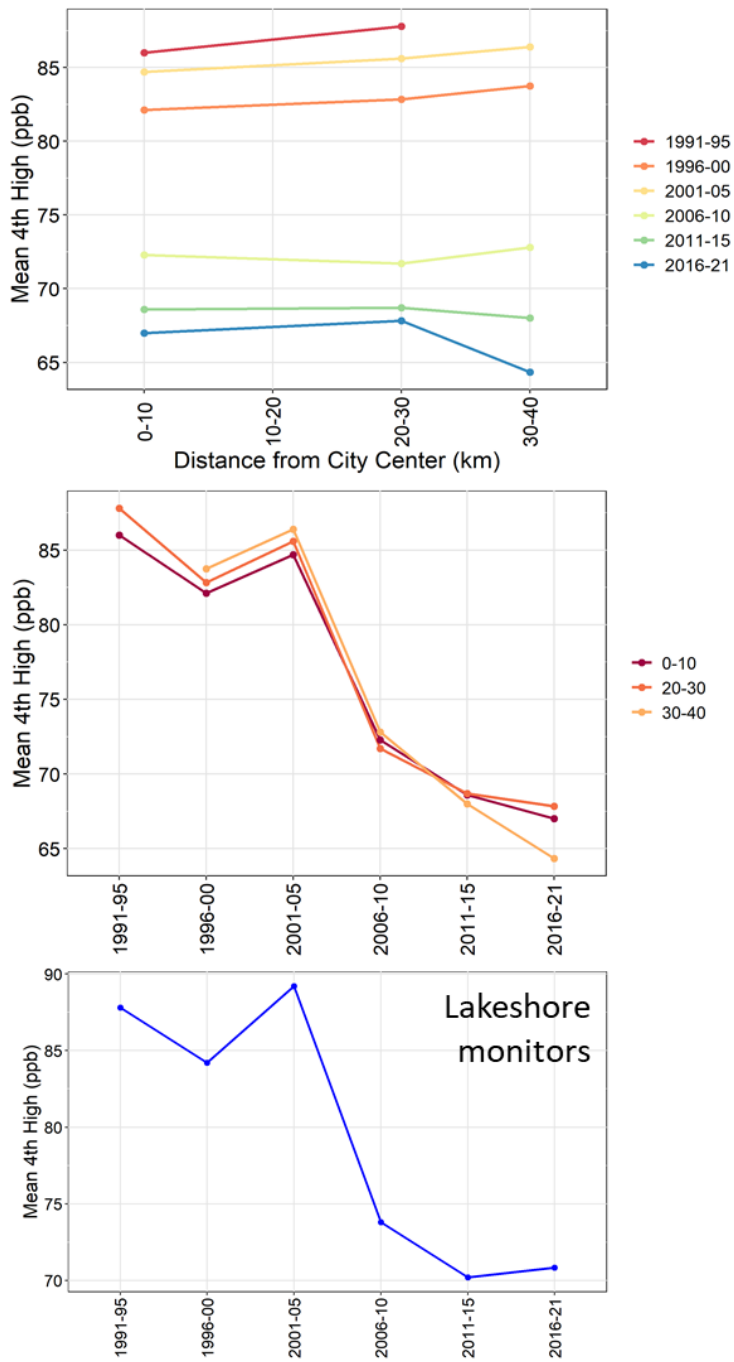

Figure A6.14. Mean fourth high MDA8 ozone concentrations for the Toledo area plotted versus (top) distance from the city center, with different lines for the different year groups, and (middle) different year groups, with different lines for the different distance bins, and (bottom) different year groups for just the lakeshore monitor(s) in the 20-30 km bin.

Synthesis: Ozone formation in areas of interest in Ohio

Figure A6.15 summarizes the ozone formation chemistry information for the Toledo area in recent years. As discussed above, $HCHO/NO_2$ ratios from the TROPOMI satellite and the CAMx model both indicate that most of the Toledo area was NOx-sensitive, with significant areas of transitional chemistry. The CAMx model also identified areas of VOC sensitivity along the lakeshore and in downtown Toledo. The W-W analysis suggested that ozone formation along the lakeshore was NOx-sensitive (positive W-W MDA8 differences) in the latest time period, and the trends analysis indicated that ozone formation in this area was transitional or NOx-sensitive. In addition, the HDDM analysis by Koplitz et al. (2022) identified a small area of transitional chemistry along the Toledo lakeshore and over Lake Erie. Considering all of this evidence, it is likely that ozone formation in most of the Toledo area is NOx-sensitive, with areas of transitional chemistry downtown and along the Lake Erie lakeshore.

Figure A6.16 summarizes the ozone formation chemistry information for the Columbus area in recent years. LADCO did not conduct a W-W or ozone trends analysis for this maintenance area, so this analysis relies upon $HCHO/NO_2$ ratios from the TROPOMI satellite and the CAMx model. Both analyses indicate that ozone formation in most of the region is NOx-sensitive, with some transitional areas located near the city center. As seen for other areas, the model predicts more VOC sensitivity than does the satellite. The HDDM analysis by Koplitz et al. (2022) found that the entire Columbus area was NOx-sensitive. Taken together, it appears that most of the Columbus area is NOx-sensitive, and that there is likely a small area with transitional chemistry located near the city center.

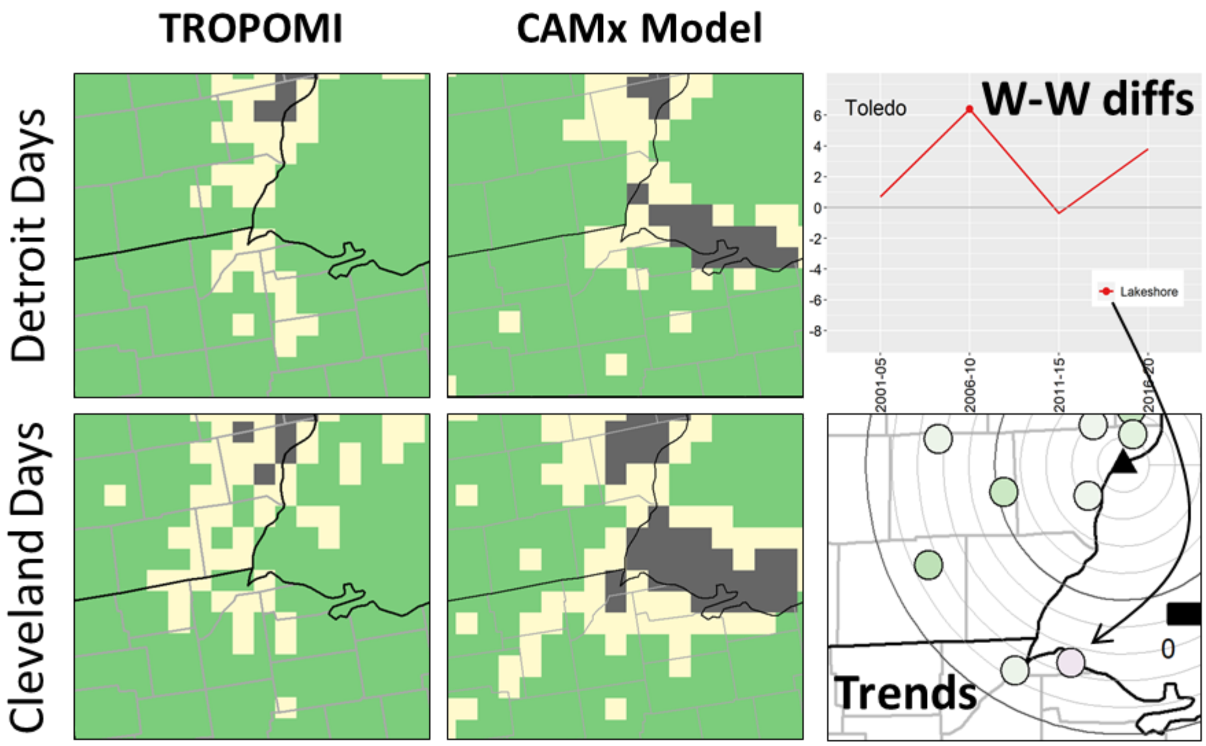

Figure A6.15. Summaries of the recent ozone-NOx-VOC sensitivity[4] for the Toledo area based on (left) TROPOMI satellite HCHO/NO_2 ratios, (middle) CAMx model HCHO/NO_2 ratios, (top right) weekday-weekend analysis, (bottom right) the trends analysis. The satellite and model figures are shown for (top) Detroit exceedance days and (bottom) Cleveland exceedance days. All analyses focused on high-ozone days.

[4] TROPOMI results are for 2018-19, CAMx model results are for 2020, trends results are the difference between 2011-15 and 2016-21, and monitor ratios and W-W results are for 2016-21. Positive trends differences indicate increases in ozone, whereas negative values indicate decreases. Monitor ratios greater than 1 are considered NOx-sensitive, and ratios less than 0.3 are VOC-sensitive. W-W differences greater than 1 are NOx-sensitive and less than -1 are VOC-sensitive. High-ozone days were defined as days with a MDA8 value greater than 70 ppb for the TROPOMI and CAMx model analyses and as days with a MDA8 value greater than 60 ppb for the monitor ratios. The W-W analysis examined days with ozone-conducive meteorology, and the trends analysis focused on the annual fourth highest MDA8 value.

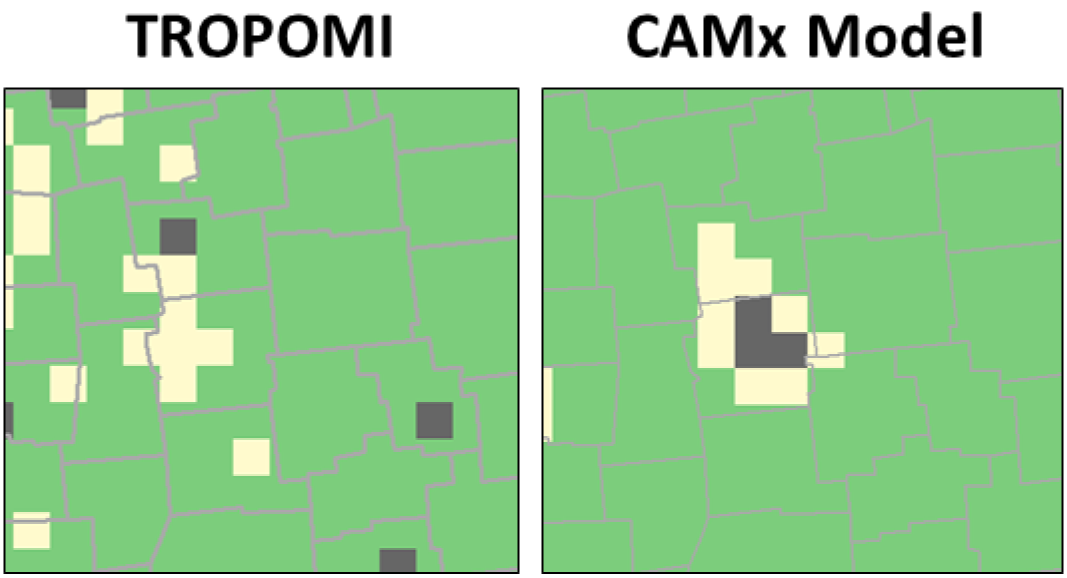

Figure A6.16. Summaries of the recent ozone-NOx-VOC sensitivity for the Cleveland area based on (left) TROPOMI satellite HCHO/NO_2 ratios, (middle) CAMx model HCHO/NO_2 ratios, (top right) weekday-weekend analysis, (bottom right) the trends analysis. The satellite and model figures are shown for (top) Detroit exceedance days and (bottom) Cleveland exceedance days. All analyses focused on high-ozone days.

APPENDIX 7

Sensitivity Observations for the Twin Cities

Ozone concentrations in the Twin Cities of Minneapolis-St. Paul, Minnesota, have typically been low, and this area has attained all of the ozone NAAQS. However, emissions of ozone precursors in this large metropolitan area are large, and it is worth understanding the ozone formation chemistry in this area.

Figure 7.1 shows maps of the area, including design values for 2019-2021. The highest design value in the area in these years was 64 ppb at the Blaine monitor. The low value of 53 ppb in central Minneapolis was at the Minneapolis-Near Road monitor, where we would expect NOx-suppression due to locally high NOx concentrations from vehicle emissions.

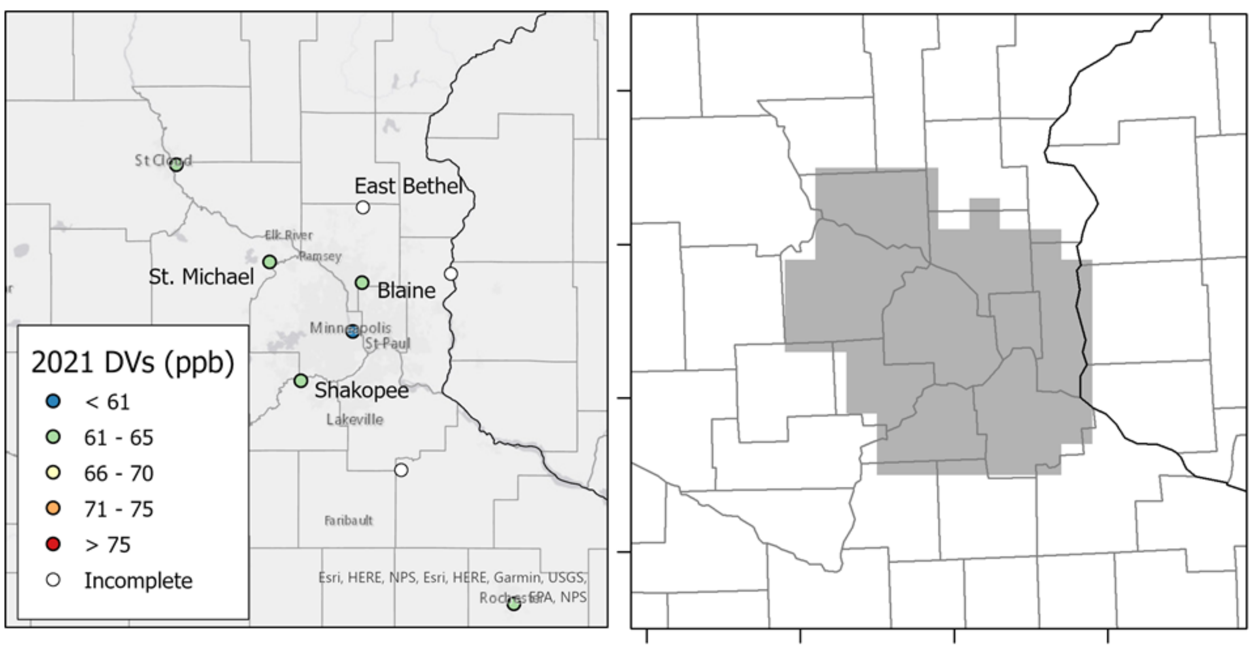

Figure A7.1. Maps of (left) the ozone monitors in the Twin Cities (Minneapolis-St. Paul, MN) area with 2019-2021 design values and (right) the grid cells included in the Twin Cities area for the TROPOMI and CAMx model indicator ratio analyses. Only monitors used in the W-W analysis are labeled.

LADCO applied the same analyses as described in the main document to data for the Twin Cities area. However, given the relatively lower ozone concentrations in the Twin Cities area relative to the ozone nonattainment areas discussed in the main document, we sometimes applied lower ozone thresholds in determining “high ozone days”. For example, in several analyses, the main analysis focused on ozone exceedance days, which we defined as days on which the MDA8 value exceeded the level of the 2015 ozone NAAQS, 70 ppb. For the Twin Cities, we often applied a threshold of 65 ppb instead to define a “high ozone day”. Using this lower threshold provided enough days to allow a more statistically meaningful analysis.

The analyses were conducted using the same methods described in the main document, except as noted. These methods are not repeated in this appendix.

Ground-Based HCHO/NO_2 Analysis

The Blaine monitor is located approximately 11 miles north of downtown Minneapolis in the suburb of Blaine (Table A7.1). This monitor measured concentrations of HCHO and NO_2 from 2012 through 2018. Median HCHO/NO_2 ratios at this suburban monitor were around 0.5 in both sets of years, suggesting that ozone formation chemistry at this site was transitional based on the ratio thresholds from Blanchard (2020) (Figure A7.1). Figure A7.2 shows that these ratios are somewhat higher (more NOx-sensitive) than those in Chicago, Milwaukee, and St. Louis but similar to ratios in Detroit and Grand Rapids.

Table A7.1. Information about the one monitor in the Twin Cities that measured both HCHO and NO_2 concentrations, as well as ozone, including the years the HCHO and NO_2 data was available.

Area	Site Name	Site ID	Years Available
Twin Cities	Blaine	270031002	2012-2018

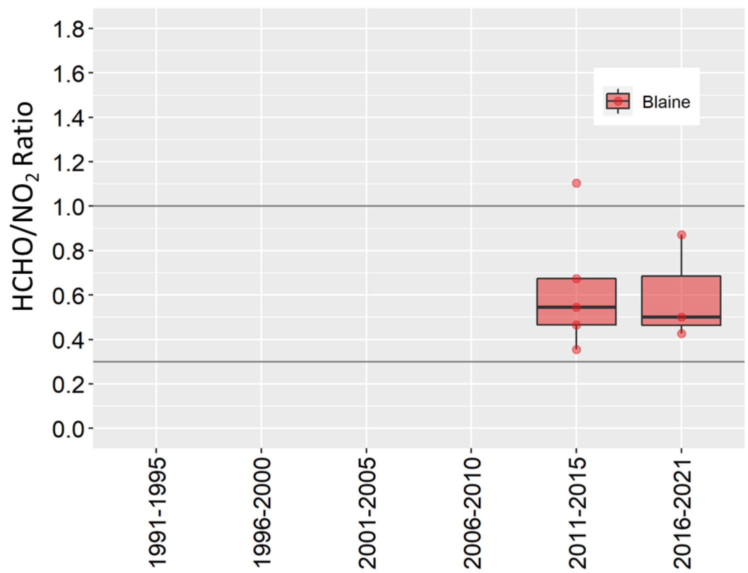

Figure A7.1. Ground-based HCHO/NO_2 ratios for monitors in the Twin Cities area on days with MDA8 ozone greater than 60 ppb. Data are shown for five-year groupings of years. The gray lines mark the ratio thresholds between VOC-sensitive (< 0.3), transitional (0.3-1), and NOx-sensitive (> 1) chemistry based on ratio thresholds from Blanchard (2020).

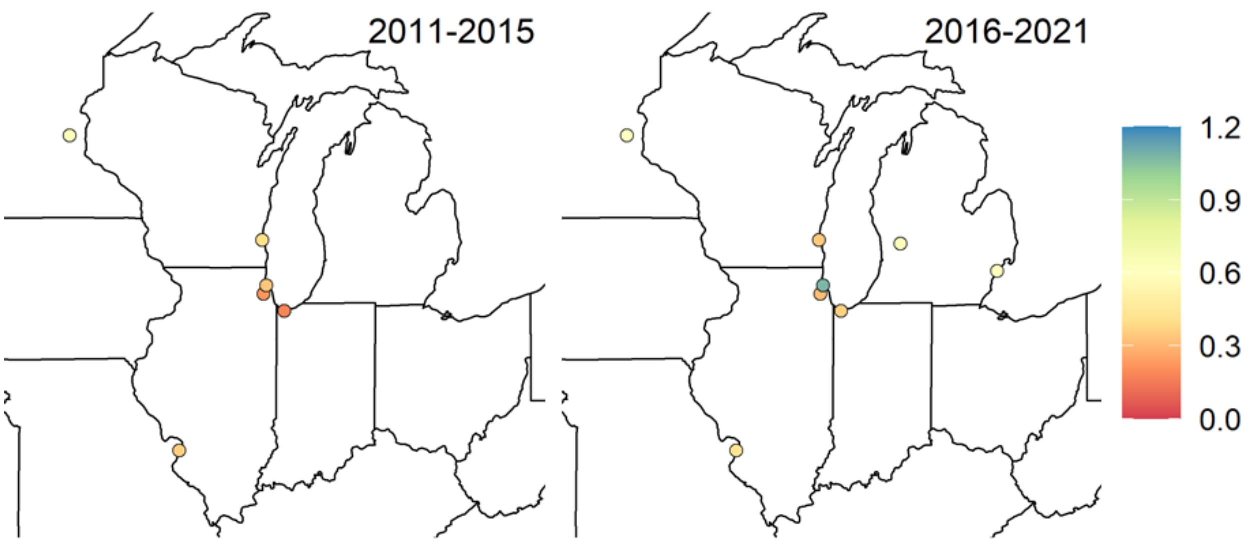

Figure A7.2. Mean ground-based HCHO/NO_2 ratios for monitors in or near LADCO nonattainment areas and the Twin Cities on days with MDA8 O_3 greater than 60 ppb. Data are shown just for the two groupings of years with data in the Twin Cities.

TROPOMI-Derived Formaldehyde-to-NO_2 (HCHO/NO_2) Ratio

For this analysis, LADCO applied a threshold of 65 ppb to determine ozone "exceedance" days. We also analyzed TROPOMI satellite data from four years (2018 through 2021) rather than from the two years (2018 and 2019) applied in the main analysis. Using this lower threshold and additional years provided additional days for the analysis, giving more confidence in the results.

Figure A7.3 shows maps of the mean NO_2 and HCHO retrievals, as well as the HCHO/NO_2 ratio and inferred sensitivity regime, on ozone "exceedance" days. The maps show peak NO_2 concentrations over downtown Minneapolis and St. Paul and also northeast of the city near the Sherco Power Plant, a large coal-fired power plant that emitted 7066 tons of NOx in the years 2018 and 2019 (Figure A7.3). HCHO concentrations also peaked in the Twin Cities urban area and north of the downtown areas. The lowest HCHO/NO_2 ratio was near the Sherco Power Plant, with a value that indicates transitional chemistry. The ratios in the downtown of Minneapolis were lower than in surrounding areas, but still fell in the NOx-sensitive range, as did all of the rest of the area.

Figure A7.1 shows the grid cells included in the boxplots for the Twin Cities. NO_2 column abundances in the Twin Cities were on the low end of those observed in other LADCO cities (Figure A7.4), similar to those observed in Cleveland and St. Louis and much lower than those observed in Chicago or Detroit. HCHO abundances were similar to those seen in other northern cities and areas. The HCHO/NO_2 ratios were very similar to those observed in many of the ozone nonattainment area, with almost all of the grid cells and days falling in the NOx-sensitive range.

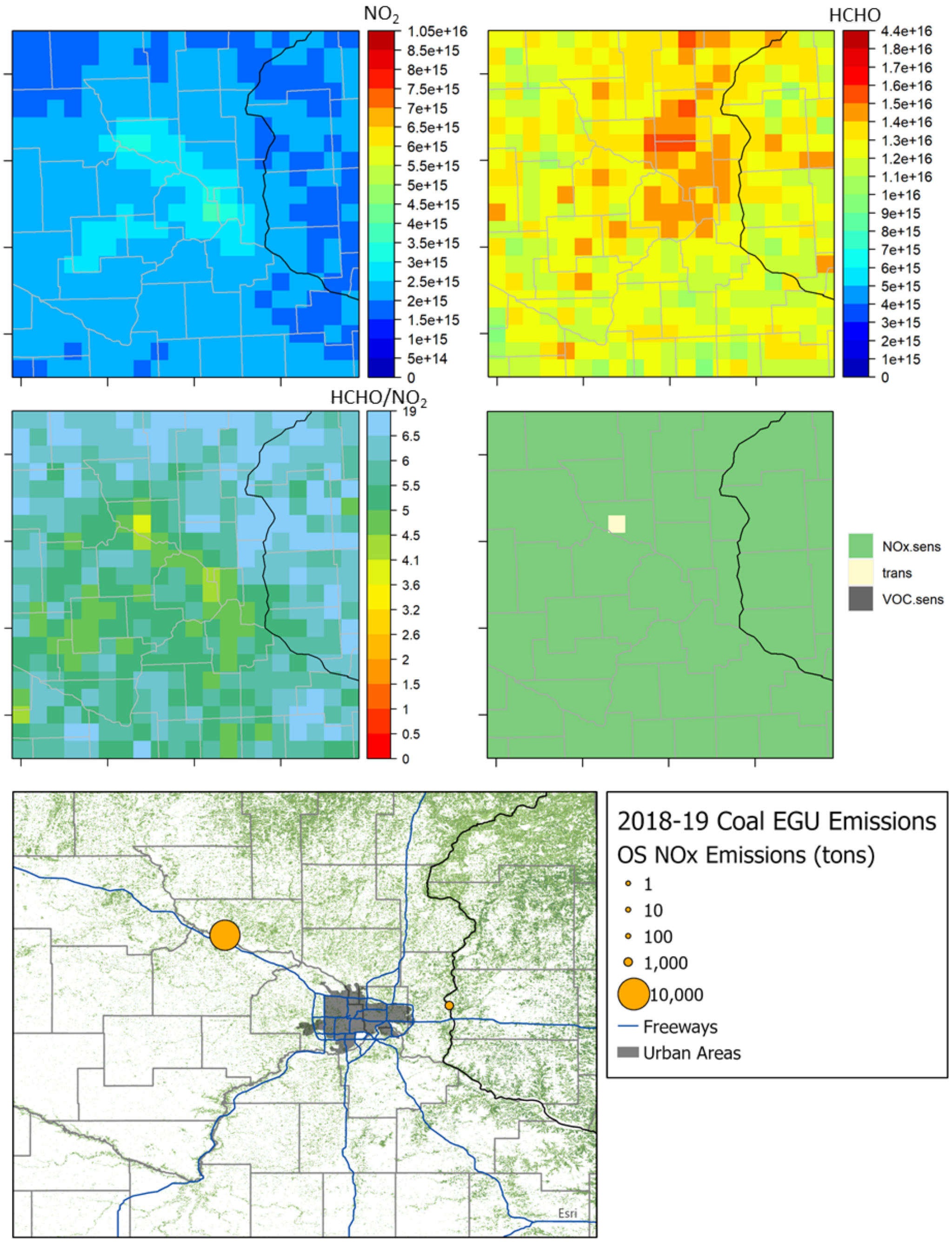

Figure A7.3. Maps of (top left) NO_2 columns (mol/cm^2), (top right) HCHO columns (mol/cm^2), (middle left) HCHO/NO_2 ratios, and (middle right) ozone formation sensitivity regimes on days when MDA8 ozone exceeded 65 ppb in the Twin Cities area of Minnesota in 2018-2021. (Bottom) Maps of large emissions sources, including total ozone season NOx emissions (tons) from coal-fired electric generating units (EGUs) in 2018 and 2019, urban areas, freeways, and tree canopy cover (green), with data sources as described in Figure 4 of the main report.

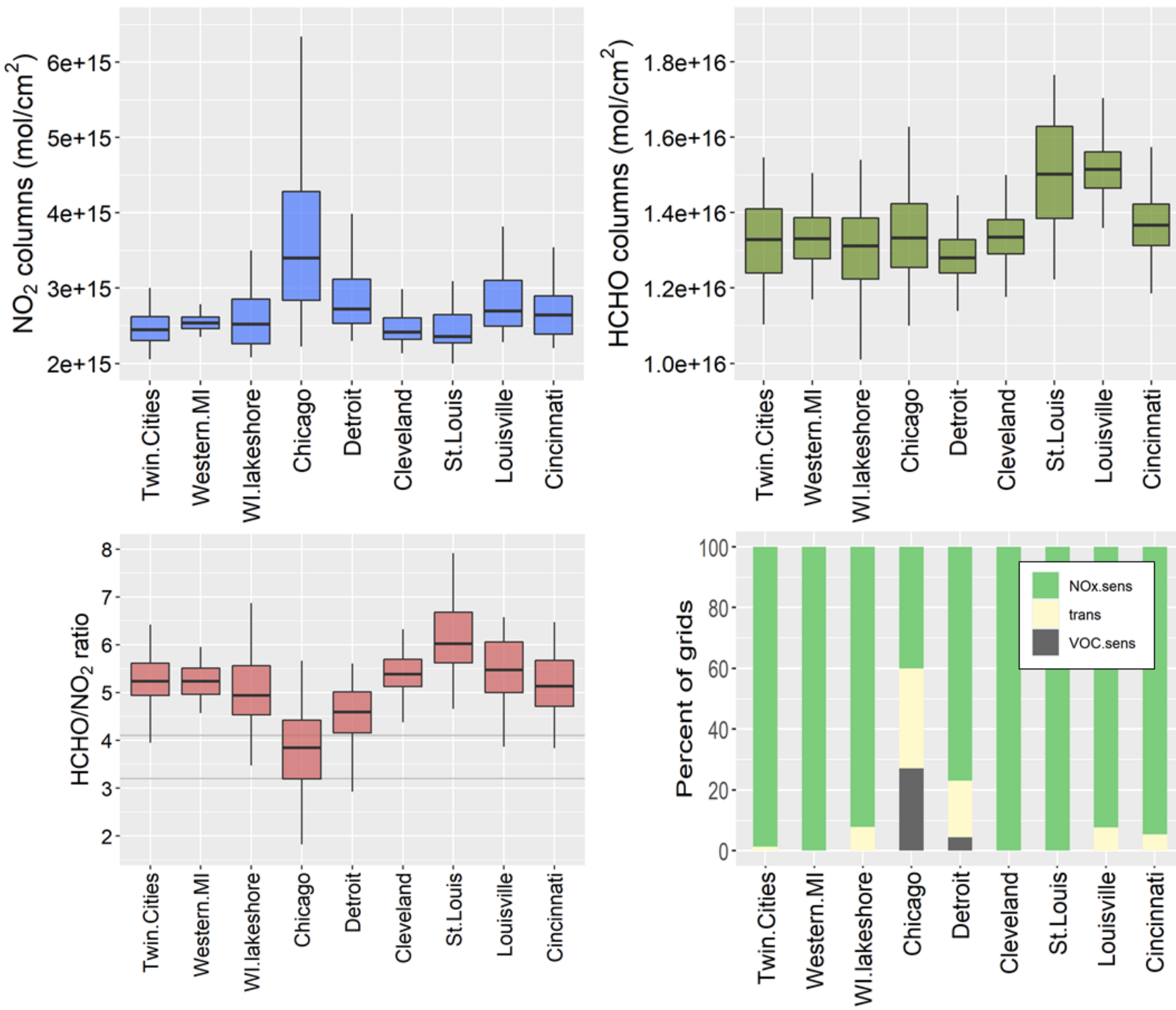

Figure A7.4. Boxplots of TROPOMI satellite NO_2 columns (top left, mol/cm^2), HCHO columns (top right, mol/cm^2), HCHO/NO_2 ratios (bottom left), and the distribution of ozone formation sensitivity. Values are for exceedance days in 2018-2021 in the Twin Cities area (applying a threshold MDA8 value of 65 ppb) compared with the different nonattainment areas (applying a threshold MDA8 value of 70 ppb). Sensitivity regimes are determined from HCHO/NO_2 ratios using ratio thresholds from Jin et al. (2020).

Model-Based Indicator Ratios: Formaldehyde-to-NO_2 ($HCHO/NO_2$) and Hydrogen Peroxide-to-Nitric Acid (H_2O_2/HNO_3) Ratios

As done for the TROPOMI satellite analysis, LADCO applied a threshold of ozone MDA8 values of 65 ppb or greater to examine high-ozone days in the Twin Cities area. Maps of the mean ozone concentrations on these days in 2016 show a peak of 65-70 ppb over the downtowns of Minneapolis and St. Paul, with concentrations decreasing away from this peak (Figure A7.5). Ozone concentrations are projected to decrease from 2016 to 2028 around the area, with the smallest decrease in the Minneapolis city center and the largest decrease in a ring around the city center, particularly to the east. $HCHO/NO_2$ ratios are lower than 0.5 in the city center in 2016, with ratios increasing everywhere in 2028. H_2O_2/HNO_3 ratios are more uniform but reach a minimum in the same city center grid cells. These ratios also increase in 2028. Figure A7.10 shows maps of the indicator and precursor species mean values in the early morning and early afternoon. This figure shows the values in 2016 and the change in values from 2016 to 2028.

Application of the ratio thresholds from Jin et al. (2020) to the $HCHO/NO_2$ ratios finds a VOC-sensitive area centered over the Twin Cities city centers in 2016, surrounded by a ring of transitional chemistry (Figure A7.6). Most of the remainder of the area is NOx-sensitive. One grid cell that includes St. Cloud, MN, northeast of the Twin Cities, is classified as VOC-sensitive, and another that contains the Sherco Generating Station is classified as transitional. The grid cell with the Sherco power plant was classified as transitional based on the TROPOMI satellite analysis as well. However, the St. Cloud grid cell was NOx-sensitive according to the satellite-based approach. Application of the H_2O_2/HNO_3 ratios classifies all of the Twin Cities area as NOx-sensitive except for one grid cell over downtown Minneapolis. The VOC-sensitive and transitional areas are projected to shrink by 2028 using both sensitivity indicator ratios, and the area of NOx-sensitivity is projected to expand.

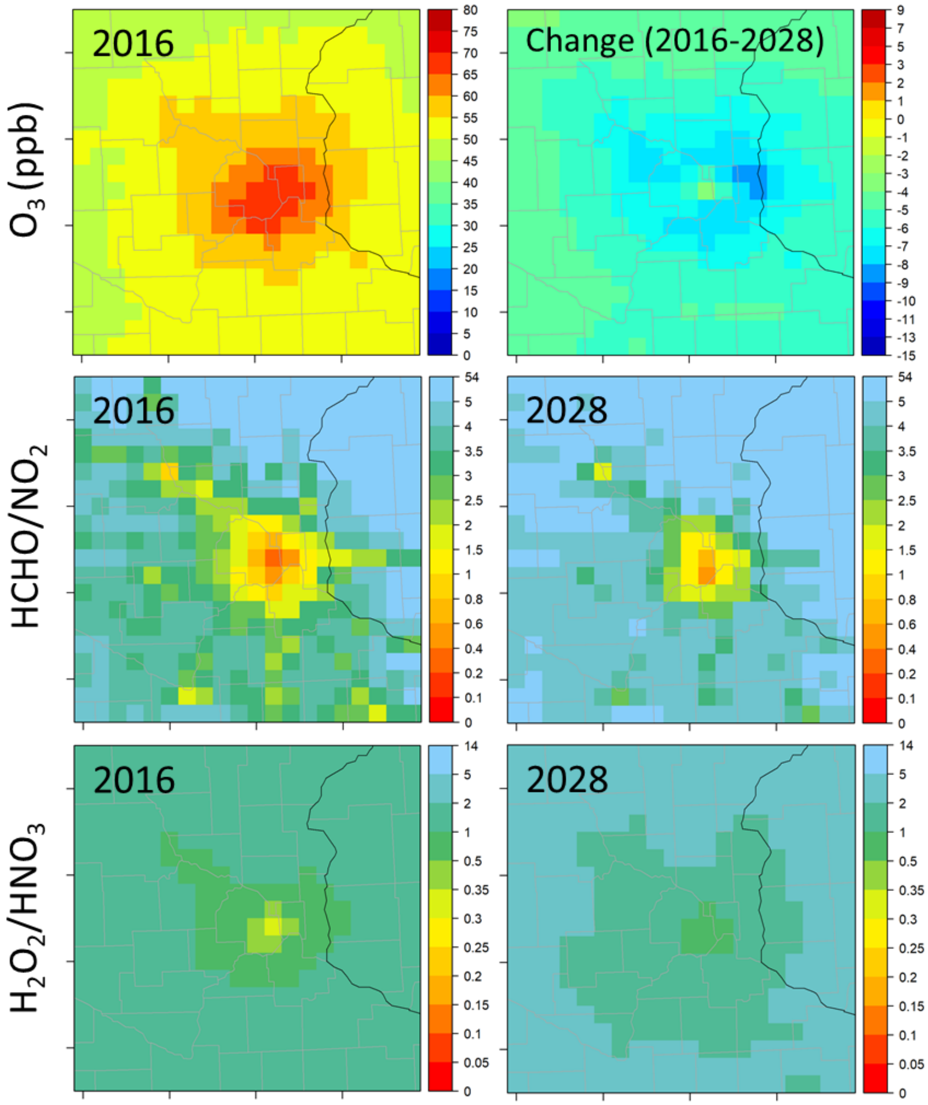

Figure A7.5. Mean (top) 2016 ozone concentrations and concentration changes from 2016 to 2028 (ppb), (middle) $HCHO/NO_2$ ratios in 2016 (left) and 2028 (right), and H_2O_2/HNO_3 ratios in 2016 (left) and 2028 (right) in the early afternoon (13:00-16:59 LDT) on days with ozone MDA8 values >65 ppb in the Twin Cities area in 2016. Values are the mean value within each grid cell based on the LADCO_2016abc model run.

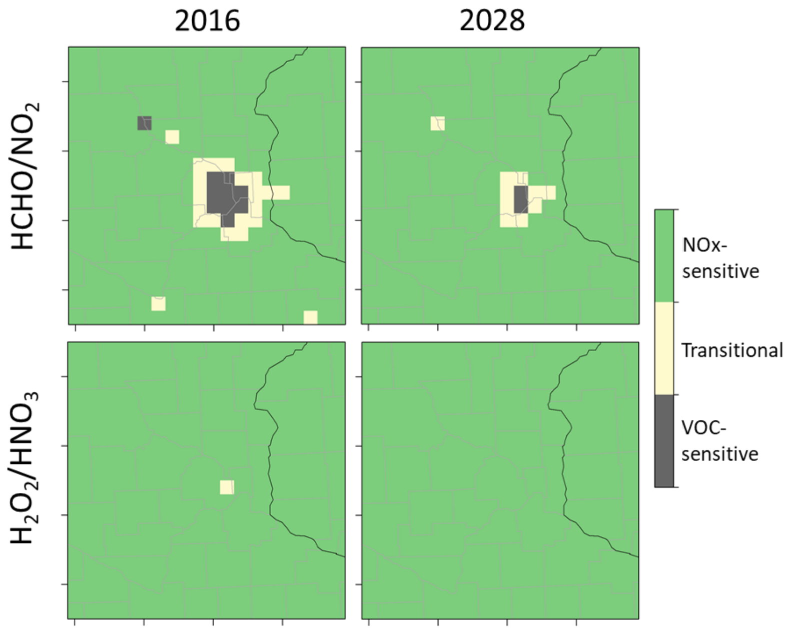

Figure A7.6. Mean ozone formation sensitivity regime in 2016 (left) and 2028 (right) in the Twin Cities area based on the (top) $HCHO/NO_2$ ratios and (bottom) H_2O_2/HNO_3 ratios in the early afternoon (13:00-16:59 LDT) on days with ozone MDA8 values >65 ppb in the Twin Cities area in 2016. Values are based on the mean ratio within each grid cell based on the LADCO_2016abc model run. Ozone formation sensitivity regimes were determined by applying ratio thresholds from Duncan et al. (2010) to the $HCHO/NO_2$ ratios and from Sillman (2022) to the H_2O_2/HNO_3 ratios.

Figure A7.7 shows that the model estimated that median early afternoon ozone concentration on days with MDA8 ozone greater than 65 ppb in the Twin Cities was similar to median values in northern nonattainment areas on similar days. However, the peak concentrations in the Twin Cities area were lower than those in the neighboring nonattainment areas, indicating that maximum concentrations in this area were lower than in the nonattainment areas. Ozone was modeled to decrease somewhat less between 2016 and 2028 than in the other northern areas. Modeled NO_2 concentrations were similar to those in western Michigan but much lower than those in Chicago and slightly lower than those in Detroit. Concentrations of HCHO, HNO_3, and H_2O_2 were all similar to those in the other areas, and VOC concentrations were lower (Figures A7.7 and A7.8).

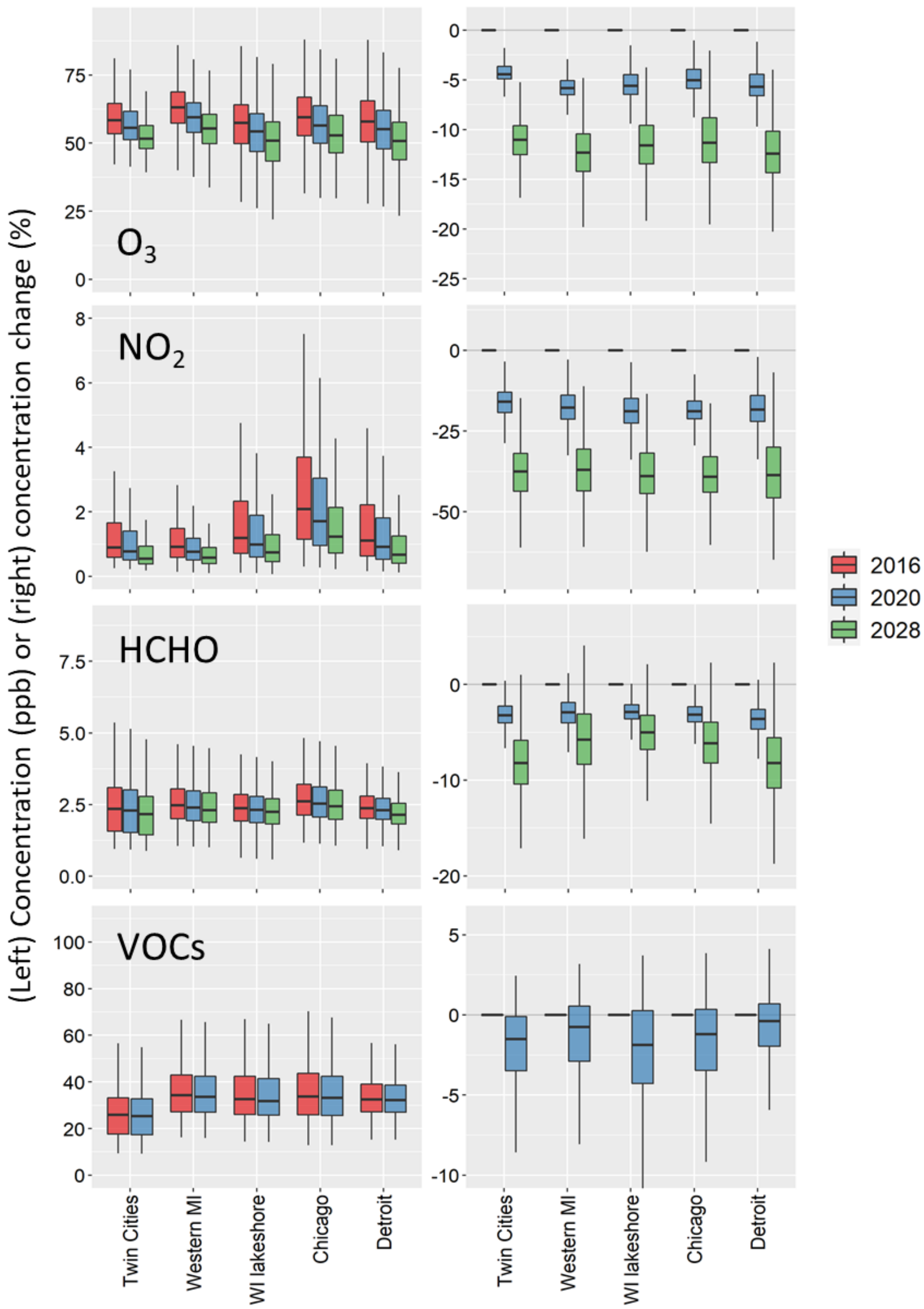

Figure A7.7. Modeled concentrations (left) and percent concentration changes (right) of O_3, NO_2, HCHO, and total VOCs in the early afternoon (13:00-16:59 LDT) on days with ozone MDA8 values greater than 65 ppb in the Twin Cities and other northern nonattainment areas. The 2016 values are from the LADCO_2016abc model run except for VOCs, which come from the LADCO_2016aa2a run.

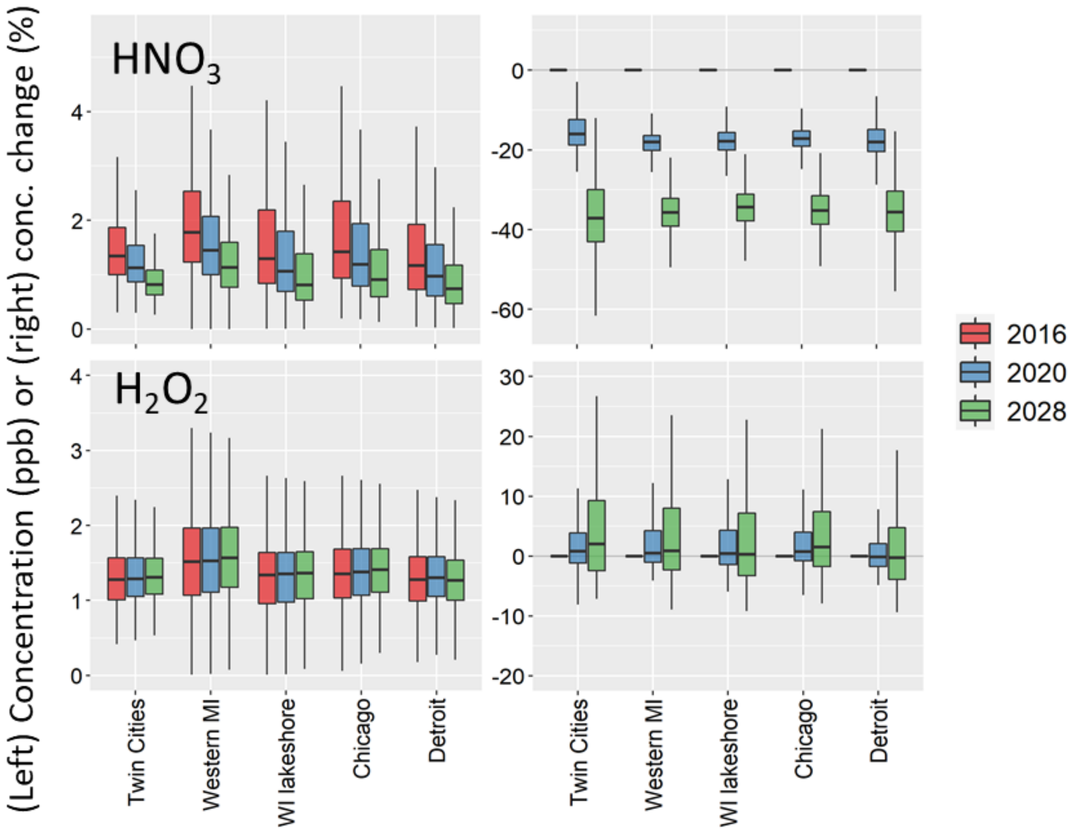

Figure A7.8. Modeled concentrations (left) and percent concentration changes (right) of HNO_3 and H_2O_2 in the early afternoon (13:00-16:59 LDT) on days with ozone MDA8 values greater than 65 ppb in the Twin Cities and other northern nonattainment areas. The 2016 values are from the LADCO_2016abc model run except for VOCs, which come from the LADCO_2016aa2a run.

The HCHO/NO_2 ratios in the Twin Cities area were generally higher than those in northern urban nonattainment areas (e.g., Chicago and Detroit) and along the Wisconsin lakeshore but lower than those found in Western Michigan(Figure A7.9). H_2O_2/HNO_3 ratios in the Twin Cities were similar to those found in the northern nonattainment areas. Application of the HCHO/NO_2 ratio thresholds from Jin et al. (2020) estimated that just over 10 percent of the Twin Cities area was VOC-sensitive in 2016, whereas 60 percent was NOx-sensitive. Application of H_2O_2/HNO_3 ratio thresholds from Sillman (2022) estimated that only about 5% of the Twin Cities area was VOC-sensitive and about 90% of the area was NOx-sensitive. Over time, the extent of the

VOC-sensitive areas is projected to decrease and the NOx-sensitive areas are projected to expand, as found for other areas.

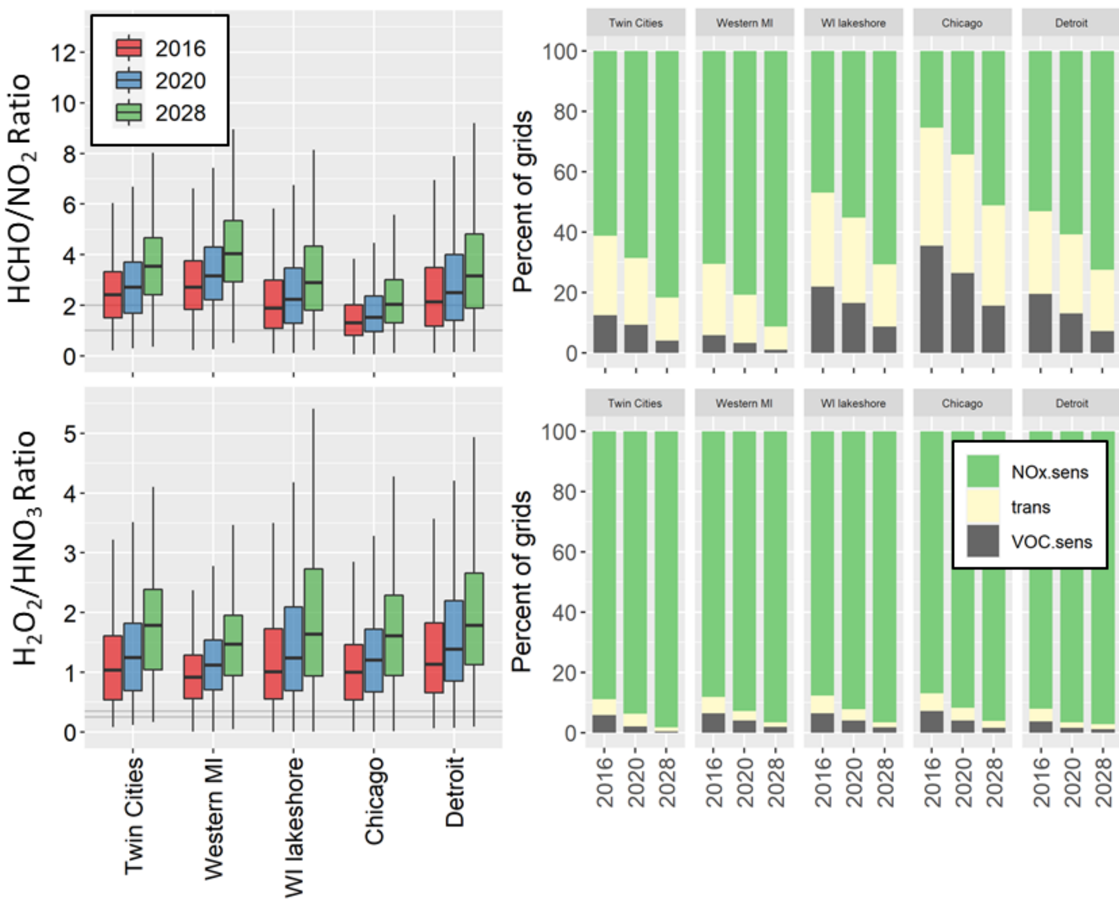

Figure A7.9. Modeled pollutant ratios (left) and ozone formation sensitivity regimes determined from the pollutant ratios (right), for $HCHO/NO_2$ ratios (top) and H_2O_2/HNO_3 ratios (bottom) for the Twin Cities and other northern nonattainment areas. The gray lines mark the ratio thresholds between VOC-sensitive ($HCHO/NO_2$ < 1; H_2O_2/HNO_3 < 0.25), transitional ($HCHO/NO_2$ of 1-2; H_2O_2/HNO_3 of 0.25-0.35), and NOx-sensitive ($HCHO/NO_2$ > 2; H_2O_2/HNO_3 > 0.35) chemistry. Values are shown for the early afternoon (13:00-16:59 LDT) on days with ozone MDA8 values greater than 65 ppb. The 2016 values are from the LADCO_2016abc model run. Ozone formation sensitivity regimes were determined by applying ratio thresholds from Duncan et al. (2010) to the $HCHO/NO_2$ ratios and from Sillman et al. (2022) to the H_2O_2/HNO_3 ratios.

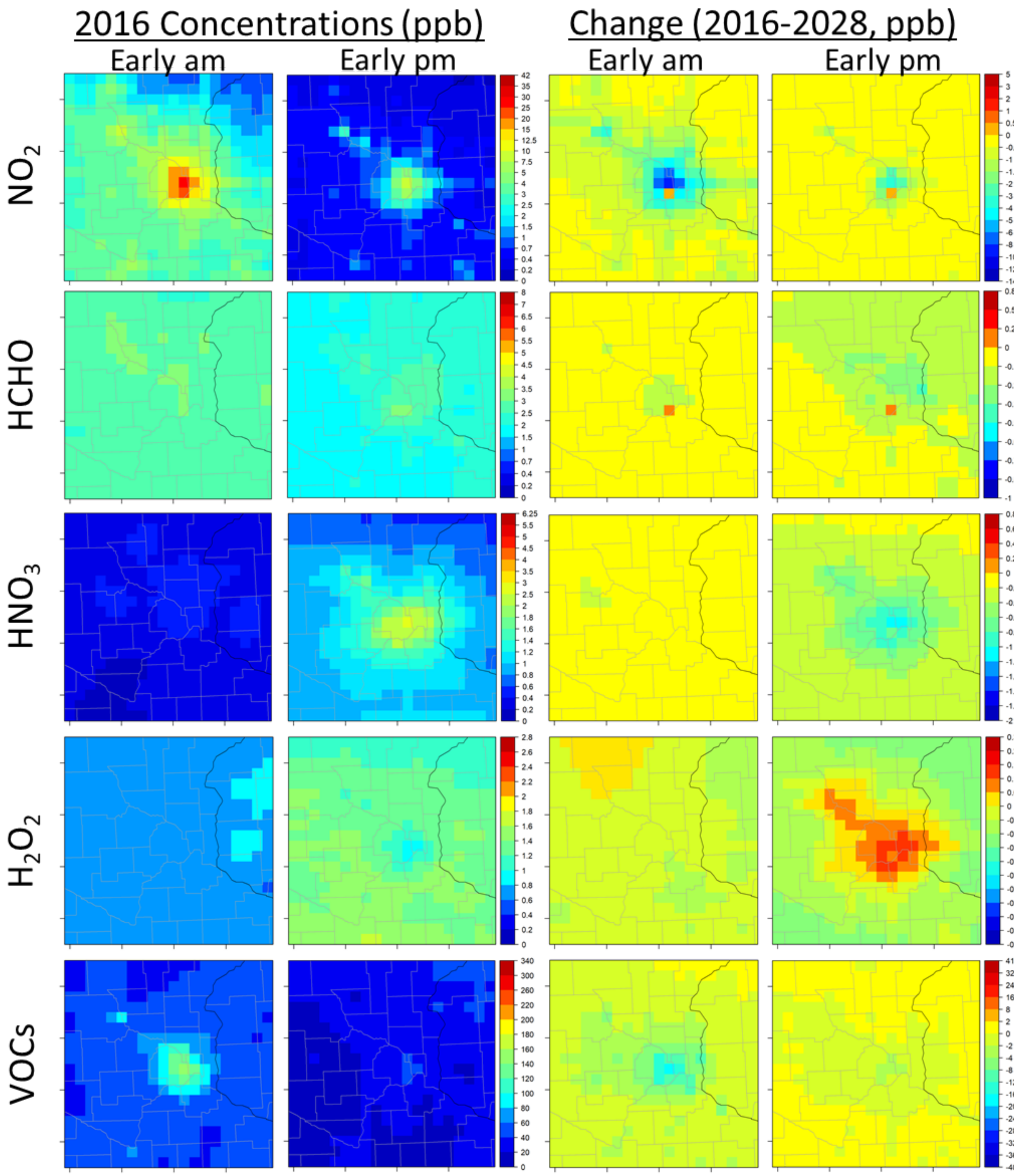

Figure A7.10. Mean concentrations of ozone sensitivity indicator compounds in the Twin Cities area on days with ozone MDA8 values greater than 65 ppb in 2016 (left) and the change in compound concentrations between 2016 and 2028 (right). Concentrations are shown for the early morning (5-8:59 LDT) and early afternoon (13:00-16:59 LDT) from the abc model.

Weekday-weekend Analysis

LADCO conducted a weekday-weekend (W-W) analysis for the Twin Cities area following the methods described in Section 3 of the main document. Table A7.2 lists the ozone and meteorological monitors used in the CART and the related W-W analyses, along with the parameters used in the CART analysis. Figure A7.11 shows the CART tree used to determine the meteorological conditions on ozone-conducive days in this area, and Table A7.3 describes the meteorological conditions on day types that were determined to be ozone-conducive. Unlike for the ozone nonattainment areas, there were no day types (nodes) with mean ozone concentrations of 60 ppb or higher. Accordingly, we defined “ozone-conducive day types” as nodes with mean ozone concentrations of 55 ppb or higher. Table A7.3 shows that high temperatures, southerly winds, and low relative humidity were the primary factors necessary for high ozone concentrations in this area. Even with the lower threshold of 55 ppb, there were relatively fewer ozone-conducive days (8 percent of all days) in this area relative to the nonattainment areas, which had 11 to 33 percent ozone-conducive days. These smaller numbers will lead to greater uncertainties in the analysis.

Table A7.2. Ozone monitors and meteorological stations used in the CART analysis, values of *ctree_control* parameters used in each CART analysis, and NO_2 monitors used in the weekday-weekend analysis.

Ozone monitors	Airport met station	*maxdepth*	*minsplit*	*minbucket*	Terminal nodes	NO_2 monitors
East Bethel Blaine Shakopee St. Michael*	Minneapolis- St. Paul (MSP)	5	400	200	15	270031002 270370020 270370423

* The St. Michael monitor was used in the CART analysis but not in the W-W analysis.

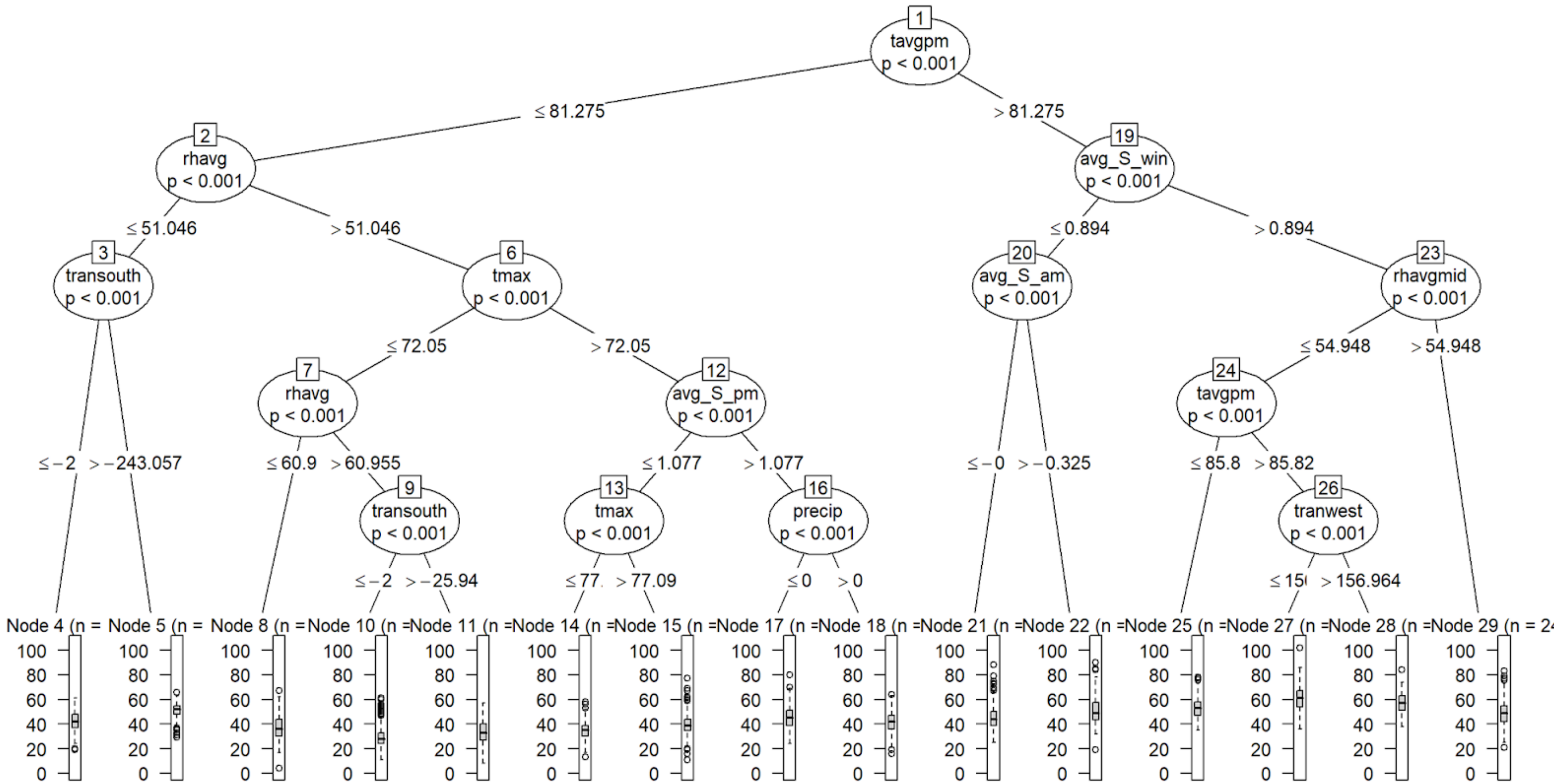

Figure A7.11. CART Tree for the Twin Cities area. The boxplots show the range of ozone MDA8 values (ppb) observed within each set of meteorological conditions ("node").

Table A7.3. Description of the meteorological conditions on ozone-conducive days in each area, along with information about each set of ozone-conducive days. The exceedance probability is the probability of a day in that group having a MDA8 value above 65 ppb (not 70 ppb as for the other analyses). The percent of exceedances is also relative to a threshold of 65 ppb.

Node	Meteorological conditions*	Mean MDA8 Ozone (ppb)	Exceedance Probability (%)	% of Days	% of Exceedances
Twin Cities					
27	T_{avgpm} > 85.8 °F, avg_S_win > 0.9 m/s, RH_{avgmid} ≤ 54.9 %, $tran_{west}$ ≤ 157.0 km	58.5	32%	5%	40%
28	T_{avgpm} > 85.8 °F, avg_S_win > 0.9m/s, RH_{avgmid} ≤ 54.9 %, $tran_{west}$ > 157.0 km	55.9	14%	3%	16%
Combined High-Ozone Nodes		*57.4*	*25%*	8%	56%

* avg_S_win = average wind south (v) vector, RH_{avgmid} = average midday relative humidity, T_{avgpm} = average afternoon temperature, $tran_{west}$ = westerly (u) component of 24-hr transport vector.

As discussed in the main document, we conducted the W-W analysis on the ozone-conducive days, as determined by the CART analysis described above. The results of this W-W analysis for the Twin Cities are shown in Figure A7.12. Mean ozone concentrations on both weekdays and weekends on ozone-conducive days decreased from roughly 64 ppb in 2001-2005 to just over 50 ppb in 2016-2020. The mean W-W MDA8 differences were positive in all sets of years, starting off very close to zero, indicating transitional chemistry, and shifting to significantly NOx-sensitive in 2006-2010. W-W differences decreased over time, with values decreasing to just under 1 in 2016-2020. This could be interpreted to indicate a shift to transitional chemistry in 2016-2020. A more likely explanation is that this is an artifact of the relatively small number of ozone-conducive days and thus reflects a methodological limitation rather than an actual change in chemistry. There were no weekend days in node 28 in 2016-2020, which adds a large amount of uncertainty to the mean weekend concentrations, which likely skewed the results.

The monitored NO_2 concentrations in the Twin Cities area decreased from 2001-05 through 2011-15 and then leveled off through 2016-20. Plots of W-W differences versus NO2 concentrations (Figure A7.12) suggest that VOC concentrations continued to decrease during this time. However, as discussed above, the mean MDA8 concentration on weekends in 2016-20 is uncertain because of the lack of one type of ozone-conducive day in this time period, so the curve fits are also uncertain for this time period. Overall, this analysis suggests that ozone formation in the Twin Cities area switched from being transitional in the early 2000s to NOx-sensitive since then.

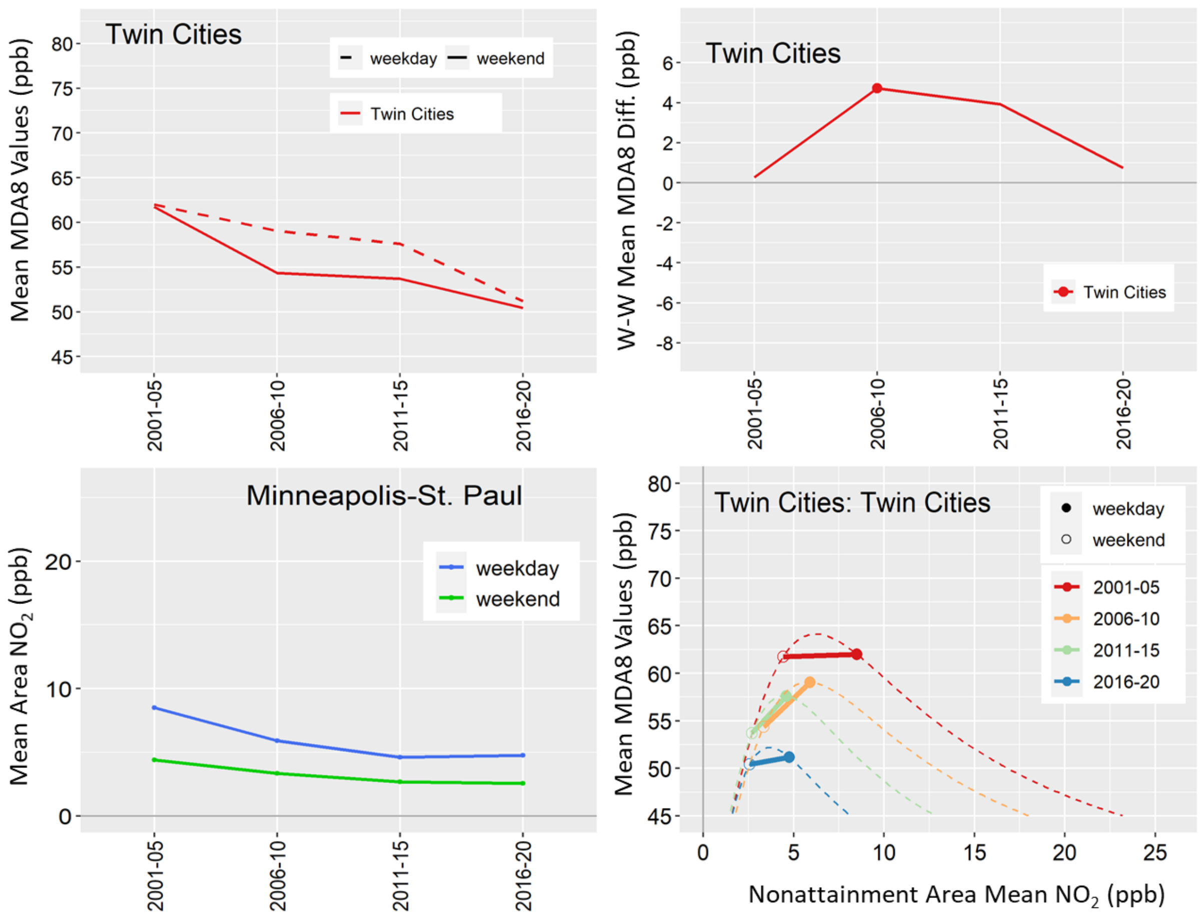

Figure A7.12. Results of the weekday-weekend analysis for the Twin Cities monitors. (Top left) trends in mean maximum daily 8-hour ozone (MDA8) concentrations on weekdays (Tue-Thu) and weekends (Sun). (Top right) the weekday-weekend (W-W) difference in the mean MDA8 value for the LADCO nonattainment areas. The filled circles indicate statistically significant W-W differences. Positive values indicate NOx sensitivity and negative values indicate VOC sensitivity. (Bottom left) Mean area concentrations of NO_2 on ozone-conducive weekdays and weekend days. NO_2 concentrations were measured during midday hours (9:00-14:59 LST) from May through September. (Bottom right) Plots of mean MDA8 ozone concentrations versus midday nonattainment area mean NO_2 concentrations on ozone-conducive weekdays (solid symbols) and weekend days (open symbols) during four sets of years. Curves (dashed lines) are included as visual aids and are not meant to be quantitative; these curves were developed as described in the main text using an analytical model in which VOCR was tuned and the curve was scaled to fit the ozone MDA8 values.

Ozone Trends Over Space and Time

LADCO conducted an analysis of ozone trends over space and time for the Minneapolis-St. Paul (Twin Cities) area, as described in section 4 of the main text. Maps of mean fourth high MDA8 ozone values in the different sets of years are shown in Figure A7.13. In the 1990s, all ozone monitors were located to the north and/or east of the city, with no monitors to the west or south of the Minneapolis (or St. Paul) city center. Starting in the early 2000s, additional monitors were added such that monitors are currently distributed fairly evenly around the city center. Ozone fourth high MDA8 values have been relatively low throughout this time period, with the highest concentrations (in the low 70s ppb) found closest to the city center in the 1990s.

Figure A7.14 shows the ozone fourth high MDA8 values plotted versus distance from the Minneapolis city center and over time. There was no monitoring in the inner 10 km of Minneapolis until the 2010s. The city center monitor added at that point is an official near-road monitor, which is sited to measure maximum emissions from roadways. The Minneapolis Near-Road monitor is located at the intersection of two interstates: I-90 and I-35W. This monitor recorded the lowest-observed ozone concentrations in the time periods it operated. This is almost certainly due to localized titration of ozone by locally high concentrations of NO emitted from the nearby highways. Accordingly, these measurements reflect local NOx titration rather than more urban-scale impacts due to a combination of NOx sources in an urban area, as observed in Chicago.

Besides the near-road site, there is no evidence of NOx saturation/VOC limitation in the Twin Cities, as ozone concentrations are generally highest near the city center and decrease away from it (Figure A7.14). There is, however, evidence of transitional chemistry in the city center in the 1990s. Ozone concentrations at the monitor in the 10-20 km distance bin were stable from the early 1990s through the early 2000s, at which point they started to decrease. Similarly, concentrations at the next-farthest monitor, at 30-40 km, were stable from 1991-95 to 1996-00 and decreased after this. These observations suggest that ozone formation in the inner 40 km was transitional during the early 1990s. The outer part of this area shifted to NOx-sensitive in the early 2000s, and the inner portion remained transitional through the early 2000s, after which point it shifted to NOx-sensitive. Ozone formation in the rest of the Twin Cities area appears to have been NOx-sensitive throughout the study period.

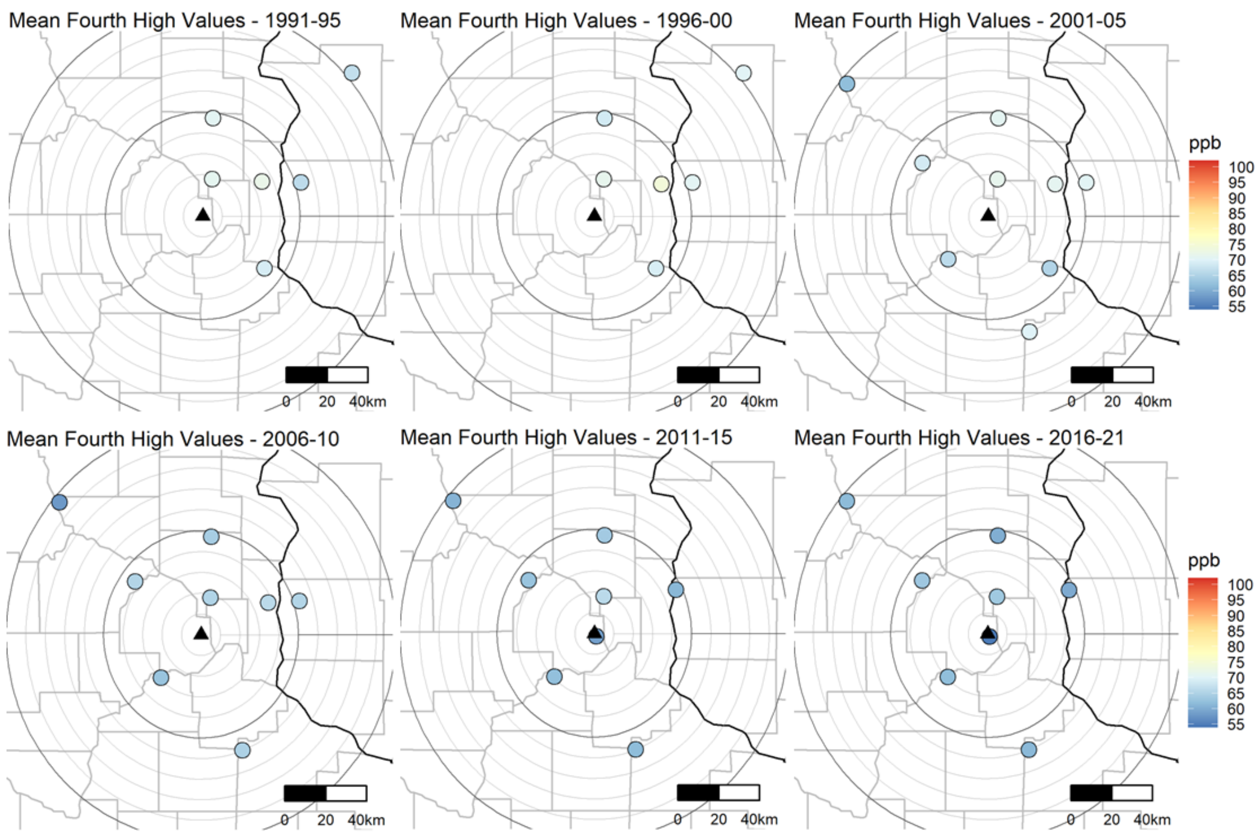

Figure A7.13. Maps of mean annual fourth high maximum daily 8-hour average (MDA8) ozone concentrations in ppb in the Minneapolis-St. Paul area in each time period, as labeled. The black triangles show the location of the Minneapolis city center. The concentric circles show the distance from the city center, with the light lines being 10 km apart and the darker lines being 50 km apart.

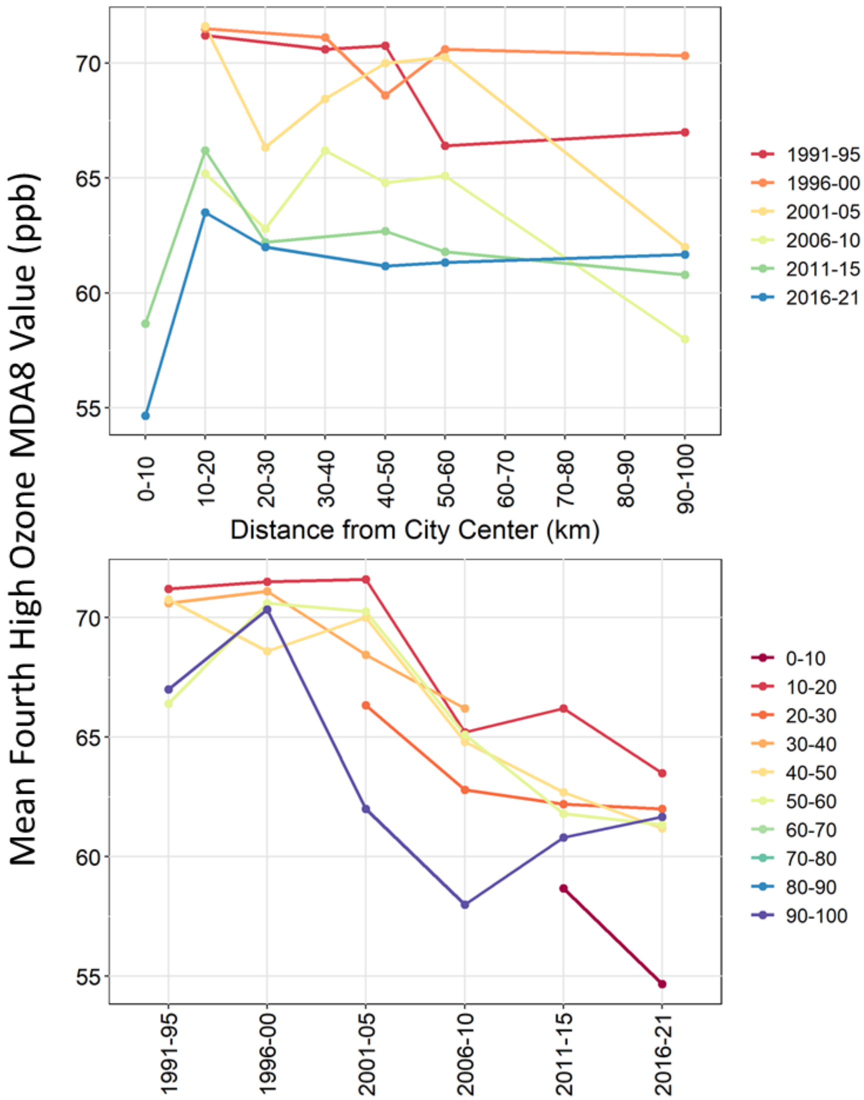

Figure A7.14. Mean fourth high MDA8 ozone concentrations for the Minneapolis-St. Paul area plotted versus (top) distance from the Minneapolis city center, with different lines for the different year groups, and (bottom) different year groups, with different lines for the different distance bins.

Over the last two time periods (2011-15 to 2016-21), mean ozone fourth high MDA8 values decreased slightly over most of the Twin Cities area (Figure A7.15). The largest change was a decrease of 4 ppb north of the city. Half of the monitors changed by less than 1 ppb, with the two sites to the northwest of the city having small increase in ozone, and the sites to the south having small decreases. Overall, ozone concentrations appear stable to slightly decreasing in the Twin Cities area.

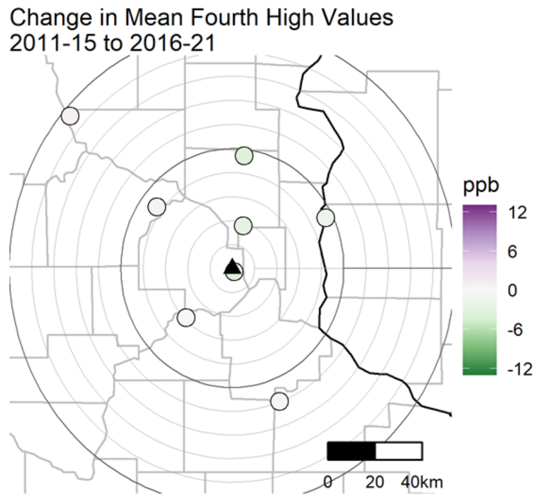

Figure A7.15. Map of the change in mean annual fourth high maximum MDA8 ozone concentrations in ppb from 2011-15 to 2016-21, with positive values indicating increasing concentrations. The black triangles show the location of the Minneapolis city center. The concentric circles show the distance from the city center, with the light lines being 10 km apart and the darker lines being 50 km apart.

Synthesis: Ozone Formation Sensitivity in the Twin Cities area

Considering all of the evidence together, it appears that ozone formation in recent years in most of the Twin Cities area is NOx-sensitive, likely with an area of transitional chemistry in the Minneapolis and St. Paul city centers. The ground-based HCHO/NO_2 ratios suggest transitional chemistry at the Blaine monitor, located 10-20 km from the Minneapolis city center. HCHO/NO2 ratios from the TROPOMI satellite indicate NOx sensitivity in the whole area except by one large power plant to the northwest. In contrast, HCHO/NO2 ratios from the CAMx model suggest an area of VOC sensitivity in the city center. However, as discussed in Section 5.4 of the main document, this method seems to consistently over-predict VOC sensitivity across all areas of the LADCO region. Both the W-W analysis and the trends analysis suggest that the Twin Cities area is NOx sensitive. In addition, HDDM modeling by Koplitz et al. (2021) found a mix of VOC-sensitive and transitional chemistry in the central Twin Cities, surrounded by areas of NOx-sensitivity. Taken together, it is likely that there is some transitional chemistry in the city center and that most of the area is NOx-sensitive.

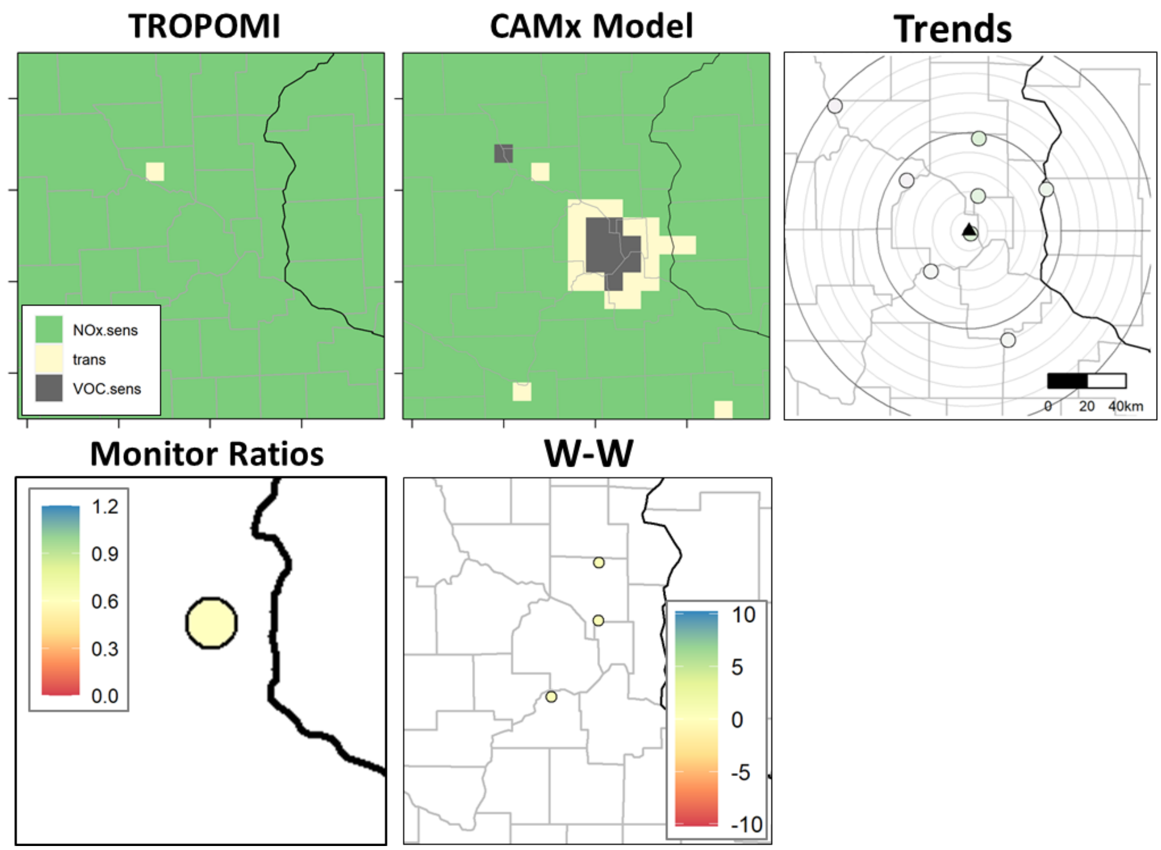

Figure A7.16. Summaries of the recent ozone-NOx-VOC sensitivity[5] for the Twin Cities area based on (top left) TROPOMI satellite HCHO/NO_2 ratios, (top middle) CAMx model HCHO/NO_2 ratios, (top right) the trends analysis, (bottom left) monitored HCHO/NO_2 ratios, and (bottom middle) weekday-weekend analysis. All analyses focused on high-ozone days.

[5] TROPOMI results are for 2018-21, CAMx model results are for 2016, trends results are the difference between 2011-15 and 2016-21, and monitor ratios and W-W results are for 2016-21. Positive trends differences indicate increases in ozone, whereas negative values indicate decreases. Monitor ratios greater than 1 are considered NOx-sensitive, and ratio less than 0.3 are VOC-sensitive. W-W differences greater than 1 are NOx-sensitive and less than -1 are VOC-sensitive. High-ozone days were defined as days with a MDA8 value greater than 70 ppb for the TROPOMI and CAMx model analyses and as days with a MDA8 value greater than 60 ppb for the monitor ratios. The W-W analysis examined days with ozone-conducive meteorology, and the trends analysis focused on the annual fourth highest MDA8 value.